

The Effects of Increased *Plp1* Gene Dosage on Expression and Processing of Myelin Proteins

A thesis presented to the Faculty of Veterinary Medicine,
University of Glasgow

for the degree of Doctor of Philosophy

2007

© Saadia Ansari Karim

Abstract

Mutations in *proteolipid protein 1 (PLP1)*, an X-linked gene causes Pelizaeus-Merzbacher disease (PMD) in humans. The most frequent cause of PMD is the duplication of *PLP1*, which encodes the major myelin membrane protein of the human CNS. The #66 transgenic mice with extra copies of the wild type *Plp1* gene are a valid model of PMD caused by increased gene dosage (Readhead *et al.*, 1994). These mice develop dysmyelinating or demyelinating phenotypes dependant on the gene dosage. This study investigated the effects of both low and high increased *Plp1* gene dosage on various different selected aspects of myelin, including morphology, message and protein levels of PLP/DM20 and other representative myelin proteins and PLP/DM20 dynamics.

Early in development mice with low increased gene dosage (hemizygous) are indistinguishable at the protein and myelin levels from their wild type littermates. During myelination these animals display elevated levels of PLP/DM20 in the oligodendrocyte cell body and alterations in other myelin protein levels and to the structure of myelin but these are transitory effects. These transient changes suggest the oligodendrocytes at low gene dosage retain the ability to regulate expression, production and incorporation of proteins into myelin thus maintaining the normal process of myelination.

At high increased gene dosage (homozygous), oligodendrocytes in culture, pre and early myelinating oligodendrocytes *in vivo* and oligodendrocytes *in vivo* during peak myelination all exhibit elevated levels of PLP/DM20 in the their cell bodies. The protein is sequestered into autophagic vacuoles and late endosomes/lysosomes (LE/Ls), while the levels in myelin are reduced compared to wild type and hemizygous cells. Synthesis, partitioning with lipids and incorporation of PLP/DM20 are all also affected in the homozygous animals. The increased *Plp1* gene dosage does affect other myelin proteins, in particular MBP, which showed a consistent and dramatic reduction in oligodendrocytes and myelin.

These results indicate the heterogeneity of phenotypes and underlying changes caused by low and high increased *Plp1* gene dosage. The cause of the dysmyelination observed in #66 mice and patients with PMD does not appear to be due to one single change in myelinogenesis. Each alteration observed in #66 transgenic mice could be a contributing factor. Importantly, the perturbation of MBP expression, in the light of this gene's pivotal

role in myelination, highlights that the relationship between *Plp1* and *Mbp* expression is implicated in the pathogenesis of dysmyelination.

Table of Contents

Abstract	ii
Table of Contents	iii
List of Figures	viii
List of Tables	x
Acknowledgements	xi
Author's Declaration	xiii
Abbreviations	xiv
1 Introduction	1-2
<i>1.1 Background</i>	<i>1-17</i>
<i>1.2 CNS structure and Function</i>	<i>1-17</i>
1.2.1 Oligodendrocytes	1-18
1.2.2 Myelin	1-22
1.2.3 Axons	1-27
1.2.4 Astrocytes	1-28
1.2.5 Microglia.....	1-30
<i>1.3 Protein and Lipid content of CNS Myelin</i>	<i>1-30</i>
1.3.1 Myelin proteins	1-30
1.3.2 Other proteins	1-36
1.3.3 Lipids	1-36
<i>1.4 The Plp1 Gene: Structure and Function</i>	<i>1-38</i>
1.4.1 The <i>PLP1</i> Gene.....	1-38
1.4.2 Evolution and Conservation of the <i>Plp1</i> gene	1-40
1.4.3 Expression of <i>Plp1</i> gene	1-42
1.4.4 Regulation of the <i>Plp1</i> gene.....	1-43
1.4.5 Splicing of the <i>Plp1</i> gene.....	1-44
1.4.6 Translation and post-translational modification of PLP/DM20 protein	1-44
1.4.7 Proposed functions of the <i>Plp1</i> gene	1-45
1.4.8 Protein dynamics.....	1-47
<i>1.5 PLP1 gene mutations and disease</i>	<i>1-50</i>
1.5.1 <i>PLP1</i> gene-related disorders in man	1-50
1.5.2 <i>Plp1</i> gene mutations in animals	1-54
1.5.3 Spontaneous mutations of other myelin genes.....	1-60
<i>1.6 Aims of thesis</i>	<i>1-62</i>
2 Materials and Methods	2-63
<i>2.1 Miscellaneous</i>	<i>2-63</i>
<i>2.2 Mouse Breeding</i>	<i>2-63</i>
2.2.1 Animal breeding facilities.....	2-63
2.2.2 Transgenic Lines.....	2-63
2.2.3 Maintenance of transgenic lines of mice	2-68
2.2.4 Crossing of transgenic lines of mice.....	2-68
<i>2.3 Isolation and manipulation of DNA</i>	<i>2-68</i>
2.3.1 Tail Biopsy and mouse identification	2-68
2.3.2 Genomic DNA (gDNA) extraction.....	2-68
2.3.3 gDNA quantification and storage	2-69
2.3.4 PCR Genotyping.....	2-71

2.3.5	Agarose gel	2-75
2.3.6	Visualisation of PCR Products	2-75
2.4	<i>Isolation and manipulation of RNA</i>	2-75
2.4.1	Tissue/Sample Collection	2-75
2.4.2	Extraction of RNA.....	2-75
2.4.3	Quantification and Quality check	2-76
2.4.4	cDNA generation from total RNA.....	2-76
2.4.5	RT-PCR	2-79
2.4.6	Northern blotting.....	2-80
2.4.7	qRT-PCR	2-87
2.5	<i>Protein Analysis</i>	2-92
2.5.1	Tissue/Sample Collection	2-92
2.5.2	Isolation of Myelin proteins.....	2-92
2.5.3	Western Blotting.....	2-94
2.5.4	Oligodendrocytes Cultures	2-98
2.5.5	Synthesis at P20	2-102
2.6	<i>Myelin Morphology/Analysis</i>	2-107
2.6.1	Tissue Fixatives and Fixation	2-107
2.6.2	Tissue Processing and Sectioning.....	2-108
2.6.3	Staining Techniques.....	2-109
2.6.4	Immunohistochemistry (2.5.6.2 Charaterisation by immunostaining)	2-109
2.6.5	Morphological Quantitative studies.....	2-113
2.6.6	Statistical analysis.....	2-115
3	Effects of #66 transgene cassette	3-116
3.1	<i>Background</i>	3-116
3.2	<i>Aims</i>	3-116
3.3	<i>Methods</i>	3-116
3.3.1	Animal breeding	3-116
3.3.2	Genotype and Sample Selection	3-117
3.3.3	Tissue Preparation.....	3-117
3.3.4	Transcript Analysis.....	3-117
3.3.5	CNS Myelin Analysis	3-118
3.4	<i>Results</i>	3-118
3.4.1	#66 transgene expression.....	3-118
3.4.2	CNS Myelin analysis	3-119
3.5	<i>Discussion</i>	3-119
4	Effects of Increased <i>Plp1</i> gene dosage on Pre- and Early Myelinating Oligodendrocytes	4-125
4.1	<i>Background</i>	4-125
4.2	<i>Aims</i>	4-126
4.3	<i>Methods</i>	4-126
4.3.1	Animal breeding	4-126
4.3.2	Sample Selection.....	4-127
4.3.3	Primary Cell Culture Analysis.....	4-127
4.3.4	Transcript Analysis.....	4-127
4.3.5	CNS Myelin Analysis	4-127

4.4	<i>Results</i>	4-128
4.4.1	Identification of Genotype	4-128
4.4.2	Immunostaining	4-128
4.4.3	Protein Analysis of Culture Lysates	4-128
4.4.4	Analysis of Early Myelination in P3 spinal cord	4-129
4.5	<i>Discussion</i>	4-129
5	Effects of Increased <i>Plp1</i> gene dosage on Peak Myelination (P20)	5-139
5.1	<i>Background</i>	5-139
5.2	<i>Aims</i>	5-140
5.3	<i>Methods</i>	5-140
5.3.1	Animal breeding	5-140
5.3.2	Sample Selection.....	5-140
5.3.3	Transcript Analysis.....	5-140
5.3.4	CNS Myelin Analysis	5-141
5.3.5	Morphometric analysis	5-141
5.3.6	Immunostaining	5-142
5.4	<i>Results</i>	5-142
5.4.1	Identification of Genotype	5-142
5.4.2	Transcript Analysis of P20 wild type, hemizygous and homozygous animals....	5-142
5.4.3	PLP/DM20 levels in CNS.....	5-143
5.4.4	Effects of increased dosage on other myelin proteins.....	5-144
5.4.5	Stress responses in #66 animals.....	5-145
5.4.6	Morphometric analysis of P20 #66 myelin in spinal cord and brain	5-145
5.4.7	Storage of PLP/DM20 in the oligodendrocyte cell body	5-146
5.5	<i>Discussion</i>	5-147
6	Effects of Increased <i>Plp1</i> gene dosage on Maintenance of Myelination (P60)	6-163
6.1	<i>Background</i>	6-163
6.2	<i>Aims</i>	6-164
6.3	<i>Methods</i>	6-164
6.3.1	Animal breeding	6-164
6.3.2	Sample Selection.....	6-164
6.3.3	Transcript Analysis.....	6-164
6.3.4	CNS Myelin Analysis	6-165
6.3.5	Morphometric analysis	6-165
6.4	<i>Results</i>	6-166
6.4.1	Identification of Genotype	6-166
6.4.2	Transcript Analysis of P60 wild type and hemizygous #66 male mice	6-166
6.4.3	Protein Analysis of P60 wild type and hemizygous #66 male mice	6-166
6.4.4	Morphometric Analysis of P60 Myelin	6-167
6.5	<i>Discussion</i>	6-168
7	Effects of Increased <i>Plp1</i> gene dosage on PLP/DM20 Dynamics	7-178
7.1	<i>Background</i>	7-178
7.2	<i>Aims</i>	7-179

7.3	<i>Methods</i>	7-179
7.3.1	Animal breeding	7-179
7.3.2	Sample Selection.....	7-179
7.3.3	Primary cell cultures	7-180
7.3.4	Brain Slice system	7-180
7.3.5	Lipid Rafts	7-180
7.4	<i>Results</i>	7-181
7.4.1	Identification of Genotype	7-181
7.4.2	Newly Synthesised PLP and DM20 in Oligodendrocytes	7-181
7.4.3	Degradation of Newly Synthesised PLP and DM20 over time	7-182
7.4.4	Blocking of Proteasome Mediated Degradation	7-182
7.4.5	Synthesis in Brain Slices.....	7-183
7.4.6	Incorporation of Newly Synthesised PLP and DM20 into Myelin	7-184
7.4.7	PLP and DM20 in Lipid Rafts	7-184
7.4.8	All Newly Synthesised Proteins in Oligodendrocytes	7-185
7.5	<i>Discussion</i>	7-185
8	Final conclusions and future work	8-195
9	Appendix	206
9.1.1	APES-coated slides.....	206
9.1.2	DEPC-treated water	206
9.1.3	Fixatives.....	206
9.1.4	Tissue processing protocols	207
9.1.5	Staining protocols	208
9.1.6	Staining solutions.....	209
9.1.7	General Buffers.....	210
9.1.8	Specific solutions and buffers.....	211
9.1.9	Tissue culture media	212
	References	214

List of Figures

Figure 1. Drawing of an oligodendrocyte and axons also showing the myelin sheaths, internodes and nodes of Ranvier and myelin. Obtained from http://members.tripod.com/blustein/Oligodendrocytes/oligodendrocytes.htm	1-21
Figure 2. Myelin in wild type mice.....	1-25
Figure 3. Organisation of <i>Mbp</i> gene in mice.	1-33
Figure 4. The murine <i>Plp1</i> gene.....	1-39
Figure 6. Pie chart showing the proportion of PMD caused by the different types of mutations with ~70% caused by duplications of the <i>PLP1</i> gene.	1-56
Figure 7. Transgene construct from the #66 and #72 lines.....	2-65
Figure 8. The steps involved in generating <i>Plp1</i> null mice.	2-67
Figure 9. gDNA separated on a 0.8% agarose gel.	2-70
Figure 10. Genotyping PCRs.	2-74
Figure 11. 500ng total RNA from P20 spinal cords.	2-78
Figure 12. cDNA from P20 mouse spinal cord.....	2-78
Figure 13. 12.5µg total mRNA separated on a denaturing agarose gel.	2-82
Figure 14. Northern blotting (very similar to Southern blotting method described by Southern).....	2-84
Figure 15. cDNA probes for northern hybridisation.....	2-86
Figure 16. TaqMan technology.	2-88
Figure 17. An example of the typical output from the ABI 7500 showing the increase in signal at each cycle.	2-91
Figure 18. Standard curve produced from serial dilutions of wild type RNA and β -actin primers and probe set.	2-91
Figure 19. Test brain slice experiment.....	2-104
Figure 20. Transcript analysis of P20 Null x #66 total RNA.....	3-122
Figure 21. Representative graph showing mRNA (message) levels in the three #66 x null genotypes using qRT-PCR.....	3-123
Figure 22. Western blot analysis of the <i>Plp1</i> wild type transgene on a <i>Plp1</i> null background.....	3-123
Figure 23. Quantitative data for <i>Plp/Dm20</i> mRNA, measured by qRT-PCR and PLP protein, measured by western blotting for <i>Plp1</i> gene null mice carrying the <i>Plp1</i> transgene.	3-124
Figure 24. Resin sections (1µm) of white matter in the ventral funiculus of P5 mice. .	4-133
Figure 25. Representative PLP/DM20 immunostained oligodendrocytes after 6 days in culture.....	4-134
Figure 26. Representative MBP immunostained oligodendrocytes after 6 days in culture.	4-135
Figure 27. Protein analysis of lysates from #66 oligodendrocyte cultures.....	4-136

Figure 28. <i>Plp1</i> and <i>Mbp</i> gene expression in spinal cord of P3 mice hemizygous and homozygous for the <i>Plp1</i> transgene.....	4-137
Figure 29. PLP/DM20 in sections of spinal cord of P3 mice homozygous for the <i>Plp1</i> transgene.	4-138
Figure 30. Transcript analysis of P20 #66 spinal cord RNA.	5-154
Figure 31. PLP/DM20 protein analysis in #66 animals at P20.....	5-156
Figure 32. Increased <i>Plp1</i> gene dosage affects expression of other myelin protein genes..	5-157
Figure 33. Stress responses in #66 transgenic mice.....	5-159
Figure 34. Electron micrographs of white matter in the ventral columns of P20 mice.	5-160
Figure 35. Oligodendrocyte cell body from spinal cord white matter of P20 homozygous transgenic mouse.....	5-160
Figure 36. Myelin status of wild type and transgenic mice at P20.	5-161
Figure 37. PLP/DM20 immunostaining of P20 homozygous forebrain.	5-162
Figure 38. Forebrain from P20 homozygous mice immunostained.....	5-162
Figure 39. Transcript analysis of P60 wild type and hemizygous message.....	6-172
Figure 40. Protein analysis of P60 brain and spinal cord myelin.	6-173
Figure 41. Electron micrographs and graphs of P60 wild type and hemizygous animals' myelin morphology.....	6-175
Figure 42. Synthesis of PLP and DM20 in wild type, hemizygous and homozygous oligodendrocytes.	7-189
Figure 43. Degradation of PLP and DM20 in wild type, hemizygous and homozygous oligodendrocytes.	7-190
Figure 44. Synthesis and incorporation of newly synthesised PLP and DM20 into myelin in brain slices from P20 wild type, hemizygous and homozygous animals.....	7-192
Figure 45. Different association of PLP/DM20 from wild type and homozygous myelin with lipid rafts.	7-194
Figure 46. Phosphorimage of lysates from oligodendrocytes after 1 hr of labelling with radiolabelled amino acids.....	7-194
Figure 47. Schematic representation of the fate of PLP/DM20 at P20 in wild type, hemizygous and homozygous #66 oligodendrocytes.....	8-205

List of Tables

Table 1. Standard PCR program used for genotyping PCRs or RT-PCRs	2-70
Table 2. PCR primers for genotyping, semi-quantitative RT-PCR and realtime RT-PCR .	2-73
Table 3. Optimisation of the forward and reverse primers for real-time RT-PCR	2-91
Table 4. Volumes for hand-poured SDS-PAGE gels.....	2-96
Table 5. Primary and Secondary Antibodies used for western blotting.....	2-97
Table 6. Primary antibodies, dilutions used and target.....	2-111
Table 7. Link antibody and Avidin biotin Complex (ABC)	2-111
Table 8. Secondary antibodies	2-111
Table 9. Summary of results in this study on #66 transgenic mice.....	8-203

Acknowledgements

Firstly I would like to thank our Merciful God for being the guide and higher support in my life. I would especially like to thank my supervisors Professor Ian R. Griffiths and Dr T. James Anderson for supporting, helping and encouraging me throughout this project. The generous funding of the Biology and Biotechnology Sciences Research Council (BBSRC) enabled me to complete this work. I would like to thank everyone in the lab, in particular, Dr Mark McLaughlin for all his advice on protein analysis, for ensuring I was never without a guiding hand and for Figure 45, to Jennifer Barrie and Prof. Griffiths for Figures 25 and 26, Mailis McCulloch for all the EM images presented in this thesis, Dr Julia Edgar for Figures 37 and 38 and to Prof. Griffiths again from the myelin morphometric analysis. Thank you also to Dr Paul Montague for all his help with all matters DNA or RNA.

Thank you to my husband for being so understanding and helpful as without his support this would not have been possible. Thank you also for willingly offering to read the entire thesis more than once. The read-throughs were very helpful and greatly appreciated. Thank you to my two boys for being patient when it was meant to be their time with me and for understanding mum was busy and could not always play with them. The time spent with them helped me unwind, relax and laugh a lot and I am very grateful to them for it. I would also like to thank my family for setting me on the path to this point in my life. Their support throughout has been a great help.

During the course of this study, I have had to learn and master new techniques and this would not have been possible without the help and advice of many people including Jennifer Barrie for advise on and demonstrating tissue culture and perfusions, Anne Terry on Level 3 of the Henry Wellcome Building and all on that floor for the use of their facilities and expertise for my northern blot experiments, Nuno for help with the analysis of the realtime qRT-PCR results and others for help with the ABI 7500 and the actual set up of the technique of realtime qRT-PCR.

The very big thank you to all the staff in Biological Services especially Neil, Catrina, Nicola and David who looked after the mice and me, they provided excellent care of the mice used in this study and all their help and advice was gratefully received. I would like to thank all in the Applied Neurobiology Group for accepting me into the group, helping me and listening to all the talking I can do, especially Marie Ward. She is a great friend

and is willing to talk about and listen to any weird and wonderful subject that arose. Thank you to my friends who are at various stages of writing up their theses for listening to and understanding the frustrations involved in this process and good luck. Finally, I would like to thank all the staff at the Vet School at the Garscube Estate for their friendliness.

Author's Declaration

I, Saadia Ansari Karim, do hereby declare that the work carried out in this thesis is original. It was carried out by myself or with due acknowledgement, and has not been presented for the award of a degree at any other University.

Abbreviations

Abbreviations

aa

ALLN

AOI

APES

ASPA

BiP

cDNA

CHAPS

CMT1A

CNP

CNS

DAB

DAPI

DEPC

DM20

DNA

dNTPs

DTT

EDTA

ER

ERAD

EM

6-FAM

FITC

gDNA

GFAP

HBSS

HRP

Ko

LAMP1

LDH

Full Name

amino acid

acetyl-leu-leu-norleucinal

area of interest

3-aminopropyltriethoxy-silane

aspartoacylase

glucose-regulated protein 78 (GRP78)

complimentary de-oxyribonucleic acid

3-[(3-chloramidopropyl)-dimethylammonio]-1-propane-sulfonate

Charcot-Marie-Tooth disease

2',3'-cyclic nucleotide 3'-phosphodiesterase

central nervous system

3, 4, 3, 4-tetraminobipheyl hydrochloride

4, 6-diamidino-2-phenylindole

di-ethyl pyrocarbonate

the small isoforms of the *Plp1* gene

de-oxyribonucleic acid

deoxynucleotides

dithiothreitol

Ethylene-di-amine-tetra-acetate

endoplasmic reticulum

endoplasmic reticulum associated degradation

electron microscopy

6-carboxy-fluorescein

fluorescein isothiocyanate

genomic DNA

glial fibrillary acidic protein

Hanks balanced salt solution

horse radish peroxidase

knockout

lysosomal membrane glycoprotein 1

lactate dehydrogenase

LE/Ls	late endosomes/lysosomes
L-MAG	large isoform of myelin associated glycoprotein
M	mean
MAG	myelin associated glycoprotein
MBP	myelin basic protein
MDL	major dense line
MFSC	myelin forming Schwann cell
MG-132	carbobenzoxy-L-leucyl-L-leucyl-L-leucinal
min(s)	minute(s)
MOBP	myelin-oligodendrocytic basic protein
MOPS	3-(N-morpholino) propanesulphonic acid
mRNA	messenger ribonucleic acid
MS	Multiple Sclerosis
MyT1	myelin transcription factor 1
NF	neurofilament
NGS	normal goat serum
NMFSC	non-myelin forming Schwann cell
OL	oligodendrocyte(s)
P	post natal age (days)
PAP	peroxidase anti-peroxidase
PCR	polymerase chain reaction
Ph	phosphorimage
<i>Plp1</i>	proteolipid protein 1 gene
PLP	proteolipid protein
PMD	Pelizaeus-Merzbacher disease
PMP22	peripheral myelin protein gene 22
PMSF	phenylmethylsulfonyl fluoride
PNS	peripheral nervous system
P0	protein zero
PVDF	polvvinylidine difluoride
qRT-PCR	realtime reverse transcript polymerase chain reaction
RER	rough endoplasmic reticulum
RNA	ribonucleic acid

rpm	revolutions per minute
RS	rabbit serum
SEM	standard error of mean
S-MAG	small isoform of myelin associated glycoprotein
SPG1	spastic paraplegia gene locus 1
SPG2	spastic paraplegia gene locus 2
SSC	standard sodium citrate buffer
SQS	squalene synthase or farnesyl-diphosphate farnesyltransferase 1
TAE buffer	tris acetate EDTA buffer
TBS	tris buffered saline
TBS-T	tris buffered saline triton X
TLCK	N α -p-tosyl-L-lysine chloro-methyl ketone
TXR	texas red
UV	ultra violet
W	western blot
WT	wild type
XBP-1	X-box Binding Protein 1

1 Introduction

1.1 Background

Myelin disorders account for a small group of incapacitating diseases in humans.

Fortunately, there are many spontaneously occurring animal models of myelin disorders allowing for the study of mechanism and pathology of disease. Over the years one focus of research has been the *proteolipid protein (PLP1)* gene. The *PLP1* gene encodes the most abundant protein found in central nervous system (CNS) myelin making up 50% of all myelin protein. The gene is highly conserved across species and regulation of the gene is also very highly controlled. A wide spectrum of myelin disorders is caused by mutations in this gene or alterations in its expression level through changes in gene copy number including Pelizaeus-Merzbacher disease (PMD) and X-linked Spastic Paraplegia type 2 (SPG2). However, the functions of the gene and how mutations of it lead to disease is still incompletely understood.

The main cause of PMD in humans is duplication of the region of the X chromosome containing the *PLP1* gene. The conservation of the gene across species makes animals such as mice and rats a valid model to study disease mechanisms. Although, there are spontaneous animal mutants of known human point mutations of the *PLP1* gene that cause PMD and SPG2 there are no naturally occurring animal models representing altered gene copy number. Transgenic animals have been generated by several groups to combat lack of suitable models and allow for the study of the mechanisms of how copy number perturbs gene function leading to the disease process. One transgenic line of mice that has been engineered with extra copies of the murine *Plp1* gene is the line #66 (Readhead *et al.*, 1994). This thesis describes the effects that extra copies of the wild type *Plp1* gene have on multiple aspects of the myelination process in the mouse CNS in these mice. The introduction to this thesis summarises the current knowledge of the *Plp1* gene, other myelin genes investigated in this thesis, background on PMD and the animal models available to allow investigation in disease mechanisms.

1.2 CNS structure and Function

The CNS consists of neurons and glial cells and can be divided into gray and white matter. Neurons constitute about half the volume of the CNS making up the gray matter and glial

cells along with neuronal processes known as axons make up the remainder. The relationship and interactions in the CNS between glial cells and neurons are highly complex and specialised. Glial cells provide support and protection for neurons. They are thus known as the "supporting cells" of the nervous system. The four main functions of glial cells are: to surround neurons and hold them in place, to supply nutrients and oxygen to neurons, to insulate one neuron from another, and to destroy and remove the remains of dead neurons. The three types of CNS supporting cells are oligodendrocytes (from the Greek literally meaning few tree cells), astrocytes and microglia. In the peripheral nervous system (PNS) the supporting cells are Schwann cells, enteric glial cells and satellite cells (Jessen 2004).

In the CNS myelination occurs after birth in rodents and happens at different times in different regions (Morell and Norton 1980). In the developing brain, neurons are formed a long way from their final resting place requiring a great amount of migration in which the glial cells are also involved. In humans the process of myelination starts in the third trimester of pregnancy and continues to up the third decade of life. Peak myelination occurs in the first year of life (Baumann and Pham-Dinh 2001).

1.2.1 Oligodendrocytes

The oligodendrocyte is the extremely specialised CNS-specific glial cell that is responsible for the production of myelin ([1.2.2 Myelin](#)) and axonal ensheathment. Each oligodendrocyte can myelinate multiple axons with the number varying depending on calibre of axon whereas Schwann cells can ensheath only one internode (one myelin/axon subunit) (Figure 1). In certain areas of the CNS oligodendrocytes myelinate up to 40 internodes, many on different axons (Morell and Norton 1980). In areas with larger myelinated fibres oligodendrocytes make fewer sheaths whereas in tracts with smaller fibres oligodendrocytes make more sheaths. The interaction between oligodendrocytes and axons appears to be determined by the diameter of axons in contact with the oligodendrocyte. In size, oligodendrocytes are smaller than another CNS cell, the astrocytes (Baumann and Pham-Dinh 2001).

Oligodendrocytes are derived from an oligodendrocyte progenitor cell (OPC) that originates in specialised areas of the ventral subventricular zone of the neural tube (Trapp *et al.*, 2004). In mature CNS, OPCs account for 5-8% of the glial cell populations (Vouyiouklis 2003). These cells migrate, divide and populate the CNS during early

development. These early OPCs go on to differentiate into late OPCs or oligodendroblasts that are committed to oligodendrogenesis (Trapp *et al.*, 2004). Late OPCs are post migratory and differentiate into oligodendrocytes in a temporal and spatial sequence that precedes myelination by a few days (Trapp *et al.*, 1997). Numbers of immature oligodendrocytes are greater than are finally required by the CNS triggering apoptosis pathways to reduce the numbers of cells (Barres *et al.*, 1992).

The cells known as premyelinating oligodendrocytes can be characterised by distinct criteria. Some of the myelin proteins such as DM20, myelin associated glycoprotein (MAG), and 2',3'-cyclic nucleotide 3'-phosphodiesterase (CNP) are expressed and are evenly distributed throughout the cell. These cells also extend multiple processes called membrane sheets, radially and symmetrically. The differentiation from a premyelinating to myelinating oligodendrocyte is again characterised by morphological and molecular changes. The most important change is from a non-polarised cell to a polarised cell with the oligodendrocyte targeting myelin proteins to specific membrane domains. PLP/DM20 is targeted to compact myelin, CNP to non-compact myelin of the internode, MAG to periaxonal membranes and myelin basic protein (MBP) mRNA along processes (Trapp *et al.*, 2004).

Findings put forward by Spassky *et al.*, (2000) showing *Plp/Dm20* progenitor cells and platelet-derived growth factor receptor alpha (PDGFR α) expressing progenitors highlight the possibility of more than one oligodendrocyte lineage in the CNS. This research is supported by findings from Le Bras and colleagues (2005) that *Plp/Dm20* progenitors generate OPCs independent of PDGFR α OPCs. Richardson *et al.*, (2006) reviewed the evidence for site(s) of origin of oligodendrocytes concluding that both dorsal and ventral sources are involved and each is active at different times during development of the CNS.

Oligodendrocytes require neurons as they produce certain factors essential for formation and maintenance of myelin in the CNS. OPCs can differentiate as normal in axon-free culture and express myelin components but later oligodendrocytes become dependant on axonal signals. One such extrinsic signal is platelet-derived growth factor-AA (PDGF-AA), which is a major mitogen in rodents (reviewed by Rogister *et al.*, 1999). The release of adenosine triphosphate (ATP) from electrically active neurons, which is then hydrolysed to adenosine, causes the inhibition of OPC proliferation and stimulates differentiation

(Stevens *et al.*, 2002). Unlike Schwann cells, oligodendrocytes do not have a basal lamina or microvilli.

In cultured oligodendrocytes, PLP is a latecomer, being expressed after MAG and MBP (Dubois-Dalcq *et al.*, 1997). PLP is translated and modified in the ER and Golgi apparatus then transported to the site of incorporation whereas MBP is actually translated at its site of incorporation into myelin. MAG and CNP are also translated in the oligodendrocyte cell body rather than their sites of incorporation. The presence of PLP is a sign of a mature myelin-forming oligodendrocyte. Oligodendrocytes express some of the same molecular components as Schwann cells in the PNS; however, two proteins expressed only by oligodendrocytes are myelin-oligodendrocyte glycoprotein (MOG) on their outer cell membrane and myelin-associated oligodendrocytic basic protein (MOBP) in the major dense line (MDL) of compact myelin (Arroyo and Scherer 2000).

Jung-Testas and co-workers (1994) have shown that oligodendrocytes synthesise pregnanolone, progesterone and their sulfated metabolites. These hormones appear to activate the synthesis of specific proteins. The production of such hormones in females may have an influence on myelination. This effect is observed in Multiple Sclerosis (MS) when in pregnancy estrogen and progesterone levels are high and improvements in disease status are seen. In animals the difference is more notable in older animals during remyelination (Li *et al.*, 2006). Cahill (2006) reviewed how sex influences the development of the brain, its anatomy and function in humans highlighting the importance of understanding there is a difference between male and female brains. This can affect any results obtained from female animals therefore all studies in this thesis were carried out on male mice. Another factor in this decision was the fact that PMD mainly affects males.

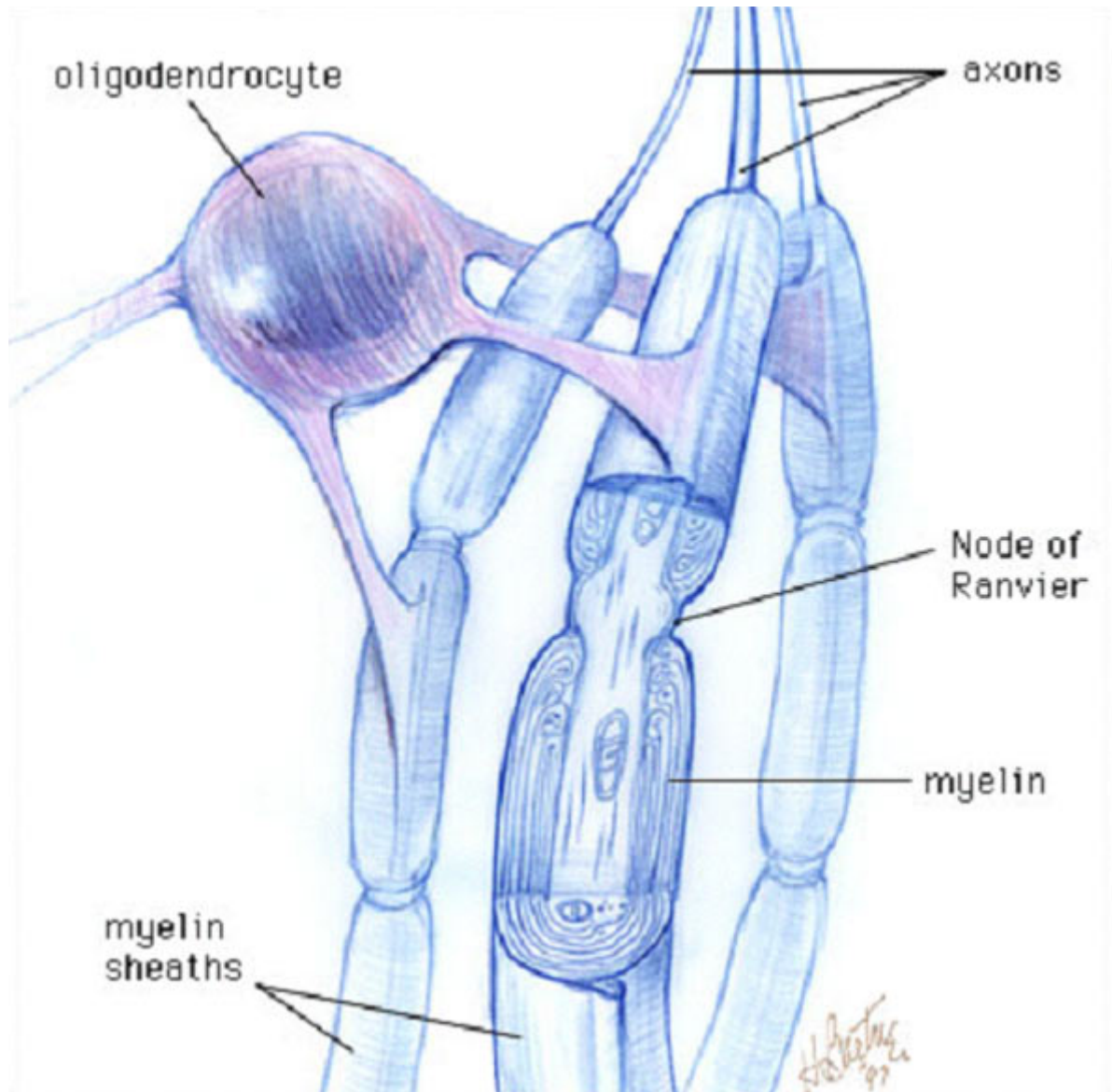


Figure 1. Drawing of an oligodendrocyte and axons also showing the myelin sheaths, internodes and nodes of Ranvier and myelin. Obtained from <http://members.tripod.com/blustein/Oligodendrocytes/oligodendrocytes.htm>.

1.2.2 Myelin

In man, more than 40% of an area of a brain section may consist of white matter (Morell and Norton 1980). This white matter is a fatty coating of axons known as myelin. Myelin derived from the Greek word for marrow (*myelos*), was first described by a German pathologist Rudolf Virchow in 1864. The main reason there is so much white matter or myelin in the brain is that it is essential for the speedy conduction of electrical signals along the axon length. To double the conduction velocity of signal on a bare fibre would require a four times increase in diameter whereas with a myelinated fibre a doubling only requires a two times increase in diameter thus saving on space and energy needed (Morell and Norton 1980). Myelination in the CNS is dependant on a balance between positive and negative axonal signals received by the myelinating cell (Colman *et al.*, 2005).

Myelination is the process of ensheathing axons with myelin extending from certain glial cells in the CNS and PNS. The myelin is formed by vast extensions of membranes of glial cells, oligodendrocytes in the CNS and Schwann cells in the PNS. Formation of myelin follows a set pattern after contact between the glial cell and the axon is made. The initial area to myelinate is the cervical spinal cord and from this region myelination spreads caudally along the spinal cord and rostrally through the brain. Small diameter fibre tracts myelinate after large diameter fibre tracts and the optic nerve myelinates later than the spinal cord. The myelin sheath forms after the plasma membrane of the glial cell process wraps around the axon and then compacts, squeezing out all the cytoplasm (Figure 2A) (Sherman and Brophy 2005). As it wraps, two different membrane appositions are generated, the intracellular or major dense line (MDL) and the extracellular or intraperiod line (IPL) (Figure 2B) (Lemke 1988). The basic ultrastructure of CNS and PNS myelin is similar although the proteins involved vary between the two. In the CNS periodicity of the IPL is maintained by PLP whereas in the PNS the regularity of IPL is determined by the P0 glycoprotein (Giese *et al.*, 1992). The structure and myelin membrane orientation of the proteins, MAG, MBP, PLP and P0 are shown in Figure 2C. As the process of myelination continues the link between the oligodendrocyte cell body and compacted membrane becomes less apparent and is less visible by electron microscopy (Deber and Reynolds 1991).

Most myelinated axons in any given animal have the same g ratio (ratio of axon diameter to fibre diameter) and this value is normally between 0.6 and 0.7 (Sherman and Brophy 2005). Neuregulin 1 (NRG1) type III protein was shown to be active in regulating myelin

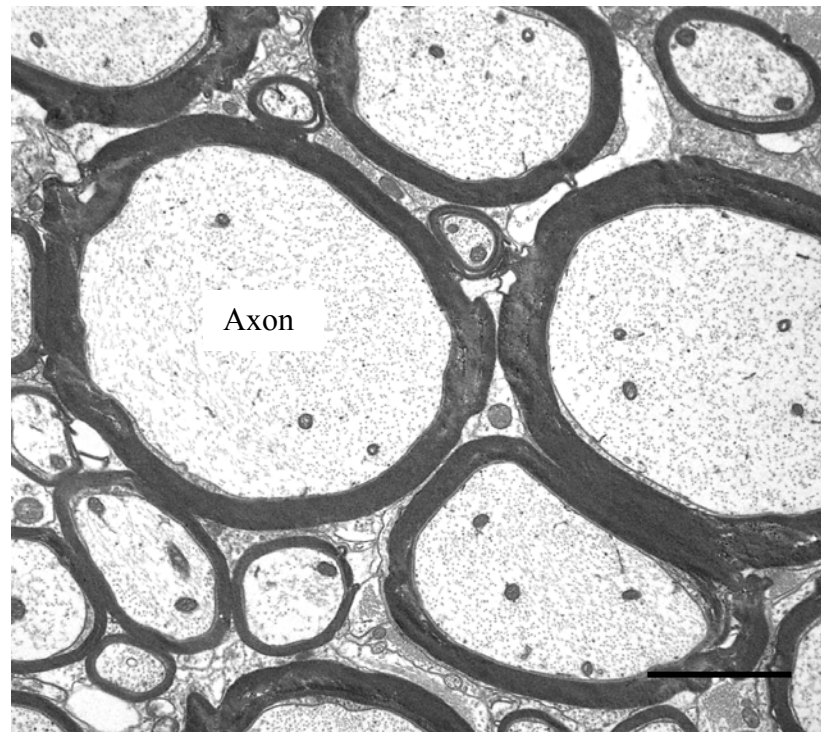
thickness in the PNS thus influencing g ratios (Michailov *et al.*, 2004, Sherman and Brophy 2005). Whether NRG1 type III has a role in the regulation of g ratios in the CNS is unknown and if it is not, the factors involved have yet to be identified. g ratio is the precise relation between axon diameter and myelin sheath thickness but the mechanism by which the myelinating cell determines the number of wraps to produce is still a matter of investigation. Transplantation of oligodendrocytes into nerve tracts demonstrated that axons, and not the glial cells, determine the number of myelin wraps (French-Constant *et al.*, 2004). Myelin periodicity in the CNS is 14nm as viewed by electron microscopy and 18nm in fresh nerves by X-ray diffraction (Arroyo and Scherer 2000). The myelin sheath is divided into two parts, compact and non-compact myelin, which contains non-overlapping groups of proteins. The bulk of myelin is compact with non-compact myelin found at the paranodes and the oligodendrocyte inner tongue.

There is little or no cytoplasm left between adjacent wraps in myelin. At the lateral margins of every wrap a membrane loop forms containing some cytoplasm known as a paranodal loop. These make up part of the non-compacted myelin and each paranodal loop forms a highly specialised cell junction with the axon called the axoglial apparatus (Boiko and Winckler 2006). The paranodal loops flank the nodes of Ranvier. All these structures contain different molecular components (Arroyo and Scherer 2000).

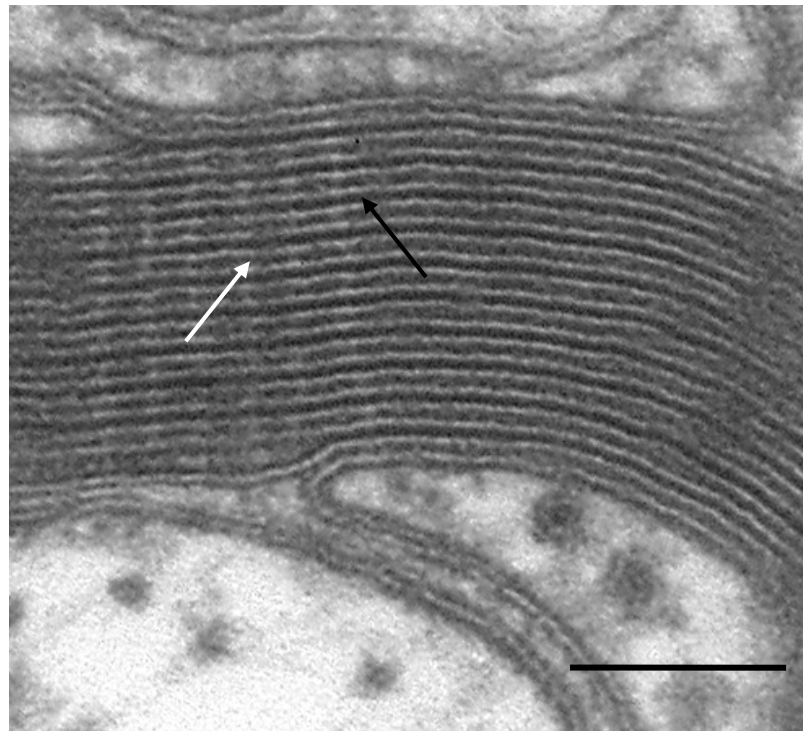
CNS myelin has a distinct structure as well as composition. One of the structural differences between CNS and PNS myelin is that CNS myelin has a radial component, which is a series of radially arranged intralamellar strands that span the sheath normally in a single strand (Arroyo and Scherer 2000). The radial component consists of a series of interlamellar tight junctions containing the protein claudin 11 (also known as oligodendrocyte-specific protein (OSP)); other components of the radial component are MOBP and MBP. Myelin is different from other cell membranes in that it has a high lipid to protein ratio (Figure 2D) (Morell and Norton 1980). This enables myelin to function as an insulator. Although other profiles of the myelin sheath have been observed the most generally accepted theory is that of spiral wrapping by a single cell process whether from an oligodendrocyte or Schwann cell (Hirano and Dembitzer 1967).

Myelin once produced by the oligodendrocyte to ensheath axons is not a stable static membrane. It is constantly renewed and replaced by the cell throughout its life span as are components of myelin. However this process occurs more slowly than for components of

other membranes in the CNS. The half-life of the lipids in myelin can be as long as several months and the same is true for most of the PLP/DM20 and MBP present (Morell and Norton 1980).



A



B

Figure 2. Myelin in wild type mice.

A) Electron micrograph of wild type myelin ensheathing axons. Bar = 2 μ m. **B)** Higher magnification EM of myelin ultrastructure showing the IPL (white arrow) and MDL (black arrow). Bar = 0.05 μ m.

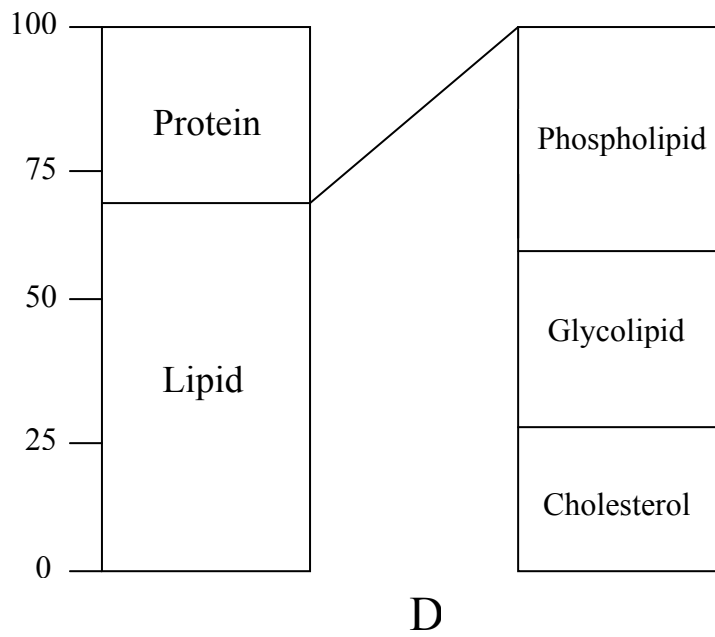
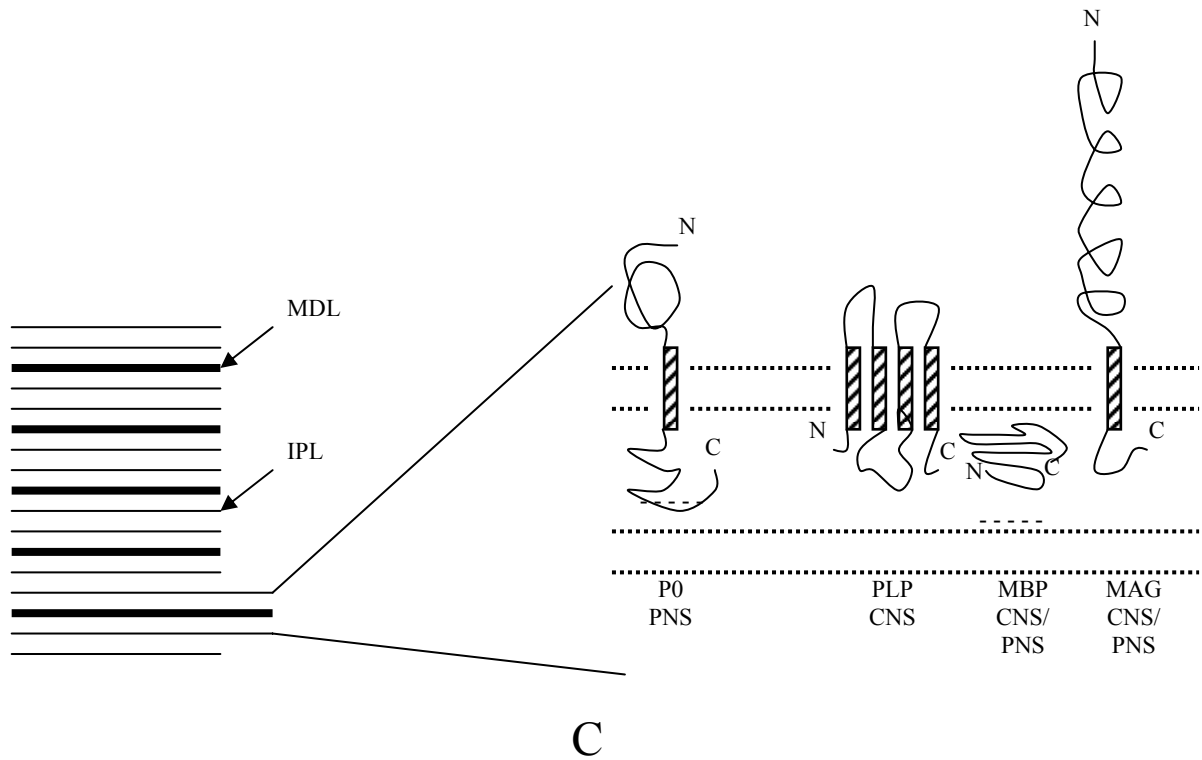


Figure 2 (continued).

C) Diagram of myelin showing MDLs and IPLs, and location of some myelin proteins within these structures. **D)** Diagram showing proportion of protein and lipids in myelin (adapted from Morell and Norton 1980).

1.2.3 Axons

The axon is the main process of neurons and conducts signals away from the cell body. Neurons are typically composed of a soma, or cell body, a dendritic tree and an axon and can vary in size. The majority of vertebrate neurons receive input on the cell body and dendritic tree, and transmit output via the axon. Axons larger than $1\mu\text{m}$ in diameter in mice are ensheathed by myelin. The membrane that forms the surface of the axon, the axolemma, maintains a difference in voltage between the inside and outside of the cell (Morell and Norton 1980). The membrane does this by concentrating potassium ions within the cell and keeping sodium ions outside with the sodium ions only getting into the cell under special circumstances. The nerve impulse or signal is the depolarization of the membrane down the length of the axon due to an influx of sodium ions. This is then followed by a decreased out-flowing of potassium ions restoring the voltage difference.

Axons are wrapped many times by the sheet-like membrane extensions to form the mature internodal myelin sheath. Some internodes can be as long as 1mm in length and are separated from the next by a very short gap of less $1\mu\text{m}$ known as the node of Ranvier (French-Constant *et al.*, 2004). In myelinated axons the membrane is depolarized at a node of Ranvier and it activates the membrane at the next node, thus, jumping along the axon from node to node increasing the speed of the impulse (Morell and Norton 1980). This is called saltatory conduction. Action potentials can reach speeds of more than 100m/s in the fastest fibres (Aldskogius 2005). The action potentials jump from node to node due to the concentration of voltage dependant sodium channels at the node and the high electrical resistance of the myelin sheath.

The node of Ranier has a distribution of highly specialised proteins to allow saltatory conduction to occur. Voltage-dependant Na^+ channels are highly concentrated in the axolemma at the node in both CNS and PNS. Molecules located at the axolemma at the node include ankyrin_G 480/270 kDa, neurofascin and Nr-cell adhesion molecule (Nr-CAM). Neurofascin is essential for the clustering of Na^+ channels at the node (Sherman *et al.*, 2005). Two proteins appear at the node of Ranier before ankyrin_G 480/270 kDa or voltage-dependant Na^+ channels (Arroyo and Scherer 2000). One, an intrinsic membrane protein called Caspr, is located at the axonal paranodal membranes in both the CNS and PNS. A binding site for protein 4.1, which binds the actin cytoskeleton, is contained in the cytoplasmic domain of Caspr (Arroyo and Scherer 2000). Caspr also binds with F3/contactin (Faivre-Sarrailh *et al.*, 2000, Rios *et al.*, 2000). Other specialized proteins are

present at the juxtaparanode, Caspr2, a homologue of Caspr, and Kv1.1/1.2/ β 2 K⁺ channels subunits (reviewed by Schafer and Rasband 2006, Rasband 2006).

Axons are very long and unable to produce the components they need to survive. Therefore, neuron cell bodies produce the majority of the components required and transport them down the length of the axon. A peripheral layer of actin microfilaments is located just beneath the axolemma which supports the axolemma and anchors the cytoskeleton to it. The shape and size of the axon is determined by the neurofilament cytoskeleton. Fast axonal transport mechanisms that move membrane-bound organelles such as mitochondria along the axon are contained within microtubular domains. The fast axonal transport mechanisms have high energy requirements utilising translocators such as kinesin for anterograde transport and dynein for retrograde transport (Edgar *et al.*, 2004). Golgi-derived vesicles are transported anterogradely away from the cell body (perikaryon), lysosomal-derived vesicles are transported retrogradely towards the cell body whereas organelles such as mitochondria move in both directions along the axon.

Although axons are not necessary for oligodendrocyte production they do play a role in regulating and modulating oligodendrocyte numbers (Trapp *et al.*, 2004). In the CNS, the generation of adenosine by the hydrolysis of ATP released from axons inhibits proliferation of OPCs and stimulates their differentiation into premyelinating oligodendrocytes in turn increasing myelination (Stevens *et al.*, 2002). Soluble factors produced and released from neurons in culture affect membrane condensation and co-culturing oligodendrocytes with neurons increases raft clustering in the cells (Fitzner *et al.*, 2006).

1.2.4 Astrocytes

Astrocytes are star shaped glial cells that perform a variety of functions in the CNS. Astrocytes provide physical support to neurons and have some ability to remove debris within the brain. They also provide neurons with some of the chemical factors needed for proper functioning playing a role in providing nourishment to neurons and help control the chemical composition of fluid surrounding neurons; they are an important component of the blood brain barrier. Oligodendrocytes are supplied factors such as PDGF by astrocytes. Volterra and Meldolesi reviewed the changing understanding of the role of astrocytes over the years (2005).

In order to provide physical support for neurons, astrocytes form a matrix to keep them in place. In addition, this matrix serves to isolate synapses from one another. This limits the dispersion of transmitter substances released by terminal buttons; thus aiding in the smooth transmission of neural messages. Astrocytes provide nourishment to neurons by 1) receiving glucose from capillaries 2) breaking the glucose down into lactate (the chemical produced during the first step of glucose metabolism) 3) releasing the lactate into the extra cellular fluid surrounding the neurons. The neurons receive the lactate from the extra cellular fluid and transport it to their mitochondria to use it for energy. In this process astrocytes store a small amount of glycogen, which stays in reserve for times when the metabolic rate of neurons in the area is especially high.

Astrocytes outnumber neurons by 10:1. Astrocytes are generated from two sources, early in development they are formed from elongated precursors that have their cell bodies in or near the ventricular zone and later in development they originate from a distinct set of cells in the subventricular zone (Jessen 2004). They have many radiating processes that interweave in complex ways between neuronal cell bodies and fibres (Jessen 2004). Some processes contact blood vessels and may have a role to play in the controlling the blood-brain barrier which protects the CNS while other processes form cuffs or veils around individual synapses (Jessen 2004). Astrocytes are also involved in the removal of excess neurotransmitters and can help control levels of potassium in the extracellular space. Astrocytes with no GFAP failed to form processes in the presence of neurons *in vitro* (Liedtke *et al.*, 1996). Glial cells were originally viewed as providers of physical and trophic support for neurons in the nervous system. Of the glial cells, astrocytes have been shown to be important in migration, positioning and maintenance of environment for neurons (Liedtke *et al.*, 1996). However, very little is known about the interaction between oligodendrocytes and astrocytes in the CNS and is a matter of ongoing study.

Astrocytes are a potential source of growth factors/mitogens such as Insulin growth factor - 1 (IGF-1) and Leukemia inhibitory factor (LIF). The *IGF-1* gene has been found to be active in areas of demyelination due to drug treatment and localised next to immature oligodendrocytes expressing the IGF-1 receptor (Komoly *et al.*, 1992). Ishibashi and colleagues (2006) reported the release of ATP after action potential firing triggers LIF release from astrocytes. LIF then goes on to promote myelination by mature late-stage MOG- positive oligodendrocytes. The role of astrocytes in promoting myelination in the

CNS has been confirmed by work carried out using 120µm slices of embryonic murine spinal cords cultured on a bed of astrocytes (Thomson *et al.*, 2006).

1.2.5 Microglia

Microglia are the smallest of the glial cells and act as the immune cells of the CNS. They are resident macrophage-like cells that originate from blood monocytes (Jessen 2004). Microglia can act as phagocytes, cleaning up CNS debris and protecting the CNS from invading micro-organisms. Microglia are close cousins of other phagocytic cells including macrophages and dendritic cells. Microglia are derived from myeloid progenitor cells (as are macrophages and dendritic cells) which come from the bone marrow. During embryonic development they migrate to the CNS and differentiate into microglia. They are highly mobile cells that play several roles in protecting the NS (Streit *et al.*, 2004). They are a rich source of cytokines and are thought to play in neurodegenerative disorders such as Multiple Sclerosis (MS), dementia, Alzheimer's and amyotrophic lateral sclerosis. Microglia are part of early component of the inflammatory response in the CNS (Perry, 1994) and there is ongoing debate as to whether they merely respond to damage or actually form part of the pathogenetic mechanism (Block *et al.*, 2007).

1.3 Protein and Lipid content of CNS Myelin

Some of the main proteins and lipids involved in myelination are discussed in this section. Many of the main proteins and lipids in myelin are produced by oligodendrocytes. Martini and Schachner (1997) reviewed glial cell surface molecules including PLP, MAG and MBP and what is known about their functions as elucidated through experiments with null mice.

1.3.1 Myelin proteins

1.3.1.1 PLP/DM20

PLP/DM20 makes up 50% of all myelin protein in the CNS. PLP is 30 kDa while DM20 the smaller isoform is 26 kDa in size. In normal myelin PLP is only incorporated after the compaction of the lamellae has started. PLP/DM20 is made up of four hydrophobic segments of more than 30 amino acids which are linked by shorter hydrophilic sequences with clusters of positively and negatively charged residues. These four hydrophobic segments make up four transmembrane domains. The protein can undergo post-

translational modifications such as acetylation and acylation or covalent linking of fatty acid chains (see [1.5 The *Pip1* Gene: Structure and Function](#)).

1.3.1.2 Myelin Basic Protein (MBP)

Myelin basic protein (MBP) is the component of myelin thought to stabilise the cytoplasmic apposition of oligodendrocyte surface membranes in compact myelin. MBP isoforms are positively charged molecules thought to play a key role in myelin compaction by bringing together cytoplasmic surfaces presumably by electrostatic interactions with the negatively charged lipid bilayer (Jacobs 2005). The nucleotide and resulting amino acid sequence of MBP is highly conserved in mammals. The *Mbp* gene is encoded by 7 exons spanning 32 kb of mouse chromosome 18 situated within a larger transcription unit known as *Golli-MBP* (Campagnoni and Campagnoni 2004). This larger unit spans 105 kb in mouse and 179 kb in humans and contains 3 transcriptional start sites (tss) with tss3 the most active one producing classic MBP. *Golli* (Gene of Oligodendrocyte Lineage) *MBP* has 11 exons in mice and 10 in humans of which the last 7 give rise to classic MBP isoforms.

At least 6 closely related extrinsic membrane proteins are encoded by the *Mbp* gene accounting for 30% of all CNS myelin proteins and 18% of PNS myelin proteins (Lemke 1988). The four isoforms produced through splicing of the transcript, seen in CNS myelin range from 14.0 kDa to 21.5 kDa and are extremely basic (Figure 3). MBP is localised to the MDL of myelin thus confined to the interior of the cell. In most species that produce myelin, the predominant form of MBP is the 18.5 kDa isoform (Zeller *et al.*, 1984). However, in mice and rats two isoforms predominate, the 18.4 kDa and 14 kDa isoforms. Alternative splicing of the exons within the *Mbp* gene leads to the production of the four isoforms seen in myelin (De Ferra *et al.*, 1985, Takahashi *et al.*, 1985). Kamholz *et al.*, (1986) identified three MBP isoforms in humans and found the 18.5 kDa isoform is the major one in man. Expression of the isoforms is different and they are located in different parts of the cell and myelin suggesting various functions.

Myelination in mouse brain occurs from postnatal day 8-10 and continues actively for 7-10 weeks with maximum activity around P18-21. Maximum synthesis of MBP isoforms is seen at peak myelination. The developmental profile of *Mbp* transcripts suggests that the *Mbp* gene is transcriptionally controlled (Cook *et al.*, 1992). The proportion of the MBP isoforms in myelin change as development and myelination continues in the mouse. MBP

mRNA may be transported to its site of incorporation in myelin for translation to avoid non-specific binding of the protein to acidic lipids (Trapp *et al.*, 2004). MBP is a structurally disordered basic protein until post-translational modifications. Post-translational modifications can enhance and regulate its multiple functions (Boggs 2006). It is involved in adhesion of cytosolic membranes of compact myelin and may have a role in interactions with the cytoskeleton and transmission of extracellular signals. It is the one protein that is essential of the formation and maintenance of myelin. Fitzner *et al.*, (2006) propose that MBP is essential for the rearrangement of the plasma membrane of the oligodendrocyte in myelin. The possible multiple functions of classic MBP in CNS myelin are reviewed by Boggs (2006).

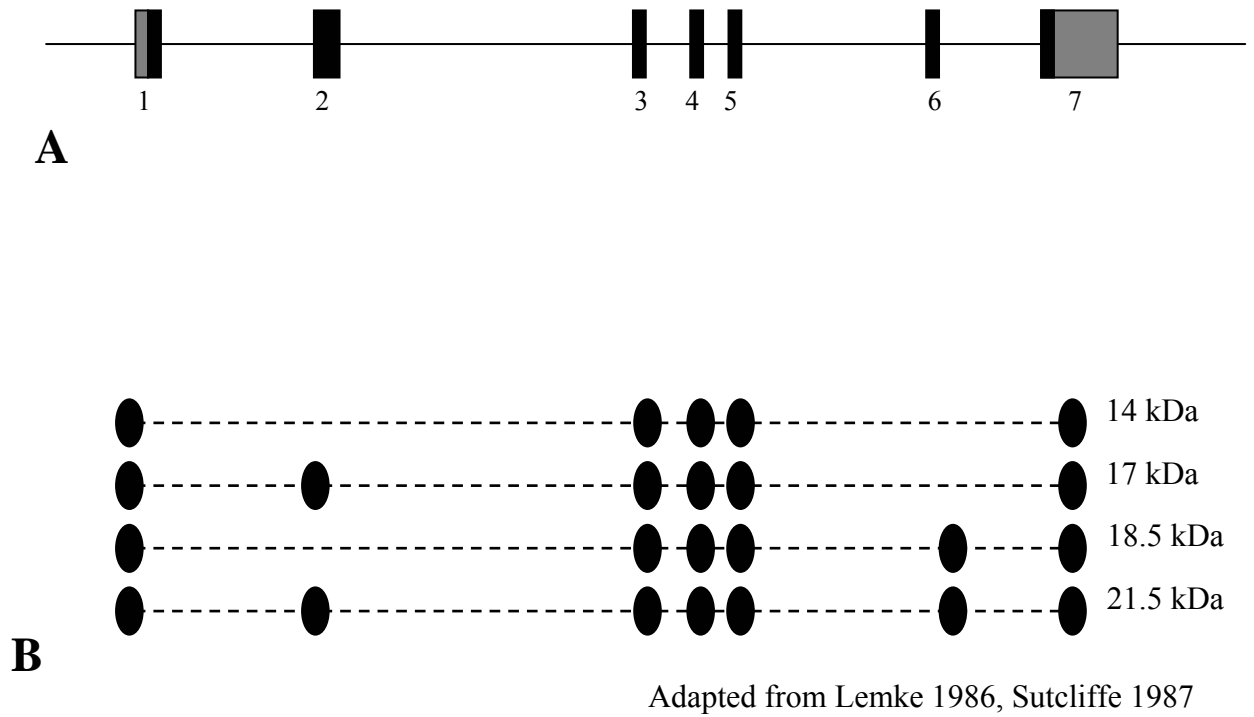


Figure 3. Organisation of *Mbp* gene in mice.

A) The *Mbp* gene containing all 7 exons (not to scale). **B)** The exon composition of the four MBP isoforms produced in myelin.

1.3.1.3 Myelin associated glycoprotein (MAG)

Myelin associated glycoprotein (MAG) was first discovered in 1973 by Quarles and colleagues (Georgiuo *et al.*, 2004). The *MAG* gene is located on human chromosome 19 and mouse chromosome 7 and consists of 13 exons spanning 16 kb. MAG is a heavily glycosylated glycoprotein expressed at low levels in both CNS and PNS myelin around 1% of all myelin proteins (Lemke 1988). The protein is located at the periaxonal margin of the myelin sheath next to the axon (Trapp *et al.*, 1984). This periaxonal space is the 12-14 nm interface between the axon and the innermost myelin layer (Georgiuo *et al.*, 2004). MAG is also present in paranodal loops and in the PNS is a prominent component of Schmidt-Lantermann incisures.

MAG is detected prior to any of the other myelin proteins at the very earliest stages of myelination suggesting a role in the initial axon-glial recognition events that occur before myelination and indicate the path of myelin deposition. Indirect evidence that MAG is an adhesion molecule important for initiation of myelination includes the fact the extracellular part of MAG is made up of five homologous immunoglobulin-like domains and contains the sequence Arg-Gly-Asp, a peptide involved in binding of extracellular matrix adhesion molecules to their receptors (Lemke 1988). The demonstration that *in vitro* MAG facilitates neuron-oligodendrocyte and oligodendrocyte-oligodendrocyte adhesion provides direct evidence for this role (Poltorak *et al.*, 1987). MAG undergoes post-translational modifications which include phosphorylation and glycosylation and shares a transport pathway to myelin with PLP/DM20 (Georgiuo *et al.*, 2004).

Two MAG transcripts, L-MAG (72 kDa) and S-MAG (67 kDa), are produced by alternative splicing of the cytoplasmically disposed C-terminus of MAG. L-MAG knockout mice which still produced S-MAG generated by Fujita *et al.*, (1998) showed CNS myelin abnormalities but not any changes in PNS myelin. L-MAG is found to dominate during early stages of CNS myelination, whereas, in mature myelination L-MAG and S-MAG are found in similar concentrations. S-MAG is preferentially expressed in PNS myelin and late in neuronal development (Lai *et al.*, 1987). During the early stages of myelination L-MAG is enriched in endosomes and therefore could play a role in membrane remodelling (Bo *et al.*, 1995, Trapp *et al.*, 1989a). The large extracellular domain of MAG dominates the extracellular spacing between the membranes in myelin leaving them at 12-14nm. MAG has been implicated in the regulation of neurofilament spacing and axonal calibre in mature myelinated axons (Yin *et al.*, 1998).

1.3.1.4 2',3'-Cyclic Nucleotide 3'-Phosphodiesterase (CNP)

2',3'-Cyclic nucleotide 3'-phosphodiesterase (CNP) hydrolyses 2'3'-nucleotides to nucleoside 2'-phosphate (Braun *et al.*, 2004). The *CNP* gene is located on human chromosome 17 and mouse chromosomes 3 and 11 with the *Cnp1* gene on mouse chromosome 11. Two CNP mRNA species of 2.4 kb and 2.8 kb generated by the presence of alternative translation start sites in the *Cnp1* gene, have been identified in the nervous system resulting in two CNP polypeptides (48 and 46 kDa) (Bernier *et al.*, 1988). CNP is synthesised like MBP on free polysomes, but unlike MBP, not at its site of incorporation into myelin but in the perinuclear regions of the oligodendrocytes (Gillespie *et al.*, 1990). CNP shows a 70% homology across species and properties of the protein suggests a regulatory role in myelination. Post translational modification of the protein by polyisoprenylation, known to confer membrane-binding capabilities on cytoplasmic proteins, hints at the regulatory role too.

The protein is localised to the uncompacted myelin in the CNS and associated with cellular membranes. While the amount of CNP activity correlates with the degree of myelination, its function in the process is unknown. Over the years studies have been carried out to elucidate the role of CNP within the CNS and the myelination process. In one such study using CNP overexpressing mice generated by Gravel *et al.*, (1996) findings highlighted CNP's role in the extension of membranous processes and in influencing the temporal myelination program. Lee *et al.*, (2005) also found that in oligodendrocytes CNP was essential for process outgrowth. Recent studies by Bifulco and colleagues (2002) highlighted a function for CNP in normal microtubule distribution within cells acting as an anchor for tubulin. The hypothesis that oligodendrocytes support axons was backed up by *Cnp1* null mice which developed axonal loss causing a severe neurodegenerative disorder and premature death but did not have any changes to myelin assembly (Lappe-Siefke *et al.*, 2003).

1.3.1.5 Myelin-associated oligodendrocytic basic protein (MOBP)

Myelin-associated oligodendrocytic basic protein (MOBP) is a small highly basic protein which has three isoforms (8.2, 9.7, and 11.7 kDa) due to alternative splicing of the *Mobp* gene on mouse chromosome 9 (Baumann and Pham-Dinh 2001, Montague *et al.*, 2006). In murine myelin they are more abundant than CNP but less so than PLP. The proteins are located in the MDL (Yamamoto *et al.*, 1994, Montague *et al.*, 1997) but their function is

still uncertain as *Mobp* null mice have no obvious phenotype (Yool *et al.*, 2002) although subtle changes in the radial component have been proposed (Yamamoto *et al.*, 1999).

1.3.1.6 Minor proteins

Some of the other proteins involved in the myelination of the CNS include oligodendrocyte-specific protein (OSP, also known as claudin 11), oligodendrocyte-myelin glycoprotein (OMgp), myelin/oligodendrocyte specific protein (MOSP), RIP antigen and NI-35/250 proteins (Baumann and Pham-Dinh 2001).

1.3.2 Other proteins

1.3.2.1 Aspartoacylase (ASPA)

Aspartoacylase (ASPA) is a marker for oligodendrocyte cell bodies as it has been shown that ASPA activity is detectable only in oligodendrocytes in the CNS thus is used as a control to compensate for any differences in oligodendrocyte cell numbers, so all samples for western analysis are normalized for ASPA (Kirmani *et al.*, 2003, Madhavarao *et al.*, 2004). ASPA is known to catalyse deacetylation of *N*-acetylaspartate (NAA), which is a highly abundant nervous system specific amino acid derivative, into acetate and aspartate (Kirmani *et al.*, 2002). Aspartate in the CNS is used for acetyl CoA synthesis and then subsequently the synthesis of fatty acid/lipid required for myelination (Kirmani *et al.*, 2003).

1.3.3 Lipids

Lipids were initially thought to play one of two roles in the body, as repositories of energy in storage fat and as structural components of cell membranes (Taylor *et al.*, 2004). Later more functions were assigned to lipids in cells. In the CNS lipids make up 70% of the dry weight of purified myelin (Morell and Norton 1980). In bulk membrane the main lipids are cholesterol and glycerophospholipids but myelin is composed mainly of cholesterol and galactocerebroside (GalC) and its sulphated derivative sulphatide. The cerebroside in myelin contain long chains which can be as long as 24 carbons and are saturated (Lee 2001). However the galactolipids, galactocerebroside (GalC) and sulphatide account for 30% of all lipids and are the most abundant lipids in CNS myelin (Coetzee *et al.*, 1999). Lipid turnover in mice is dependant on age, the younger the animal the longer the half-life of the lipid (Taylor *et al.*, 2004). As oligodendrocytes, during active myelination, produce huge amounts of myelin membrane per cell per day they must also produce and transport

masses of lipids. During active myelination the concentration of GalC in the brain is directly proportional to myelin accumulation. Mice lacking galactolipids appear to form myelin sheaths with normal periodicity and compaction but animals' deficient in cholesterol show severe hypomyelination (Coetzee *et al.*, 1999, Saher *et al.*, 2002).

Mice lacking both galactolipids and PLP however, have abnormal myelin in that it is poorly compacted but they have relatively normal IPL formation. PLP was shown to interact with cholesterol and galactosylceramide-enriched membrane domains, known as myelin rafts and this association of PLP with lipids in rafts may be critical to proper sorting of the protein ([1.3.3.1 Myelin rafts](#)) (Simons *et al.*, 2000). Simons and colleagues (2002) went on to show the accumulation of PLP, cholesterol and other raft components in late endosomes/lysosomes (LE/Ls) at the perinuclear region in BHK cells (hamster fibroblast line) and oligodendrocyte cultures and transgenic mice overexpressing PLP. As import of cholesterol is poor in the brain oligodendrocytes produce their own through the same pathway as PLP, the ER/Golgi apparatus.

Cellular mechanisms in oligodendrocytes ensure cholesterol levels are kept low in late endosomes (LEs). Any accumulation of cholesterol by co-transport with PLP into these organelles is an obvious change. Mutant PLP/DM20 with either the *rumpshaker* (*rsh*) or *msd* mutation has a perturbed relationship with lipids and myelin rafts impairing the vital cholesterol binding. Both *rsh*-PLP and *msd*-PLP have impaired cholesterol binding and lipid raft association (Kramer-Albers *et al.*, 2006). They suggest this impairment of PLP and lipid association contributes to disease phenotype in humans.

1.3.3.1 Myelin rafts

Rafts are liquid-ordered domains that are more tightly packed than the surrounding lipid bilayer (Rajendran and Simons 2005). This is due to the saturated hydrocarbon chains in raft sphingolipids and phospholipids. As rafts are dynamic, both proteins and lipids can move in and out of raft domains; however, this movement and the rafts themselves can be too small to visualise. Rafts in biological membranes are thought to be microdomains with a lipid structure like the liquid ordered (L_o) phase surrounded by liquid disordered (L_d) phase membrane (Hancock 2006). It is thought rafts modulate the biological function of proteins and molecules that are associated with them (reviewed by Gielen *et al.*, 2006). Proteins associated with lipid rafts can be identified by their resistance to detergent extraction and PLP was recovered from detergent resistant membrane fractions.

Compact myelin represents the bulk of the sheath and contains myelin rafts composed of proteins and lipids specific to the membrane (Kramer *et al.*, 2001). There are several mechanisms by which oligodendrocytes could transport components of myelin to produce the final myelin sheath, directed transport, transcytosis or endosomal sorting, regulated exocytosis or myelin rafts. The sorting of PLP/DM20 with lipids in fluid myelin rafts supports the final method of transport although they may not all be mutually exclusive (Simons *et al.*, 2000). However, none of the other myelin proteins co-localise with PLP/DM20 (Kramer *et al.*, 2001).

1.4 The *Plp1* Gene: Structure and Function

The structure and function of the human and mouse *PLP1* genes are highly homologous therefore many details in this section relate to the human *PLP1* gene. Where there are notable differences these are mentioned.

1.4.1 The *PLP1* Gene

PLP was first discovered in 1951 by Folch and Lees in bovine white matter (Lerner *et al.*, 1973). The *PLP1* gene in humans consists of 7 exons spanning 17kb at a single locus (Macklin *et al.*, 1987) mapping to Xq21.33-22 in humans next to glycine receptor, alpha 4 subunit (*Glr4*) gene. Exon 1 of the gene contains 5' non-coding region, the codon for initial methionine and the first base of next codon (glycine) which due to cleavage of the methionine will become the amino-terminal of the mature *PLP1* gene products. Exon 2 encodes amino acids 1-63. The 7th and last exon encodes the C terminus and 3 polyadenylation sites. The coding sequence of the *PLP1* gene is highly conserved with 100% identity between human, mouse and rat sequences (Wight *et al.*, 1997). There is also a high degree of conservation in the 5' and 3' un-translated regions among species (Macklin *et al.*, 1987). However, in the mouse the *Plp1* gene contains an extra exon 1.1 within intron 1 located 122 base pairs downstream from exon 1 (Figure 4A). These produce splice variants that are expressed in neuronal subpopulations known as soma-restricted PLP (sr-PLP) and soma-restricted DM20 (sr-DM20) (Figure 4B) (Bongarzone *et al.*, 1999). Splicing of the 3rd exon in humans and mice at the mRNA level leads to two protein isoforms, PLP and DM20 (Nave *et al.*, 1987).

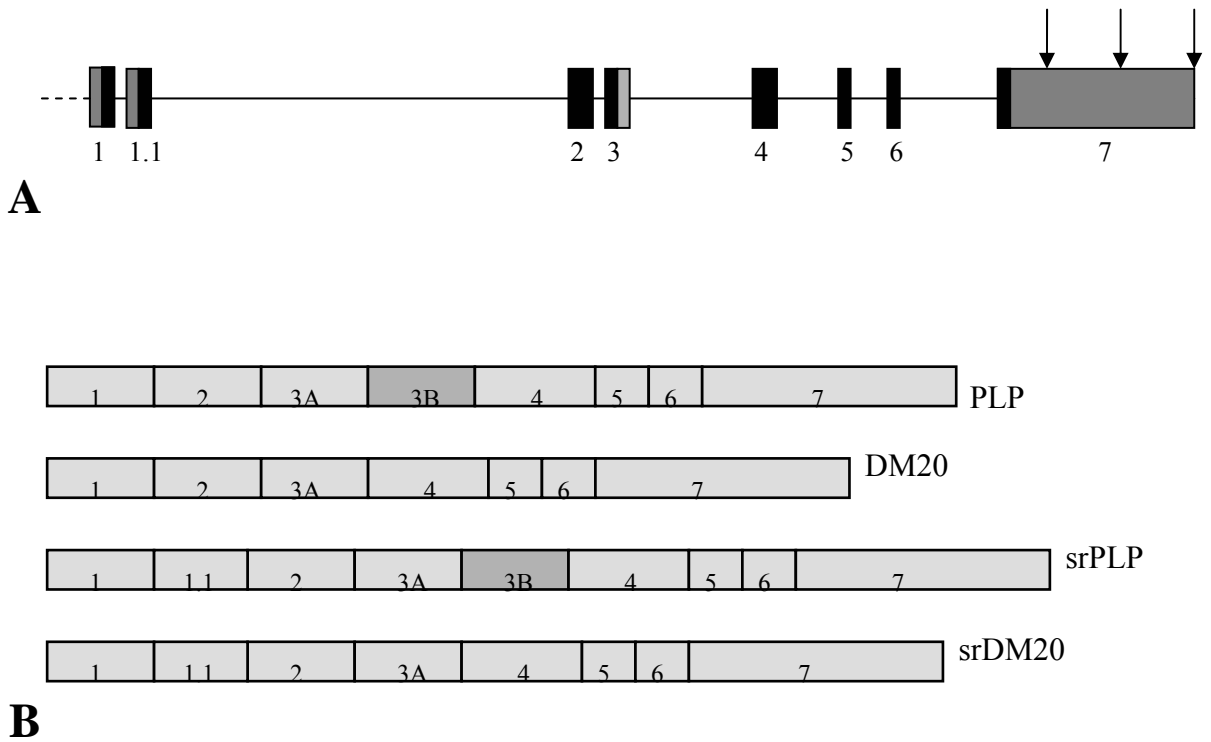


Figure 4. The murine *Plp1* gene.

A) The murine *Plp1* gene with all exons (light grey section of exon 3 is alternatively spliced exon 3B); arrows depict the three polyadenylation sites (not to scale). **B)** The four isoforms produced by the *Plp1* gene through alternative splicing, PLP and DM20 and soma-restricted (sr) PLP and DM20.

1.4.2 Evolution and Conservation of the *Plp1* gene

1.4.2.1 Evolution of the *Plp1* gene

The evolution of early vertebrates led to the requirement of insulation of the axons for the speedy conduction of electrical impulses. P0 was the initial structural protein of the CNS along with the DM20 protein which was expressed by the ancestral vertebrate *Plp1* gene in cartilaginous fish as early as 440 million years ago (Yoshida and Colman 1996, Hudson 2004, Yin *et al.*, 2006). The PLP protein appeared around 400 million years ago after the divergence of bony fish (Yoshida and Colman 1996). Mammals, birds and reptiles all express both PLP and DM20 and in these species the proteins have developed to perform different functions in CNS myelin. The change from P0 to PLP as the main structural protein in CNS myelin also provides a neuroprotective function as seen in transgenic mice with P0 expression in place of *Plp1* expression (Yin *et al.*, 2006). These animals have myelin in the CNS with a highly regular and compact PNS-like structure but developed degeneration of myelinated axons and their lifespan was reduced by 50% (Yin *et al.*, 2006). The slow evolution of the *Plp1* gene over the past 80 million years implies the intense selective pressure that led to the modern mammalian PLP and DM20 proteins.

1.4.2.2 Conservation of the *Plp1* gene

A remarkable level of sequence conservation between species at both the amino acid and nucleotide levels in the *Plp1* gene restricts the further reshaping of PLP and DM20. Amino acid sequence homology achieves 100% in rodents, >99% in the dog and >97% in the cow when compared to PLP and DM20 sequence in man (Milner *et al.*, 1985, Macklin *et al.*, 1987). Any nucleotide changes that are tolerated tend to be silent. Any other nucleotide changes lead to disease in man and animals as evidenced by PMD/SPG2 in humans and *rumpshaker*, *jimpy* and *shaking pup* disorders in animals.

This conservation also extends to the non-coding and non-transcribed regions of the *Plp1* gene. There is greater than 95% identity at the nucleotide level of the coding regions and at least 90% conservation between man and mouse for the 5' and 3' UTRs (Wight and Dobretsova 2004). The homology of the entire 3'UTR between mouse and rat is greater than 90% and some regions within the 3'UTR have almost 100% homology (Macklin *et al.*, 1987). The proximal region of the 5'UTR is one of the most highly conserved areas, at 100% between rodents and man, of the *Plp1* gene (Macklin *et al.*, 1987). Of all the introns, intron 3 is the most highly conserved with 80% homology between man and mouse (Wight

and Dobretsova 2004). This intron is important in the splicing of exon 3B to form DM20 (Nave *et al.*, 1987).

This level of conservation in non-coding regions is almost unique to the *Plp1* gene. Other genes have a lower homology of sequence between species in non-coding regions. Another X chromosome gene, hypoxanthine phosphoribosyltransferase (*Hprt*) shows 74% homology between the human and mouse genes which is considered high for the 3'UTR. The high level of conservation within the non-coding and non-transcribed regions of the *Plp1* gene is highly unusual and may be of more interest than the conservation of the amino acid sequence (Macklin *et al.*, 1987). This high level of conservation could indicate that the *Plp1* gene is under tight regulatory control that may be vital for the function of the gene. This suggests mutations in the gene whether in the coding or non-coding regions are not tolerated. The almost complete conservation of the transcription initiation sites and the adjacent 5' flanking sequence of the *Plp1* gene supports this hypothesis (Macklin *et al.*, 1987).

1.4.2.3 The *DM* gene family

PLP is part of a large proteolipid protein gene family with sequence homology, the *lipophilin/DM* family which may encode pore-forming polypeptides (Gow 1997). There are two other members of the $DM\alpha/DM20/PLP$ family, $DM\beta/M6A/EMA$ and $DM\gamma/M6B/Rhombex\ 29$ and these have been isolated from fish, amphibians and mammals (Hudson *et al.*, 2004). These gene products are mainly located in the CNS and include the glycoprotein-encoding genes *DM α* , *DM β* and *DM γ* in bony fish (Kitagawa *et al.*, 1993) and *M6A* and *M6B* in mammals (Yan *et al.*, 1993).

The main features of this family are four transmembrane (TM) domains, a large extracellular loop between TM domains 3 and 4 and an intracellular part between TM domains 2 and 3 (Figure 5). All the members of this protein family share a remarkable level of amino acid conservation in the four transmembrane domains and the four cysteine residues present in PLP and DM20 that are for fatty acid attachment are also conserved (Weimbs and Stoffel 1992). Expression of these family members does however differ with $DM\alpha/DM20/PLP$ the main structural component of myelin in the CNS. The neuronal components of the family are $DM\beta/M6A/EMA$, whereas $DM\gamma/M6B/Rhombex\ 29$ are expressed in both cell types, neurons and myelinating glia (Hudson 2004).

1.4.3 Expression of *Plp1* gene

Plp and *Dm20* cDNAs have been isolated from human, bovine, canine, rodents as well as chickens, zebra finch, trout and zebrafish (Wight and Dobretsova 2004). The *Plp1* gene is primarily expressed in oligodendrocytes, although it is transcribed in low levels in Schwann cells in the PNS, cardiac myocytes and foetal thymus and spleen (Puckett *et al.*, 1987, Campagnoni *et al.*, 1992, Pribyl *et al.*, 1996). As the gene is so highly conserved across species it is likely regulation of the gene is equally well maintained. There are two closely spaced (30bp) transcriptional initiation sites in the *Plp1* gene beginning 147-160 bases upstream of ATG initiator methionine. Homology is strong between human and mouse for this region suggesting functional constraints on this region (Hudson 2004). The two transcriptional initiation sites are used differentially during development, in different tissues and following injury. Both sites are utilised in the CNS but the downstream site is mainly utilised in the PNS. At peak myelination, most transcription is initiated from upstream site. Promoter usage is known to affect splice site selection. During early myelination downstream site is utilised and DM20 is predominantly expressed. This is also the case in Schwann cells where DM20 is mainly expressed and the downstream site is utilised (Scherer *et al.*, 1992). The inclusion of exon 1.1 in mice produces two different proteins, srPLP and srDM20, soma-restricted isoforms which are not targeted to compact myelin (Figure 4B) (Bongarzone *et al.*, 1999). Their function is still not known.

1.4.3.1 Temporal and spatial control of expression of *Plp1* gene

The intronic sequence between exons 1.1 and 2 in mice is the largest of the *Plp1* gene and possibly has important regulatory functions, similarly the intron between exon 1 and 2 in other species (Wight and Dobretsova, 1997). Maintenance of *Plp1* gene regulation control is preserved across species lines. The high levels of conservation in non-coding regions in the *Plp1* gene suggest these have a role in gene regulation and/or expression. In oligodendrocytes the gene is temporally regulated and there is a dramatic surge in its expression during active myelination in the CNS although PLP is present in pre-myelinating oligodendrocytes. PLP becomes the predominant isoform as development progresses. Deletion-transfection studies by Dobretsova and Wight (1999) using *Plp-lac Z* fusion genes suggested that intron 1 contains an enhancer element involved in the increase in expression. Experiments characterised this region as autosilencer/enhancer (ASE) (Li *et al.*, 2002b). The functional core of the ASE, refined to positions 1093-1117 of intron 1, contains target sites that are recognised by a number of proteins from a large superfamily

of basic leucine zipper (bZIP) transcription factors. These can function as positive or negative regulators of expression and may be critical in the assembly of a nucleoprotein complex required for the dramatic upswing in expression mentioned above (Dobretsova *et al.*, 2004).

Along with temporal control, intron 1 plays a role in the spatial control of *Plp1* gene expression. Deletion-transfection experiments with constructs containing the 5' UTR, promoter and/or intron 1 identified intron 1 as the essential region for spatial control (Li *et al.*, 2002b). Intron 1 confers this control through a transcription repression mechanism in non-expressing cell types via a negative regulatory element near the 3' end of the intron. This element is active in mouse liver cells but not in glial cells whereas the opposite is true for the ASE, which is inactive in +/- Li liver cells (Li *et al.*, 2002a)

1.4.4 Regulation of the *Plp1* gene

There are three polyadenylation sites in the *Plp1* gene leading to three major classes of mRNA, 1.6, 2.4 and 3.2 kb (Gardinier *et al.*, 1986, 1990). Both *Plp* and *Dm20* transcripts are present in the three mRNA classes. The most abundant *Plp* mRNA is 3.2 kb and it contains all 5 regulatory elements situated within the 3'UTR. The main area of control of the *Plp1* and also the *Mbp* gene is at transcription. mRNA synthesis of the two genes mirrors steady state transcript levels and protein levels throughout myelinogenesis. The molecular basis for transcriptional control includes *trans*-acting regulatory elements and their *cis*-acting enhancer/promoter elements (Hudson 1990). Although oligodendrocytes do produce myelin transcripts in the absence of neurons, these transcript levels increase 4 fold in the presence of neurons (Macklin *et al.*, 1986).

Findings, such as partial rescue of dysmyelination by the insertion of both *Plp* and *Dm20* only transgenes suggests both isoforms are required for oligodendrocyte maturation (Nadon *et al.*, 1997). The levels of expression of the two transgenes were however; lower than levels of wild type PLP and DM20 observed in wild type mice suggesting the endogenous *Plp1* gene had an effect on expression of the transgenes (Nadon *et al.*, 1997). The discovery that overexpression of 3' UTR of the *Plp1* gene caused down regulation of the endogenous *Plp1* gene mRNA showed transgenes also have an effect on expression and regulation of PLP/DM20 in oligodendrocytes in culture and in animals (Mallon and Macklin 2002).

1.4.5 Splicing of the *Plp1* gene

Alternative splicing of the *Plp1* gene precursor mRNA (pre-mRNA) leads to two mRNAs producing PLP (30kDa) and the smaller isoform DM20 (26 kDa) (Nave *et al.*, 1987). Alternative 5' splice site selection is utilised in pre-mRNA splicing within exon 3 splicing out exon 3B to produce a transcript with a 105bp deletion resulting in a loss of 35 amino acids from Val-116 to Lys-150 (Nave *et al.*, 1987). The part of PLP absent in DM20 is highly hydrophilic thus making DM20 more hydrophobic than PLP.

The splicing of exon 3 is the rate-limiting step in *Plp/Dm20* transcript synthesis. Significant levels of pre-mRNA were found to contain intron 3 (Vouyiouklis *et al.*, 2000). Of all the introns, intron 3 is the most highly conserved and disrupting intron 3 selectively reduces *Plp* mRNA levels. In studies by Hobson *et al.*, (2002) deletion of nucleotides +28-+46 within intron 3 led to disablement of *Plp* splicing and a late onset, mild neurological phenotype similar to PMD characterised by dysmyelination and axonal loss. This region is a purine rich sequence located near the intron's 5' end which can act as a splicing enhancer and is required for efficient PLP-specific splice site selection in oligodendrocytes but not useful in non-glial cells (Hobson *et al.*, 2002).

1.4.6 Translation and post-translational modification of PLP/DM20 protein

1.4.6.1 Translation and post-translational modification

Both PLP and DM20 are modified with long chain fatty acids. Palmitate, oleic acid and stearate, all acyl moieties attach to PLP via thioester bonds to cysteine residues 5, 6, 9, 108, 138 and 140 (Weimbs and Stoffel 1992). PLP has six sites whereas there are only four sites in DM20 as Cys138 and Cys140 are not present in this isoform. Bizzozero and colleagues (2002) showed that the majority of PLP and DM20 in CNS myelin is fully acylated using mass spectrometry. Palmitoylation deficient mutants of PLP highlight the necessity of palmitoylation for the targeting of PLP to myelin-like-membranes (Schneider *et al.*, 2005).

1.4.6.2 PLP and DM20 protein topology

Of all the models proposed for the topology of PLP, the one put forward by Popot *et al.*, (1991) is the most widely accepted (Figure 5). As the DM20 isoform lacks amino acids

116-150, it is more hydrophobic than PLP and therefore its topology may be different which could indicate varying roles for the two *Plp1* isoforms.

1.4.7 Proposed functions of the *Plp1* gene

PLP is an intrinsic protein which is responsible for the stabilising of the apposition of extracellular surfaces of the plasma membranes of oligodendrocytes (Boison *et al.*, 1995) (Klugmann *et al.*, 1997). There is a structural role for PLP ensuring the regularity of the IPL but there may also be a role in oligodendrocyte/axon communication. The axon appears to require ongoing interaction with glial cells for its normal development and also continued maintenance after myelination. Null mice develop normally and assemble compact myelin ensheathing both small and large calibre axons (Klugmann *et al.*, 1997). However, from 6-8 weeks onwards, these mice develop increasing numbers of focal axonal swellings which contain organelles throughout the CNS (Griffiths *et al.*, 1998). The myelin sheath was eventually lost around larger swellings. These axonal swellings are related to the loss of PLP/DM20 in the null mice supporting a function for the proteins in oligodendrocyte/axon communication and interactions. Both retrograde and anterograde fast axonal transport along the length of the axon shows a progressive impairment in null mice (Edgar *et al.*, 2004). This supporting function of the oligodendrocyte and possibly PLP/DM20 is reviewed by Edgar and Garbern (2004).

DM20 is expressed in a wide range of embryonic and adult tissues independent to myelination. A *Dm20* only transgene constructed to contain the “shaking pup” mutation conferred embryonic lethality to the recipient animals suggesting a role in the function of many cell types (Nadon *et al.*, 1997). When *Plp* or *Dm20* only transgenes were introduced into *jp* mice, PLP incorporated into PNS compact myelin whereas DM20 was retained in the cytoplasmic regions of the Schwann cells but the periodicity of the myelin did not change (Anderson *et al.*, 1997). It is possible a signal is contained in the part of the protein present in PLP but absent from DM20. Yamada *et al.*, (1999) proposed function for PLP/DM20 early in CNS development. A portion of PLP/DM20 was found to be secreted into medium *in vitro* and increased the number of GalC- and GFAP-positive cells in culture. This activity could be mimicked by a synthetic peptide corresponding to PLP amino acids (aa) 215-232 (Yamada *et al.*, 1999). However, the exact function, cells stimulated and pathway involved in the activity of this portion of PLP/DM20 is still unclear.

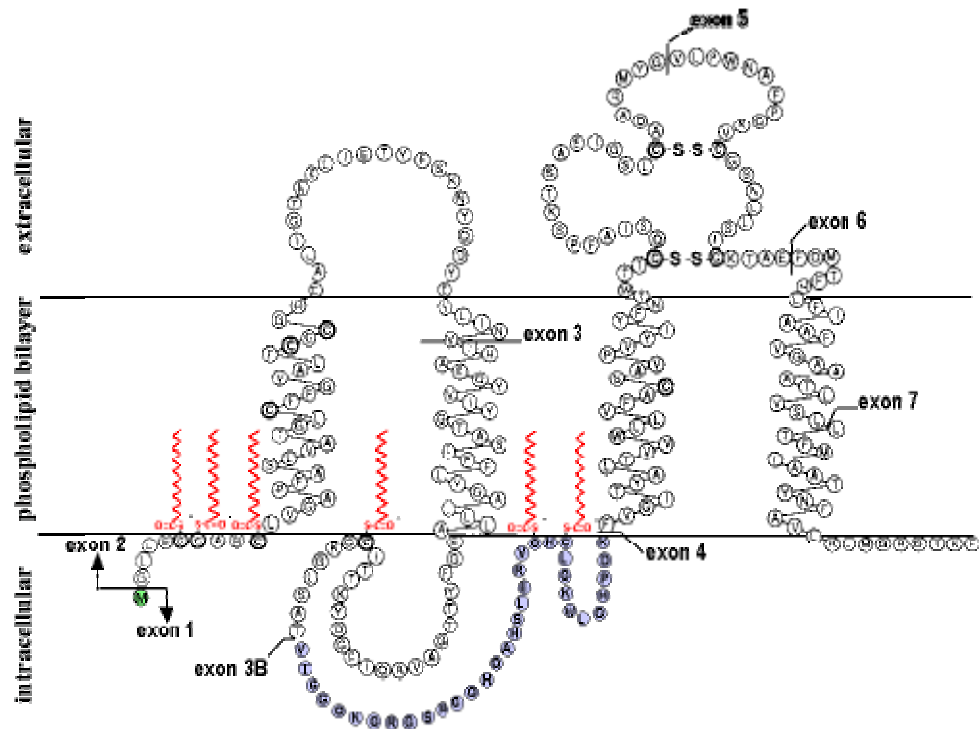


Figure 5. Proposed topology of the PLP isoforms.

Shows each exon, the exon 3B in blue missing from DM20, the six acylated cysteine residues (red zigzag lines) located at the cytoplasmic membrane surface and the two disulfide bridges in the hydrophilic loop connecting TMD III and TMD IV. (Yool 2000, Weimbs and Stoffel, 1992).

1.4.8 Protein dynamics

Niemann *et al.*, (1999) highlighted the necessity of maintaining a steady balance of myelin synthesis and turnover to prevent demyelination in a mature myelin sheath. The synthesis and degradation of PLP/DM20, the major protein of myelin can be studied at the culture and brain slice level.

1.4.8.1 Synthesis

The predicted site of PLP/DM20 synthesis was the RER and using intracranial injections of ³⁵S-methionine, PLP was initially observed in the rough microsomal membrane fraction which contains the RER. More specific investigations found PLP/DM20 is synthesised in bound polysomes at the RER (Nussbaum and Roussel 1983). After synthesis in the RER and prior to transport to myelin PLP/DM20 is packaged and modified in the Golgi apparatus (Nussbaum and Roussel 1983). Current knowledge is that PLP/DM20 is translated on the ER and modified in the Golgi apparatus before transportation to the cell surface for incorporation into compact myelin as are lipids

Using techniques such as protease domain protection assays, immunocytochemical epitope mapping and glycosylation scanning, the orientation of PLP/DM20 in the ER and plasma membrane was elucidated. Wahle and Stoffel (1998) proposed that only PLP/DM20 with the correct topology of both the N and C termini on the cytoplasmic face is transported to the cell surface. The synthesis of *rumpshaker* PLP and DM20 occurs at a rate comparable to wild type PLP and DM20 synthesis. McLaughlin and colleagues (2006) showed that the misfolded *rumpshaker* PLP/DM20 can be transported to the cell surface in cultured oligodendrocytes but to a lesser extent than wild type PLP/DM20.

1.4.8.2 Degradation

The concept of protein turnover is fairly new being barely 60 years old as originally proteins were thought to be stable. Rodulf Scheonheimer challenged this in 1942 and showed proteins are continuously synthesised and degraded. Proteins are degraded at different rates, giving them varying half-lives. Housekeeping proteins have a long half-life while proteins involved in events such as development or cell cycle are likely to have short half-lives. There are two major systems for protein turnover in eukaryotic cells, the lysosome and proteasome. Originally the lysosome, first discovered in 1953, was thought to be the main site of protein degradation. The lysosome carries out degradation by

microautophagy, a process where a membrane-bound compartment containing cellular proteins fuses with a lysosome resulting in digestion of proteins (Ciechanover, 2005). However, this is a rather non-selective method of degradation and does not fit with the varying protein half-lives observed. Lysosomal inhibitors further elucidated the role of the lysosomes in degradation highlighting many proteins not turned over by this method.

The discovery of the proteasome in 1986 led to the advancement of the investigation into degradation. The majority of proteins whether they are misfolded, unfolded and in excess are hydrolysed via the ATP-dependant proteasome pathway. ER-associated proteins, short-lived proteins such as p53, cyclins and activating transcription factor 3 (ATF3) and long-lived proteins are also degraded via the proteasome (Lee and Goldberg 1998).

1.4.8.2.1 Proteasome mediated degradation

The 20S proteasome is a cylinder or barrel shaped protein core which can assemble with other proteins complexes to form the 26S proteasome complex and is involved in the degradation of proteins in eukaryotes and certain archaeobacteria (Peters, 1994). The proteasome in mammalian cells accounts for 1% of all cell proteins (Lee and Goldberg 1998) and is located mainly in the cytosol of cells (Nandi *et al.*, 2006). It is involved in the degradation of short-lived proteins such as transcription factors, tumour suppressors and rate limiting enzymes and also in the degradation of long-lived proteins too. Proteins labelled by a small (76 residues) heat stable, highly conserved protein ubiquitin, and are preferentially degraded by the proteasome. (Ciechanover 2005, Von Mitecz 2006). Not all proteins are ubiquitinated as the proteasome has a role in ubiquitin independent degradation. The ubiquitin-proteasome system is involved in many biological processes such as regulation of cell cycle, immune response, protein misfolding, and disease progression (Nandi *et al.*, 2006). Previously, it was assumed that only lysosomes were involved in turnover of long lived proteins. However, by using proteasome inhibitors such as MG132, a peptide aldehyde, which is a substrate analogue and potent transition-state inhibitor of chymotrypsin-like activity of the proteasome, 80-90% of protein degradation was blocked thus confirming the involvement of the proteasome (Lee and Goldberg 1998). Cell viability and growth was not generally affected for 10-20 hrs after exposure to these inhibitors.

Accumulation of unfolded or misfolded protein in the ER can trigger the unfolded protein response (UPR). BiP ([1.4.8.2.1 BiP \(GRP78\)](#)) has been identified as the master regulator of

this process and X-box DNA-binding protein 1 (XBP1) ([1.4.8.2.2 X-box DNA-binding protein 1 \(XBP1\)](#)) can participate either directly or indirectly in this process too (Shang 2005). The misfolding of PLP/DM20 due to mutations such as *rumpshaker* can lead to the activation of the UPR as evidenced by McLaughlin and co-workers (2007). Southwood and colleagues (2002) presented data showing UPR activation in animals with *Plp1* coding mutations but there was no activation of the UPR in transgenic mice that had extra copies of the wild type *Plp1* gene. This demonstrates that the UPR has the potential to modulate PMD disease severity dependant of the mutation involved. Turnover of the mutant PLP/DM20 protein was increased when compared with wild type PLP/DM20 with *msd* PLP/DM20 degraded faster than *rumpshaker* PLP/DM20 (Kramer-Albers *et al.*, 2006). The rate of degradation of PLP/DM20 appears to be dependant on the mutation in the *Plp1* gene with the mutation that causes the most severe disease phenotype (*msd*) the fastest degraded.

1.4.8.2.2 BiP (GRP78)

BiP also known as glucose regulated protein 78 (GRP78 (78kDa)) an ER chaperone protein, is a peptide-dependant ATPase and member of the heat shock 70 protein family, that binds transiently to newly synthesised proteins translocated into the ER and more stably to misfolded, unassembled or unglycosylated proteins (Zhang and Kaufman 2004). It has also been implicated in calcium sequestration in the ER. When the cells are subjected to ER stress, in particular the depletion of stored calcium and/or the accumulation of abnormal proteins, the rate of transcription of *grp78* is enhanced (Zhang and Kaufman 2004).

1.4.8.2.3 X-box DNA-binding protein 1 (XBP1)

Xbp1 mRNA splicing is initiated by release of BiP from *Irelp* upon accumulation of unfolded protein in the ER. Spliced *Xbp1s* mRNA encodes a potent transcription factor which binds to consensus sequences of many UPR target proteins (Shang 2005). The splicing event converts a 267 amino acid *Xbp1u* encoded by unspliced *Xbp1* (U) mRNA to a 371 amino acid *Xbp1(S)* encoded by the spliced product (Lee *et al.*, 2003). *Xbp1s* is then translocated to the nucleus where it binds its targets, chaperone genes inducing their transcription. The unspliced *Xbp1u* can act as a negative regulator of the spliced form XBP-1(S) during the recovery phase of ER stress (Yoshida *et al.*, 2006).

1.4.8.2.4 Lysosome-Associated Membrane Protein 1 (LAMP-1)

Lysosome-Associated Membrane Protein 1 (LAMP-1) is one of the major lysosomal membrane glycoproteins along with the structurally related LAMP-2. Both LAMP-1 and LAMP-2, which are highly glycosylated, contribute 50% of protein in of the lysosomal membrane (Eskelinen 2006). The lysosomal membrane itself is responsible for the acidification of the interior of the organelle, sequestration of active lysosomal enzymes, transport of degradation products from the lumen to the cytoplasm and regulation of fusion and fission events between lysosomes and other organelles (Andrejewski *et al.*, 1999). The *Lamp-1* gene is expressed ubiquitously encoding a polypeptide of 382 amino acids corresponding to 42 kDa. However, the final product after *N*- and *O*-glycosylation is 92 kDa (Andrejewski *et al.*, 1999). Staining with anti-LAMP1 antibody labels up all the lysosomes within cells.

1.5 *PLP1* gene mutations and disease

1.5.1 *PLP1* gene-related disorders in man

PMD is the main disease focus of this thesis. It is an inherited dysmyelinating disorder caused by mutations in the *PLP1* gene on the X chromosome. MS is the most well known demyelinating disorder associated with oligodendrocyte cell loss in man and is thought to involve an autoimmune response to a myelin protein such as MBP.

1.5.1.1 Pelizaeus-Merzbacher disease

Pelizaeus-Merzbacher disease (PMD) (OMIM 312080) is an X-linked dysmyelinating disorder of the CNS caused by mutations in the *PLP1* gene in humans. PMD is considered a leukodystrophy with a variable clinical and neuropathological phenotype (Koeppen 2005). In Germany the incidence of the disorder is low accounting for 6.5% of all leukodystrophies (Heim *et al.*, 1997) and this is probably similar elsewhere. The disorder is characterized clinically by nystagmus, delayed psychomotor development, spasticity, cerebellar ataxia, optic atrophy, laryngeal stridor, seizures and mental deterioration (Inoue, 2005).

1.5.1.1.1 History of PMD

Pelizaeus first described PMD in meticulous detail in 1885 as a clinical entity in five of his patients from one family. He observed all the patients were males and sons of healthy sisters thus identifying it as an X-linked disorder (Koeppen 2005). Merzbacher performed

the first autopsy study on a patient in 1910 confirming it as a disorder of the white matter of the CNS.

A marked variation in severity of symptoms of PMD was noted in patients leading to classification of the types of PMD in the later half of the last century (Renier et al., 1981). These include the most common, classic PMD with an onset of within the first 5 years and death in 3rd to 7th decade of life. Congenital or connatal PMD is the severest form with onset from birth and death in childhood to 3rd decade. The mildest form of PMD merges with X-linked SPG2 in regards to phenotype (Hudson *et al.*, 2004). The link between PMD and the *PLP1* gene was made in 1964 by Zeman and colleagues.

1.5.1.1.2 *Symptoms of PMD*

The connatal form begins in infancy as early as the eighth day and usually no later than the third month and is progressive so that the victim may survive to middle age. Initial symptoms are hypotonia (decreased muscle tone), respiratory distress, stridor (high pitched sound from upper airway), nystagmus (involuntary eye movement), and occasional seizures. The patients go onto develop severe spasticity with very little voluntary movement and never walk (Hudson *et al.*, 2004).

Patients suffering from classic PMD develop symptoms as early as the first year of life. Symptoms include but are not exclusive to nystagmus, hypotonia, weakness of lower limbs and head titubation. Muscle tone decreases throughout infancy progressing to spasticity later in childhood. The patients develop spastic quadriparesis which is worse in the lower limbs than upper (Hudson *et al.*, 2004). Axonal loss was seen in the white matter of the centrum semiovale in a patient whose mutation was a duplication of the *PLP1* gene (Koeppen and Robitaille 2002). Many of the patients survive until they are in their 50s. The mildest form of PMD is very similar to SPG2 ([1.5.1.2 X-Linked Spastic Paraplegia Type 2](#)).

1.5.1.1.3 *Clinically affected Females*

As PMD is a recessive X-linked disorder it mainly affects males with females as carriers of the mutation. However the incidence of PMD in females is higher than the incidence of Duchenne Muscular dystrophy (DM), which is also a recessive X-linked disorder. Females who carry duplication of the *PLP1* gene have heavily skewed X-inactivation in favour of the normal X chromosome inactivating the duplicated X chromosome. Therefore these

females are asymptomatic whereas, females carrying a copy of the *PLP1* gene with point mutations are unlikely to undergo any skewing thus 50% of cells will be expressing the mutant *PLP1* gene (Woodward *et al.*, 2000). Oligodendrocytes expressing a mild phenotype survive; thus, females go onto develop late onset neurological symptoms.

1.5.1.2 X-Linked Spastic Paraplegia Type 2

X-linked spastic paraplegia 2 (SPG2) is a rare disorder that occurs in two clinically distinct forms in humans. The mild or pure spastic form is characterised by spasticity of the lower limbs with normal mental function (Hudson *et al.*, 2004). Most cases reported take on a more complicated phenotype of spasticity, cerebellar ataxia, mental retardation and, occasionally, congenital malformations. SPG1 (OMIM 312920) results from mutations of the L1 cell adhesion molecule (*LICAM*) gene at Xq28 locus. Other cases of complicated SPG and uncomplicated (pure) SPG map to the *PLP1* gene locus and are known as SPG2 (OMIM 312920) (therefore allelic to PMD). SPG2 begins with pure spastic leg weakness but gradually developed other symptoms such as sensory loss, optic atrophy, nystagmus, dysarthria and dementia (Koeppen and Robitaille 2002). Some of the clinical features of SPG2 are similar to those of PMD including the mental retardation, nystagmus and optic atrophy. As with PMD males are mainly affected.

1.5.1.3 Genetic basis of *PLP1* related disorders

PMD in humans occurs as a consequence of a number of mutations, including point mutations in coding regions, mis-splicing at the transcript level, deletion, duplication/triplication of the gene or changes in gene expression regulation. Figure 6 shows the genetic mechanisms for PMD in patients. The main cause of PMD in humans is duplication of the *PLP1* gene accounting for 50 to 75% of all cases (Sistermans *et al.*, 1998, Garbern *et al.*, 1999). The breakpoints in the duplications causing PMD vary as does the size of the duplication from 300Kb to 4.6Mb (Woodward *et al.*, 1998, Inoue *et al.*, 1999). Very rare cases of PMD are caused by triplication of the *PLP1* gene and the severity of the disease is greater than cases caused by duplication (Wolf *et al.*, 2005). Real-time quantitative PCR can now be utilised to detect *PLP1* copy numbers for diagnosis of humans (Regis *et al.*, 2005). Mimault and colleagues (1999) describe analysis of 82 sporadic cases of PMD caused by duplications showing that the duplications arise most frequently in the male germline.

Point mutations make up a further 15-20%, 2-3% is caused by null mutations and the rest have no known cause. Some mild forms of PMD cases with no known mutation in the coding region may be caused by mutations in splicing at other exon-intron borders within the *PLP1* gene. A point mutation at the 3' border of exon 6 was found in a patient with mild PMD (Hobson *et al.*, 2000, Hubner *et al.*, 2005). This mutation did not cause an amino acid change but did affect splicing and caused partial skipping of exon 6 in the *PLP1* mRNA. The reading frame remained intact however it led to the absence of amino acids 232-253 which represent the main part of the fourth transmembrane domain. However wild type *PLP1* mRNA was also produced leading to the milder phenotype (Hubner *et al.*, 2005). To date there have been three further mutations affecting the exon 6 donor splice site leading to disease published. The severity of the disease phenotype depends on whether any wild type splicing also occurs. (*Jimpy* mice mirror this with skipping of exon 5/partial rescue with wild type PLP and DM20). A case of PMD caused by mis-splicing at the exon 5 donor site due to a point mutation has also been documented (Aoyagi *et al.*, 1999).

Recent cases of PMD (and SPG2) caused by a positional effect have been reported. A duplication of a region of the X chromosome downstream from the *PLP1* gene in a patient is the cause of the disease (Lee *et al.*, 2006a). Lee *et al.*, (2006a) proposed that this duplication leads to *PLP1* gene silencing, thus, causing the disease. An inverted X chromosome with a breakpoint within *GLRA4*, a putative pseudogene similar to glycine receptor alpha-2 chain was found in a patient with a subset of PMD symptoms (Muncke *et al.*, 2006). They suggest that a positional effect spanning 70kb is the cause of the symptoms and that *GLRA4* is not involved. Carango and colleagues (1995) described two brothers with PMD with no mutations in the coding regions of the *PLP1* gene. The brothers had a 6-fold higher level of *Dm20* mRNA in their cultured skin fibroblasts compared to RNA from an unaffected male which could be mirrored in their CNS tissue. This reflects the patients with PMD who have duplications or triplications of the *PLP1* gene. Any change in the expression of this gene has a detrimental effect on myelination.

PMD in humans involves at least three mechanisms, loss of function, gain of toxic function and increased dosage. The loss of function pertains to null mutations and is the least severe whereas the gain of toxic function relates to point mutations and causes a range of severity depending on the specific mutation. PMD caused by duplication lies in between the two but the rare cases of triplications increase severity.

1.5.1.4 Other myelin disorders caused by gene dosage

The disorders Charcot-Marie-Tooth disease type 1 (CMT1A) and Hereditary neuropathy with liability to pressure palsies (HNPP) are examples of other myelin disorders caused by dosage effects and mutations of a myelin protein gene. The major cause of CMT1A is duplication of the peripheral myelin protein 22 (*PMP22*) gene, and HNPP by a decrease in dosage of the same gene (Woodward and Malcolm 1999). Other human diseases such as Familial Hypercholesterolemia, Duchenne Muscular Dystrophy (DMD) and Lesch-Nyhan syndrome, another x-linked disorder, have been found to be caused by partial gene duplications (Hu and Worton 1992).

1.5.2 *Plp1* gene mutations in animals

1.5.2.1 Spontaneous mutants

The *jimpy* (*Plp^{jp}*) (abbreviated to *jp*) mouse was described in 1954 and since then several other animal myelin deficiencies caused by mutations of the *Plp1* gene have been discovered. These include the myelin synthesis-deficient *jp* mouse (*Plp^{jp-msd}*) (abbreviated to *msd*), *Plp^{jp-4j}*, myelin deficient (*md*) rat, the shaking (*sh*) pup, the rabbit with paralytic tremor (*pt*) and the *rumpshaker* (*Plp^{jp-rsh}*) (abbreviated to *rsh*) mouse.

1.5.2.1.1 *Jimpy (jp) mouse and myelin synthesis-deficient jp (msd) mouse*

The *jp* and *msd* are the most severely affected mutants and are characterised by an almost complete absence of myelin, reduction in mature oligodendrocyte numbers and death by 3-4 weeks. The *msd* mutation (A242V) occurs in patients with severe PMD.

1.5.2.1.2 *Rumpshaker (rsh) mice*

The *rumpshaker* mouse is a spontaneous occurring mutant with a mild disease phenotype dependant on genetic background. The *rsh* mutation leading to an amino acid substitution (I186T) in mice is identical to a mutation in humans causing SPG2 (Kobayashi *et al.*, 1994). This mouse is hypomyelinated, with some naked axons and thinner sheaths on axons that are myelinated. While many of the axons have normal periodicity, some have condensed IPLs (Griffiths *et al.*, 1990). Genetic background has a role in the severity of disease in mice with the *rsh* mutation causing a lethal phenotype in the C57BL/6 mice with death around postnatal day 30 (P30) (Al-Saktawi *et al.*, 2003). Wallerian-type degeneration is also seen in these mice (Edgar *et al.*, 2004).

1.5.2.1.3 *Other known mutants*

Yool *et al.*, (2000) and Nave and Griffiths (2004) reviewed the known animal mutants of PMD and SPG2.

Mutations causing PMD

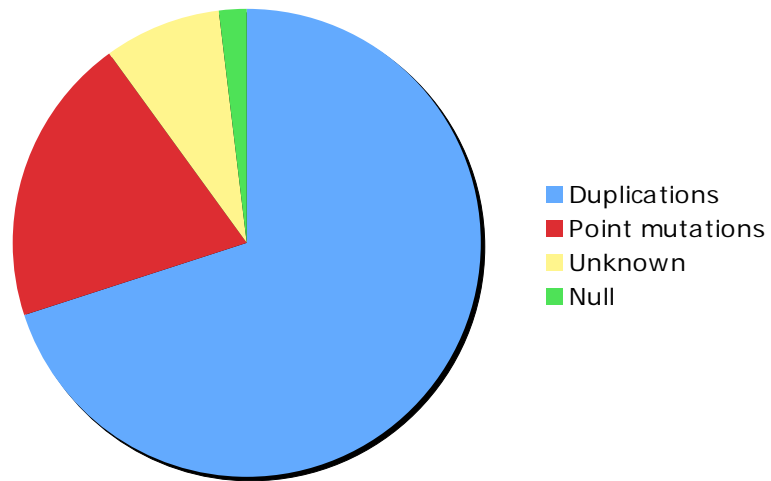


Figure 6. Pie chart showing the proportion of PMD caused by the different types of mutations with ~70% caused by duplications of the *PLP1* gene.

1.5.2.2 Transgenic animals

1.5.2.2.1 #66 and #72 transgenic mice

Readhead *et al.*, (1994) generated two lines of transgenic mice containing a cassette with extra copies of the wild type murine *Plp1* gene. One line, #72 had a cassette with 3 extra copies and could be bred to homozygosity with 6 extra copies with an endogenous copy of the *Plp1* gene on the X chromosome. The other line, #66, had 7 extra copies of the *Plp1* gene in tandem and when bred to homozygosity had 14 extra copies of wild type gene as well as the endogenous copy on the X chromosome. The entire *Plp1* gene containing 8 exons and 3.5kb of the 5' regulatory region was present in 7 copies in the cassette which was inserted into an unknown autosome in the mouse genome. The transgene was checked for mutations and was found to be indistinguishable from the endogenous copy of the gene. Both dysmyelination and demyelination are seen in the #66 transgenic mice. Dysmyelination or the aberration of the normal myelination process is seen the animals with the highest *Plp1* gene copy numbers (homozygous) with premature death around 2 months. The homozygous #66 mice develop a tremor that is visually noticeable after 2 weeks and continues throughout their life. These animals are fertile but tend to die by seizures prior to mating. Although the *Plp1* transgenic cassette is inserted into an autosome the gene's expression is still area and cell specific. Readhead and colleagues (1994) noted that the dysmyelination in the homozygous animals was less severe in the spinal cord and brain stem and more prominent in the forebrain and optic nerve. This may suggest that areas that myelinate later in CNS development are more severely affected by loss of myelin.

Astrocytosis is increased in the homozygous #66 animals with increased numbers of processes noted in early and late CNS development. It was noted that mature oligodendrocytes in #66 transgenic mice accumulate PLP/DM20 and other myelin proteins and have a high level of oligodendrocyte death (Anderson *et al.*, 1999). Dysmyelination occurring in mice with extra copies of wild type *Plp1* gene was previously thought to be caused by a defect in oligodendrocyte differentiation; however it may be due to the cell's inability to maintain contact and/or remyelinate nearby axons (Woodward and Malcolm 1999).

Demyelination is noted in animals with the lower *Plp1* gene copy number (hemizygous) and is the loss over time of properly laid down myelin. Demyelination, as well as axonal degeneration is seen in older #66 hemizygous animals (Anderson *et al.*, 1998). These

animals are able to reproduce and are clinically normal for several months. However, they go on to develop a progressive neurological disorder characterised by loss of weight, ataxia, tremors and seizures. The loss of myelin in the hemizygous mice is different from that seen in other mutants with signs of tract and fibre size specificity observed. A significant level of axonal degeneration is also observed in these animals. Clinically unaffected animals older than 1 year usually show changes in the brain and spinal cord but the optic nerve showed abnormalities at 4 months. Ip and colleagues (2006) discovered that in these mice the immune response contributes to the degeneration of the myelin. CD8+ lymphocytes and CD11b+ macrophage like cells are elevated in the white matter of these animals.

A viral expression construct used to infect primary oligodendrocyte cultures, causing overexpression of PLP, led to mistrafficking of the protein to LE/Ls instead of the normal route of the Golgi apparatus. It also led to the sequestering of cholesterol to these cellular compartments (Simons *et al.*, 2002). Transgenic #66 mice accumulate PLP and cholesterol in LE/Ls and this leads to the perturbation of the myelination process affecting the viability of the oligodendrocytes (Simons *et al.*, 2002). Accumulation of the protein in the ER of oligodendrocytes with extra copies of the *Plp1* gene can also trigger apoptosis (Gow *et al.*, 1998).

Oligodendrocytes die by apoptosis in homozygous #66 transgenic mice. Apoptosis involves the cleavage/activation of caspase family members which occurs in a cascade manner and the pathways leading to apoptosis activation in *Plp1* mutants vary dependant on the mutation involved as seen by evidence from the *jimpy* and #66 transgenic animals (Cerghet *et al.*, 2001).

1.5.2.2.2 Other transgenic animals

Yool *et al.*, (2000) also reviewed the known animal models of PMD and SPG2. Several transgenic and knockout animals have been generated over the years to investigate different aspects of human dysmyelinating and demyelinating diseases. These include the aforementioned #66 transgenic and *Plp1* null mice. Other transgenic animals include the #72 line generated by Readhead *et al.*, (1994), *4e-Plp* transgenic mice (Kagawa *et al.*, 1994), PLP or DM20 only lines (Nadon *et al.*, 1994) and ND3A and ND4 transgenic mice generated to express high levels of DM20 only (Barrese *et al.*, 1998, Mastronardi *et al.*, 1993, Johnson *et al.*, 1995).

The *4e-Plp* transgenic line of mice containing extra copies of the wild type *Plp1* gene show evidence pointing to the dual role PLP plays in myelination (Kagawa *et al.*, 1994). The cassette here contains 40kb gDNA encompassing all 8 exons of the mouse *Plp1* gene as well as 20kb of the 5' flanking region and 4kb of the 3' flanking sequence. The copy number is estimated to be 2 *Plp1* genes per transgene cassette thus hemizygotes have 2 extra copies of *Plp1* while homozygotes have 4. The expression of the transgene has been found to similar to the endogenous gene in this case the *jimpy Plp1* gene. In hemizygous mice the message levels were up to 132% of wild type levels while in homozygous mice the levels were down to 60% of wild type levels. Protein levels were reduced even further than transcript levels in the *4e-Plp* animals.

Both homozygous males and females exhibit ataxia, tremors and convulsions leading to premature death around postnatal day 30. At P20 in homozygous 4e mice the majority of axons are found to be naked or ensheathed by a thin myelin sheath in white matter of spinal cords. Oligodendrocyte maturity is compromised in these animals with oligodendrocytes producing less *Mbp* mRNA than wild type controls. Kagawa *et al.*, (1994) confirmed also the hypomyelination seen in their animals was not caused by insertional mutagenesis.

A line of transgenic rats LewPLP, were generated by Bradl and colleagues (1999). These homozygous animals have a dysmyelinating phenotype with the death of mature oligodendrocytes as well as the arrest in immature oligodendrocyte development. The homozygous rats die before weaning age while the hemizygous animals myelinate normally then go on to develop myelin degeneration throughout their life. When studying the hemizygous animals further Bauer *et al.*, (2002) uncovered oligodendrocytes with swollen and aberrant RER in the CNS gray matter. All these models are useful in studying the underlying pathological mechanisms leading to disease in humans.

1.5.2.2.3 *Plp1* null mice

The complete loss of the *PLP1* gene products in humans leading to a mild form of PMD is caused by point mutations like a (C-to-A) mutation in the initiation codon of the gene (Sisternans *et al.*, 1996). As there were no spontaneous animal models of complete loss of the *PLP1* gene, Klugmann *et al.*, (1997) generated a transgenic mouse lacking the *Plp1* gene by targeting a vector to delete the translation start site of PLP/DM20. These mice did not go on to develop the expected dysmyelinating phenotype seen in *Plp1* mutants and

developed normally showing no other signs usually associated with dysmyelinating disorders (Griffiths *et al.*, 1998). The myelin did not immunostain for PLP or DM20 but did for MBP as expected. Myelin sheaths were of approximately normal thickness but exhibited variability in the amount of compaction with some sheaths showing normal periodicity and others having widely spaced IPLs (Klugmann *et al.*, 1997). There were no signs of astrocytosis when stained with GFAP and the PLP/DM20 deficient oligodendrocytes showed no evidence of increased cell death or degenerative changes.

The main difference in the myelin ultrastructure was the loss of distinction between the IPL and MDL (Klugmann *et al.*, 1997). Griffiths *et al.*, (1998) discovered that the PLP/DM20 null mice generated by Klugmann *et al.*, (1997) went on to develop axonal swellings and degeneration of axons later in life suggesting the progressive impairment of fast retrograde and anterograde transport in axons (Edgar *et al.*, 2004). Patients with mutations causing a complete lack of PLP/DM20 in the CNS, exhibit the same length dependant axonal degeneration seen in null mice (Garbern *et al.*, 2002). This axonal degeneration in mouse and human may be caused by the loss of PLP/DM20 mediated axonal-oligodendrocyte interactions. Studies by Rosenbluth and colleagues (2006) highlighted ultrastructural changes in PLP null myelin such as irregularly filled and diffuse interlamellar spaces and distorted radial components that may be the cause of the axonal damage. As this is one of the major phenotypic symptoms in *Plp1* null mice and is not seen in *shiverer* mice (deficient in MBP) it suggests the correct expression of PLP and DM20 is essential for the oligodendrocyte function of maintaining the interaction between the cell and axons.

1.5.3 Spontaneous mutations of other myelin genes

1.5.3.1 *Shiverer (sh)* mice

The *shiverer* mutation was mapped to mouse chromosome 18 by Sidman and colleagues (1985). Both Roach *et al.*, (1985) and Kimura *et al.*, (1985) showed that *shiverer* mice had a deletion of a large proportion of their *Mbp* gene. *Shiverer* animals show behavioural changes from postnatal day 14, developing shivers, then tonic seizures and finally premature death.

Information on the function of MBP has mainly come from this recessive neurological mutant *shiverer*. The *shiverer* mutation causes a defect in CNS myelination which leads to tremors, then convulsions and eventually premature death (Lemke 1988). In homozygous

shiverer animals there is almost no CNS myelin present and where there is myelin, the MDL is uncompacted. Around 20 kb of the *Mbp* gene which maps to mouse chromosome 18 is deleted from the *shiverer* genome (Roach *et al.*, 1985). The reintroduction by Readhead *et al.*, (1987) of a cloned MBP gene restored the mutant phenotype to a wild type phenotype. One surprising finding with the *shiverer* mouse was the lack of effect on the PNS where MBP is also expressed suggesting another protein compensates for the loss of MBP. Alterations in phosphorylation of cytoskeleton proteins and neuronal perikaryon functions like cytoskeletal gene expression are seen in these mice suggesting compact myelin is important for normal maturation of the neuronal cytoskeleton in the CNS (Brady *et al.*, 1999).

Kimura and colleagues (1998) showed that overexpression of one of the major MBP isoforms (14 kDa) in *shiverer* mice restores CNS myelination in these mice. They also demonstrated a similar restoration of CNS myelination in *shiverer* animals with a minor isoform (17.2 kDa). Shine *et al.*, (1992) generated *shiverer* mice crossed to carry MBP transgene producing a range of mice with varying MBP expression levels. Mice with MBP expression above 50% of wild type levels showed no difference in numbers of myelinated axons and myelin thickness.

1.5.3.2 Myelin deficient (*shi^{md}*) mouse

The *myelin deficient* mouse is allelic to the *shiverer* animal and was shown to carry a duplication rather than a deletion of the MBP gene with one copy containing an inversion at its 3' end (Popko *et al.*, 1988). *Shi^{md}* mutation is caused by an inversion of exons 3-7 and a duplication of exons 2-7 resulting in the formation of antisense MBP heterogeneous nuclear RNA eliminating MBP mRNA from the nucleus (Okano *et al.*, 1991).

Shi^{md} mice produce 2.5-5.0% MBP mRNA compared to normal wild type levels. In neonatal *md* mice MAG and MBP are both present, the MAG in the cell body and early myelin sheaths and the MBP only in the myelin sheaths. However, at P17 when dysmyelination is evident MAG is less obvious in the oligodendrocytes.

1.5.3.3 Quaking mice

Quaking mice show a generalised hypomyelination in both the CNS and PNS caused by an autosomal recessive mutation on chromosome 17 (Bray *et al.*, 1981). This mutation is in

the quaking (*qkl*) gene, of which one protein isoform is involved in the alternative splicing of MAG (Trapp 1988, Georgiou *et al.*, 2004). The MDL does not form in these mutants.

1.6 Aims of thesis

This study aims to investigate the effects of increased *Plp1* gene dosage in #66 transgenic mice (Readhead *et al.*, 1994). The contribution of only the transgene cassette with an endogenous *Plp1* gene to PLP/DM20 message and protein amounts is investigated to get a better measure of the control on transgene expression. The effects of increased *Plp1* gene dosage on message and protein levels of its own products and other myelin gene products have been explored. In addition to steady state levels, the effects on protein dynamics have been studied. Changes to myelin ultrastructure have also been described and quantified using morphometric analysis.

In the final discussion, the findings from this study and any future work that could help answer questions raised are discussed.

2 Materials and Methods

2.1 Miscellaneous

All procedures were conducted in accordance to health and safety guidelines outlined in specific risk assessments. Inorganic chemicals were sourced from Sigma or BDH and were of AnalaR® or molecular biology grade. Solutions were sterilised as appropriate, bulk solutions were autoclaved whereas smaller volumes that could not autoclaved were filter sterilised using a Flowpore 0.22µm filter (Sartorius, Epsom, UK). Toxic powders, fixatives and other volatile liquids were prepared in fume cupboards.

The Appendix (page 207) gives details of the preparation of fixatives, stains, buffers and solutions as well as of staining and processing protocols. These are all cross-referenced to pages in this section.

2.2 Mouse Breeding

2.2.1 Animal breeding facilities

Mice were bred at the Glasgow Parasitology Unit, University of Glasgow Veterinary School. The breeding facility at Glasgow is known to have evidence of murine hepatitis virus and picorna virus infections both of which have been associated with neurological disease in mice (Lipton *et al.*, 1994, Fujiwara, 1994). During the period of this study, the mice were routinely screened and monitored for pathogens that may have a detrimental effect and there was no evidence of clinical disease and the phenotypes and pathology identified in transgenic mice were not identified in wild type controls also bred in this facility. Similarly, mice bred at ZMBH, a specific-pathogen free facility, had phenotypes and pathology that were consistent with those seen in the mice bred at Glasgow. This suggests that these viruses did not contribute to the phenotypes and pathology described in this study.

2.2.2 Transgenic Lines

2.2.2.1 #66 mice

#66 mice were generated by Readhead *et al.*, (1994). The murine *Plp1* gene was isolated from a cosmid library and used to construct a 26.6kb transgene insert. The transgenic

cassette is predicted to include all eight exons of the *Plp1* gene, 3.5kb of the 5' regulatory region and a small vector fragment containing the T7 promoter sequence at the 3' end of the transgene (Figure 7A). This was introduced into B6D3F2-fertilised ova by pronuclear microinjection and produced two lines of transgenic mice containing the intact *Plp1* transgene (#66 and #72). These were assessed by Southern blot analysis and were estimated to respectively contain seven and three copies of the transgene per haploid genome. The transgene copies co-segregated in subsequent generations following an autosomal inheritance pattern suggesting that, in both lines, the transgenes had inserted in tandem at autosomal sites (Readhead *et al.*, 1994). The presence of the transgene can be detected by conventional PCR using primers for the end of exon 7 and beginning of the 5' UTR (forward primer) and the T7 sequence (reverse primer) (Figure 7B and C).

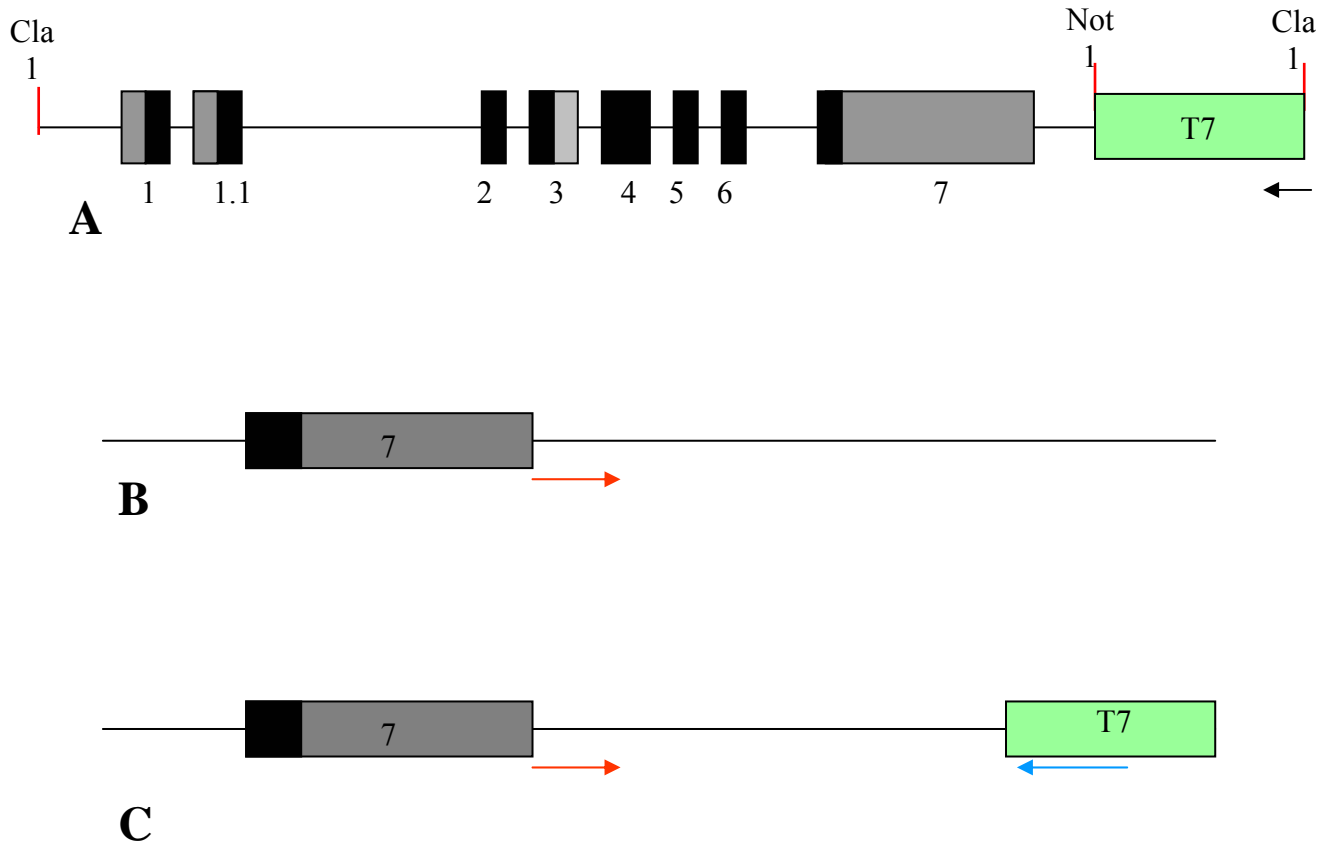


Figure 7. Transgene construct from the #66 and #72 lines.

The figure shows PCR primer positions for identifying the transgene (the exons are represented by numbered boxes, coding regions are shaded black with exon 3B shaded light grey; the transgene-specific T7 promoter sequence is represented by a green box, a black arrow indicates the orientation of this sequence) (Readhead *et al.*, 1994). **A)** The transgene construct with relevant restriction sites shown. **B)** The primer positions on the endogenous *Plp1* gene. **C)** The transgene construct (forward primer in red and reverse primer in blue).

2.2.2.2 *Plp1* gene null mice

Plp1 gene null transgenic mice were generated by Klugmann *et al.*, (1997) at ZMBH, Heidelberg. The endogenous *Plp1* gene was disrupted by introducing a targeting vector designed to disrupt the ATG translation start codon in exon 1 (Figure 8A-E). The targeting vector is also predicted to disrupt exon 1.1, preventing the transcription of *srPlp* and *srDm20* mRNA (Bongarzone *et al.*, 1999). The targeting vector replaced exons 1 to 3 of the wild type allele by homologous recombination and was introduced into R1 embryonic stem cells by electroporation. The *neo* gene, in reverse orientation to the *Plp1* gene and under the control of the herpes simplex virus (HSV) promoter, was used to disrupt the translation start codons. It replaced the 3' end of exon 1 and 2.5kb of intron 1 between the BamH1 site in exon 1 and the Kpn1 site in intron 1. A negative selector, the thymidine kinase (*tk*) gene also under the HSV promoter, was used to select against random (non-homologous) vector insertion as it was located immediately upstream of the 5' homology region of the targeting vector (Figure 8B). Construct-mediated G418 resistance positively selected for stem cells containing the targeting construct and cells that had random vector insertion were negatively selected against using gancyclovir. Homologous recombination and a single integration event were confirmed by Southern blot analysis. Cells containing the *Plp1* gene-null allele (*Plp^{tmkn1}*) were microinjected into blastocysts from C57BL/6J mice to produce chimeras. The chimeras were used to establish founder stock of *Plp1* gene null mice containing the *Plp^{tmkn1}* allele by back crossing onto C57BL/6J mice (Klugmann *et al.*, 1997). The wild type *Plp1* gene and the disrupted *Plp^{tmkn1}* allele are shown in Figure 8D and 8E with primer positions marked by arrows.

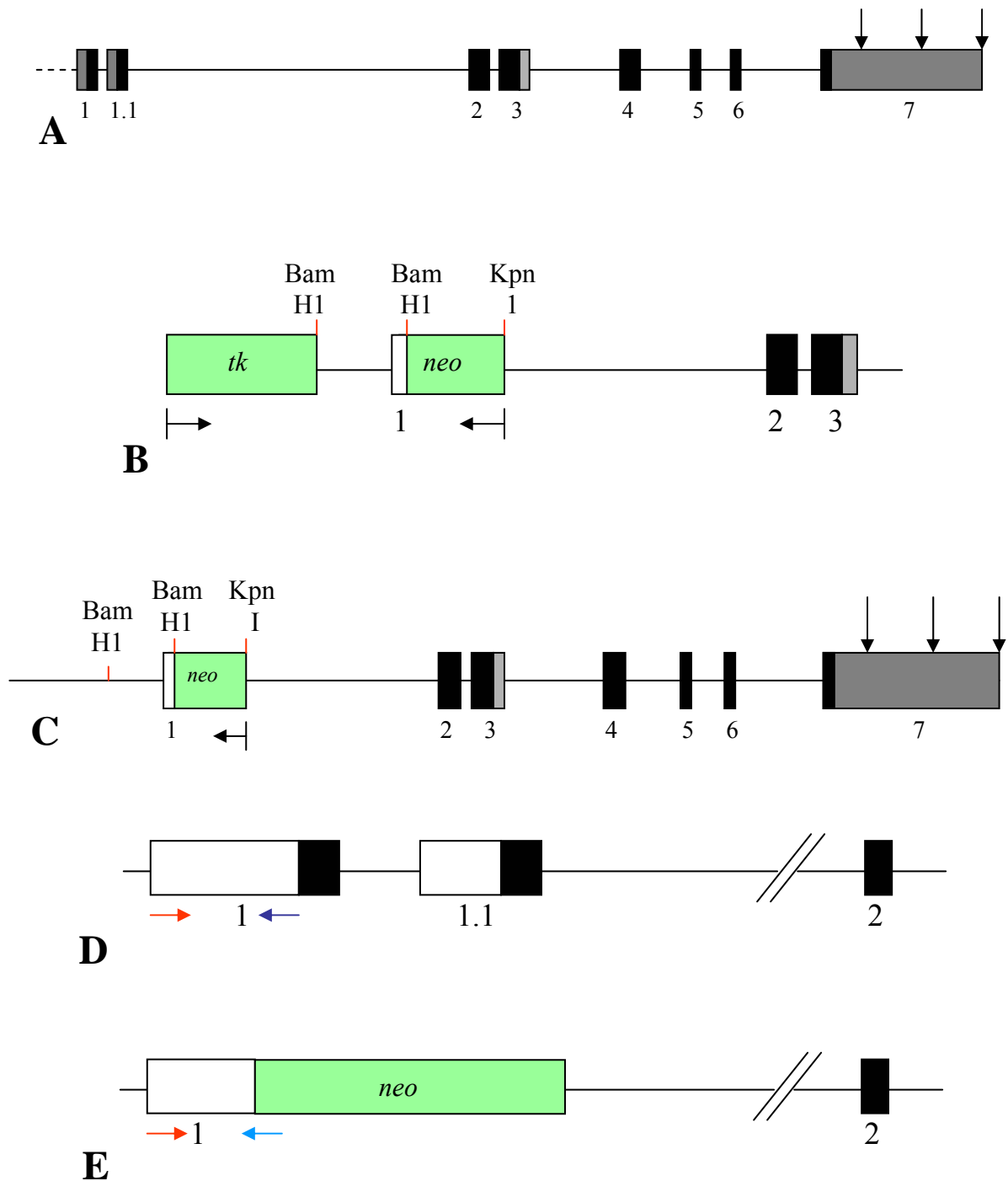


Figure 8. The steps involved in generating *Plp1* null mice.

A) The endogenous murine *Plp1* gene with all numbered exons (coding regions in black; exon 3B shaded light grey, arrows in exon 7 representing polyadenylation sites). **B)** The targeting vector containing the negative selectable marker (*tk* gene) which is lost during homologous recombination and the positive selectable marker (*neo* gene) which is retained (selectable markers are denoted by green boxes). **C)** The resulting recombined null gene. **D)** The endogenous *Plp1* gene (forward primer in red and reverse primer in dark blue). **E)** The mutated *Plp1^{tmknl}* gene (forward primer in red and reverse primer in light blue).

2.2.3 Maintenance of transgenic lines of mice

The #66 line of transgenic mice was maintained by creating harems containing transgene positive and negative animals of 2 months and older from the same background. Brother-sister matings were avoided and background strains were not mixed. The *Plp1* gene null transgenic line was maintained by creating harems of *Plp^{tmkn1}* hemizygous male and homozygous female mice. In addition, harems containing wild type mice from this line and mice carrying the *Plp^{tmkn1}* allele ensured the production of *Plp^{tmkn1}* heterozygotes and wild type littermate controls.

2.2.4 Crossing of transgenic lines of mice

For transgenic complementation of the *Plp1* gene null mice with the #66 transgene, hemizygous transgene positive #66 males were bred with *Plp^{tmkn1}* heterozygous females. This ensured that all F1 males were *Plp^{tmkn1}* hemizygotes or wildtype and that a number were also transgenic hemizygotes. Transgene negative littermates from the same breeding programme were used as internal controls.

2.3 Isolation and manipulation of DNA

2.3.1 Tail Biopsy and mouse identification

The mouse was anaesthetised in a chamber using Halothane (Rhone-Poulenc Chemicals Ltd, Stockport, UK). Once anaesthetised, 5mm of the tip of the tail was removed using aseptic techniques with a clean scalpel blade on a glass slide. The wound was cauterised and treated with Rimadyl analgesic (Pfizer, Tadworth, UK) which contains 50mg/ml Carprofen. The dose rate for the mice is 5mg/kg. While the mouse was still unconscious the ear was punched to allow for identification later. The mouse was returned to cage and allowed to recover under a heat lamp while regularly checked for wound bleeding.

The tail tip was placed into labelled tube and stored at -20°C until needed.

2.3.2 Genomic DNA (gDNA) extraction

gDNA for genotyping was extracted from tail samples collected at biopsy and at post mortem. This was conducted using a Promega kit following the manufacturer's protocol. Over night protein digestion with 7µl 50 mg/ml Proteinase K solution with 120µl 0.5M

EDTA in Nuclei Lysis solution was carried out. Frozen tail tips were placed in a 1.5ml fresh tube on ice.

The following morning 200µl ammonium sulphate containing Protein Precipitation solution (Promega, Southampton, UK) was added to aid precipitation. The DNA was extracted by mixing supernatant with 600µl iso-propanol and gently inverting. After a high speed spin (13,000rpm for 5 minutes) the pellet was washed with 600µl 70% ethanol. Finally, the pellet was resuspended in DNA Rehydration solution (Promega). Volume for resuspension was dependent on size for pellet.

Alternatively, a 3mm piece of tail was placed into a fresh tube containing 100µl 50mM Sodium Hydroxide and heated to 95°C for 1 hour 30 minutes. 10µl 1M Tris pH5.0 was added and samples vigorously vortexed. The crude DNA extractions could then be stored at 4°C or diluted 1 in 10 in ddH₂O and stored at -20°C.

2.3.3 gDNA quantification and storage

gDNA was quantified using a GeneQuant RNA/DNA calculator with a spectrophotometer cell. gDNA was assessed for degradation by electrophoresis on an agarose gel (Figure 9). The gDNA was diluted for genotyping PCRs to working concentrations of 25 ng µl⁻¹ in ddH₂O and stored at -20°C.

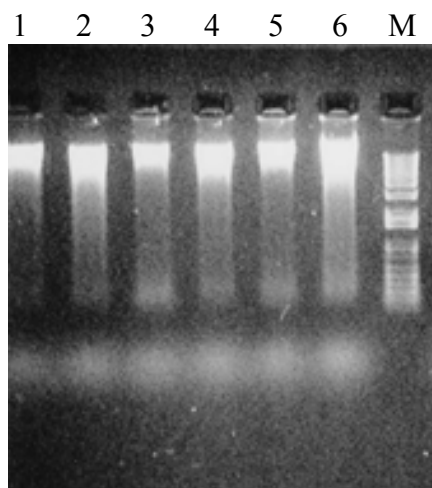


Figure 9. gDNA separated on a 0.8% agarose gel.

Lanes 1-6 show 250ng DNA separated on a 0.8% agarose gel, Lane M shows 1kb plus DNA ladder.

Initial cycle	denaturing temperature	94° C	3 min
	annealing temperature	58° C	1 min
	extension temperature	72° C	2 min
Step cycles (25 cycles)	denaturing temperature	93° C	40 secs
	annealing temperature	58° C	1 min
	extension temperature	72° C	40 secs
Final cycle	denaturing temperature	93° C	40 secs
	annealing temperature	58° C	1 min
	extension temperature	72° C	2 min

Table 1. Standard PCR program used for genotyping PCRs or RT-PCRs (annealing temperature can be altered depending on temperature of primers).

2.3.4 PCR Genotyping

2.3.4.1 PCR Program

Amplifications for genotyping were performed on a DNA thermal cycler following the program in Table 1.

2.3.4.2 Genomic PCR

25µl PCR reaction were carried out in 0.5ml thin walled tubes containing Ready-to-go PCR beads (Amersham, Chalfont St.Giles, UK). 25ng gDNA, forward and reverse primers at 0.2M concentration and ddH₂O was added to the beads. The reaction was overlaid with 50µl of molecular biology grade mineral oil (Sigma, Poole, UK) to prevent evaporation of the reaction mix. The reaction was stopped by storing at 4° C before analysis.

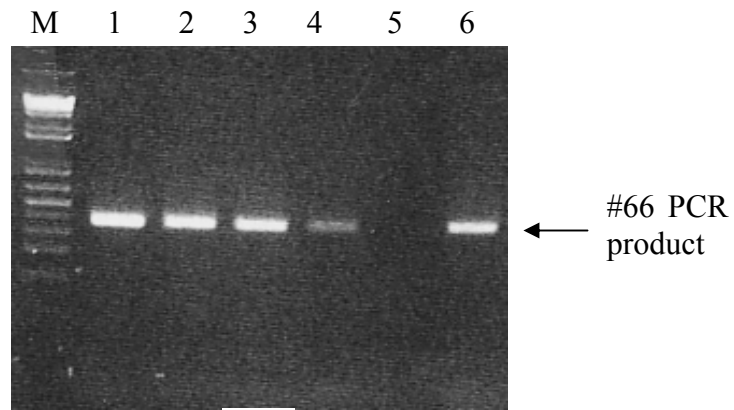
2.3.4.3 PCR Primers

Primer sequences and product sizes are listed in Table 2 and the PCR products are demonstrated in Figure 10. Primer positions are represented graphically in Figures 7 and 8 describing the transgenes and are cross-referenced in the text. A positive control (a known DNA sample) was included with each set of samples dependant on the PCR. A negative control reaction where the sample was replaced by ddH₂O was also included to ensure that there were no contaminating nucleic acids.

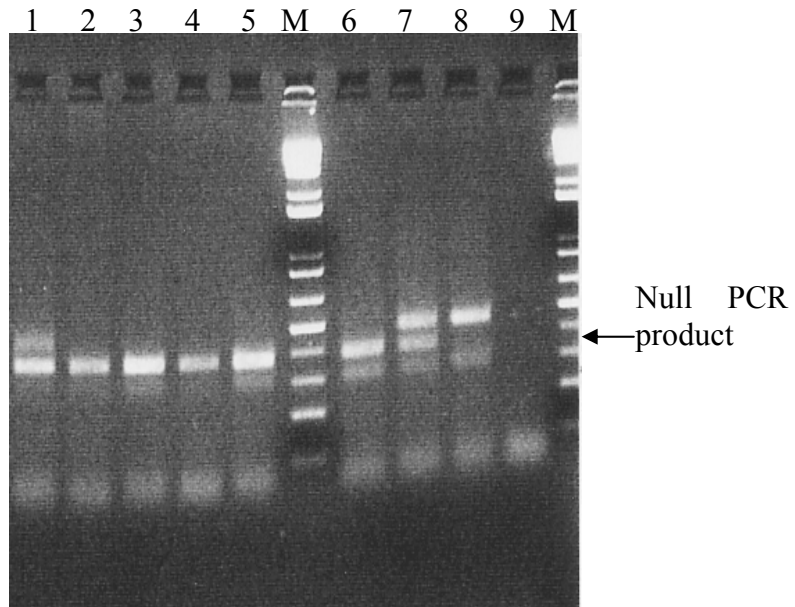
Amplify	Primer	Sequence	Size	Reference
#66 and #72 transgenes	PLP	5' CAG-GTG-TTG-AGT-CTG-ATC-TAC-ACA-AG 3'	~400bp	Readhead <i>et al.</i> , 1994
	α T7	5' GCA-TAA-TAC-GAC-TCA-CTA-TAG-GGA-TC 3'		
<i>Plp1</i> wild type allele	Ex1f	5' GGA-GGA-TTA-AGA-ACC-CCT-CC 3'	389bp	Griffiths <i>et al.</i> , 1995
	α PLP5'anti	5' CTG-TTT-TGC-GGC-TGA-CTT-TG 3'		
<i>Plp^{tmkn1}</i> allele	Ex1f	5' GGA-GGA-TTA-AGA-ACC-CCT-CC 3'	429bp	Griffiths <i>et al.</i> , 1995
	α MKneo1	5' TAC-GGT-ATC-GCC-GCT-CCC-GAT-TCG-CA 3'		
<i>Cyclophilin</i> transcript cDNA	CyclC	5' ACC-CCA-CCG-TGT-TCT-TCG-AC 3'	300bp	Danielson <i>et al.</i> , 1988
	α CyclG	5' CAT-TTG-CCA-TGG-ACA-AGA-TG 3'		
<i>Xbp1</i> transcript cDNA	XBP1.3S	5' AAA-CAG-AGT-AGCTCA-GAC-TGC 3'	~ 500bp	Marciniak <i>et al.</i> , 2004
	XBP1.12AS	5' TCC-TTC-TGG-GTA-GAC-CTC-TGG-GAG 3'		
<i>B-actin</i> transcript (Probe 3' Blackhole Quencher, 5' 6-FAM) (NM_007393)	Forward	5' AGA-GGG-AAA-TCG-TGC-GTG-ACA-T 3'	~180bp	Karim <i>et al.</i> , 2007
	Reverse	5' AGG-AAG-GCT-GGA-AAA-GAG-CC 3'		
	TaqMan Probe	5' TGG-CCA-CTG-CCG-CAT-CCT-CTT-C 3'		
<i>Mbp</i> transcript	Forward	5' AGA-CCC-TCA-		

all isoforms (Probe 3' Blackhole Quencher, 5' 6- FAM) (NM_0010252 59)		CAG-CGA-TCC-AA 3'	~130bp	Karim <i>et al.</i> , 2007
	Reverse	5' CCC-CTG-TCA- CCG-CTA-AAG-AAG 3'		
	TaqMan Probe	5' CAA-GTA-CCA- TGG-ACC-ATG-CCA- GGC-A 3'		
<i>Plp1</i> transcript both isoforms (Probe 3' Blackhole Quencher, 5' 6- FAM) (NM_011123)	Forward	5' GTA-TAG-GCA- GTC-TCT-GCG-CTG- T 3'	200bp	Karim <i>et al.</i> , 2007
	Reverse	5' AAG-TGG-CAG- CAA-TCA-TGA-AGG 3'		
	TaqMan Probe	5' TGG-CAA-GGT- TTG-TGG-CTC-CAA- CCT-T 3'		

Table 2. PCR primers for genotyping, semi-quantitative RT-PCR and realtime RT-PCR



A



B

Figure 10. Genotyping PCRs.

A) #66 PCR of wild type, hemizygous and homozygous samples using *Plp1* forward primer and T7 reverse primer (Lane M 1kb plus ladder, Lanes 1-4 and 6 transgene positive (hemizygous or homozygous) and Lane 5 transgene negative (wild type)). **B)** *Plp1* and *Plp^{tmkn1}* allele PCR (Lanes M 1kb plus ladder, Lanes 1-5 samples and Lane 6-9 controls, wild type, heterozygous, null and blank).

2.3.5 Agarose gel

Regular analysis of DNA and PCR products was performed in 1-2% agarose gels in 1 x TAE (Tris acetate ethylene-di-amine-tetra-acetate) buffer ([appendix](#)). 1% agarose gels were used to examine DNA and 2% for PCR products (Figures 9 and 10). Gels were made from ultra pure electrophoresis grade agarose (Invitrogen, Paisley, UK) melted in TAE buffer. Once cooled Ethidium Bromide 1mg/ml was added to the gel to give final concentration of 0.5µg/ml. Samples were loaded with 6x Orange G loading dye ([appendix](#)) and 1 x TAE used as electrophoresis buffer.

2.3.6 Visualisation of PCR Products

Agarose gels were viewed with a “Fotoprep I” ultraviolet (UV) transilluminator (Fotodyne Inc.)

2.4 Isolation and manipulation of RNA

2.4.1 Tissue/Sample Collection

Mice were culled by CO₂ inhalation. Tissues were removed immediately after death, placed in freezer tubes (Nunc, Loughborough, UK) and snap frozen in liquid nitrogen. The tissues were then stored at -80°C until required.

2.4.2 Extraction of RNA

The extraction of RNA from tissue using RNAsol B is a modification of a one step procedure described by Chomczynski and Sacchi (1987) and was carried out following manufacturer’s recommendations. RNAsol B contains a monophasic solution of guanidium and phenol chloroform. Guanidium rapidly inactivates RNase activity and forms complexes with RNA and water allowing the RNA to be retained in the aqueous phase while DNA and proteins separate in the phenol/chloroform phase.

1 ml prechilled RNAsol Bee (TelTest Inc) was added to previously prepared tissue (powdered in liquid nitrogen then snap frozen and stored in -80°C) on ice. The tissue was homogenised by titration through sterile needles of decreasing sizes (23-14g) until the RNAsol Bee was clear. The resulting solution was aliquoted into a fresh 1.5ml tube. 200µl Chloroform was added to each tube, the tubes vortexed for 30 seconds and placed on ice

for 5 minutes. The samples were then centrifuged for 15 minutes at 13,000 rpm at 4°C. The upper aqueous layer (~500µl) was transferred to a fresh tube.

Depending on starting material 4µl glycogen was added (cultures, spinal cord). Equal volume 100% isopropanol (Sigma) was added to the samples. After 10 minutes at room temperature the samples were centrifuged for 15 minutes at 13,000 rpm at 4°C (RNA forms pellet and is visible to eye). The supernatant was discarded and 1ml 70% Ethanol was added to the pellet. After vortexing, the samples were centrifuged for 8 minutes at 13,000 rpm at 4°C. The supernatant was once again removed and a further spin for 2 minutes at the same setting was performed. The excess ethanol was removed using a P200 Gilson pipette and tip. The pellet was left to air dry for no more than 10 minutes and pellet resuspended using 100µl DEPC treated H₂O ([appendix](#)). For long term storage the RNA was kept at -80°C.

2.4.3 Quantification and Quality check

Prior to storage the RNA was checked for concentration and quality. For quantification, RNA samples were initially diluted 1 in 10 with milliQ H₂O. A blank of only milliQ H₂O was also prepared. On a Genequant (Pharmacia Biotech, Little Chalfont, UK) the blank was read for single stranded RNA at absorption of 260/280nm. This gave a reading of zero after which all the samples were read. The resulting concentration was multiplied by a factor of 10 to give final concentration for each RNA sample.

500ng RNA was run out on a 1.5% agarose gel in 1xTAE at 75 volts for 45 minutes to resolve the major RNA species and assess their integrity (Figure 11). The gel was photographed using UV image capture system.

2.4.4 cDNA generation from total RNA

Ensuring all tubes and tips were RNase free and H₂O DEPC treated, cDNA was produced from total RNA. Prior to reverse transcription 2µg total RNA was treated with 2 units of DNase I for 45 minutes at 37°C. This was to remove genomic DNA contamination. To stop the reaction 5µl de-act slurry was added to each sample. The samples were left for 2 minutes at room temperature then centrifuged for 2 minutes at 10,000 rpm.

Fresh tubes were prepared for reverse transcription. 25µl supernatant (1µg DNase I treated RNA) was heated at 65°C for 5 minutes to denature any secondary structures then mixed

with reverse transcription reaction mix [1x RT buffer (Invitrogen), 5mM DTT, 1mM dNTPs, Random primers, 20 units RNAsin (Promega), 200 units RTase (Invitrogen) in total volume of 25 μ l] to give 50 μ l reaction volume. Three incubation/heating steps followed: 37°C for 30 minutes, 40°C for 1 hour and finally 72°C for 15 minutes. 150 μ l DEPC treated was added to each sample to give final working volume of 200 μ l (Figure 12).

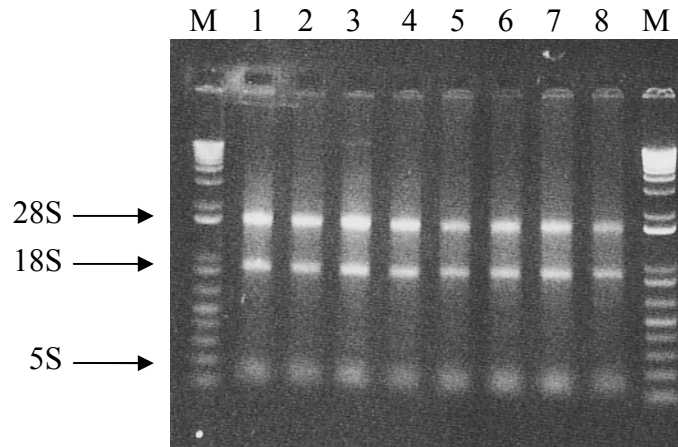


Figure 11. 500ng total RNA from P20 spinal cords.

Lanes 1-8 show 500ng aliquots of total cellular RNA separated on a 1.5% non-denaturing agarose gel, Lane M shows 1kb plus DNA ladder. All three bands of ribosomal RNA are visible (28S, 18S and 5S bands).

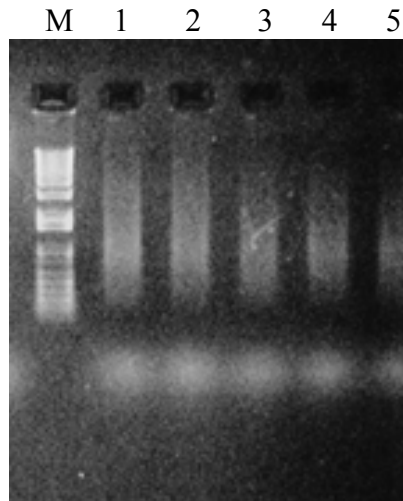


Figure 12. cDNA from P20 mouse spinal cord.

Lane 1-5 show 10 μ l cDNA separated on a 0.8% agarose gel, Lane M shows 1kb plus DNA ladder.

2.4.5 RT-PCR

The amino acid mutation leading to a misfolded protein or the introduction of extra wild type gene copies resulting in protein overproduction, may induce an additional process burden for the ER. One consequence is the activation of cellular quality control mechanisms which involve the upregulation of many chaperone proteins. One way of measuring ER stress is by studying the X box protein 1 (*Xbp1*). *Xbp1* was used as it is one effector of the UPR which is expressed on ER stress-mediated splicing of the *Xbp1* mRNA. XBP1 induces certain ER-targeted proteins, eg, glucose-regulated protein 78 (GRP78), which help resolve the ER stress and foster cell survival. cDNA produced from spinal cord RNA was utilised for X box protein 1 (*Xbp1*) and cyclophilin RT-PCR (Marciniak *et al.*, 2004). The cyclophilin message was used as an endogenous control as levels of message are not altered during development or between tissues. Also used as a control was cDNA from cultured oligodendrocytes, which had been exposed to stress inducing conditions such as treatment with tunicamycin and were processed in tandem with the spinal cord tissue. The samples were taken out of the freezer and placed on ice to thaw slowly. While the samples thawed, primers (Table 2) were also allowed to thaw. As the cDNA was not quantified 2µl of each sample was used. The PCR was set up as normal gDNA PCRs were ([2.3.4.2 Genomic PCR](#)). The PCR conditions were similar to gDNA PCR conditions (Table 1).

4µl from each PCR was run out on a 2% agarose gel to confirm PCR was successful alongside cyclophilin. The PCR products for *Xbp1* were cleaned up using the Qiagen PCR clean up kit (Qiagen, Crawley, UK) following the manufacturer's instructions. The *Xbp1* PCR products could be digested with *PstI*, which cuts only the unspliced cDNA. The spliced product is a result of ER stress. A varying volume for each test PCR was selected dependant on cyclophilin levels and put into a fresh tube. Into these a digestion mix (1.5µl enzyme, 3µl 10x buffer and ddH₂O up to 30µl) was added and all were placed into a 37°C waterbath for 2 hours. The digestion was put on ice to stop the reaction then 15µl digest and 5µl orange G loading dye were placed in a fresh tube. The products were resolved on a 2% agarose gel containing ethidium bromide for visualisation. Finally the captured images were quantified using Scion Image for Windows software (Scion Corporation, Maryland, USA). The intensity of the signal was corrected for the relative density of cyclophilin.

2.4.6 Northern blotting

Hayes *et al.*, (1989) reviewed the general principles of Southern, northern and western blotting.

2.4.6.1 Sample preparation

RNAs were removed from -80°C on dry ice and put at 60°C until thawed. RNA requires a rapid thaw to avoid degradation and thawing at 60°C ensures there is minimal degradation of the samples. $20\mu\text{g}$ each RNA was aliquoted into RNase-free tubes on ice. The tubes were placed on dry ice and the original samples were returned to the -80°C freezer. The $20\mu\text{g}$ samples were put in dry ice to freeze. As sample concentration varied thus leading to varying sample volumes, each was reduced to a final volume of approximately $5\mu\text{l}$ by a sequential process of freezing and evaporation under vacuum. Once frozen their volumes were reduced to $5\mu\text{l}$ using a vacuum pump. Once the pump was stopped if the volumes were not down to $5\mu\text{l}$ then the samples were placed in dry ice again. This process continued until all samples were reduced to $5\mu\text{l}$. The RNAs were then resuspended in $20\mu\text{l}$ RNA loading buffer ([appendix](#)) on ice in a fume hood. $20\mu\text{l}$ RNA loading buffer was also added to two aliquots of $5\mu\text{l}$ RNA ladders (Gibco, Paisley, UK). Both the samples and RNA ladders were heated at 65°C for 15 minutes to denature the RNA secondary structure and placed on ice. Prior to loading onto the gel $5\mu\text{l}$ RNA loading dye ([appendix](#)) was added to each sample including ladders.

2.4.6.2 Denaturing agarose gel for northern blotting

A 1% denaturing agarose was prepared to run out RNA for northern blotting. 2g agarose was weighed out, added to 147ml ddH₂O and melted in a microwave oven. The agarose was put into a water bath at 60°C to cool. 20ml 10x MOPS ([appendix](#)) was dispensed and also placed into the 60°C water bath. This was to allow easier mixing of MOPS with agarose. 33ml 37% formaldehyde was aliquoted into a 50ml tube in a fume hood and placed in a 37°C water bath.

The gel caster apparatus was set up in a fume hood ensuring it was level. Aliquoted 10x MOPS and formaldehyde were mixed in with the agarose in a fume hood making a final volume of 200ml. This was then poured into the gel caster and left to set. After 30 minutes the gel caster apparatus was dismantled and the gel was placed into a tank containing 2 litres 1x MOPS.

2.4.6.3 Running of gel

The samples were loaded onto the gel and the gel was electrophoresed at 100 volts for 10 minutes without buffer circulation. This allowed the samples to run into the gel. The power was turned off and 1µl normal BPB/XC glycerol loading dye ([appendix](#)) was loaded into the empty wells. The power was turned on again as was buffer circulation using a peristaltic pump. The gel electrophoresed until the dye front was 2/3rd down the gel.

2.4.6.4 Staining of gel and ladders

At the end of the run the buffer was discarded down the fume hood sink. The gel was trimmed and stained for 10 minutes in ddH₂O containing a few drops of 3mg/ml Ethidium bromide. The gel was washed twice in ddH₂O the once in 10x SSC ([appendix](#)). It was photographed with an UV ruler (Figure 13). The ladders were cut off and left in ddH₂O overnight to destain some more. The ladders were also photographed using an UV ruler.

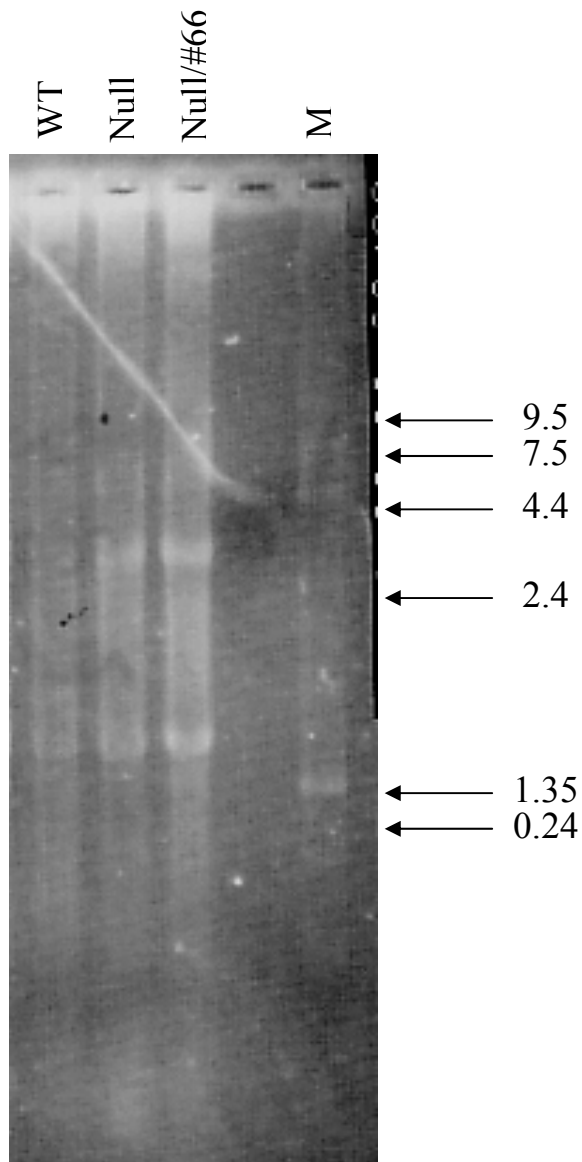


Figure 13. 12.5 μ g total mRNA separated on a denaturing agarose gel.
A) P20 *Plp1* null x #66 northern gel, WT wild type, Null *Plp1* null and Null/#66 *Plp1* null x #66, M RNA molecular ladder. **B)** Destained photograph of RNA ladder with sizes of bands in Kb.

2.4.6.5 Northern transfer and Cross-linking blot

The RNA was transferred from the agarose gel to nitrocellulose membrane by upwards capillary action. This was based on the transfer technique for DNA used in Southern blotting devised by Dr E. Southern (Southern, 1975) (Figure 14).

Three large pieces of 3MM Whatman paper were cut. Three smaller pieces of 3MM whatman paper measured to the size of the gel as well as one piece of Hybond N membrane (Amersham) were cut. Paper towels and a heavy weight were also obtained. The three large pieces of paper were wetted in 10x SSC and placed over a glass sheet placed in the centre of a tray. All air bubbles were rolled out using a clean pipette. The gel was placed in the centre of the paper, well side up and dry membrane placed very carefully on to it ensuring there were no air bubbles. The three smaller pieces of whatman paper were wetted in 10x SSC and placed on top of the membrane. Paper towels were placed over these ensuring that they were not touching around the side of the gel. A heavy weight was placed on the very top. 500ml 10x SSC was added to the tray and the transfer was left over night.

After 16-18 hours the blotting apparatus was dismantled, the gel was discarded safely and the blot UV cross-linked at optimum energy, dried and stored until required.

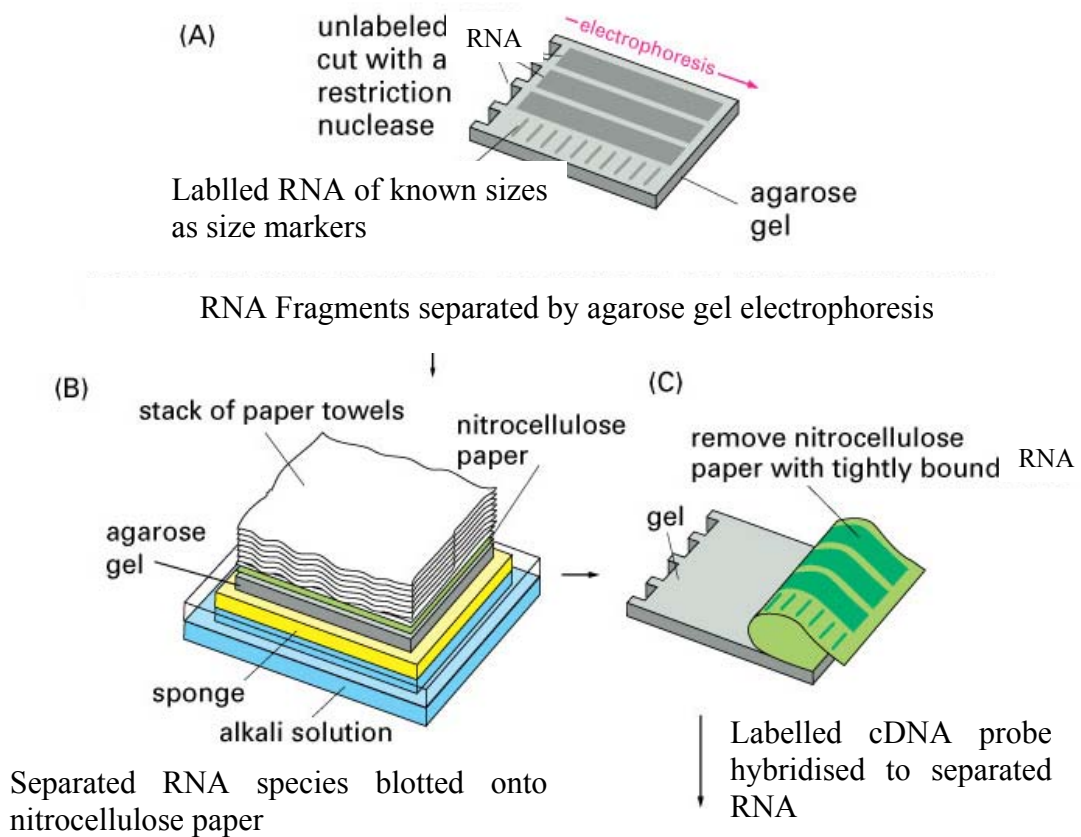


Figure 14. Northern blotting (very similar to Southern blotting method described by Southern).

A) The total RNA is separated according to length by electrophoresis. **B)** A sheet of either nitrocellulose paper or nylon paper is laid over the gel, and the separated RNA is transferred to the sheet by blotting. The gel is supported on a layer of sponge in a bath of alkali solution, and the buffer is sucked through the gel and the nitrocellulose paper by paper towels stacked on top of the nitrocellulose. As the buffer is sucked through, it denatures the RNA and transfers the single-stranded fragments from the gel to the surface of the nitrocellulose sheet, where they adhere firmly. This transfer is necessary to keep the RNA firmly in place while the hybridization procedure is carried out. **C)** The nitrocellulose sheet is carefully peeled off the gel and RNA UV-crossed link to membrane.

Figure modified from Essential Cell Biology, Second Edition.

2.4.6.6 Preparation of cDNA probe

A specific probe complementary to the target mRNA species was generated by PCR. A PCR was set up using 2µl cDNA of wild type origin with primers from exons of gene of interest (Table 2), ddH₂O and beads ([2.3.4.2 Genomic PCR](#)). In all respects including programme this PCR was identical to gDNA PCR only the product contained no introns. Specific probes for *β-actin* as a control and *Mbp* and *Plp1* as test probes were produced.

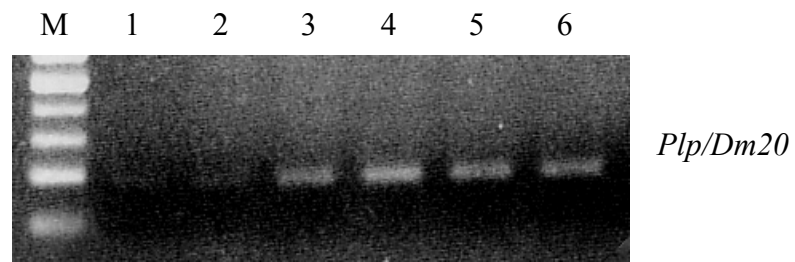
The generation of a PCR product of the appropriate size was confirmed by running a small aliquot on an agarose gel (Figure 15). The rest of the PCR product was cleaned up following manufacturer's protocol using a PCR clean-up kit (Qiagen). The final volume of EB solution added was 30µl to give a more concentrated cDNA probe product.

2.4.6.7 Incorporation of isotope

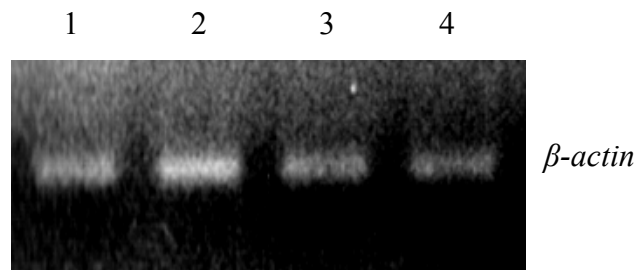
Before hybridisation of the probe to the northern blot, a radiolabelled probe is required. All appropriate precautions were taken when handling and working with radio-isotopes.

³²P αCTP was removed from -20°C and thawed on bench behind a screen. A 50µl labelling reaction contained the following: [20ng cDNA previously boiled for 5 minutes, 20µl RadPrime buffer (Invitrogen), 1µl NTPs except CTP, 2.5µl ³²P αCTP (Amersham), 1µl Kleonow enzyme and ddH₂O to volume]. The mixture was incubated for 15 minutes at 37°C.

A NICK column (Amersham) was prepared by washing it through with TE ([appendix](#)). The reaction was stopped by placing on ice and all 50µl was added to the centre of the column. 350µl TE was added and allowed to run through column allowing any unincorporated isotope to be removed and discarded. A further 400µl TE was added and collected in a screw top tube as the final probe. The cleaned probe was put into a lead container and stored at -20°C until use. All waste was disposed off either in a waste bin or down the sink. Blots were hybridised with probes 0.5x10⁶ to 1x10⁶ cpm/ml specific activity with amounts determined by liquid scintillation counting.



A



B

Figure 15. cDNA probes for northern hybridisation.

A) *Plp/Dm20* cDNA probes, the strongest probe in Lane 4 was used for northern hybridisation. **B)** β -actin cDNA probes, where again the probe with the strongest signal in Lane 2 was used for northern hybridisation.

2.4.6.8 Pre-hybridisation, hybridisation and washes

10ml RapidHyb solution (Amersham) was aliquoted into a 20ml universal and placed into a hybridisation oven (Hybaid) set at 65°C. Meanwhile the blot was wetted in 2x SSC ([appendix](#)), rolled up and put in a hybaid bottle ensuring RNA side faced in and there were no air bubbles.

100µl Salmon sperm was boiled for 5 minutes, put in ice and then added to RapidHyb solution. This was poured into the hybaid bottle containing the blot and bottle put into the oven. The bottle was rotated for 30minutes and this was the pre-hybridisation step. The probe was also boiled for 5 minutes and left on ice. The probe was added to the solution at bottom of bottle behind a screen ensuring the probe did not touch the blot at any point. After at least 2 hours the hybridisation solution was poured down the sink. The blot was rinsed quickly in the bottle with 2x SSC then high stringency wash buffer (0.1x SSC, 0.5% SDS) which had been heated in a 60°C waterbath was added. The temperature on the oven was turned down to 60°C and blot washed by rotation three times for 20 minutes each.

After the third wash the blot was removed from the bottle and sealed in a plastic bag. The blot was then taped into a cassette and exposed to x-ray film overnight at -70°C. The film was developed and exposures of various durations obtained. The blot could be reprobbed with a second cDNA probe for a control mRNA species such as *β-actin* after the initial signal had decayed usually after 3-4 weeks.

2.4.7 qRT-PCR

PCR is a popular method to amplify specific nucleic acid sequences. Reverse transcription polymerase chain reaction (RT-PCR) is an *in vitro* method of enzymatically amplifying defined regions of RNA allowing quantification of transcript produced by a certain gene. Conventional RT-PCR is an end-point quantification of transcript amounts and therefore not accurate with low resolution, low sensitivity and the results are not expressed as a number. A more accurate measurement would be of transcript amounts in each cycle of the PCR and fluorescence based qRT-PCR utilising TaqMan technology is one way to achieve this (Figure 16). Bustin (2000) and Lie *et al.*, (1998) both reviewed the principles of the method, instrumentation available and possible applications of real-time RT-PCR.

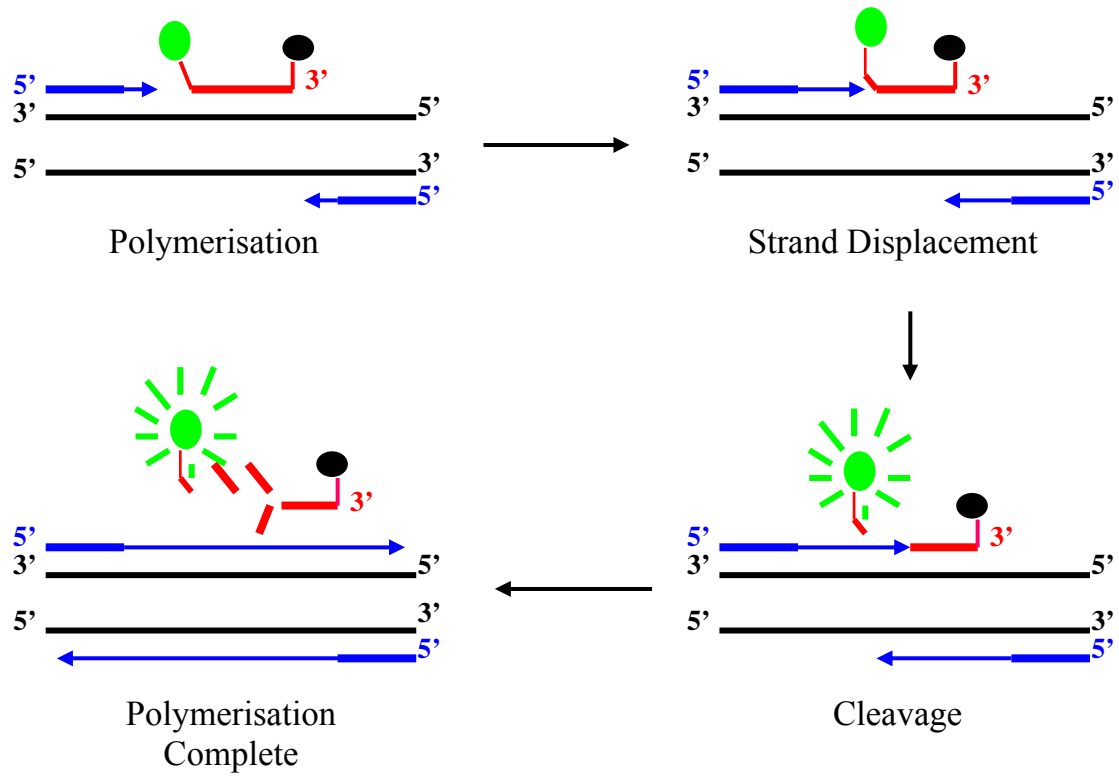


Figure 16. TaqMan technology.

Two fluorescent dyes, a reporter (green circle) and a quencher (black circle), are attached to the 5' and 3' ends of a TaqMan probe which anneals to a central region in the target sequence, when both dyes are attached to the probe, reporter dye emission is quenched, and during each extension cycle, the Taq DNA polymerase cleaves the reporter dye from the probe, once separated from the quencher, the reporter dye emits its characteristic fluorescence.

Both one- and two-step real-time RT-PCRs are possible. In two-step RT-PCR the total RNA is first used to produce cDNA by reverse transcription then the qRT-PCR step using fluorescence is carried out. This process is time consuming and also limited by sample handling numbers by the operator. Also required are two kits, one to complete the RT step and one for the PCR step. The one-step qRT-PCR requires one kit to carry out both the RT and PCR steps in the one tube. This kit can be expensive but the time saved counteracts this. The one-step RT-PCR was utilised in this study due to the number of samples. However, choice of real-time RT-PCR method is only one of the decisions required and Bustin (2002) reviewed practical issues and problems with this technique.

2.4.7.1 Sample/tissue collection ([see section 2.4.1](#))

2.4.7.2 RNA Preparation ([see section 2.4.2](#))

2.4.7.3 RNA Quantification and Quality Check ([see section 2.4.3](#))

2.4.7.4 qRT-PCR primers and probes

The Primer Express program (Applied Biosciences) was used to design possible primer and probe sets from the relevant mRNA sequences following guidelines laid out by Dorak. The primer/probes sets were selected using the program's recommendations and taking any limits into consideration. The accession numbers for the mRNA sequences and selected primer/probe sets are shown in Table 2. Primer and Taqman probes for *Plp1* and *Mbp* were to amplify transcripts for all the isoforms produced by the genes and were labelled *Plpall* and *Mbpall* respectively. Primers and TaqMan probes were purchased from MGI with a blackhole quencher on the 3' end and a 6-Fam reporter on the 5' end of the TaqMan probe. These were stored in the dark at -20°C until required.

2.4.7.5 qRT-PCR on ABI 7500

The ABI 7500, a Personal Computer (PC) based real-time PCR machine was utilised for this study. The threshold, baseline setting and internal ROX dye (from kit) as a reference remained the same for all reactions with all primer and probe sets. These were set from the standard curves produced for each primer and probe set.

2.4.7.5.1 Primer and probe reconstitution

Both the primers and probes were reconstituted to a stock concentration of 100µM with DEPC treated water. Once reconstituted, the primers and probes were diluted to 10µM working stocks with DEPC treated water. 100µl and 50µl aliquots of the probes were made, the tubes wrapped in foil, placed in a light resistant bag and stored at -20°C. MGI

recommend no more than two freeze thaws for the probes as it reduces the fluorescence emitted during real-time PCR.

2.4.7.5.2 Primer and Taqman Probe Optimisation

A 96 well plate was set up with various combinations of forward and reverse primers and a set concentration of probe (100nM) to optimise the PCR reaction (Table 3). 50ng wild type RNA per reaction was utilised as the template for all optimisation reactions. As this was a one-step RT-PCR the SuperScript III Platinum One-Step qRT-PCR kit (Invitrogen) was used to perform the experiment on the ABI 7500. The basic PCR program was 50°C for 2 mins; 95°C for 10 mins; 40 cycles of 95°C for 15 secs, 60°C for 60 secs. The total run was 2 hour however, the initial 50°C was extended to 30 mins to reverse transcribe the cDNA from the RNA template. In order to ensure the entire product was amplified the 60°C for 60 sec step was altered to best match/fit the melting temperatures for all three primer and probe sets and also extended to 2 mins.

The primer pair that gave the highest deltaRn and the lowest Ct (cycle at which threshold is crossed) was chosen for each primer set (800nM/800nM) (Figure 17). The same process of optimisation was carried out for the probe with varying concentration of the probe used with the most efficient primer concentrations.

2.4.7.5.3 Test plate set-up

96 well plates (ABgene) were used to set the real-time RT-PCR experiments. A standard curve was generated using serial dilutions of an abundant wild type RNA sample (Figure 18). Dilutions of 1000ng, 100ng, 10ng, 1ng, 0.1ng and 0.01ng were used with β -actin primers and probe initially, then the other primer/probe sets. Each sample was loaded in the duplicate for the standard curve

The ideal assay will have a slope of -3.3 with a R^2 of 0.99999 (as close to 1 as possible). The standard curves were optimised using the PCR conditions, threshold and baseline settings until as close to the ideal as possible. Once the conditions to achieve a good standard curve were obtained they were applied to the plates with test samples.

	Forward primer			
Reverse primer	800 nM	400 nM	200 nM	50 nM
800 nM	800/800	400/800	200/800	50/800
400 nM	800/400	400/400	200/400	50/400
200 nM	800/200	400/200	200/200	50/200
50 nM	800/50	400/50	200/50	50/50

Table 3. Optimisation of the forward and reverse primers for real-time RT-PCR

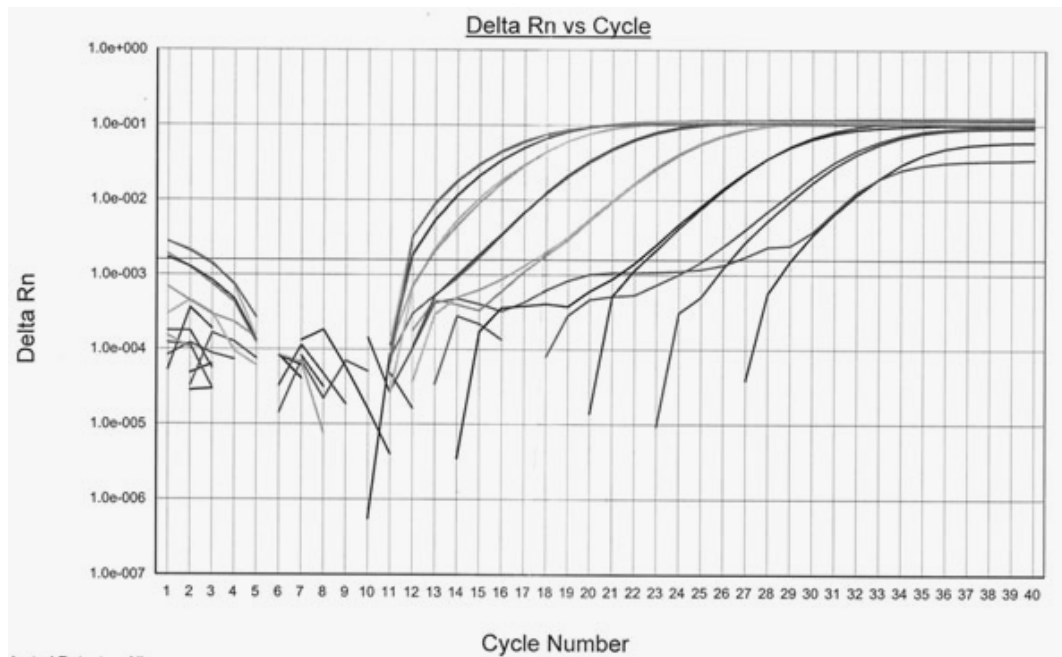


Figure 17. An example of the typical output from the ABI 7500 showing the increase in signal at each cycle.

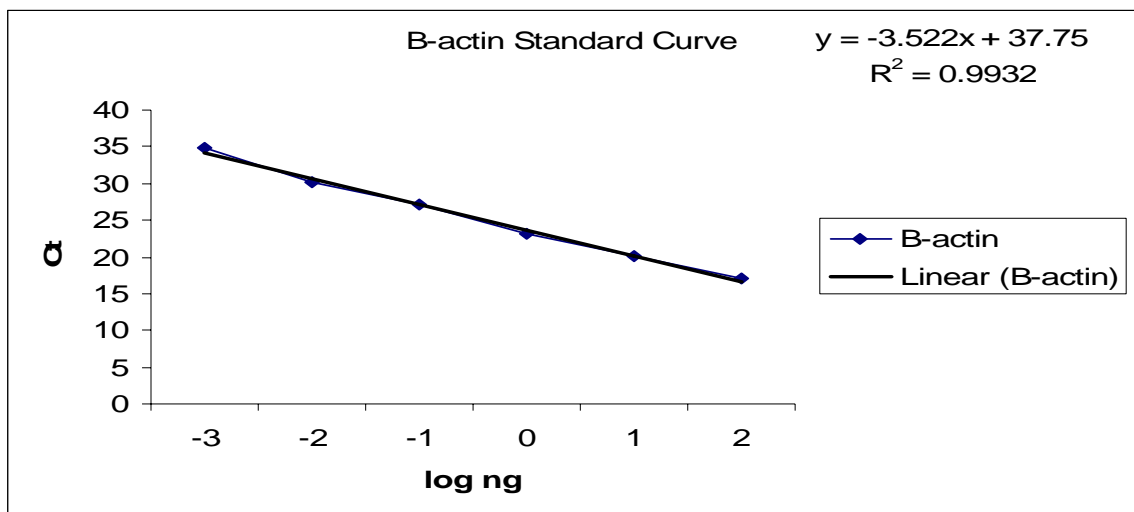


Figure 18. Standard curve produced from serial dilutions of wild type RNA and β -actin primers and probe set.

2.4.7.5.4 Set up of reaction plate

Each plate was set up to include all the wild type, hemizygous and homozygous samples available for that experiment with all three primer/probe sets if possible to reduce variability between the reactions. This also ensured the threshold and baseline settings were the same for the reactions.

2.4.7.5.5 Analysis of results

The standard curve produced is then used as a reference standard for extrapolating quantitative information for mRNA targets of unknown concentrations. The use of absolutely quantitated RNA standards helps generate absolute copy number data. The variation introduced due to variable RNA inputs, can be corrected by normalisation to a housekeeping gene. The other method of analysis, the comparative C_t method was not utilised in this study.

The C_t values from each sample were then used for the analysis. The calculation is as follows $(C_t - \text{intercept})/y$ or slope value then \ln LOG. This is the un-normalised amount in ng of message in initial 50ng total RNA sample. The average of the duplicated or triplicated values are then normalised to β -actin values (ng Test/ng β -actin) to give the final normalised message amount in initial 50ng total RNA used.

2.5 Protein Analysis

2.5.1 Tissue/Sample Collection

Mice were killed by CO_2 asphyxiation; tissues rapidly removed and snap frozen in liquid nitrogen in labelled freezer tubes. The tissue was stored at -80°C until required.

2.5.2 Isolation of Myelin proteins

This technique was used to extract myelin from CNS tissue and is based on the method of Norton and Poduslo (1973). The principle is based on centrifugal enhanced flotation of the myelin fraction due to the highly buoyant nature of lipids. By-products of the technique include the pellet fraction containing the membranous and nuclear components of the spinal cord and brain homogenate and supernatant fraction is enriched in cytoplasmic components.

2.5.2.1 Myelin preparation

Firstly the cord was thawed in 7.5ml high sucrose buffer (0.85M sucrose, 10mM Hepes, 2mM Dithiothreitol (DTT) and 1mM N α -p-tosyl-L-lysine chloro-methyl ketone (TLCK)) and homogenised using an ultra turrax polytron homogeniser at high speed for 12-15 strokes. 500 μ l of this total homogenate were removed and frozen. For tissue dissected from P3 mice only the total homogenate was produced. For older (P20 and P60) mice the remainder of the total homogenate was transferred to a Beckman centrifuge tube and overlain slowly with 3ml of buffer (0.25M sucrose, 10mM Hepes (pH7.4), 3mM DTT) and centrifuged at 70,000g for 90 minutes at 4°C using SW41 rotor on a Beckman ultracentrifuge. This produced a biphasic solution with cellular debris left in the lower phase (0.85M sucrose) and myelin protein trapped at the interface between the 0.25M/0.85M phases. The myelin haze between the two phases, the supernatant from lower phase and the pellet were removed and also kept. When CNS tissue is homogenised myelin spontaneously forms micelles. Trapped within the micelles are also cytoplasmic components. Hypotonic shock bursts open micelles and helps wash away contaminants. 6ml of ddH₂O was added to the myelin sample and this was centrifuged at 23,000g for 30 minutes to sediment the protein. The supernatant was discarded and the process was repeated another two times with the final centrifugation at 17,000g to ensure that only proteins were sedimented. The protein pellet was resuspended in 100 μ l of ddH₂O.

2.5.2.2 Lipid Raft Preparation

PLP and DM20 are known to associate in CHAPS insoluble lipid rafts. Lipid rafts can be isolated from the myelin fraction by density gradient centrifugation as different lipids float differently (Simons *et al.*, 2000). Myelin can further be fractionated into lipid rafts using a method modified from Simons and colleagues (2000).

250 μ g myelin from wild type and homozygous brain were utilised to prepare the lipid rafts. 250 μ g myelin was added to 60 μ l 5xTE ([appendix](#)) (final concentration 1xTE), 30 μ l CHAPS (20mM) and added ddH₂O to make a final volume of 300 μ l. Each sample incubated with rotation at 4°C for 30 mins. For the density gradient centrifugation, a discontinuous gradient was prepared. After rotation, 300 μ l sample was added to 600 μ l Optiprep (60%) to make a 40% solution. This was overlaid with 1.2ml 30% Optiprep (600 μ l 5xTE, 900 μ l ddH₂O and 1.5ml Optiprep, 3ml total volume) and finally 500 μ l extraction buffer. The samples were centrifuged for 2hrs at 40,000rpm in a SW50.1 rotor (Beckman). Six fractions of 430 μ l were collected and labelled 1-6. Fraction 1 was the

lightest (at top) and fraction 6 the heaviest (at bottom). After quantification the samples were treated as normal to prepare a western blot or phosphorimage if radiolabelled samples used.

2.5.2.3 Protein Assay

Total protein concentrations were quantified in order to ensure equal loading of samples on subsequent SDS-Page gels.

The assay was performed using the Pierce protein BCA assay system (Perbio) based on the Lowry Method using bicinchoninic acid (BCA) as the reagent. The reaction was initiated by the addition of the reagent and incubated at 37°C for 30 minutes. 2mg/ml BSA standards (Perbio) were diluted (0.025, 0.05, 0.1, 0.2, 0.4, 0.6mg/ml) and prepared at 10X the concentration of the samples which were routinely 5µl of sample/1ml of reaction reagent. Measurement of the absorbance of the final product was performed on a spectrophotometer (Cecil 1100) set to a wavelength of 562nm. A standard curve was generated and the sample concentrations calculated from this.

2.5.3 Western Blotting

The transfer of size separated proteins onto a membrane was described by Burnette (1981).

2.5.3.1 Sample preparation

Aliquots of the protein samples (1-2.5µg of myelin extracts and 10-15µg of total homogenate extracts dependant on protein investigated) were made up to a volume of 24µl in 3x Sample buffer (62.5mM Tris (pH6.8), 40mM DTT, 5% 2-mercaptoethanol, 0.002% bromophenol blue, 2% SDS, 10% glycerol) and denatured by placing in water heated to 90°C for 5 minutes. The process linearises the protein with the addition of SDS to give an unique negative charge and permit migration towards the anode. Separation is based in size. The samples were loaded onto the gel with size markers as controls for transfer efficiency.

2.5.3.2 SDS PAGE (sodium dodecyl (lauryl) sulphate polyacrylamide gel electrophoresis)

At the onset of the project hand-poured gels from stock solutions were utilised (Table 4). However precast gels were employed later for safety, convenience and economy of time. Precast gels employed were NuPage 4-12% 10 or 12 well (Invitrogen) with MES Page buffer (Invitrogen). Both types of gels were run with identical samples to investigate the

efficiency, speed and resolution of each with both types to buffer and showed no difference.

2.5.3.3 Protein electrophoresis

Hand-poured gels were electrophoresed in SDS-PAGE running buffer ([appendix](#)). Pre-cast gels were electrophoresed in a discontinuous buffer system using 1x MES buffer (Invitrogen). The samples were electrophoresed for 1 hour at 100volts to resolve the proteins. Towards the end of this project the hand-poured gels were replaced with precast gels. The resolution and sensitivity of the western blots were not significantly different.

2.5.3.4 Electrophoretic protein transfer

The gel was removed from the plates, wells were cut off and the gel was placed in cathode buffer. The proteins were transferred to PVDF membrane (Millipore) using a semi dry blotter and a buffering system based on the Towbin method which enabled the transfer ([appendix](#)). The transfer was carried out at 225mA for 1 hour. To confirm the transfer was successful the blot was stained briefly with Ponceau S (0.1% Ponceus S w/v, 5% Acetic acid v/v), a water soluble stain which highlighted the separated proteins and allowed a visible inspection of loading.

2.5.3.5 Immunostaining

The membrane was blocked for 2 hours at room temperature or overnight at 4° C by soaking in blocking buffer containing 5% dried milk in 0.1% TritonX-100 in TBS (pH 7.4) to ensure no non-specific proteins were picked up by the antibodies. Blocking buffer was removed and antibody in freshly 5% dried milk in 0.1% TritonX-100 in TBS (1x T-TBS) (pH 7.4) was added for at least 2 hours or overnight at 4° C (Table 5). The membrane was washed repeatedly in T-TBS (pH 7.4) for 3 x 10 minutes and the appropriate secondary antibody conjugated to horse radish peroxidase (HRP) was applied at 1:10,000 in 5% dried milk in T-TBS (pH 7.4) for 60 minutes. The membrane was washed again in T-TBS (pH 7.4). The membrane was incubated in equal volumes of luminol enhancer solution and stable peroxide solution (both from Amersham) for five minutes at room temperature, dried slightly and wrapped in Saran wrap. X-omat imaging film (Agfa) was exposed to the membrane for a range of exposures to give optimal signals. The film was developed in an automatic processor (Dupont Cronex CX-130).

	12.5%	14%	Stacker (4%)
Acrylamide	8.3ml	9.7ml	880µl
1.5M Tris pH8.8 (Resolver) 0.5M Tris pH6.8 (Stacker)	5.0ml	5.0ml	1.64ml
10% SDS	200µl	200µl	30µl
10% Ammonium Persulphate	150µl	150µl	75µl
MilliQ H ₂ O	6.4ml	5.0ml	4.0ml
Temed	10µl	10µl	9µl

Table 4. Volumes for hand-poured SDS-PAGE gels.

Primary antibody	Host	Dilution	Target	Source
226	Rabbit Polyclonal	1:20,000	Myelin, mature oligodendrocytes	NP Groome
AA3	Rat Monoclonal	1:5,000	Myelin, mature oligodendrocytes	S Pfeiffer
ASPA	Rabbit Polyclonal	1:1,000	Oligodendrocyte marker	J Garbern
β -actin	Mouse Monoclonal	1:1000	Actin	Sigma
CNP	Mouse Monoclonal	1:500	Myelin, mature oligodendrocytes	Chemicon
GFAP	Monoclonal, Polyclonal	1:250,000	Astrocyte marker	Dako
MAG	Monoclonal, Polyclonal	1:10,000	Myelin, mature oligodendrocytes	Chemicon, NP Groome RH Quarles
MBP	Mouse monoclonal Rabbit polyclonal	1:5,000	Myelin, mature oligodendrocytes	NP Groome Chemicon
BiP	Rabbit polyclonal	1:5,000	ER Stress response	Stressgen
Anti-Rabbit 2°		1:10,000		New England Biolabs
Anti-Mouse 2°		1:10,000		New England Biolabs
Anti-Rat 2°		1:10,000		New England Biolabs

Table 5. Primary and Secondary Antibodies used for western blotting.

2.5.4 Oligodendrocytes Cultures

2.5.4.1 Primary cell culture

Oligodendrocytes were prepared from the spinal cord of postnatal 5 day animals. The animals were euthanased in a halothane chamber and decapitated to ensure exsanguination. The tail was removed and frozen and part of the brain stem and spinal cord was placed in bottle containing Karnovsky's modified fixative for aid genotyping (Montague *et al.*, 1998).

Using sterile technique and with the aid of a dissecting microscope the spinal columns were removed and the cord dissected out into Hanks balanced salt solution (HBSS) (Invitrogen). The meninges were stripped from the cord and the cord masticated with a sterile scalpel. The connective tissue of the cord was digested by the addition of 2ml 0.25% trypsin and 200µl 1% collagenase and incubation at 37°C for 1hour. The digestion was quenched by the addition of 1ml stop solution ([appendix](#), Fanarraga *et al.*, 1995). The cord was then triturated through 23g needle (three times) and 26g needle (three times) before the addition of 10ml Dulbeccos modified eagle medium (DMEM) (Invitrogen) containing 10% Foetal bovine serum (FBS) (Invitrogen) and centrifugation at 800rpm for 5minutes. The supernatant was removed and the pellet resuspended in 1ml DMEM containing 10%FBS. The cell density was determined and plated out in 2x35mm poly-L-Lysine coated dishes at an approximate density of ~250,000 cells/dish. The cells allowed to settle down onto the plate for 2 hours at 37°C 5%CO₂ before the addition of 1.5ml Sato conditioned medium ([appendix](#), Fanarraga *et al.*, 1995). The cells were grown in culture for at least six days with medium change every second/third day. At harvest the cultures comprised 70-80% O4 positive cells along with astrocytes, occasional neurons and other cells (McLaughlin *et al.*, 2006).

2.5.4.2 Charaterisation by Immunostaining

Paraffin and resin (Trapp *et al.*, 1981) sections were stained for PLP/DM20 and MBP using either the PAP or the ABC techniques. Immunostaining for caspase-3 and the CC-1 antigen was carried out on cryosections from animals perfusion fixed with 4% paraformaldehyde. Sections were washed in PBS for 20 min followed by 0.5% Triton X-100/PBS 30 min at room temperature, and blocked in 0.1% Triton X-100, 0.2% pigskin gelatin in PBS for 30 min at room temperature. Primary antibodies were applied overnight at 4°C and the secondary fluorescent conjugates for 30 min at room temperature, in the blocking buffer.

Cryosections were fixed in 4% paraformaldehyde for 20 min at room temperature and treated with 50% HCl/1% Triton X-100 for 10 min at room temperature. Sections were permeabilised with methanol for 10 min at -20°C, before primary antibodies were applied overnight at 4°C. Sections stained for CC-1 antigen were labelled with 4, 6-diamidino-2-phenylindole (DAPI) 2.2 µg/ml in ddH₂O for 1 min at room temperature. To determine the nature of the apoptotic cells, sections stained for caspase-3 were double labeled with various cellular markers. All cryosections were mounted in Citifluor antifade medium.

2.5.4.2.1 Immunostaining of coverslips

For immunochemistry cells were plated out onto coverslips at ~20,000 cells in a volume of 140µl /coverslip. The cultures were incubated for 7days at 37°C 5%CO₂ with the media being changed every two days before harvesting. Although the cultures were a mixed population of cells including neurons and astrocytes the conditioned growth medium employed favoured oligodendrocyte proliferation. All immunostaining was carried out under aseptic conditions. O10 antibody is used to label PLP on live cells when it reaches the surface of the cell in a certain conformation (Sommer *et al.*, 1982). The existing media was drained from each coverslip and 100µl O10 antibody (diluted 1:6 in SATO media) was added. The coverslips were left to incubate for 1 hour at RT then washed 5-6 times in media. Secondary antibody mouse IgM texas red was added at 1:50 dilution in media and incubated for 30 mins at RT. The secondary antibody was washed off with 1x PBS and 150-200µl 4% paraformaldehyde was added for 15 mins thus fixing the cells. Once again the coverslips were washed with 1xPBS and ice cold 20% methanol was added for 10 mins to permeablise the cells. The coverslips were then washed well with 1xPBS 5-6 times one coverslip at a time to avoid drying out.

Double staining was carried out to label surface and internal PLP/DM20 within the cultured cells. 100µl AA3 antibody diluted 1:10 in 1% Normal Goat Serum was added and coverslips kept at 4° over night. 18-20 hours later the coverslips were washed 5-6 times in 1xPBS. Secondary antibody rat FITC diluted 1:50 in PBS was added for 30 mins. The coverslips were again with 1xPBS and DAPI was added at 1:1200 in PBS for 1 min before mounting face down onto slides with a drop of citifluor. The coverslips were sealed with clear nail varnish ready to view with fluorescence microscope.

2.5.4.3 Harvesting for Biochemistry

The 35mm dishes were removed from the incubator and placed on the bench. All media was removed using either a tip or pipette and put into a beaker for waste. The dishes were then rinsed with 1ml chilled PBS twice. At this stage the second and final rinse with PBS was removed and either the dishes were snap frozen in liquid nitrogen or 75µl lysis buffer ([appendix](#)) was added on ice.

If the dishes were frozen then they were stored in -80°C until needed. If lysis buffer was added, cells were scraped using a cell scraper and buffer transferred to 1.5ml tube. The samples were then rotated for 30 minutes at 4°C to achieve complete cell lysis. Following a 5000g spin for 5 minutes at 4°C the supernatant was transferred to a fresh tube and stored at -20°C.

2.5.4.4 Radiolabelling for dynamic investigation

For investigating protein turnover dynamics [³⁵S]-Pro-Mix (cysteine/methionine) (Amersham) was added to the serum free HBSS. The hot amino acids were incorporated into all newly synthesised proteins over time and the rate of nascent protein formation could then be measured using a phosphorimage cassette which generates an autoradiographic image.

The initial few steps were the same regardless of type of dynamic study. The media was removed and 1.5ml of fresh warmed Sato media was added to the cultures which were incubated for 2 hours at 37°C 5%CO₂. 50ml HBSS was prepared and put into the 37°C waterbath. After 2 hours the SATO media was removed and each dish was washed with 1ml HBSS. 1ml HBSS was then added and cultures incubated for 30 minutes at 37°C 5%CO₂. This starved the cells allowing for a more efficient uptake of isotope when it was added. For each spinal cord used for culture 2 dishes were plated and for each cord 100µCi (3.7MBq) of [³⁵S]-Pro-Mix was added to 1ml of HBSS. At this stage the steps differ depending on type of study (see below). Due to mixed litters from hemizygous/hemizygous crosses and the necessity for genotyping only two time points were achievable from individual animals in any of the primary cultures studies.

2.5.4.4.1 Synthesis

To investigate synthesis two time points for incubation with isotope were selected, 45 minutes for one dish and 90 minutes for the second dish. This would enable the study of

levels of newly synthesised protein over a doubling in time. After 30 minutes the HBSS was removed and 500µl HBSS containing [³⁵S]-Pro-Mix was added to each dish. The cultures were incubated for 45 minutes or 90 minutes at 37°C 5%CO₂. After the first time point one dish was washed quickly with HBSS then three times with ice cold PBS and snap frozen. The second dish was washed with HBSS and as with the first dish washed with ice cold PBS three times and snap frozen.

2.5.4.4.2 Degradation of proteins using Pulse/Chase experiments

Degradation was determined by the pulse chase technique. This involves radiolabelling proteins during a short pulse period and monitoring their fate “chase” by saturating the cells with cold amino acids. To investigate decay of proteins, cells were labelled for 60 minutes, the pulse phase and chased by replacing the HBSS with Sato medium supplemented with 2.5mM cysteine/2.5mM methionine for 24 hours.

After 30 minutes the HBS was removed and 500µl HBSS containing [³⁵S]-Pro-Mix was added to each dish. After 1 hour the HBS was removed then each dish was washed once with HBSS. One dish labelled 0 hours (T₀) was washed with chilled PBS and snap frozen. The second dish labelled 24 hours was chased by adding Sato medium supplemented with 2.5mM cysteine/2.5mM methionine. After 24 hours incubation at 37°C 5%CO₂ the second dish was washed with PBS as before and snap frozen.

2.5.4.4.3 Blocking of Degradation

The nature of the biochemical pathway involved in protein decay can be determined by including specific inhibitors during the chase phase of the experiment. The cultures were treated as before and put through the pulse phase of the experiment. To show that the chosen compound had an effect initially both dishes were put through the chase, one with media containing the compound and the other either ddH₂O or solvent the compound was made up in.

As before on day 6 the cells had fresh SATO added then HBS. After 30 minutes the HBS was removed and 500µl HBSS containing [³⁵S]-Pro-Mix was added to each dish. After 1 hour the HBSS was removed and each dish washed once with HBSS. The two dishes were chased by adding Sato medium supplemented with 2.5mM cysteine/2.5mM methionine. The Sato for one dish labelled 24 hours + also contained 50µM MG132 and the other labelled 24 hours - contained an equal volume DMSO as MG132 was dissolved in this.

Both dishes were incubated for 24 hours at 37°C 5%CO₂ after which they were washed with chilled PBS and snap frozen.

Once it was confirmed the compound in this case MG132 was having an effect on rate of degradation then pulse/chase experiments were set up. One dish was snap frozen directly after the pulse phase and labelled 0 hour. The second dish labelled 24 hours + was put through the chase phase with Sato medium supplemented with 2.5mM cysteine/2.5mM methionine and 50µM MG132.

All these cultures were lysed in the same way as previously described ([2.5.4.3 Harvesting for Biochemistry](#))

2.5.5 Synthesis at P20

In order to investigate PLP dynamics in a system containing an oligodendrocyte, myelin and axon unit, a brain slice system was employed. This investigation involved generating the 300µm thick slices of brain and maintaining them in a metabolically active state oxygenated artificial CSF media supplemented with [³⁵S]-Pro-Mix. A proportion of the slices were removed over set periods of time and levels of newly synthesised radiolabelled protein studied. Prior to the dynamics study a series of experiments were carried investigating the stability of the system (Figure 19).

2.5.5.1 Brain slice

250ml Kreb's buffer (pH 7.4) ([appendix](#)) was prepared and oxygen (95% O₂ 5% CO₂) was bubbled through it for at least 30 minutes. The pH was re-checked and flow of the oxygen bubbling was continued. Following rapid removal, the brain was halved through the midline and each half immersed in a 2% agarose DMEM solution and allowed to solidify on ice. This allowed vibratome sections to be prepared and minimised movement and distortion of the brain during slicing.

A P20 male mouse was sacrificed with CO₂, the brain was dissected out and placed in chilled O₂ saturated Kreb's buffer in a Petri dish. The meninges were striped using fine forceps and the brain was cut in half down the midline. Each half was transferred to fresh chilled buffer. The agarose was transferred to a beaker in the 37°C waterbath to cool and the foil cups were put on ice then the cooled agarose was poured into the foil cups. Each brain hemisphere, held by the cerebellum as straight as possible, was submerged in the

agarose. The hemispheres in their individual moulds were carefully orientated so the frontal lobes were pointing down. The agarose was left to cool and set.

The foil cup was removed from around one hemisphere. The agarose cylinder was placed on its side and cut through by the cerebellum, this surface acted as a base. The cylinder was stood on its base and the excess agarose was trimmed from the top to the base to form a pyramid like structure. One half razor blade was wiped and placed onto the vibratome. Some superglue was added to the vibratome platform and the tissue block was gently pressed onto it. The platform with block was put in place and wound down to start.

Chilled Kreb's buffer was gently dropped into blade and block using a glass pasteur pipette. The block was trimmed at 600µm until the blade reached the tissue. 300 micron thick slices were continuously cut from the tissue; ensuring chilled buffer was added as the blade was slicing. The slices were transferred to a petri dish containing chilled Kreb's buffer. Slicing was stopped when the cerebellum was reached. The agarose around each slice was removed and the same was done for the 2nd hemisphere of the brain.

Once both hemispheres were cut and agarose removed, the slices were transferred to a flask containing 10ml room temperature O₂ saturated buffer. 5ml was removed and a fresh 5ml added. The slices were incubated for 10 minutes at RT with oxygenation. 5ml was again removed and replaced with fresh buffer, the slices were gently agitated and 5ml buffer removed, leaving the slices in 5ml buffer. This process diluted any cellular components such as proteolytic enzymes that could have been released by ruptured cells.

Before the actual experiments were carried out a test of the actual slice protocol was undertaken. The brains of two wild type animals were used for the test. One half of one brain was homogenised without slicing and the other half of the brain was sliced then immediately homogenised. One half of the 2nd brain was sliced and treated as a normal slice experiment without any isotope in the Kreb's buffer. The other half was treated the same except the addition of MG132 into the buffer. The resulting fractions from the myelin preparation were separated on a gradient NuPage gel and the blots stained for MBP (Chemicon, Chandlers Ford, UK) (Figure 19)

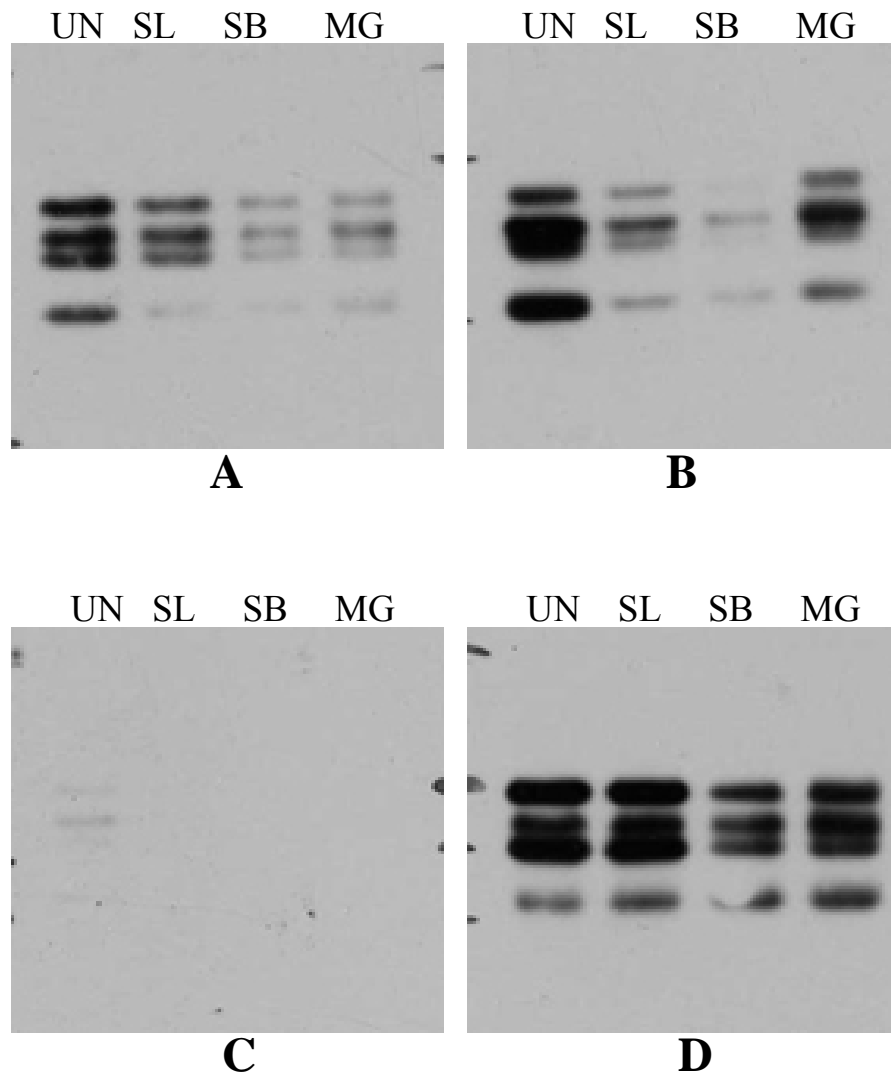


Figure 19. Test brain slice experiment.

A) MBP signal in 15µg total homogenate. **B)** MBP signal in 15µg pellet fraction. **C)** MBP signal in 15µg supernatant. **D)** MBP signal in 1µg myelin fraction (also showing the enrichment of MBP from total homogenate to myelin) (UN unsliced brain half, SL sliced brain half, SB sliced buffered half and MG sliced half buffered in presence of MG132).

2.5.5.2 Isotope incorporation

Once the slices were washed and had equilibrated in the buffer the [³⁵S]-Pro-Mix could be added to start the experiment. The flask containing slices in 5ml Kreb's buffer was transferred to the 37°C waterbath with gentle agitation and continual oxygenation. After 10 minutes [³⁵S]-Pro-Mix (100µCi/ml) was added to start the experiment. Dependant on the experiment, the slices were removed at certain time points of incubation.

For synthesis and incorporation studies the slices were removed at 2, 4 and 6 hours after the addition of isotope. The slice experiments were not left for longer than 6 hours as the integrity of the slices was comprised as demonstrated by a lactate dehydrogenase (LDH) assay which is measured to evaluate the presence of tissue or cell damage (McLaughlin, M. personal communication). The slices were washed three times in a 15ml tube with 10ml RT Kreb's buffer. After the final wash as much of the buffer was removed as possible using a 1000µl tip and pipette, and snap frozen in tube with liquid nitrogen. The slices were stored at -20°C short term or -80°C long term.

2.5.5.3 Myelin prep ([2.5.2.1 Isolation of Myelin proteins](#))

2.5.5.4 Protein Assay ([2.5.2.1 Protein Assay](#))

2.5.5.5 Covalent linking of Antibodies to sepharose beads

The covalent linking of antibodies to sepharose beads allows the precipitation of the relevant protein from a tissue or cellular lysates. pH is important in this experiment as the change in pH for one solution to the other allows the proteins to bind to the antibody and beads, be washed while bound and then be eluted off. AA3, an anti-PLP antibody was used for PLP/DM20 immunoprecipitations (Yamamura *et al.*, 1991).

Prior to carrying out immunoprecipitation covalently coupled beads with required antibodies were needed. This method allows covalent linking of antibody molecules to sepharose beads. The coupled bead then can be utilised to extract a specific protein from a sample to which the antibody is targeted. Dependent on the antibody two types of sepharose bead are available. Protein A Sepharose beads are better for cross-linking to polyclonal and Protein G Sepharose beads for monoclonal antibodies.

Initially 200µl beads were washed three times in 1ml PBS to remove any alcohol from the beads and resuspended in a final volume of 1ml PBS. 10-50µl of antisera was added to beads dependent of efficiency of antibody. The sample was then rotated for 1-2 hours at

4°C. After rotation the beads were washed three times in 100mM sodium borate pH 9.2 and resuspended in 900µl sodium borate pH 9.2. 100µl 200mM DMP (dissolved in sodium borate pH 9.2) was added and the sample rotated for a further 30 minutes at room temperature (RT). This step was repeated (900µl +100µl RT). Once the beads had been rotated twice with DMP they were washed three times with 50mM glycine pH 2.5. Then the beads were washed further with 50mM Tris pH 8.0 three times and finally resuspended in 1ml 50mM Tris pH 8.0 and stored at 4°C until required.

2.5.5.6 Immunoprecipitation and western blotting

Using antibody coupled beads immunoprecipitation (IP) was performed on the radiolabelled protein samples. This allowed the extraction and study of specific proteins from the mixture of proteins obtained from a myelin preparation. Using sepharose beads coupled with AA3 antibody (Yamamura *et al.*, 1991) ([2.5.5.5 Covalent linking of Antibodies to sepharose beads](#)) immunoprecipitations were performed on either radiolabelled protein extracts from brain slices or oligodendrocyte cultures.

Four fractions of proteins were obtained from brain slices; total homogenates, pellet (containing membranous organelles), supernatant (containing mainly the cytosolic components) and the myelin fraction. Set amounts of protein were used for each IP. For the total homogenate, pellet and supernatant fractions 200-400µg protein was utilised. 20 times less protein was used from the myelin fraction (10-20µg). This ratio gave a roughly equal signal of PLP/DM20 from the total and myelin fractions, highlighting the enrichment of PLP/DM20 in myelin. The amounts selected were determined by the yield recovered from the homozygous mice which produce the least amount of myelin.

The appropriate volume of protein for each sample was added to a 1.5ml tube to which 1ml lysis buffer ([appendix](#)) was also added. The samples were rotated at 4°C for 30 minutes. The tubes were then centrifuged at 5,000 rpm for 5 minutes also at 4°C. The supernatant was transferred to a fresh tube containing 40-50µl AA3 coupled beads. The samples were then rotated for at least 4 hours or overnight at 4°C. During this rotation PLP/DM20 bound to the antibody linked to the beads.

After the rotation the beads were washed three times with chilled wash buffer (1x TBS, 1% Triton X 100). On the final wash all the supernatant was removed ensuring no beads were lost. 8µl 3x SB with DTT giving a final 1x concentration was added to each tube and the

beads were then either stored at -20°C until use or heated in waterbath at 90°C for 6 minutes.

2.5.5.7 Phosphorimage

Once heated the samples were separated out on a hand poured SDS-Page gel or a pre-cast Nu-Page gel ([2.5.3.3 Protein electrophoresis](#)). The proteins were transferred onto PVDF membrane as described previously ([2.5.3.4 Electrophoretic protein transfer](#)). Once transferred the blot was air dried rather than blocked with 5% milk and wrapped in saran wrap. The blot was then put down on a Phosphorimage screen (Fugi) for a short exposure of a few days and a long exposure of two weeks. The screen was scanned using a STORM scanner (Molecular Dynamics). Each image was then analysed using the Image Quant programme.

2.5.5.8 Reprobe blot

Once all exposures were obtained from the blot, it was reprobbed with the appropriate antibody to ensure loading was equal across the gel. The blot was activated by placing it in a dish containing methanol for 1 min. After a quick wash with 1x TBS-T the blot was then blocked with 5% milk for 1 hr. The blocking milk was poured off and milk containing antibody was added. In most cases the antibody used was 226 in a 1:20,000 dilution. The immunostaining process continued as previously described ([2.5.3.5 Immunostaining](#)) and the exposed films developed to provide images of the blot.

2.6 Myelin Morphology/Analysis

2.6.1 Tissue Fixatives and Fixation

2.6.1.1 Karnovsky's modified fixative (paraformaldehyde/glutaraldehyde 4%/5%)

Karnovsky's modified fixative ([appendix](#)) was used for the preservation of tissues for resin embedding before light and electron microscopy.

2.6.1.2 4% Paraformaldehyde in PBS

4% paraformaldehyde in PBS ([appendix](#)) was used for the preservation of tissues used for immunohistochemistry and for post fixation of cryopreserved sections.

2.6.1.3 Immersion

Brain and spinal cord from mice under 10 days were immersion fixed in Karnovsky's modified fixative prior to identification of genotype.

2.6.1.4 Cardiac perfusion

All perfusions were carried out in a fume cupboard. Mice under 10 days were killed in a halothane chamber. Mice over 10 days of age were humanely euthanased using an overdose of carbon dioxide in a closed chamber. Following death the carcass was weighed and the tip of the tail was removed to aid genotyping. Once the carcass was pinned out on a cork board, the thoracic cavity was opened and the right atrium of heart nicked. This allowed blood and perfusion fluids to escape. Perfusion was carried out by instilling solutions into the left ventricle through a 21 or 25 gauge hypodermic needle dependant on body size.

The blood was flushed from circulation with 0.85% saline and this was followed by the fixative. 20ml to 60ml fixative was used dependent on carcass size. After fixation the carcass was immersed in fixative for up to 2 hours. Tissue was dissected using a low power dissection microscope and microsurgical instruments. The brain, optic nerves and spinal cord were removed, cut into appropriate blocks, placed in fixative and stored until further processing.

2.6.2 Tissue Processing and Sectioning

2.6.2.1 Resin processing and sectioning

Tissue blocks prepared for resin embedding were processed using a Lynx el microscopy tissue processor (Leica). The tissues were passed through increasingly graded alcohols and infiltrated with araldite resin ([appendix](#)). The tissue blocks were oriented in resin-filled silicone moulds and placed at 60°C for 24 hours to allow polymerisation. Utilising an Ultracut-E ultratome (Reichert-Jung), 1µm light microscopy sections were cut with a glass knife from the resin blocks and the sections mounted on cleaned glass microscope slides, while for electron microscopy 70nm sections were cut with a diamond knife and mounted on 200-mesh 3.05mm-diameter copper grids.

2.6.2.2 Cryopreservation and sectioning

Tissue blocks from fresh and 4% paraformaldehyde or P-L-P fixed animals were suspended in a foil mould filled with Tissue-Tec O.C.T compound (Miles Inc) and frozen

in isopentane cooled in liquid nitrogen. The frozen blocks were wrapped with NescoFilm (Bando Chemical Ind. Ltd.) and stored at -20°C. 15µm sections were cut using an OTF cryostat (Bright Instrument Company) and mounted onto APES-coated microscope slides ([appendix](#)) which were then stored at -20°C.

2.6.3 Staining Techniques

2.6.3.1 Methylene blue/azure II

1µm resin sections were dried onto microscope slides on a 60°C hot plate. The sections were flooded with methylene blue/azure II stain ([appendix](#)) for 30-60 seconds and rinsed in running water. After drying, slides were mounted in DPX.

2.6.3.2 Electron microscopy (EM)

For electron microscopy, the 70nm resin sections on copper grids were “stained” with uranyl acetate and lead citrate ([appendix](#)).

2.6.4 Immunohistochemistry ([2.5.6.2 Characterisation by immunostaining](#))

2.6.4.1 ABC Technique (Avidin biotin complex)

This technique was utilised for immunolabelling resin sections with anti-MBP in order to facilitate the measurement of myelin density.

To enable staining the araldite resin was etched from the sections by agitation of the slides in sodium ethoxide (50% ripened sodium ethoxide 50% absolute alcohol) for 30 minutes. Slides were washed in absolute alcohol (6 changes) over 30 minutes. Endogenous peroxidase activity was quenched using 3% hydrogen peroxide in water for 30 minutes. Sections were again washed in running water for 30 minutes.

Non specific immunoglobulins were blocked with 10% normal goat serum (NGS) in PBS for 2 hours at room temperature. Excess NGS was removed and primary antibody, diluted in 1% NGS/PBS, was immediately applied and the sections incubated overnight in a humidity chamber at 4°C. The following day sections were allowed to warm to room temperature and washed in several changes of PBS. The appropriate biotinylated link antibody diluted in 1% NGS was applied for 1 hour at room temperature and then washed in PBS six times over 30 minutes. Sections were then incubated with ABC complex for 30

minutes at room temperature and washed again six times in PBS. The chromogen was developed in filtered PBS containing 0.5 mg/ml 3, 4, 3, 4-tetraminobipheyl hydrochloride (DAB) and 0.003% hydrogen peroxide for up to 5 minutes. Excess DAB was removed by washing in PBS for 2 minutes and running water for 5 minutes. The chromogen was intensified with 1% osmium tetroxide. The slides were then dehydrated in alcohols, cleared in xylene and mounted in DPX.

2.6.4.2 Immunofluorescence

Indirect immunofluorescence was the preferred method of labelling frozen cryostat sections. The sections were allowed to come to room temperature before washing in PBS to remove the tissue-tec. If the animal had not been perfused with fixative then the sections would be immersed in 4% paraformaldehyde for 20 minutes and then washed once more in PBS. Some antibody labelling required permeabilisation in -20°C methanol or 0.5% triton X-100 (Sigma), others require the non specific immunoglobulins to be blocked with 10% Normal goat serum (NGS) or 0.1% tritonX-100 with 0.2% Pig skin Gelatin (Sigma). Primary antibodies were diluted in 1% NGS or triton/gelatin blocking buffer as above; the sections were incubated in primary antibody overnight at 4°C. On day two sections were allowed to come to room temperature before being washed in several changes of PBS. Secondary antibodies labelled with fluorescein isothiocyanate (FITC) or Texas red (TxR) were diluted in PBS or the blocking buffer as before and applied to the sections for 30 minutes at room temperature. Slides were briefly washed in PBS before mounting in citiflour antifade mounting medium (citifluor). Sections were examined by epifluorescence. FITC absorbs light with a wavelength 495 nm and emits it at 525 nm, which can be visualised as green light using a blue filter. TxR absorbs light at 596 nm and emits it at 620 nm, which can be visualised as red light using a green filter. 4, 6-diamidino-2-phenylindole (DAPI), a nuclear marker employed, produces a blue fluorescent light with excitation of 345 nm and emission of 455 nm.

2.6.4.3 Antibodies and Markers

Commercially available and gifted antibodies were used and their sources and dilutions are illustrated in Table 6.

Anti-Caspase-3 antibody (R&D systems) was used to recognise apoptotic cells. The CC-1 antibody (Oncogene) was employed to distinguish mature oligodendrocytes (Fernandez *et al.*, 2000). Anti-MBP antibody (N.P. Groome, Oxford, UK) was used to stain central compact myelin.

Primary antibody	Host	Isotype	Dilution	Target	Source
Anti-Lamp1	Rabbit polyclonal	Clone ID4B		Late endosomes /lysosomes (LE/Ls)	Developmental Studies Hybridoma Bank
Anti-MBP	Rat monoclonal	IgG	1:500	Myelin, mature oligodendrocytes	N.P. Groome
CC-1	Mouse monoclonal	IgG _{2b}	1:100	Mature oligodendrocytes	Oncogene
Anti-caspase-3	Rabbit polyclonal	IgG	1:4000	Apoptotic cells	R&D
226			1:600	Myelin, mature oligodendrocytes	Applied Neurobiology Grp
AA3	Rat Monoclonal		1:15	Myelin, mature oligodendrocytes	S. Pfeiffer
O10	Monoclonal	IgM	1:6	Conformationally sensitive cell-surface epitope of PLP	M. Jung

Table 6. Primary antibodies, dilutions used and target.

Link antibody	Dilution	ABC Dilution	Source
Rabbit-anti-rat IgG Biotinylated	1:100	10 µl of A and B in 625 µl PBS	Vector labs

Table 7. Link antibody and Avidin biotin Complex (ABC)

Secondary antibody	Dilution
Goat anti-rabbit IgG FITC	1:80
Goat anti-rat IgG FITC	1:50
Goat anti-mouse IgG _{2b} FITC	1:100

Table 8. Secondary antibodies
(Sourced from Southern Biotech)

2.6.4.4 CC-1 staining of oligodendrocytes

Sections were permeabilised in 0.5% triton X-100 for 30 minutes and non-specific binding blocked with 0.1% triton x-100, 0.2% pig skin gelatin in PBS for 30 minutes. Excess blocking solution was removed and CC-1 antibody at 1:100 diluted in blocking solution applied and the sections and incubated at 4°C overnight. The slides were washed and incubated with goat anti-mouse IgG_{2b} FITC secondary antibody diluted in blocking solution for 30 minutes, the nuclei stained with DAPI and the slides washed and mounted. APC has been used to label mature oligodendrocytes (Fernandez, 2000).

2.6.4.5 Caspase-3 staining of apoptotic cells

Following permeabilisation in 0.5% triton X-100 sections were blocked with 0.1% triton X-100, 0.2% pig skin gelatin in PBS for 30 minutes. Excess blocking solution was removed and anti-caspase-3 antibody diluted in blocking solution applied and the sections incubated at 4°C overnight. The sections were washed and incubated with goat anti-rabbit IgG FITC secondary antibody diluted in blocking solution for 30 minutes the nuclei stained with DAPI and the slides washed and mounted.

2.6.4.6 DAPI Staining

Following immunolabelling cell nuclei were stained with 1µg/ml 4, 6-diamidino-2-phenylindole (DAPI), the fluorescent dye, for 30-60 seconds.

2.6.4.6.1 Quantification of Labeled Cells in Cryosections.

Cells were quantified in the ventral columns adjacent to the ventromedian fissure in 15-µm cryosections. Multiple sections were cut with at least 15 µm between sections. Fluorescent images were recorded using a 20x objective and a digital camera (Colour CoolView, Photonic Science, Robertsbridge, England, UK) and stored on computer. In all instances, cells were counted within a defined area of interest using Image-Pro Plus-4 software set to count objects wholly within the frame or touching two of the sides. Caspase-3-labeled cell bodies were counted together with DAPI-labelled nuclei. Approximately 20 fields were counted from each animal. CC-1 antigen labelled cells were counterstained with DAPI and separate images of the two fluorophores were merged (Adobe Photoshop 6, Adobe Systems, San Jose, CA, USA) and the number of labelled cell bodies containing a nucleus were counted, as above. Cell densities were derived and, where appropriate, the labelling index or percentage of labelled cells calculated in relation

to the total number of DAPI stained nuclei. APC CC-1 antibody labels mature oligodendrocytes and lightly labels progenitors and astrocytes.

2.6.5 Morphological Quantitative studies

2.6.5.1 Myelin volume

Cervical segment 2 (C2) of spinal cords were dissected out following perfusion-fixation in Karnovsky's Modified Fixative and processed for resin embedding. Following polymerisation the resin blocks were trimmed and thin sections (70nm) cut and placed onto copper grids which were subsequently stained with uranyl acetate and lead citrate (appendix). All measurements were performed on the ventral columns of the white matter tract.

Myelin volumes were derived using a point counting technique {Williams, 1977}. Ten electron micrographs (Jeol CX-100) at 4,000x magnification were obtained by random photography of the ventral columns and printed at ~3.5 enlargement to occupy an A4 sheet of printing paper. A transparent grid square (2cm) was placed over each print and the number of intercepts overlying compact myelin was expressed as a ratio of the total intercepts. This was superseded by the digital method very early on where this analysis was carried out on the computer using a grid generated by the software (Image Pro-Plus 4.1 software (Media Cybernetics, Silver Spring, MD, USA)) (Karim *et al.*, 2007).

$V_v = \text{Points overlying compact myelin} / \text{Total points available on grid.}$

2.6.5.2 Axon status

Utilising the same photomicrographs as above a simple line grid (2 lines running diagonally from corner to corner) was overlaid and the number of non-myelinated and myelinated axons touching the line were counted. The number of each was expressed as a percentage of total fibres. Once again this was superseded by the digital method very early on where this analysis was carried out on the computer using a grid generated by the software (Image Pro-Plus 4.1 software).

2.6.5.3 Myelin Density

Myelin area was measured on semi thin (1µm) resin sections immuno-labelled with anti Myelin Basic Protein using the ABC technique. Four areas, two either side of the ventromedian fissure were captured with x40 dry lens using a CCD camera (Colour

Coolview, Photonic Science). The digital images were converted to black and using Image Pro Plus software (Media Cybernetics). An area of interest (AOI) of $2500\mu\text{m}^2$ was placed over two separate areas of each of the four captured images and the total area of black objects (MBP labelled myelin) measured. The density of myelin ($\mu\text{m}^2/\text{mm}^2$) of white matter was calculated.

2.6.5.4 Quantification of APC+ cells

Cell counts were performed on cryosections ($15\mu\text{m}$) of the ventral columns, adjacent to the ventromedian fissure, from rostral cervical spinal cord. Images of APC-labelled cells (green channel) and DAPI-labelled nuclei (blue channel) from the same sampling area were collected at x20 objective using a CCD camera system (Photonic Science Colour Coolview) and stored in the computer. The green and blue channels were merged using Adobe Photoshop (Adobe systems Inc., San Jose) and the image quality adjusted. For each combined image, a frame ($35804\mu\text{m}^2$) outlining the AOI was placed on the screen. The number of APC+ cell bodies containing a DAPI-stained nucleus was counted within the AOI or those touching the top or left side but excluding those touching the bottom or right sides. The density of DAPI-labelled nuclei was counted automatically with an AOI of $10,000\mu\text{m}^2$. The density of APC-labelled cells and DAPI-stained nuclei (nuclei/ mm^2) and the percentage of APC+ cells (APC cells/DAPI nuclei x 100) were calculated.

2.6.5.5 Quantification of caspase-3+ cells

Cell counts were performed on cryosections ($15\mu\text{m}$) of the ventral columns, adjacent to the ventromedian fissure, from rostral cervical spinal cord. Images of caspase-3-labelled cells were collected at x20 objective using a CCD camera system (Photonic Science Colour Coolview) and stored in the computer. For each image, a frame ($35804\mu\text{m}^2$) outlining the AOI was placed on the screen. The number of caspase-3+ cell bodies was counted within the AOI or touching the top or left side but excluding those touching the bottom or right sides. The density of DAPI-stained nuclei was taken from the sections stained for APC/DAPI. The density of caspase-3-labelled cells and the percentage of caspase-3+ cells (Caspase-3+ cells/DAPI nuclei x 100) were calculated.

2.6.5.6 Calculation of cell numbers

Quantification of cells or nuclei was determined by their density in the ventral funiculi. As the area of the white matter varied between different genotypes, the total number of cells/nuclei in the white matter of a transverse section was calculated. This calculation

assumed that the density was equally distributed throughout the white matter when there was variation between tracts and at different ages. In fact the nuclear density altered across the width of the ventral column, being greater in the central region adjacent to the grey matter. The alternative strategy was to define a precise sub-region of the ventral column in which to calculate total numbers, a task that would be problematic to ensure consistent identification of the same region. The calculation based on the total white matter area therefore offers an acceptable way of comparing cell numbers between different genotypes and ages.

2.6.6 Statistical analysis

2.6.6.1 Group sizes

The number of animals included in a group varied between ages, genotype and technique. In general, 4 or more animals were included in a group and where possible littermates were used. At P3 and P5 no phenotype was displayed by any of the animals therefore identification of genotype by carried out by PCR and morphology therefore no pooling of samples was possible for cultures. Homozygous animals could be identified by P20 as the phenotype was displayed. Wild type and hemizygous animal selection was random and genotype was confirmed subsequently. In the case of the brain slice experiments identification occurred after the completion of the experiment. In general this factor put a practical appreciation of the experimental design.

2.6.6.2 Data presentation

Graphs are presented as mean \pm SEM.

2.6.6.3 Statistical tests

As group sizes were always relatively small no assumptions were made that the data was distributed normally. Groups were first compared using one-way **Analysis Of Variation** (ANOVA). If a significant difference ($p < 0.05$) was detected, individual groups were compared using the Bonferroni multiple comparison test. P value was taken at < 0.05 (one star $< * 0.05$, two stars $< ** 0.01$ and three stars $< *** 0.001$). Analyses and curve fittings were performed using Graphpad Prism4 software (GraphPad Software, San Diego, CA, USA).

3 Effects of #66 transgene cassette

3.1 Background

The #66 transgene cassette contains no sequence tags or mutations to distinguish its expression from the endogenous copy of *Plp1* gene on the X chromosome. However, it is necessary to investigate the contribution of the transgene to total PLP message and protein levels in the CNS. Readhead *et al.*, (1994) did this by quantifying *Plp1* expression in the F2 generation after breeding transgenic male mice with heterozygous *jimpy* (*jp/+*) females. The two *Plp1* messages were distinguishable from one another via PCR as the endogenous *jimpy Plp* and *Dm20* mRNA contained a 74 nucleotide deletion of exon 5 allowing for the quantification of the transgene message.

3.2 Aims

The aims of this chapter were to investigate the levels of *plp/dm20* message and PLP/DM20 protein attributable solely to the transgene cassette utilising the *Plp1* gene null mice generated by Klugman *et al.*, (1997).

3.3 Methods

The study of activity of the transgene cassette was performed at P20 (peak of myelination). Spinal cord was collected for RNA and myelin preparation and tail for DNA preparation. The steady state mRNA levels of *Plp1* were assessed by northern hybridisation and qRT-PCR using β -*actin* as an internal endogenous control. The protein levels were assessed by western blot analysis of the myelin fraction from spinal cord.

3.3.1 Animal breeding

The breeding of the #66 hemizygous males with *Plp1* gene null females was carried out as described in [2.2 Mouse Breeding](#). The offspring were genotyped as described ([2.2.4 Crossing of transgenic lines of mice](#)) for the transgene and the null locus (Figure 10) and only male animals were used for this study.

3.3.2 Genotype and Sample Selection

Brain and spinal cord tissue from three genotypes was utilised: from male mice that were wild type for the transgene and wild type for the *Plp1* gene null locus; from male mice that were wild type for the transgene and null positive; and from male mice that were transgene and null positive (Figure 10).

3.3.3 Tissue Preparation

Total cellular RNA was extracted from powdered spinal cord as described in [2.4 Isolation and Manipulation of RNA](#). Preparation of myelin from spinal cord is described in [2.5 Protein Analysis](#). gDNA from tails was prepared for genotyping as described in [2.3 Isolation and Manipulation of DNA](#).

3.3.4 Transcript Analysis

3.3.4.1 Northern analysis

This experiment was performed on total cellular RNA extracted from spinal cord. The procedure of northern transfer and hybridisation is described in [2.4.6 Northern Blotting](#). The preparation of radiolabelled probes is described also in [2.4.6 Northern Blotting](#).

Staining of the gel with ethidium bromide was used to check for equal loadings of sample and presence of bands in ladder (Figure 14A and B) and hybridisation with β -actin (a measure of invariant expression) was used to monitor equivalence of transfer. Hybridisation analysis was undertaken using labeled cDNA products from PCRs using primers for *Plp1* (Table 2) (Figure 15). The blot was left for a 3-4 weeks to allow the signal to decay then probed for β -actin and finally *Mbp* 3-4 weeks later.

3.3.4.2 qRT-PCR analysis

Standard curves were produced using serial dilutions of an appropriate wild type RNA sample as described in [2.4.7 qRT-PCR](#). Once all the parameters for the reactions were set and equivalent for both genes, the test plate, containing both *Plp1* and β -actin reactions for the relevant samples selected, was run ([2.4.7 qRT-PCR](#)).

Each sample was loaded in duplicate or triplicate and blanks containing ddH₂O were also loaded as controls. Once the PCR was complete then the results were stored on a CD for analysis. Following the analysis protocol in [2.4.7 qRT-PCR](#) the uncorrected concentrations

of *Plp1* and β -*actin* mRNA in 50ng total RNA loaded was calculated. The *Plp1* concentration was then normalised to β -*actin* and expressed as a percentage of WT/WT levels giving the actual concentration of *Plp1* message in total RNA.

3.3.5 CNS Myelin Analysis

3.3.5.1 Myelin Preparation

Myelin was prepared from spinal cord, protein was quantified and analysed by western blot as described in [2.5 Protein Analysis](#). Blots were immunostained for PLP/DM20 using C-terminal antibody 226 and for MAG (Table 6).

3.4 Results

3.4.1 #66 transgene expression

3.4.1.1 Northern Hybridisation

Transcript analysis by northern hybridisation of the *Plp1* transgene on the *Plp1* null background is demonstrated in the Figure 20 where the results were compared to wild type (WT/WT) and null (Ko/WT) littermates. There was no detectable signal for *Plp1* in the null sample (Figure 20A Null) whereas the β -*actin* signal (Figure 20B Null) confirmed presence of RNA and amount transferred to the membrane. The signals for both *Plp1* and β -*actin* message in the null/#66 (Ko/#66) sample (Figure 20A and B Null/#66) were higher than those for wild type (Figure 20A and B WT). Two classes of *Plp/Dm20* mRNAs were detected 2.4kb and 1.6 kb (Figure 20A). Both *Plp* and *Dm20* transcripts are present in the two bands seen on the northern blot (Figure 20A). The β -*actin* signal is also around 1.6kb in size which masks the lower *Plp/Dm20* mRNA signals as seen in Figure 20B. Once the *Plp1* signal was corrected for the β -*actin* signal and normalised to wild type levels the message levels in both wild type and null/#66 were comparable. The wild type levels are 100% and null/#66 levels 115%. However, this analysis has been carried out only two sets of samples. The same blot was reprobbed for *Mbp* (Figure 20C) showing an increase in *Mbp* levels in both the null and null/#66 samples compared to the wild type sample. However when corrected for β -*actin* this increase was not so marked as demonstrated by the northern.

3.4.1.2 qRT-PCR analysis

Transcript analysis by qRT-PCR of the *Plp1* transgene on the *Plp1* gene null background is demonstrated in Figure 21. As with northern hybridisation analysis there is no *Plp1* signal for the null (Ko/WT) genotype whereas the β -actin signal in all three genotypes is similar.

Once the signals were analysed and normalised to β -actin they were expressed as a percentage of wild type levels (standard, 100%). No difference is seen between the message levels for wild type and null/#66 (Figure 21).

3.4.2 CNS Myelin analysis

3.4.2.1 Western analysis

Protein analysis by western blotting of wild type, null and null/transgene (null/#66) animals is demonstrated in Figure 22. All three samples show positive staining for MAG confirming the presence and equal amount of myelin proteins on the blot as MAG was used as control for loading (Figure 22A). Neither PLP nor DM20 protein isoforms are detected in null mice (Figure 22B Null). There is no difference between PLP and DM20 protein levels between wild type and null/#66 samples (Figure 22B and Figure 23).

3.5 Discussion

Data presented in this chapter demonstrates that mice positive for the *Plp1* wild type transgene cassette and null for the endogenous *Plp1* gene produced similar levels of *Plp/Dm20* message and PLP/DM20 protein isoforms as wild type littermates. The 7 extra copies of the *Plp1* gene did not produce a 7 fold increase at either the transcript or protein level as might have been expected.

Readhead *et al.*, (1994) measured transcription efficiency of the transgene on a *jimpy* background. In mice that were #66 transgene and *jimpy* positive the message level measured 115% by RT-PCR with an error margin of 10%. In this study the transcript levels of only transgene cassette on a null background were comparable. These experiments also confirmed previous studies showing the *Plp1* gene null mouse produces no *Plp/Dm20* message or PLP/DM20 protein (Griffiths *et al.*, 1998).

The slight difference in message levels between the northern hybridisation and qRT-PCR can be explained by the fact only one set of animals was used in the former and the

different quantity of RNA at the start of each experiment. 12.5µg total RNA was used for the northern hybridisation experiment and 50ng for the qRT-PCR experiments. Leske *et al.*, (2004) also found discrepancies between their northern and qRT-PCR results. Although they observed differences in absolute values, the overall trends in mRNA levels were very similar between the methods.

Originally the *Plp1* gene promoter was thought to control the gene transcription in oligodendrocytes. However *Plp1* promoter activity was discovered to be distinct from the rate of accumulation of *Plp/Dm20* mRNA (Mallon and Macklin 2002), therefore there must be another mechanism controlling the transcription rate of the wild type *Plp1* gene. Previously it had been discovered the nucleotide sequence of exon 7, the largest exon (>2kb) of the mouse *Plp1* gene, which contains the 3' untranslated region (UTR) and the three polyadenylation sites, has a high degree of conservation between species. The homology of the entire 3'UTR between mouse and rat is greater than 90% and some regions have almost 100% homology (Macklin *et al.*, 1987). Other genes have a lower homology between species in this region. Another X chromosome gene Hypoxanthine phosphoribosyltransferase (*Hprt*) shows 74% homology between the human and mouse genes which is considered high for this region.

Studies to investigate whether the 3' UTR region regulates the transcription rate and expression of *Plp/Dm20* mRNA in cells were undertaken by Mallon and Macklin (2002). The 3'UTR of *Plp1* gene was fused to luciferase under CMV promoter control and transfected into C6 cells in excess amounts. Results showed a dramatic decrease of the endogenous *Plp1* mRNA in these cells. They then confirmed this data using a different vector and promoter. Thus overexpressing of the *Plp1* 3'UTR downregulated the transcription of the endogenous *Plp1* mRNA and also changed the adhesion properties and morphology of the C6 cells. The cells took longer to attach to the tissue culture dish than cells without the 3'UTR and formed aggregates at high density.

In transgenic mice generated to express the EGFP protein fused to the *Plp1* 3'UTR and under control of the *Plp1* regulatory regions the endogenous *Plp1* mRNA in total brain RNA decreased by 30-54% (Mallon and Macklin 2002). As there is no endogenous *Plp1* gene present in the null/#66 mice in this study and the transgene contains all 17kb of the wild type gene, it is a possibility that the 3'UTR is having an effect on the expression of the transgene itself. There is no difference between the endogenous *Plp1* gene and the

copies in the transgene therefore cells may be unable to distinguish between the two and thus regulate both in the same way.

Readhead *et al.*, (1994) were unable to demonstrate that PLP is overexpressed at the protein level in the #66 transgene and *jimpy* positive mice in their studies. In this study PLP/DM20 protein isoforms produced in the null/#66 animals was equivalent to the levels in wild type littermates. The 7 copies of the wild type *Plp1* gene in the transgene produced around 100% protein. The oligodendrocyte can control the expression of the 7 copies of the *Plp1* gene ensuring adequate transcript and protein is produced. In conclusion, data presented in this chapter suggests that there is a mechanism by which the oligodendrocyte controls transcription and translation of the *Plp1* gene to ensure tight regulation of levels of PLP/DM20 present in myelin. As PLP/DM20 is the most abundant protein in the CNS it is essential that the oligodendrocytes have the ability to maintain the levels required to produce myelin. The possible breakdown of controls in place to carry out this process may contribute to disease in humans and animals.

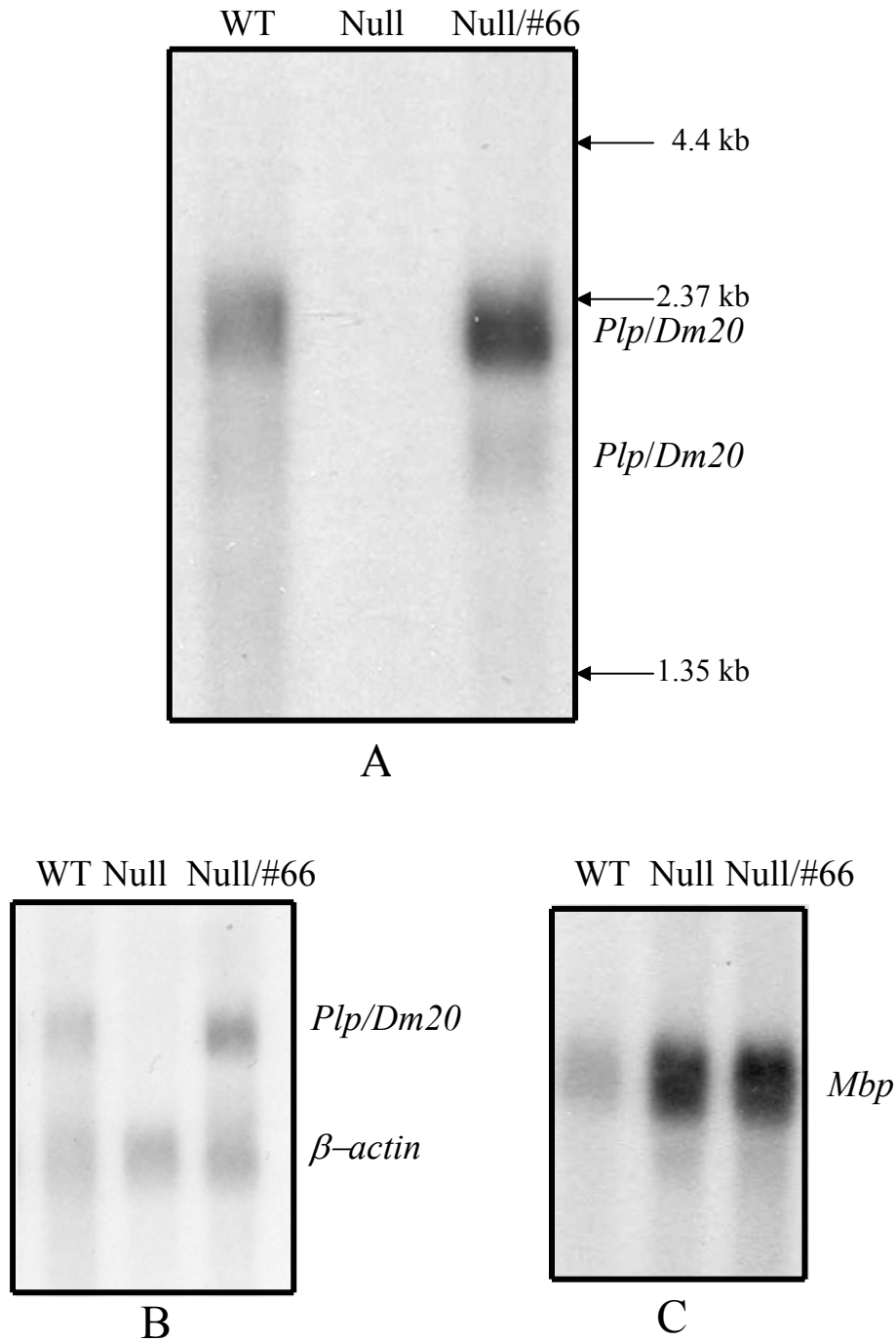


Figure 20. Transcript analysis of P20 Null x #66 total RNA.

A) Northern hybridisation analysis of *Plp1* gene transcription showing the two major murine mRNA species with no mRNA signal present in the null sample (Null). **B)** Northern hybridisation analysis of *Plp1* and β -actin gene transcription confirming the presence of RNA in the middle lane with a β -actin signal. **C)** Same blot left for 3-4 weeks for signal to decay and then reprobed for *Mbp* showing an increase in *Mbp* message in the null and null/#66 samples. 12.5 μ g spinal cord total RNA loaded per lane and 5 μ l RNA ladder loaded.

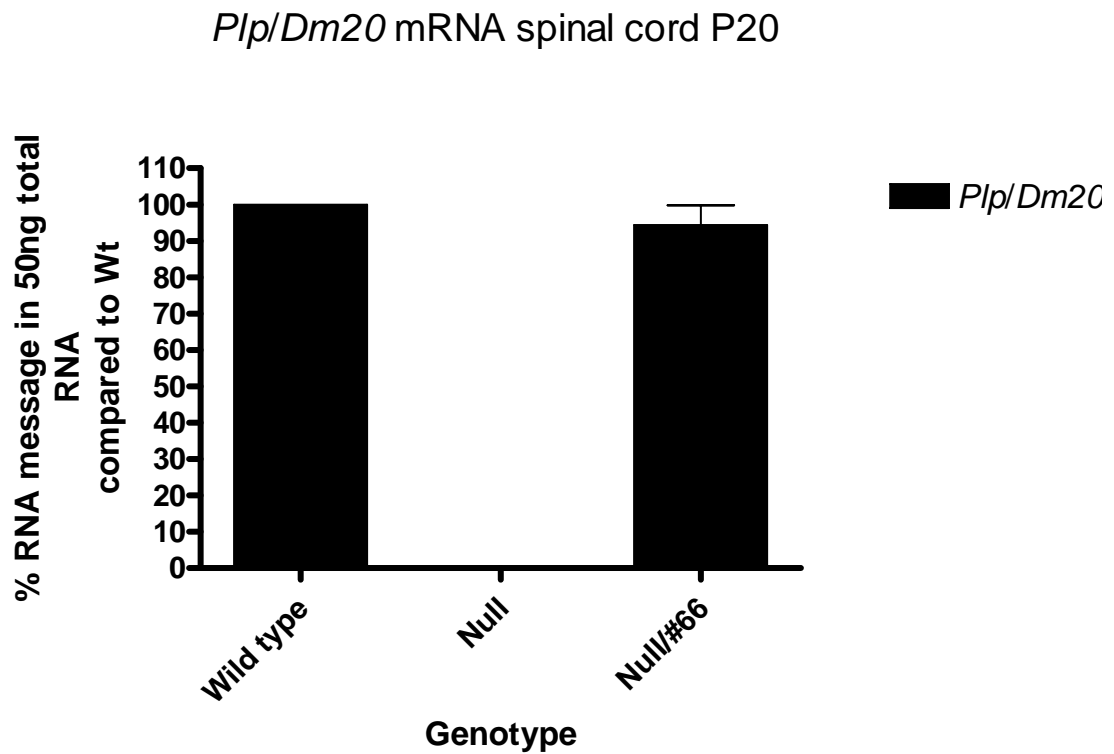


Figure 21. Representative graph showing mRNA (message) levels in the three #66 x null genotypes using qRT-PCR.

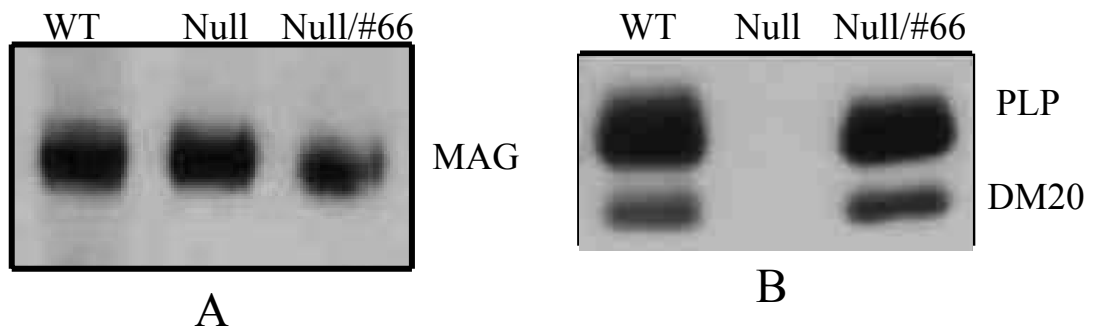


Figure 22. Western blot analysis of the *Plp1* wild type transgene on a *Plp1* null background.

A) Western blot immunostained with MAG antibody (WT wild type, Null *Plp1* null and Null/#66 *Plp1* null x #66) highlighting the presence of MAG in the null sample. **B)** Same blot washed then re-immunostained for PLP/DM20 highlighting the lack of PLP/DM20 signal in the null sample (WT wild type, Null *Plp1* null and Null/#66 *Plp1* null x #66).

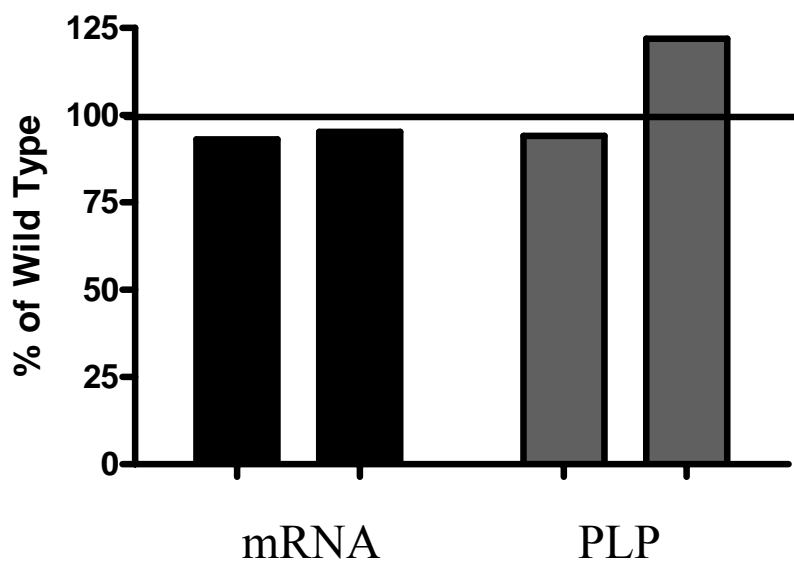


Figure 23. Quantitative data for *Plp/Dm20* mRNA, measured by qRT-PCR and PLP protein, measured by western blotting for *Plp1* gene null mice carrying the *Plp1* transgene.

Results (M, N = 2) are expressed as a percentage of a wild type mouse from the same litter. There is no difference between groups for either parameter.

4 Effects of Increased *Plp1* gene dosage on Pre- and Early Myelinating Oligodendrocytes

4.1 Background

The principle function of oligodendrocytes is to provide support to axons and to produce the myelin sheath, which insulates axons. Oligodendrocytes begin to produce myelin when they enter terminal differentiation and contact neurons. This occurs at a remarkable scale $>10^4 \mu\text{m}^2$ myelin membrane surface area/cell/day (Pfeiffer *et al.*, 1993). Oligodendrocytes, unlike Schwann cells of the PNS, form myelin internodes of numerous axons. The processes of a given oligodendrocyte wrap themselves around portions of the surrounding axons. As each process wraps itself around, it forms layers of myelin. Each process thus becomes a segment of the axon's myelin sheath. This process of myelination by oligodendrocytes is highly organized and coordinated. However it has been shown that oligodendrocytes cultured without neurons, as in my study, produce considerable amounts of myelin proteins and possibly attempt a few myelin whorls (Dubois-Dalcq *et al.*, 1986). The expression of myelin proteins is not dependant on the presence or absence of neurons (Lemke *et al.*, 1986). However recent evidence has shown that there is communication between oligodendrocytes and neurons which may involve a cAMP modulating factor (Trajkovic *et al.*, 2006).

In the early stages of myelination the oligodendrocytes come into contact with axons and produce membranous sheets extending as cell processes to the axon. These membranous sheets are not yet myelin. Changes in protein to lipid ratio or levels of proteins produced may have adverse effects on myelination. Originally studies on spontaneous *Plp1* gene mutants provided evidence for the roles of the *Plp1* gene in oligodendrocyte development. Mutants such as *jimpy* and *rumpshaker* have dysmyelinating phenotypes and display reduced numbers of mature oligodendrocytes and small numbers of thin myelin sheaths. However unlike these mutants the #66 line have extra copies of the wild type *Plp1* gene. In humans extra copies of the *PLP1* gene cause PMD (reviewed in introduction of this thesis) although the mechanisms of the disease process are not yet known. Any light shed on the effects of extra wild type copies of the gene on oligodendrocytes and the early myelination process would be useful.

4.2 Aims

At the beginning of this project there was very little information on the effects of increased *Plp1* gene dosage on the early stages of myelination or on the oligodendrocytes themselves. Therefore one of the first aims of this study was to investigate the effects of increased *Plp1* gene dosage on oligodendrocytes and on the early stages of myelination when the oligodendrocytes are just coming into contact with axons.

This chapter describes the *in vitro* studies into protein composition in oligodendrocytes via immunostaining and western blot analysis in homozygous mice in comparison to age-matched wild type and hemizygous animals. Also described is analysis of P3 spinal cord at morphologic, message and protein levels.

4.3 Methods

These studies were carried on spinal cord from P3 and P5 male #66 mice. Spinal cord was collected for RNA and myelin preparation and tail for DNA preparation. The steady state mRNA levels of *Plp1* and *Mbp* were assessed by northern hybridization and qRT-PCR using β -actin as an internal control. The protein levels were assessed by western blot analysis of the myelin fraction from spinal cord.

4.3.1 Animal breeding

The breeding of the #66 hemizygous males with #66 hemizygous females was carried out as described in [2.2 Mouse Breeding](#). The offspring were genotyped as described ([2.3 Isolation and Manipulation of DNA](#)) for the transgene and only male animals at P3 or P5 were used for this study. As there is no visible phenotype in young #66 mice another method was used to further identify the hemizygous and homozygous animals. Readhead *et al.*, (1994) correlated gene copy number with pathology and this was verified in subsequent publications (Anderson, 1997, Anderson *et al.*, 1999). Homozygous mice can be distinguished from hemizygotes by the dysmyelination that is evident at all ages in the present study. A small block of cervical spinal cord from mice used for RNA, protein or tissue culture studies was immersion-fixed in paraformaldehyde/glutaraldehyde fixative and processed for resin sections, and where necessary EM ([2.6.3 Staining Techniques](#)).

4.3.2 Sample Selection

Tissues from mice wild type and hemizygous or homozygous for the #66 transgene were used. Tails were taken for genotyping, spinal cord for tissue culture studies, or RNA and protein extractions.

4.3.3 Primary Cell Culture Analysis

Primary cell cultures for oligodendrocyte analysis were set up from P5 mice as described in [2.5.4.1 Primary Cell Culture](#). Cells on coverslips were immunostained to highlight presence or absence of proteins ([2.5.4.2 Characterisation by Immunostaining](#)) and cells in culture dishes were lysed to study proteins ([2.5.4.3 Harvesting for Biochemistry](#)).

4.3.4 Transcript Analysis

4.3.4.1 Northern analysis

This experiment was performed on total cellular RNA extracted from spinal cord. The procedure of northern transfer and hybridisation is described in [2.4.6 Northern Blotting](#). The preparation of radiolabelled probes is described also in [2.4.6 Northern Blotting](#).

Staining of the gel with ethidium bromide was used to check for equal loadings of sample and presence of bands in ladder and hybridisation with β -actin (a measure of invariant expression) was used to monitor equivalence of transfer. Hybridisation analysis was undertaken using labeled cDNA products from PCRs using primers for *Plp1* and *Mbp* (Table 2) (Figure 15). The blot was left for 3-4 weeks to allow the signal to decay then probed for β -actin.

4.3.5 CNS Myelin Analysis

4.3.5.1 Myelin Preparation

Myelin was prepared from powdered spinal cord, protein was quantified and analysed by western blot as described in [2.5 Protein Analysis](#). Blots were immunostained for PLP/DM20 using C-terminal antibody PLP₂₂₆, MAG, MBP, ASPA and β -actin (Table 6). To compensate for any differences in oligodendrocyte cell numbers in culture lysates, samples for western analysis were normalised for aspartoacylase (ASPA), a marker of oligodendrocyte cell bodies (Kirmani *et al.*, 2003, Madhavarao *et al.*, 2004).

4.4 Results

4.4.1 Identification of Genotype

Homozygous animals have to be distinguished from hemizygous animals after PCR as both are transgene positive and there is no phenotype at P5. Many axons in hemizygous spinal cord are surrounded by myelin sheaths (Figure 24A) and at this age hemizygous spinal cord is indistinguishable from wild type spinal cord. However there are naked axons and axons with thin myelin sheaths visible in homozygous spinal cord (Figure 24B). The cord at P3 is very similar to spinal cord at P5 therefore all animals used for either tissue culture or P3 analysis were identified using this method.

4.4.2 Immunostaining

Oligodendrocytes in cultures were immunostained using fluorescent techniques. PLP/DM20 is present in the cell bodies and rudimentary processes of oligodendrocytes from wild type animals (Figure 25A) cultured for 6 days from P5 spinal cord. No obvious difference is noted in the cellular distributions of PLP/DM20 between oligodendrocytes cultured from wild type and homozygous animals (Figure 25B).

Oligodendrocytes in culture from each genotype were also immunostained for MBP (Figure 26). There appears to be no visual difference in MBP staining in the wild type and hemizygous cells (Figure 26A and C) whereas, there is a reduction in MBP staining in the homozygous cells (Figure 26D). MBP-stained membranes in the wild type cultures that are not obvious in the homozygous culture are shown in Figure 26B.

4.4.3 Protein Analysis of Culture Lysates

Protein analysis by western blotting of lysates from cultured oligodendrocytes of wild type, hemizygous and homozygous mice are illustrated in Figure 27A. ASPA, a marker for oligodendrocyte cell bodies is used as a control to compensate for any differences in oligodendrocyte cell numbers between samples. Whereas the level of PLP/DM20 is elevated in the homozygotes, the amount of the MBP isoforms is decreased in the same cells. PLP/DM20 levels in homozygotes are significantly elevated ($p < 0.05$) compared with wild type and hemizygote levels, once normalised to ASPA and expressed relative to wild type (Figure 27B). Steady state levels of PLP/DM20 in hemizygotes and wild types are similar.

4.4.4 Analysis of Early Myelination in P3 spinal cord

4.4.4.1 Transcript Analysis

Transcript analysis by northern analysis is demonstrated in Figure 28A. Both *Plp1* and *Mbp* messages in total RNA from spinal cord of P3 hemizygotes are not different from wild type message levels. However in homozygotes both *Mbp* and *Plp1* messages are significantly reduced compared with wild type ($p < *0.05$).

4.4.4.2 Protein Analysis

Protein analysis by western blotting of wild type, hemizygous and homozygous P3 spinal cord lysates (total homogenates) is demonstrated in Figure 28B. As found in the cultured oligodendrocytes there is a progressive increase of PLP/DM20 levels with gene dosage with the homozygotes (Figure 28B Homo) having the highest protein levels. Conversely, (Figure 28B Homo) there is a marked decrease in MBP levels in the homozygote spinal cord total homogenate (Figure 28B Homo).

4.4.4.3 Morphological Analysis of P3 spinal cord

A 1 μ m resin section of a P3 spinal cord immunostained for PLP/DM20 is shown in Figure 29. Strongly stained oligodendrocyte cell bodies and myelin sheaths are evident showing the oligodendrocyte contains significant amounts of PLP/DM20. Some oligodendrocyte cell bodies contain dark immunopositive structures (arrow in Figure 29A). In immediately adjacent EM sections (Figure 29B, C) the immunopositive cells have distended RER and autophagic vacuoles/lysosomes, which probably correspond to the dark structures seen in the resin section.

4.5 Discussion

Data presented in this chapter demonstrate that there is increased PLP/DM20 protein present in oligodendrocytes from homozygous mice *in vitro* and in P3 spinal cord. Conversely there is a marked reduction in message levels for PLP/DM20 in the homozygous lysates. MBP at both message and protein levels is reduced in the homozygous oligodendrocytes and P3 spinal cord RNA and lysates.

To understand how oligodendrocytes cope with increased *Plp1* gene dosage and how axonal factors might interact with or influence this, PLP/DM20 levels were studied in naïve oligodendrocytes with no axonal contact and in the absence of a myelin sheath. It is

generally accepted that the presence of PLP in oligodendrocytes defines a mature myelin-forming oligodendrocyte (Griffiths *et al.*, 1998) therefore the oligodendrocytes present in the primary cell cultures from spinal cord in this study can be classed as such. O10 immunostaining confirmed cultured oligodendrocytes produced PLP/DM20 and the protein reached the cell surface. O10 antibody stains the surface of live cells and recognizes a conformation-sensitive epitope within the large extracellular loop (C-D loop) of PLP/DM20 (Figure 5) (Jung *et al.*, 1996). Oligodendrocytes *in vitro* produce PLP/DM20 protein and it can reach the cell surface in the absence of neurons.

During normal *in vivo* development the level of *Plp1* gene expression closely parallels myelination. However, expression commences prior to myelin formation and is influenced by axonal contact and the amount of myelin produced by the cell (McPhilemy *et al.*, 1990, Thomson *et al.*, 2005). In the homozygous P3 spinal cord there is reduction in mRNA for *Plp/Dm20* compared with wild type and hemizygous levels but an increase in protein levels. There is evidence to show that there is not a one-to-one relationship between message and protein levels. One message does not necessarily translate into only one polypeptide molecule. The oligodendrocyte has the ability to increase production of protein from the respective transcript. This may be the case the homozygous oligodendrocytes prior to full scale myelination.

Intuitively, one would anticipate increased *Plp1* gene dosage to result in higher levels of PLP/DM20 in oligodendrocytes. However, other factors, such as the myelination status, can have a major influence. To separate these influences in cultured oligodendrocytes which, lack myelin sheaths, PLP/DM20 levels were investigated and showed that levels in cells from homozygous mice were elevated. PLP/DM20 was also elevated in homozygous mice during very early myelination in P3 spinal cords, and to a lesser extent in hemizygous mice. However in these same cells *in vitro* and in P3 spinal cord MBP was reduced. Oligodendrocytes from homozygous animals do not produce membranous sheets as the oligodendrocytes from wild type animals do.

Premyelinating oligodendrocytes express many but not all the myelin proteins they need during myelination and they extend processes radially in many directions. All the myelin proteins detected in premyelinating oligodendrocytes appears to be evenly distributed throughout the entire cell body. However in the homozygous oligodendrocytes (Figure 29A) there are highly PLP/DM20 immunostained structures seen in the cell bodies. The

accumulation of PLP/DM20 protein overexpressed in the homozygous oligodendrocytes in the cell body whether it is in the RER or in autophagic vacuoles/lysosomes may tax or saturate the availability of molecules that help fold or move PLP/DM20 through the cell. P0 protein is also concentrated due to the lack of available myelin in the cell bodies of Schwann cells overexpressing P0 (Yin *et al.*, 2000). Similarities also exist with increased dosage of the *PMP22* gene, the commonest cause of Charcot-Marie-Tooth disease type 1A. Transgenic rodent models of the disorder exhibit dysmyelination proportionate with *Pmp22* dosage (Huxley *et al.*, 1998, Niemann *et al.*, 2000) and Schwann cells contain autophagic vacuoles reminiscent of those seen in oligodendrocytes described in this chapter (Chies *et al.*, 2003, Niemann *et al.*, 2000).

Immunostaining and EM show that the strongly immunopositive oligodendrocyte cell bodies contain numerous autophagic vacuoles and lysosomes. PLP, when overexpressed, is known to associate with the endosomes/lysosome system (Simons *et al.*, 2002). In normal myelination PLP may also associate temporarily with endosomes before axon-derived signals promote its insertion into myelin (Trajkovic *et al.*, 2006). An increase in PLP/DM20 levels and a reduction in available myelin and decreased axonal contact, as occurs in the homozygous state, would exacerbate the accumulation of PLP in lysosomes.

Prior to myelination, MBP production at message and protein levels is impaired, this is seen in the reduction of steady state MBP by western blotting in cultured oligodendrocytes and premyelinating spinal cord. *Mbp* message is translocated in granules containing hnRNP A2, ribosomal RNA, the elongation factor EF1- α and arginyl-transfer RNA synthetase (Trapp *et al.*, 2004). These granules are transported at speeds consistent with microtubule-mediated transport to the myelin internode. The excessive load/burden on the homozygous cell may impair the production or this transport of *Mbp* mRNA to the myelin. A very similar paradoxical effect has been observed in the nerves of mice “overexpressing” *P0* the major myelin gene of the PNS. A reduction in the levels of MBP was noted in mice hemizygous and homozygous for the *P0* transgene (Wrabetz *et al.*, 2000).

The levels of *Plp1* gene expression are strictly regulated in oligodendrocytes (Wight *et al.*, 2004). This is highlighted by the fact that any change in *Plp1* gene expression at message or protein levels can lead to disease in man or animal. These changes can be point mutation or gene dosage changes as seen in the #66 mice in this study. How these alterations in

expression lead to disease is still unknown and the major question to be answered. Whether the increase of PLP/DM20 in homozygous oligodendrocytes is an important clue to the disease mechanism is a matter for further investigation.

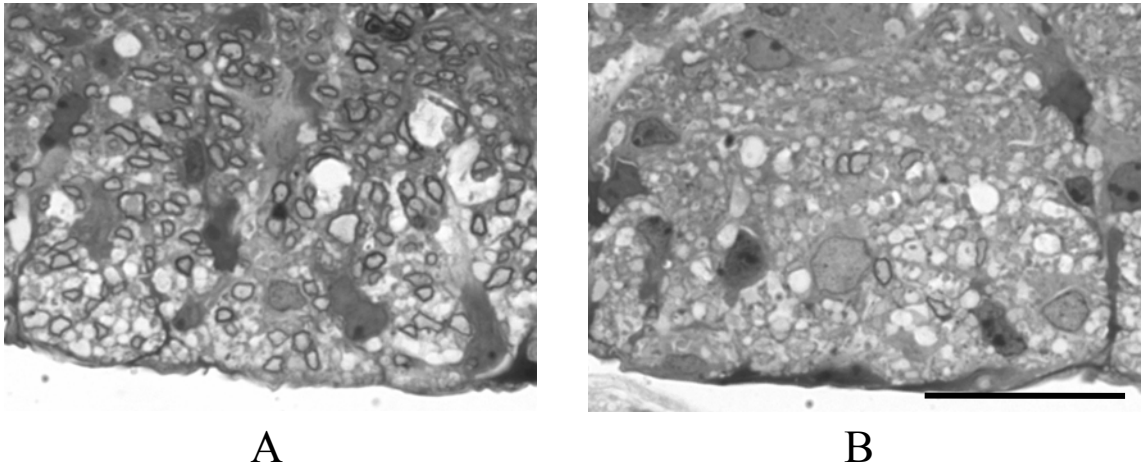


Figure 24. Resin sections (1 μ m) of white matter in the ventral funiculus of P5 mice. **A)** Hemizygous mouse with many axons surrounded by a myelin sheath indistinguishable from wildtype at this age. **B)** The homozygous mouse is dysmyelinated with thin myelin sheaths around a few axons but the majority of axons lack a sheath. Bar = 50 μ m.

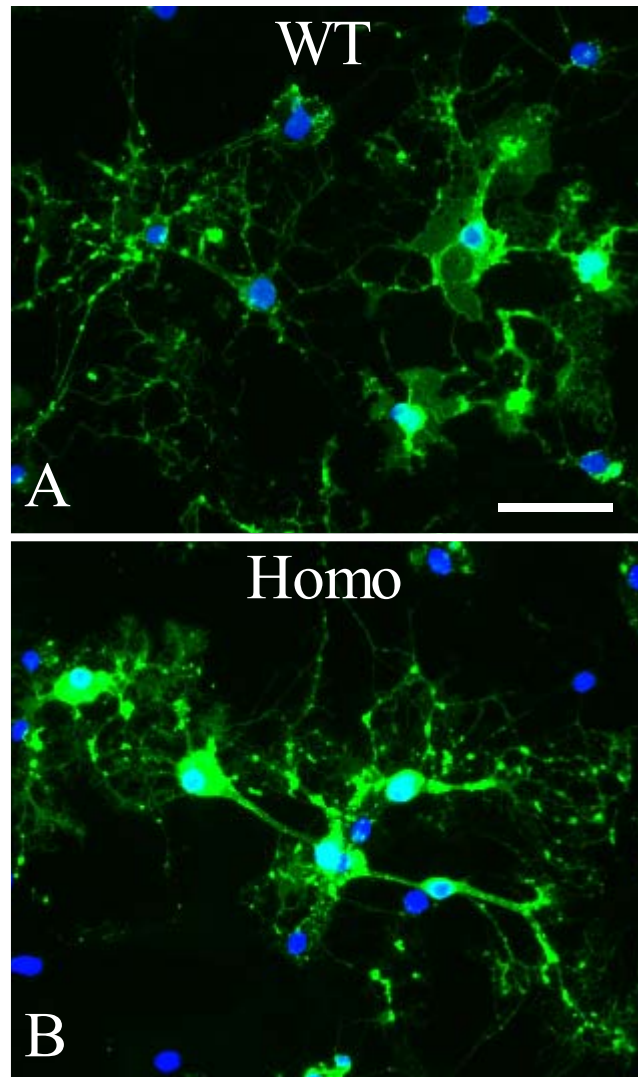


Figure 25. Representative PLP/DM20 immunostained oligodendrocytes after 6 days in culture.

A) PLP/DM20 staining of wild type oligodendrocytes in culture and **B)** PLP/DM20 staining of homozygous oligodendrocytes in culture. (Green = PLP/DM20, Blue = DAPI staining of nucleus) Bar = 50 μ m

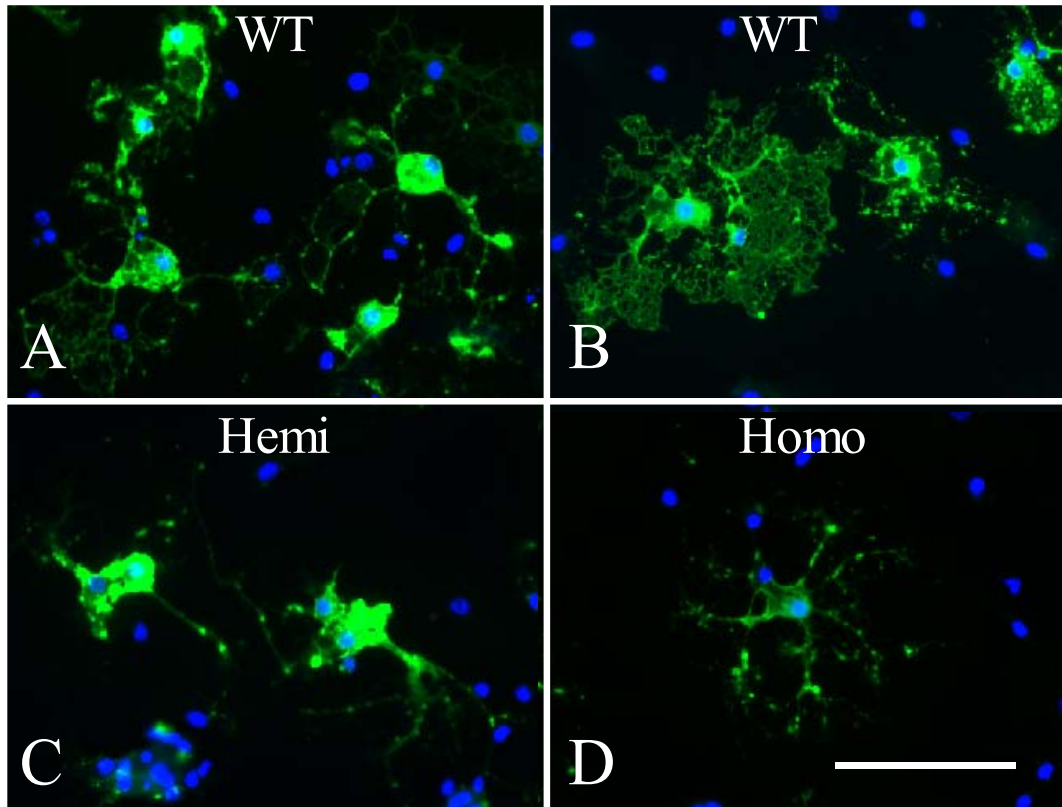


Figure 26. Representative MBP immunostained oligodendrocytes after 6 days in culture.

A) MBP staining of wild type oligodendrocytes in culture. **B)** MBP staining of wild type oligodendrocytes to show the membranous sheets not seen in homozygous oligodendrocytes. **C)** MBP staining of hemizygous oligodendrocytes in culture. **D)** MBP staining of homozygous oligodendrocytes in culture showing much lower MBP immunofluorescence compared to in both wild type and hemizygous cells. (Green = MBP, Blue = DAPI staining of nucleus) Bar = 50 μ m

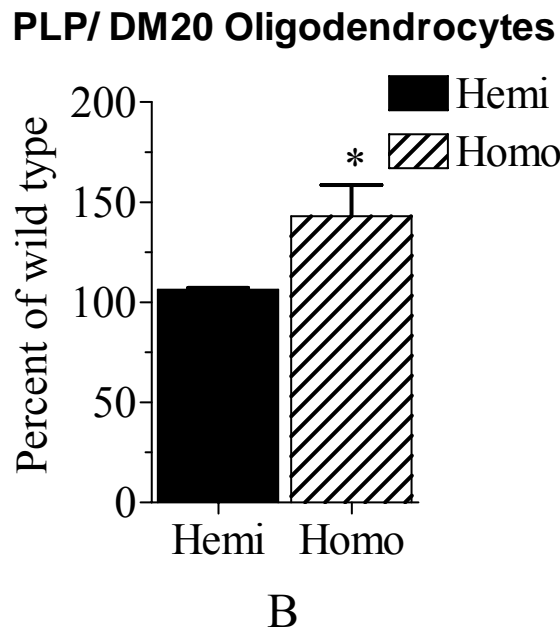
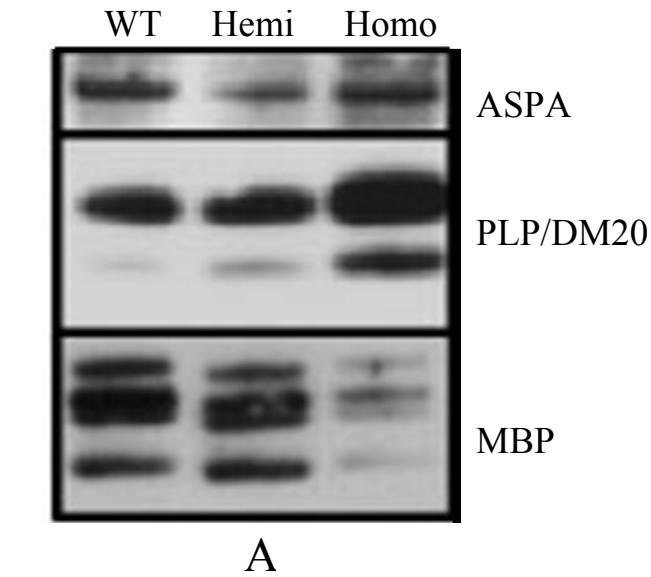


Figure 27. Protein analysis of lysates from #66 oligodendrocyte cultures.

A) Western blot immunostained for ASPA, an oligodendrocyte-specific cell body protein, PLP/DM20 and MBP showing an increase in PLP/DM20 with a reduction in MBP in the homozygous cultures compared to the other two genotypes (WT wild type, Hemi hemizygous and Homo homozygous). **B)** Levels of PLP/DM20 in oligodendrocytes normalised to ASPA and expressed relative to wild type (WT) showing a significant increase in PLP/DM20 in homozygous oligodendrocytes $p < *0.05$ but no difference in hemizygous amounts of the protein.

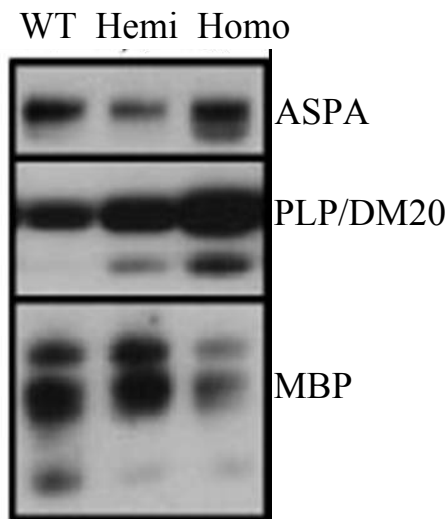
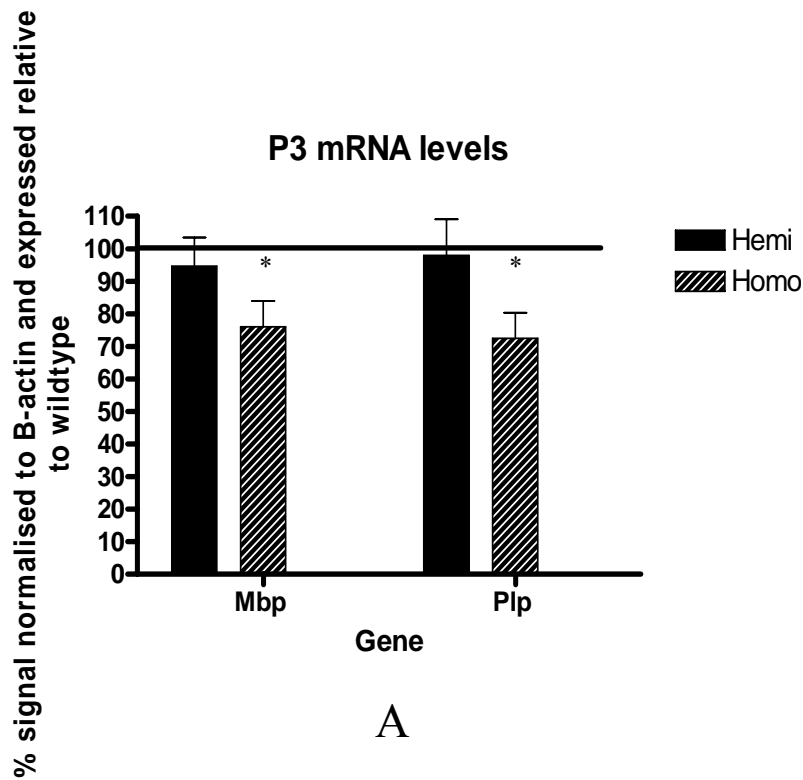


Figure 28. *Plp1* and *Mbp* gene expression in spinal cord of P3 mice hemizygous and homozygous for the *Plp1* transgene.

A) Transcript analysis graph of northern blotting showing lower mRNA levels in homozygous CNS tissue compared to wild type levels (100%) for both *Plp* and *Mbp* and no difference between hemizygous and wild type levels ($p < *0.05$). **B)** Representative western blots of total homogenates from P3 spinal cords probed for ASPA (to check loading), PLP/DM20 and MBP showing similar results to the culture profile with an increase in PLP/DM20 with decrease in MBP (WT wild type, Hemi hemizygous and Homo homozygous).

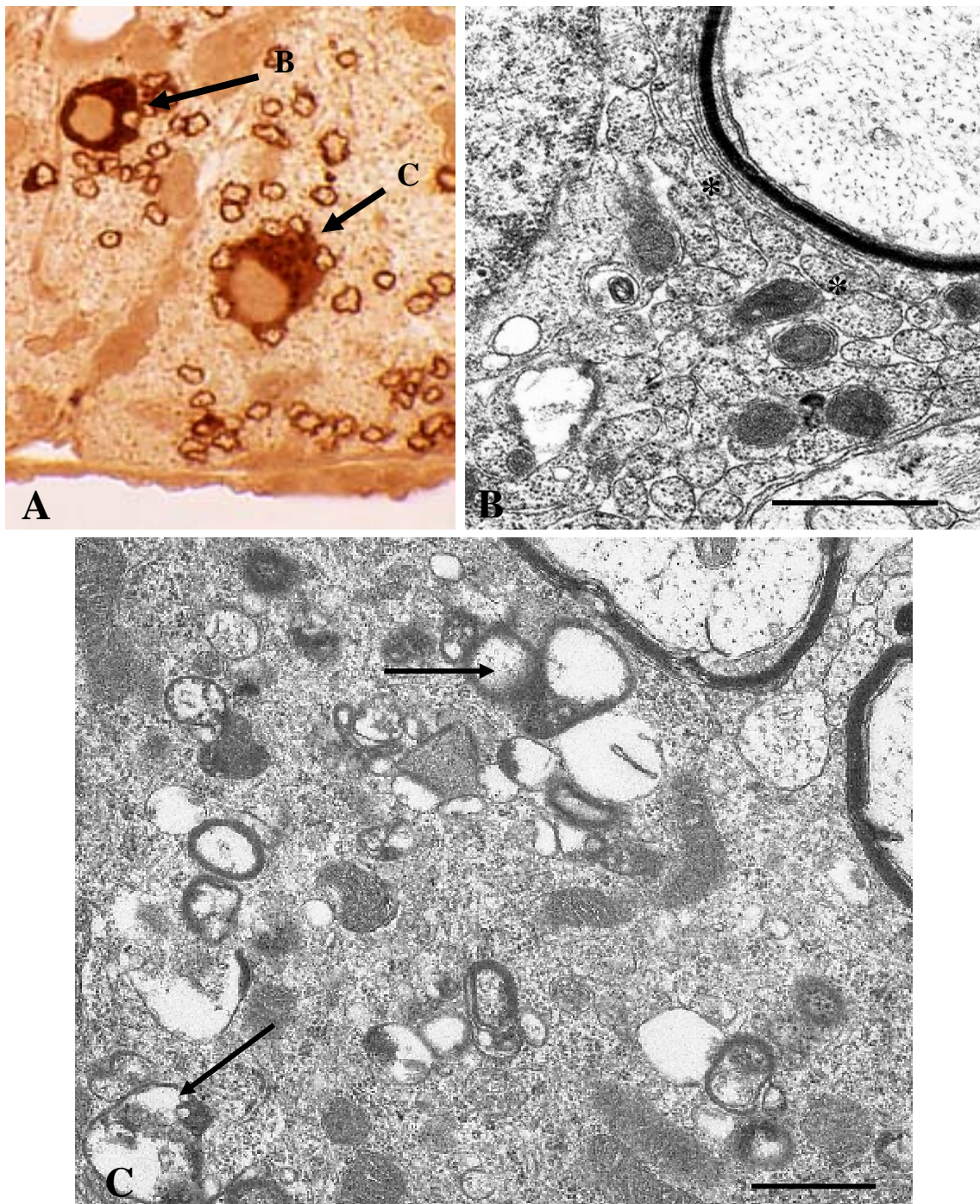


Figure 29. PLP/DM20 in sections of spinal cord of P3 mice homozygous for the *Plp1* transgene.

A) Accumulation of PLP/DM20 in cell bodies of oligodendrocytes from a P3 mouse homozygous for the transgene. Resin section immunostained for PLP/DM20 showing two oligodendrocytes with strongly immunopositive cell bodies. The thin myelin sheaths are also stained. The ventral pial surface is to the bottom. The arrows (B, C) indicate the sites of the EM images shown in Figures B and C, which were obtained from an immediately serial thin section. **B)** Part of oligodendrocyte soma showing loss of the normal cristernal arrangement of the RER (*). **C)** Oligodendrocyte soma showing autophagic vacuoles (arrows). Bars = 1 μ m.

5 Effects of Increased *Plp1* gene dosage on Peak Myelination (P20)

5.1 Background

The main cause of PMD in humans is duplication of the chromosome region containing the *PLP1* gene. This gene is highly conserved therefore mice can be used as an animal model for the disease. Unfortunately there are currently no spontaneous models of disease caused by gene dosage differences. Readhead *et al.*, (1994) amongst others generated a transgenic mouse (#66) carrying extra copies of the entire mouse *Plp1* gene including regulatory sites in 5' and 3' regions (to act as a model for PMD).

Both dys and demyelination are seen in the #66 animals dependant on the genotype of the transgenic mice. Mice with two copies of the *Plp1* gene cassette classed as homozygous showed severe dysmyelination, causing tremors, seizures and premature death. The hemizygous animals with only one copy of the cassette developed normally early on, however, in later life went on to suffer from tremors and seizures caused by demyelination. Anderson *et al.*, (1998) carried out an in-depth study of late onset demyelination observed in the hemizygous #66 animals.

Peak myelination in mouse occurs around postnatal day 20-21 in mouse. This is when the oligodendrocytes are producing the most proteins and lipids to incorporate into myelin sheaths. The burden on the oligodendrocytes is greatest at this point in CNS development. There is a huge quantity problem to be overcome by the oligodendrocytes in the CNS at peak myelination. They have to produce up to 3 times their weight in proteins and lipids per day of myelinogenesis. Transcription of the genes, trafficking of the mRNAs, translation and then trafficking of the protein is all very carefully coordinated and regulated. Gain or loss of one copy of the *Plp1* gene produces CNS myelinopathies as can be seen in humans with PMD and in transgenic rodents. The effects of increased *Plp1* gene dosage on the myelination process are the focus of this study; therefore, P20 is ideal age to investigate the effects on peak myelination.

5.2 Aims

The aim of this chapter was to investigate the effects of increased *Plp1* gene dosage at peak myelination. This was on several fronts; 1) at the message/transcript levels of Plp/Dm20 and other myelin genes, 2) at the PLP/DM20 protein level in CNS tissue, 3) how increased dosage affects other myelin proteins in the CNS, 4) what happens to the PLP/DM20 produced, 5) whether stress responses such as the UPR are activated and 6) finally how myelin morphology overall is affected by any changes/differences caused by increased *Plp1* gene dosage.

5.3 Methods

5.3.1 Animal breeding

The breeding of the #66 hemizygous males with #66 hemizygous females was carried out as described in [2.2 Mouse Breeding](#). The offspring were genotyped as described ([2.3 Isolation and Manipulation of DNA](#)) for the transgene and only male animals at P20 were used for this study (Figure 10). All three genotypes were used for this study. Hemizygous mice in this study were used prior to any demyelination changes in their myelin state. In contrast, mice homozygous for the transgene exhibit tremors from the second week followed later by seizures and thus were easily identified by eye.

5.3.2 Sample Selection

Tissues were collected from wild type, hemizygous and homozygous male mice at P20. Tails were taken for genotyping, brain and spinal cord for RNA and protein extractions. Brain cryosections were used for single or double immunofluorescence. Spinal cord sections were used to confirm genotypes and also for myelin morphology studies.

5.3.3 Transcript Analysis

5.3.3.1 Northern analysis

This experiment was performed on total cellular RNA extracted from spinal cord. The procedure of northern transfer and hybridisation is described in [2.4.6 Northern Blotting](#). The preparation of radiolabelled probes is described also in [2.4.6 Northern Blotting](#).

Staining of the gel with ethidium bromide was used to check for equal loadings of sample and presence of bands in ladder and hybridisation with β -actin (a measure of invariant expression) was used to monitor equivalence of transfer. Hybridisation analysis was undertaken using labelled cDNA products from PCRs using primers for *Plp1* and *Mbp* (Table 2) (Figure 15). The blot was left for 3-4 weeks to allow the signal to decay then probed for β -actin.

5.3.3.2 qRT-PCR analysis

Standard curves were produced using serial dilutions of an appropriate wild type RNA sample as described in [2.4.7 qRT-PCR](#). Once all the parameters for the reactions were set and equivalent for the genes, the test plate, containing *Plp1*, *Mbp* and β -actin reactions for the relevant samples selected, was run ([2.4.7 qRT-PCR](#)). The *Plp1* and *Mbp* are labelled *Plpall* and *Mbpall* as the primer/probe sets were designed to amplify all isoforms.

Set up of the experiment was as before and following the analysis protocol laid out in [2.4.7 qRT-PCR](#) the uncorrected concentrations of *Plp1*, *Mbp* and β -actin mRNA in 50ng total RNA loaded were calculated. The *Plp1* and *Mbp* concentrations were then normalised to β -actin and expressed as a percentage of wild type levels giving the actual concentration of *Plp1* or *Mbp* message in total RNA.

5.3.3.3 RT-PCR analysis of stress responses

Standard RT-PCR experiments using *cyclophilin* and *Xbp1* primers were carried out on cDNA from P20 spinal cord as described in [2.4.5 RT-PCR](#).

5.3.4 CNS Myelin Analysis

5.3.4.1 Myelin Preparation

Myelin was prepared from powdered spinal cord or brain, protein was quantified and analysed by western blot as described in [2.5 Protein Analysis](#). Blots were immunostained for myelin proteins using AA3 (for PLP/DM20), MAG, MBP and CNP antibodies (Table 5). Blots were also immunostained for BiP, an ER resident protein.

5.3.5 Morphometric analysis

To study neural development and maturation, glial cell quantification and myelin morphometry were performed on the ventral columns of spinal cord (C2-3) ([2.6 Myelin](#)

[Morphological Analysis](#)). Analysis at 20 days was chosen as a stage when the myelination process was at its peak in the CNS.

To count the number of mature oligodendrocytes in sections of spinal cord CC-1 immunostaining was carried out as described in [2.6.4.5 CC-1 staining of oligodendrocytes](#).

5.3.6 Immunostaining

Cyrosections from P20 brain were immunostained as described in [2.6.4.2 Immunofluorescence](#).

5.4 Results

5.4.1 Identification of Genotype

PCR using the *Plp* and T7 primers identified the presence or absence of the #66 transgene cassette. All animals negative for the PCR product were wild type and all animals positive for the PCR product were considering transgene positive. Dependant on age the transgene positive animals could either be homozygous or hemizygous. At P20 however the two genotypes are distinguishable by sight as the homozygous animals have tremors whereas the hemizygous animals look normal. To confirm the genotypes immersion fixed sections of spinal cord were also examined.

5.4.2 Transcript Analysis of P20 wild type, hemizygous and homozygous animals

Prior to electrophoresis on a denaturing northern gel 500ng total RNA from each animal was electrophoresed on a 1.5% agarose gel to check quality (Figure 11). 20 μ g total RNA from wild type, hemizygous and homozygous P20 spinal cord was then electrophoresed on a denaturing northern gel (Figure 13). In Figures 11 and 13 the three ribosomal species of RNA can be seen verifying the RNA has not degraded. The resulting blot was probed with *Plp/Dm20* and β -*actin* (Figure 30A). The signals of the hemizygous for β -*actin* and *Plp/Dm20* (Hemi) are very similar to the signals of the wild type RNA (WT) suggesting no difference in *Plp/Dm20* levels in the hemizygous animals in comparison to the wild type control. The signal for β -*actin* for the homozygous sample (Homo) is comparable but the *Plp/Dm20* signal is lower than the signals for both wild type and hemizygous samples (Figure 30A WT and Hemi).

When analysed and normalised to β -actin, the message levels of *Plp/Dm20* for the hemizygous RNA are not statistically different from wild type as demonstrated in Figure 30B at 122% compared to 100%. This is true for the northern analysis and the qRT-PCR. However, there is a difference in *Plp/Dm20* mRNA levels in homozygous samples. There is a decrease in message to 60% of wild type levels which is statistically significant ($p < **0.01$) in the northern analysis.

The same blot was then hybridised with *Mbp* and shows there is no difference in *Mbp* levels between wild type and hemizygous samples but there is a decrease in *Mbp* message levels in homozygous RNA (Figure 30C). *Mbp* mRNA levels, representative of other myelin genes, are not different from wild type in the spinal cords of P20 hemizygous mice but reduced ($p < **0.01$) in homozygotes. The data ($M \pm SEM$, $N = 5$) are expressed relative to wild type (Figure 30D).

Wild type RNA from different time points was used to investigate development profiles of the two messages by qRT-PCR. Figure 30E shows the profile for *Plp/Dm20* and *Mbp* from embryonic day 12 to postnatal day 80. The message levels for both peaks between postnatal day 10 and 20 then drop off towards P80. This concurs with the myelination state in the CNS where peak myelination is around P20 and then the oligodendrocytes are involved in maintenance of myelin in the CNS.

5.4.3 PLP/DM20 levels in CNS

Protein extracts from CNS tissue were studied in this section. Total homogenates, produced from spinal cord or brain from each genotype, were fractionated into myelin and pellet fractions. Western blots of each of the three sample types were immunostained for PLP/DM20 using the AA3 antibody (Figure 31A). There is a gradual decrease across the genotypes in PLP/DM20 levels in the total homogenate fraction with wild type having the most protein and the homozygous spinal cord the least. PLP/DM20 levels in the wild type and hemizygous myelin fractions are very similar but there is less PLP/DM20 protein in the homozygous myelin.

Surprisingly the pellet fraction shows a different PLP/DM20 profile. There is more PLP/DM20 protein in the pellet fractions of the hemizygous and homozygous spinal cord relative to the wild type spinal cord. The levels of PLP/DM20 in the total homogenate and

myelin fraction from homozygous mice are reduced compared with wild type whereas in the pellet fraction the converse applies (Figure 31A).

In the spinal cord of hemizygotes at P20, the levels of PLP and DM20 in myelin-enriched fractions are not different from wild type littermates but are significantly lower in homozygous animals (Figure 31B). Similar results were obtained for myelin fractions from the brain (data not shown). In comparison with wild type (100%), the levels of PLP and DM20 are greater in pellet fractions from hemizygotes ($158\% \pm 9$ and $227\% \pm 28$, respectively, $N = 5$, $p < *0.05$) while for homozygotes PLP was similar ($124\% \pm 10$, NS) and DM20 is elevated ($207\% \pm 38$, $p < *0.05$).

5.4.4 Effects of increased dosage on other myelin proteins

CNP, MAG and MBP were chosen to represent other myelin proteins in the CNS. As mentioned previously, MBP makes up 30% of myelin proteins in the CNS whereas MAG shares a similar translation and transport pathway with PLP/DM20. These proteins are present in the myelin fraction from spinal cord; therefore, myelin was immunostained on western blots for each protein (Figure 32A).

All three proteins are reduced in homozygous mice (Figure 32A Homo) and MBP and CNP are also lower in hemizygotes (Hemi), compared with wild type (WT). In the hemizygotes, MBP ($p < ***0.001$) and CNP ($p < **0.05$) are reduced relative to wild type while MAG levels are similar. All proteins are markedly lower ($p < ****0.001$) in homozygous mice (Figure 32B). Only MBP is reduced in myelin prepared from hemizygous brain compared to in homozygous brain myelin where all three proteins are reduced (Figure 32C).

To ensure equal loading 10 μ g myelin fraction from each genotype was separated on a SDS-Page gel and stained with coomassie blue (Figure 32D). Many proteins are present on the gel and PLP and MBP stain very well and can be seen near the bottom of gel. A visual reduction of these proteins in homozygous myelin (Figure 32D Homo) can be observed compared to the wild type and hemizygous myelin fractions (Figure 32D WT and Hemi). Not all proteins stain well using coomassie blue, for example DM20 and one of the MBP isoforms are not visible on this gel.

However not all proteins are reduced in the homozygous animals relative to their wild type and hemizygous littermates (Figure 32D). A western blot of myelin proteins immunostained with anti-MOBP antibody shows a higher nonspecific protein in the myelin that is increased in the homozygous CNS.

5.4.5 Stress responses in #66 animals

No difference is seen in the induction of *Xbp1* transcription between the three genotypes (Figure 33A). There are two forms of the *Xbp1* mRNA, the inactive form *Xbp1* (Unspliced) (*Xbp1* (U)) and the active form *Xbp1* (Spliced) (*Xbp1* (S)). The message levels are similar for all the mice in spinal cord. Activation of *Xbp1* converts some if not all the unspliced message to a spliced mRNA that is resistant to digestion by the restriction enzyme *PstI*. When digested with *PstI*, only the unspliced form is digested (Figure 33B).

BiP, a molecular chaperone implicated in protein folding, is upregulated when a cell is subjected to ER stress. However, no difference in BiP levels is seen between the three #66 genotypes (Figure 33C). The levels of BiP are the same throughout the changes of *Plp1* gene dosage.

5.4.6 Morphometric analysis of P20 #66 myelin in spinal cord and brain

As shown above, *Plp1* gene dosage has an influence on its transcript and protein levels as well as on other myelin gene products especially MBP. This in turn could have an impact on the formation of myelin in the CNS. Electron micrographs of cervical ventral columns of all three genotypes are shown in Figures 34A-C.

A higher magnification electron micrograph of an oligodendrocyte cell body in a P20 #66 homozygous spinal cord section is shown in Figure 35. There is a well developed RER, which is not obviously disrupted in this cell, vacuolation of the Golgi apparatus (arrow 1) and numerous autophagic vacuoles (arrow 2).

The volume of myelin from P20 spinal cord of all the genotypes was quantified from electron micrographs of cervical ventral columns using a point counting method (Figure 36A). Hemizygous animals contain slightly less myelin (81%) than wild type and are not significantly different whereas homozygous mice have considerably less myelin than the other two genotypes.

Morphometric analysis indicates that while axon diameters are similar in the three genotypes, the mean g ratio is elevated in hemizygous and more especially homozygous transgenic mice compared with wild type, due to a reduction in myelin thickness (Figure 36B, C). The morphometric changes are reflected by differences in cervical cord area; both hemizygous ($2.54 \pm 0.03 \text{ mm}^2$, $n=6$) and homozygous (2.14 ± 0.02) mice have reduced areas compared with wild type (2.89 ± 0.06 , $p < ***0.001$) and the two mutants differ from each other as well ($p < **0.01$).

The myelin recovery from whole brain (expressed as myelin protein per unit weight of brain tissue) obtained during the biochemical fractionation is also assessed. There is no difference in recovery between wild type and hemizygous mice but markedly less myelin is obtained from the dysmyelinated homozygous mice (Figure 36D).

The calculated number of CC-1+ oligodendrocytes in white matter per transverse section for P20 wild type, hemizygous and homozygous mice are 337 ± 13 , 358 ± 12 and 349 ± 52 cells/ mm^2 , respectively; these values are not significantly different (data not shown).

5.4.7 Storage of PLP/DM20 in the oligodendrocyte cell body

As observed there is more PLP/DM20 present on the pellet fraction of CNS tissue from homozygous mice compared to wild type and hemizygous counterparts. To investigate where in the oligodendrocyte cell body the protein is situated cyrosections of brain were immunostained with a PLP antibody, anti-Lamp1 (an antibody for lysosomes) and DAPI for cell nuclei (Figure 37A, B). An oligodendrocyte cell body is strongly stained for PLP/DM20 throughout the majority of cytoplasm including regions containing Lamp1+ structures (Figure 37A). Further magnification shows intense co-labelling of structures within the cell body for PLP/DM20 and Lamp-1 (Figure 37B). Analysis of the circled area (Image-Pro Plus 6 co-localisation software) shows co-localisation ($r = 0.68$, overlap correlation = 0.925) between the two markers.

MAG, which shares the same biosynthetic pathway as PLP/DM20, is also concentrated in oligodendrocyte cell bodies in homozygous mice whereas MBP, which has a different pathway, is not enriched in the soma and is present in the myelin ensheathing axons (Figure 38A, B).

5.5 Discussion

In this chapter the effects of increased *Plp1* gene dosage on peak myelination in mouse were investigated. In previous chapters the effects of the increased gene dosage on pre and early myelination were investigated as well as the contribution of the transgene only on the null background on message and protein levels. Very similar results are seen for *Plp1* transcript levels in #66 hemizygous animals pre myelination (Chapter 4) and during peak myelination at P20. Levels of *Plp1* gene message are consistent with the levels seen with the transgene on a null background in Chapter 3. The hemizygous oligodendrocytes regardless of stage of CNS myelin development can produce normal levels of message.

Readhead *et al.*, (1994) found there were higher *Plp1* transcripts levels in the hemizygous animals compared to the homozygous mice. In *4e-Plp* mice generated by Kagawa *et al.*, (1994) which contain 2 or 4 extra copies of the entire *Plp1* gene including 5' and 3' noncoding regions, the *Plp1* messages levels were at 132% in hemizygous animals. The message levels in homozygous mice were reduced to 60% of wild type levels. This reflects the findings in the #66 transgenic animals in this chapter. Mallon and Macklin (2002) put forward the proposal from evidence in their transfected cells and transgenic mice showing a decrease in endogenous *Plp1* mRNA ranging from 30%-54% that extra copies of the 3'UTR of the *Plp1* gene can cause a downshift in endogenous *Plp1* gene expression compared to wild type counterparts. As the *Plp1* genes in the transgenic cassette are wild type and there is no distinguishable factor between them and the endogenous copy this down regulation may go some way to explaining the levels of *Plp* and *Dm20* message in the hemizygous mice where levels are close to wild type levels. In homozygous mice the message levels are much lower and other issues such as threshold could be an influencing factor.

There is a discrepancy between the message levels from qRT-PCR analysis and northern analysis. The trends are the same; *Plp/Dm20* message is lower in the homozygous animals than in the hemizygous mice. Leske *et al.*, (2004) also found discrepancies between their northern and qRT-PCR results. Although they observed differences in absolute values, the overall trends in mRNA levels were very similar between the methods. One of the major differences in the methods is quantity of initial sample, in the qRT-PCR it is only 50ng whereas the sample loaded onto a northern gel is 20µg.

With *Mbp* the message levels are reduced in homozygous mice (50%) but not in hemizygous CNS tissue. This is the case at all stages of myelinogenesis in the CNS. This reflects the changes seen prior to peak myelination. The *Mbp* message is reduced in P3 spinal cord at the stage where oligodendrocytes are just coming into contact with axons and only rudimentary sheaths are formed. The *Mbp* message levels in *4e-Plp* mice were also similar to those in the #66 transgenic mice. The transcript levels were reduced from wild type > hemizygous > homozygous (Kagawa *et al.*, 1994). *Mbp* message and protein levels were also reduced in *Cnp* overexpressing transgenic mice (Gravel *et al.*, 1996)

There is an increase in PLP/DM20 levels in oligodendrocytes prior to peak myelination in the homozygous animals compared to wild type animals. This, however, is reversed at peak myelination where there is less PLP/DM20 protein in the total homogenates. Less PLP/DM20 is also seen in the myelin enriched fraction from CNS tissue in the homozygous transgenic mice. Conversely, the pellet fraction of homozygous mice which is enriched in membranous organelles, nuclei and non-soluble components has more PLP/DM20 protein compared to wild type littermates.

Wrabetz *et al.*, (2000) generated transgenic mice with extra copies of the P0 PNS myelin protein. Animals with more than 20 copies of the *Mpz* gene developed a severe phenotype similar to homozygous #66 animals. In one line, Tg80.3, containing 2 extra copies of the gene, P0 protein was overexpressed at P28 in sciatic nerves. Like the #66 mice at higher copy numbers the level of P0 protein fell and was associated with severe dysmyelination. Tg80.2 with 31 copies of *Mpz* gene had significantly reduced levels of P0 protein compared to controls. These findings are very similar to data from the #66 transgenic animals in this study. The PLP/DM20 protein levels in the *4e-Plp* mice were lower than the message levels indicating, as in #66 animals, translational or post-translational irregularities affect levels. McLaughlin *et al.*, (2006) also reported discrepancies between message and protein levels in the *rumpshaker* mice. They noted that although levels for PLP and DM20 per unit of myelin were 9% and 15% respectively, *Plp* mRNA was 66% of wild type levels.

The increase in *Plp1* gene dosage in these transgenic animals also causes a disruption to the other myelin protein studied in this project. CNP, MAG and MBP are all significantly reduced in the homozygous mice compared to wild type in both brain and spinal cord. In the hemizygous mice CNP and MBP are down in the spinal cord but CNP is not reduced

relative to wild type in the brain. In P0 overexpressor mice MBP levels were reduced in sciatic nerves to 50% normal wild type levels, as was PMP22, another PNS myelin protein (by 33%) (Wrabetz *et al.*, 2000). As in #66 transgenic mice myelin protein levels are disturbed in *Mpz* transgenic mice regardless of dysmyelination.

Over the course of this study more variability was found in the brain tissue for message, protein and also myelin status compared to spinal cord in all genotypes. This may possibly be due to the fact that the spinal cord is more uniformly myelinated compared to the brain. It was also noted that in general, hemizygous animals as a group showed more variability than the wild type or homozygous mice. This variation could be reflected in the differing ages of onset of demyelination and neurodegeneration seen in these animals. One possible theory is that the hemizygous animals with the lowest MBP at message and protein levels are the ones that will show signs of demyelination the earliest. MBP was suggested as the possible vital factor in causing disease pathology in myelination by McLaughlin *et al.*, (2006) as MBP is critical for myelin formation and influences the amount of myelin formed (Shine *et al.*, 1992).

There is a marked reduction in PLP/DM20 and other myelin proteins in the homozygous CNS. As PLP/DM20 and MBP makes up to 80% of the myelin proteins in the CNS, this reduction has a marked effect on overall protein concentration in the sample. Wrabetz *et al.*, (2000) suggested that in their P0 transgenic mice, overexpression of P0 may cause a reduction in the amount of other proteins detected by western blotting. However, there is an increase in *Plp1* gene products at either the message or protein level in the #66 transgenic mice that could explain the lowering of other myelin protein levels to such a degree.

Equal loading of protein from the biological fractionation process is essential for proper quantification of protein levels so after meticulous quantification equal concentrations of proteins were loaded into the wells of SDS-Page gels. Coomassie blue staining of the myelin fraction allowed a visual check of loading. Unfortunately many proteins do not stain well therefore were not visible. Bands of unknown proteins appeared stained to the same intensity across the three genotypes. PLP and three isoforms of MBP were visible reduced in the homozygous sample when compared to the wild type and hemizygous myelin. It is possible that as proteins are reduced in the #66 transgenic animals, protein levels can also be increased. One example of this increase in protein levels was noted on

the MOBP stained western blot. Although like the other myelin proteins investigated in this study MOBP levels were decreased in homozygous mice a second nonspecific band higher up on the same blot was increased in the same sample. It is entirely possible there is a subpopulation of proteins in the homozygous mice that are increased due to the *Plp1* gene increase.

The UPR (unfolded protein response) is triggered by the accumulation of unfolded or misfolded proteins in the ER (Shang 2005). It has a role to play or can be activated in the disease process in other myelin mutants such as *rumpshaker* (McLaughlin *et al.*, 2007). *Xbp1* and BiP both take part in this process and are upregulated in the CNS of these animals. The expression of the *Xbp1* gene changes from the unspliced RNA product to the spliced RNA product upon the activation of the UPR. The spliced product is resistant to digestion by *PstI* therefore the difference in UPR between samples can be measured. Unlike in *rumpshaker* where there is a slight activation of *Xbp1* producing the spliced products, all the *Xbp1* gene product is digested in all three genotypes in #66 transgenic mice. No difference is observed in the induction of BiP between the wild type, hemizygous and homozygous #66 mice. These findings suggest that the UPR does not come into play in the #66 mice and this may be due to the fact that the protein produced by the transgenic cassette is wild type and not unfolded or misfolded in any way.

Increase in *Plp1* gene dosage causes a clear change in myelination state in the #66 mice. The axons myelinate in proportion to their diameter; the bigger the diameter of axon then the thicker myelin sheath insulating it. The hemizygous animals have slightly thinner sheaths than those of the wild type mice. However in the homozygous animals there is very little myelin ensheathing axons leaving many axons naked. An increase in *Plp1* gene dosage, therefore, leads to a commensurate reduction in myelin formation in spinal cord. In the case of hemizygous mice this is subtle and due only to slightly thinner myelin sheaths. In the more severely affected homozygous mice this reduction is a combination of markedly thinner sheaths and amyelinated axons. Homozygous LewPLP rats also have a dysmyelinated CNS and this is due to the death of mature oligodendrocytes and the arrested development of immature oligodendrocytes (Bauer *et al.*, 2002). The hemizygous rats are normal then demyelinate later in life, as do #66 hemizygotes (Chapter 6).

Closer examination of the #66 homozygous oligodendrocytes showed abnormalities of the Golgi apparatus and vacuolar structures within the cell body. Similar abnormalities are

seen in LewPLP rats (Bauer *et al.*, 2002) and *4e-Plp* mice therefore are very unlikely to be an insertional effect or due to disruption of an important gene. In *4e-Plp* mice at P14 and P20 the white matter in spinal cord of the homozygous animals contained either naked or very thinly sheathed axons. Swelling of the Golgi apparatus and abnormal vacuolar structures were observed in the oligodendrocytes of these animals (Kagawa *et al.*, 1994).

Overall myelin volumes in the spinal cord of #66 transgenic mice differ significantly between all three genotypes. There is a step reduction from wild type to homozygous myelin. This reduction in myelin volume is reflected in the increase in g ratios in the transgenic animals. The g ratio is the ratio between axon diameter and total fibre diameter including the sheath. As the myelin around the axon decreases the g ratio increases. Myelin sheath thickness (MT) should increase with axon diameter as shown by the scatter graph for wild type mice and the corresponding linear regression. However the slopes of regression lines for the transgenic mice are reduced compared with wild type and also differ from each other.

As myelin recovery in the spinal cord was reduced, the myelin recovery from whole brain (expressed as myelin protein per unit weight of brain tissue) obtained during biochemical fractionation was also assessed. There was no difference in recovery between wild type and hemizygous mice but markedly less myelin was obtained from the dysmyelinated homozygous mice. The failure to detect subtle differences between wild type and hemizygous mice may indicate differences between myelination in brain and spinal cord or reflect the lower sensitivity of this technique compared with the morphometric analyses.

Total levels of PLP/DM20 (as contained in total homogenates) are slightly lower than wild type, the reduction probably reflecting downregulation of myelin genes associated with dysmyelination. What is striking though is the alteration in distribution of PLP/DM20 with the somal pellet fractions containing more protein, relative to the low levels in the myelin sheath. There is more PLP/DM20 present in homozygous mice in oligodendrocytes *in vitro*, in P3 oligodendrocytes in spinal cord and in the pellet fraction of P20 spinal cord and brain.

Where this extra protein is situated in the cell is a major question to be answered. Forebrain sections of P20 brain were immunostained for PLP/DM20 and Lysosomal-associated membrane protein 1 (Lamp-1). Lamp-1 is a highly glycosylated protein in lysosomal membranes. Lysosomes represent the final destination for many endocytic,

autophagic and secretory molecules targeted for destruction or recycling but have more complex functions than simply being the end-point on a degradative pathway (Eskelinen *et al.*, 2003). Co-localisation of PLP/DM20 and Lamp-1 was noted in the sections suggesting PLP/DM20 is stored in lysosomes in the oligodendrocyte cell body. Trajkovic *et al.*, (2006) report degradation of PLP/DM20 does not occur in the late endosomes/lysosomes the protein is stored in as these organelles appear to be utilised for storage by the oligodendrocytes. Intense immunostaining of oligodendrocyte cell bodies in P3 spinal cord sections points to the likelihood the increased levels of PLP/DM20 are stored in the cell body from early on in the myelinogenesis.

The quantitative change in PLP/DM20 protein amounts in myelin and pellet is matched by immunocytochemical demonstration of strong PLP/DM20 reactivity in the cell bodies in #66 transgenic mice and in the transgenic LewPLP rat model (Bauer *et al.*, 2002, Bradl *et al.*, 1999). Immunostaining and EM show that the strongly immunopositive oligodendrocyte cell bodies contain numerous autophagic vacuoles and lysosomes. PLP, when overexpressed, is known to associate with the endosomes/lysosome system (Simons *et al.*, 2002).

In normal myelination PLP may also associate temporarily with endosomes before axon-derived signals promote its insertion into myelin (Trajkovic *et al.*, 2006). A reduction in the available myelin and decreased axonal contact, as occurs in the #66 homozygous mice, would exacerbate the accumulation of PLP in lysosomes. Trajkovic *et al.*, (2006) report PLP and Lamp-1 co-localisation only occurs in immature oligodendrocytes suggesting the oligodendrocytes in the #66 homozygous animals at peak myelination have arrested in development prior to full maturity. A range of membrane proteins of both myelin and non-myelin origin were also concentrated in oligodendrocyte cell bodies in the *Plp1* transgenic rats (Bauer *et al.*, 2002). Schwann cells overexpressing P0 also concentrate the protein in their cell bodies due to the paucity of available myelin (Yin *et al.*, 2000). PLP positive vacuoles were also observed in brain sections of *Cnp* overexpressing transgenic animals (Gravel *et al.*, 1996).

Similarities also exist with increased dosage of the *PMP22* gene, the commonest cause of Charcot-Marie-Tooth disease type 1A. Transgenic rodent models of the disorder exhibit dysmyelination proportionate with *Pmp22* dosage (Huxley *et al.*, 1998, Niemann *et al.*, 2000) and Schwann cells contain autophagic vacuoles reminiscent of those seen in

oligodendrocytes in this study (Chies *et al.*, 2003, Niemann *et al.*, 2000). Additionally with increased *Pmp22* dosage, dysmyelination of the peripheral nerves is associated with reduced levels of myelin proteins (Sereda *et al.*, 1996), as occurred with the #66 *Plp1* transgenic mice.

As suggested by Yin *et al.*, (2000) and Wrabetz *et al.*, (2000) there is dose dependant mechanisms involved in the myelination process in the three genotypes of the #66 animals. This is similar to the disease process in humans as PMD severity does correlate with levels of *PLP1* copy number (Wolf *et al.*, 2005). Patients with 3 copies of the *PLP1* gene were more severely affected than patients with a duplication of the gene. However the patient with 5 copies of the gene was not any more severely affected than the patients with 3 copies again suggesting a threshold effect of the disease process. How the threshold effect and the different fates of PLP/DM20 in the homozygous #66 animals induce dysmyelination in the CNS is still a matter for ongoing study.

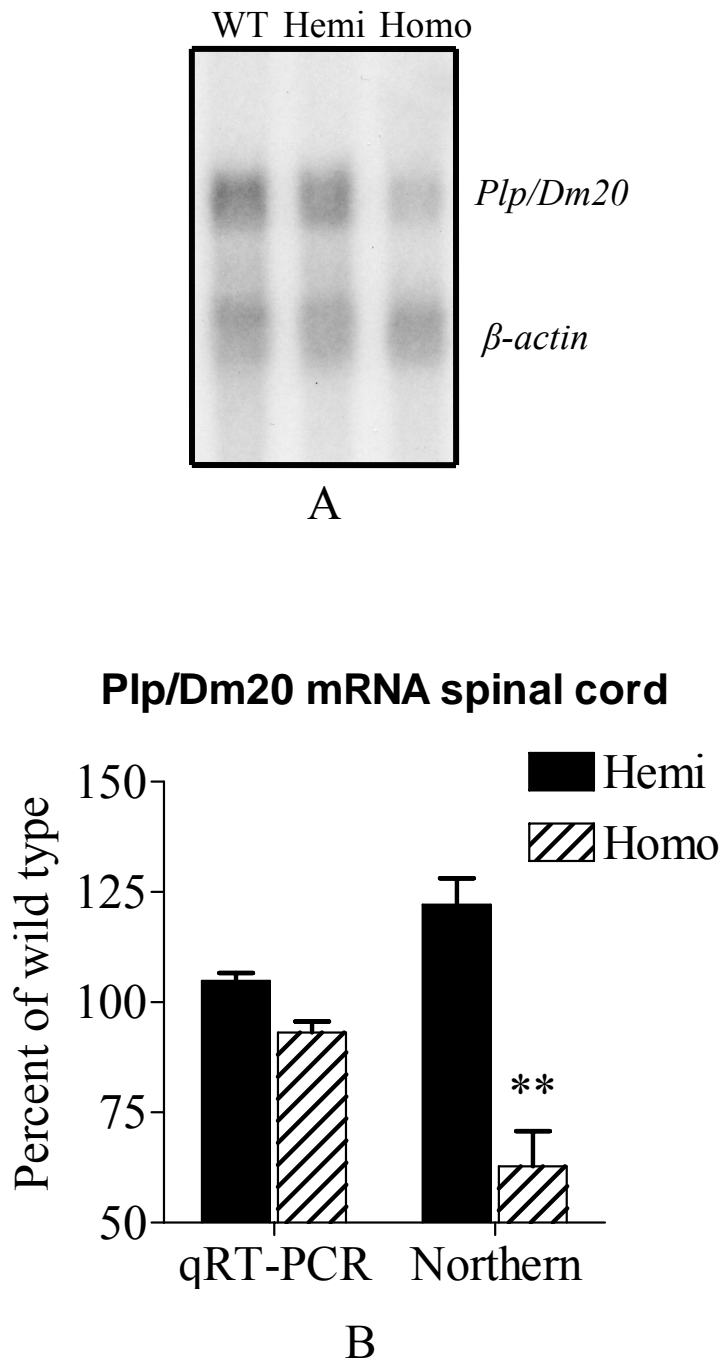


Figure 30. Transcript analysis of P20 #66 spinal cord RNA.

A) Representative northern blot for *Plp/Dm20* and *β-actin* mRNA from spinal cord of P20 mice demonstrating reduction in *Plp1* transcript levels in homozygous P20 spinal cord. **B)** Quantification of *Plp/Dm20* mRNA in P20 spinal cord, ($M \pm SEM$, $N = 5$), expressed relative to wild type. The increase in hemizygotes is not significant whereas the level in homozygotes is reduced ($p < **0.01$).

Mbp mRNA spinal cord. P20

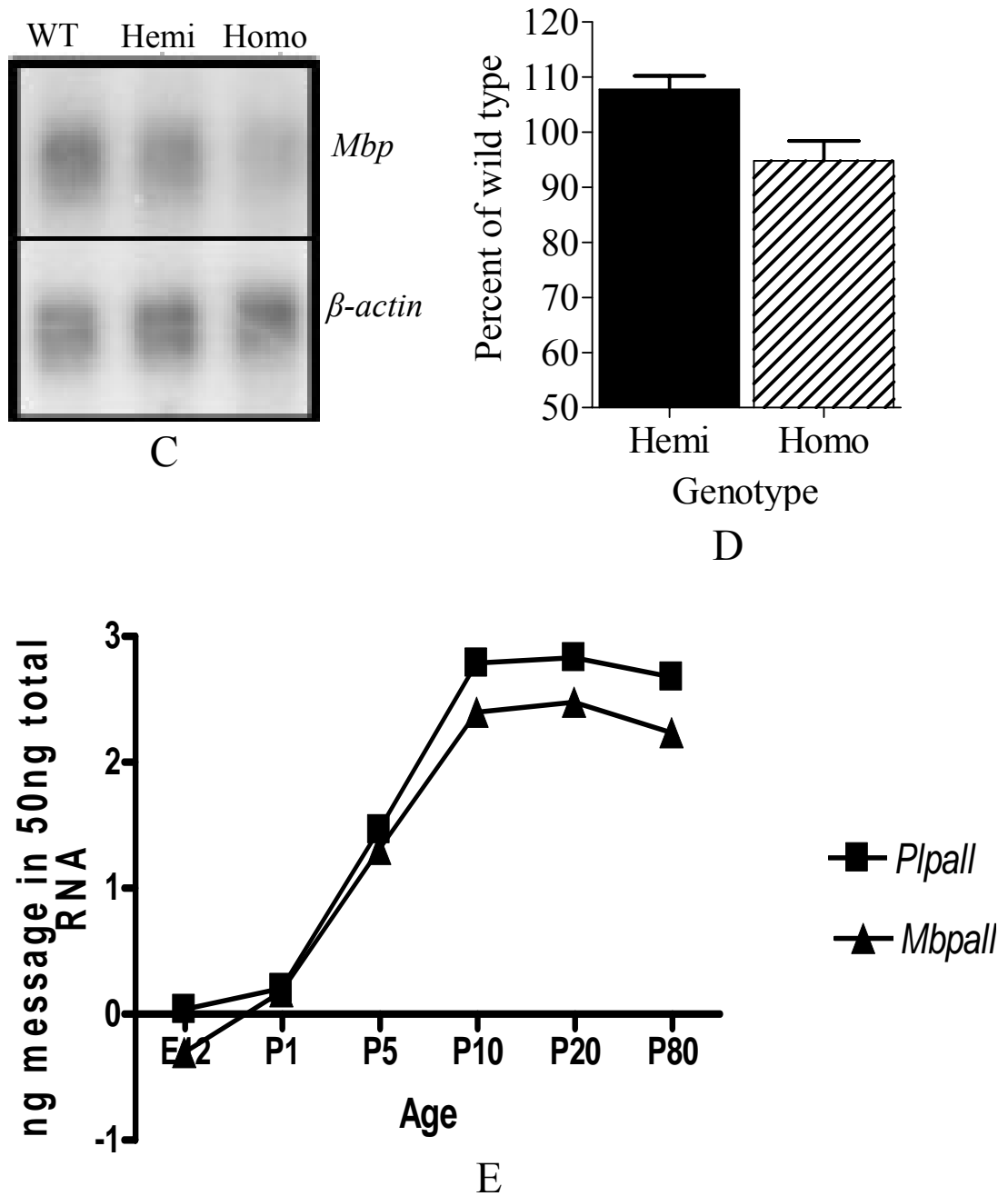


Figure 30 (continued).

C) Representative northern blot for *Mbp* and β -actin mRNA from spinal cord of P20 mice showing a reduction in *Mbp* mRNA in homozygous spinal cord (Lane 3) compared to both wild type (Lane 1) and hemizygous spinal cord (Lane 2). **D)** *Mbp* mRNA levels, representative of other myelin genes, are not different from wild type in the spinal cords of P20 hemizygous mice but reduced ($p < **0.01$) in homozygotes. The data ($M \pm SEM$, $N = 5$) are expressed relative to wild type. **E)** Graph of steady state levels of all the transcripts produced by *Plp1* and *Mbp* at different ages showing a very similar developmental profile for the two genes with an increase in levels in the lead up to peak myelination at P20 then a slight reduction at P80.

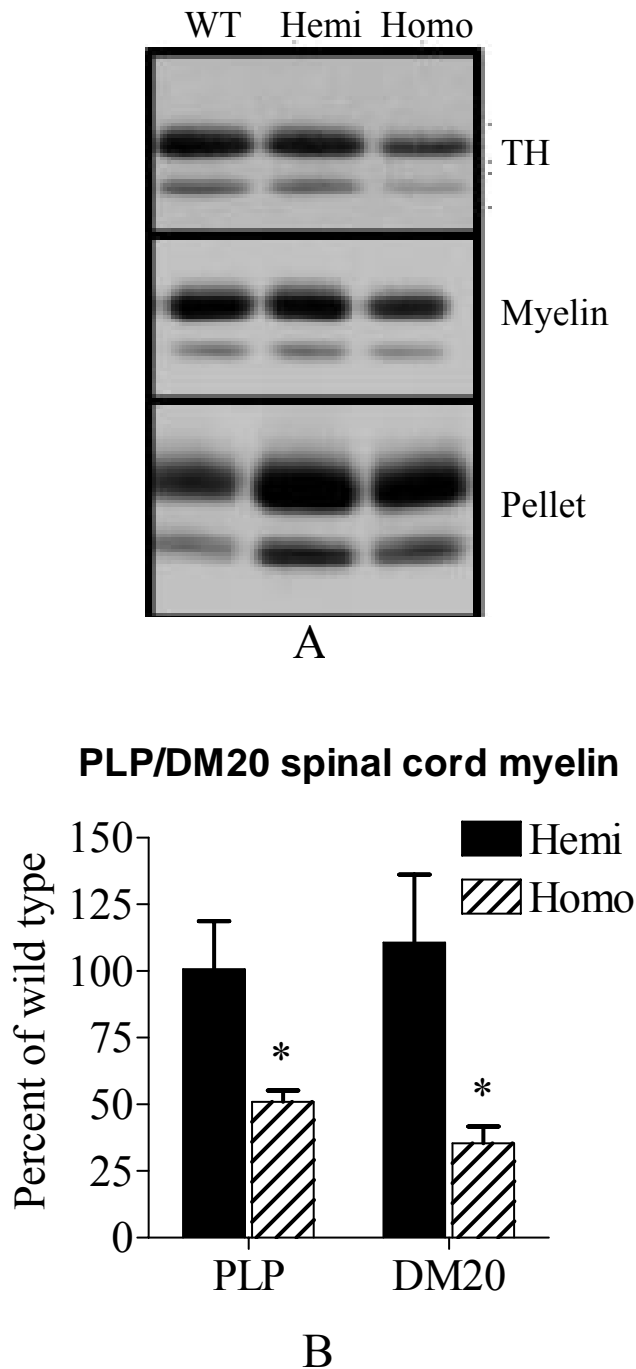


Figure 31. PLP/DM20 protein analysis in #66 animals at P20.

A) Representative western blot for PLP/DM20 of myelin enriched and pellet fractions and the total homogenate (TH) from spinal cord of P20 mice highlighting a reduction in total PLP/DM20 amounts (as seen in TH) and amount in myelin in the homozygous spinal cord (Homo) with a corresponding increase in the amounts of PLP/DM20 in the pellet fraction.

B) Steady state levels of PLP and DM20 proteins in myelin fractions from P20 mice show no change from wild type in hemizygous animals but significant reductions down to 50% of wild type levels in homozygous mice ($M \pm SEM$, $N = 5$, $p < *0.05$).

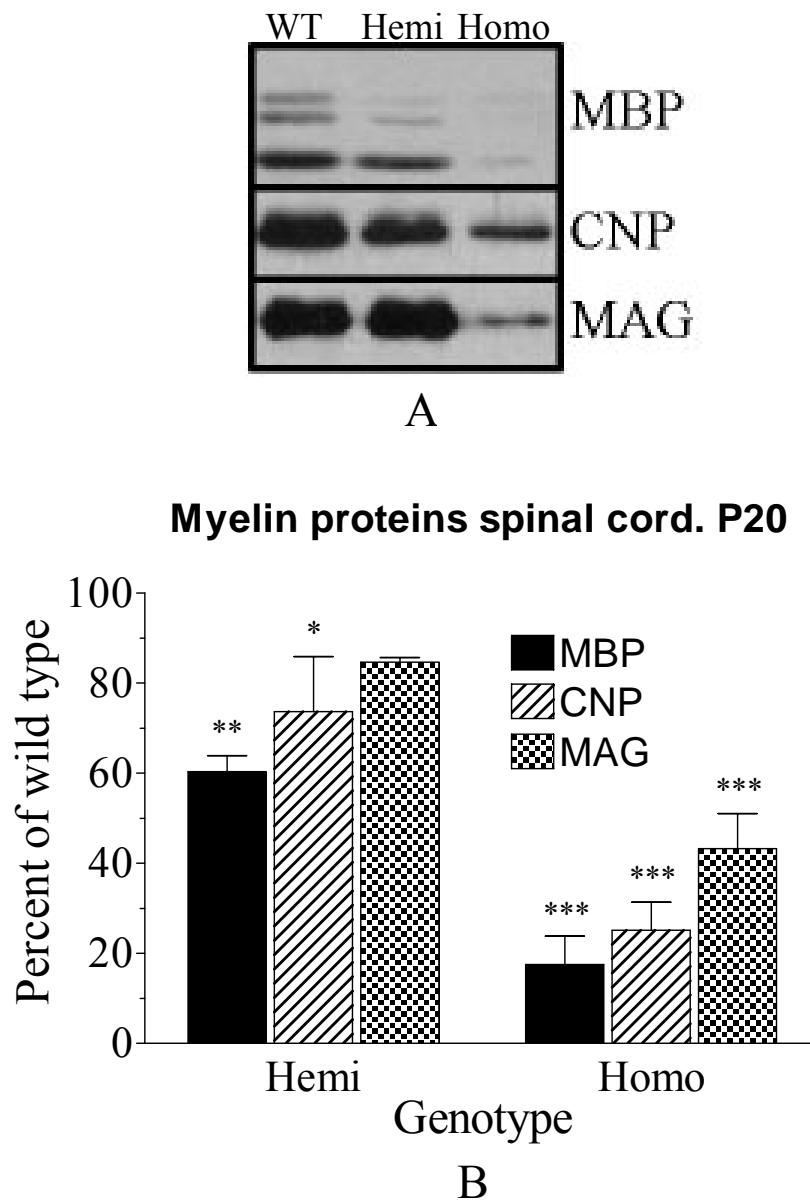


Figure 32. Increased *Plp1* gene dosage affects expression of other myelin protein genes.

A) Representative western blots of myelin enriched fractions from P20 spinal cord probed for MBP, CNP and MAG showing a marked reduction in amounts of all three proteins in homozygous spinal cord (Homo). **B)** Levels of MBP, CNP and MAG in myelin enriched fractions from spinal cord of P20 hemizygous and homozygous mice highlighting the significant decrease in all three proteins in homozygous tissue ($p < ***0.001$) and a less marked reduction in CNP and MBP levels in hemizygous tissue ($p < *0.05$, $**0.01$) ($M \pm SEM$).

Myelin proteins brain. P20

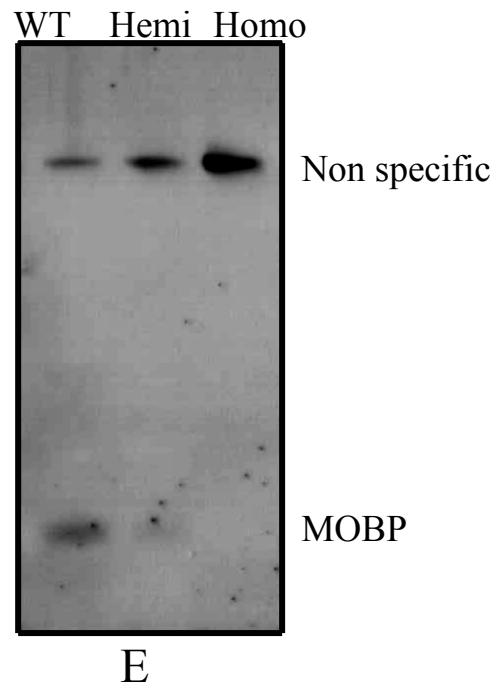
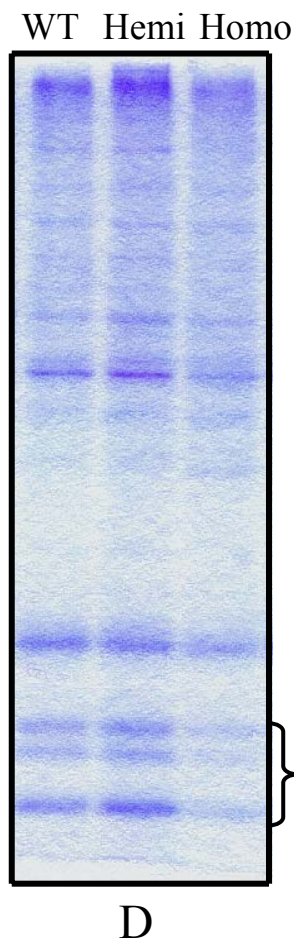
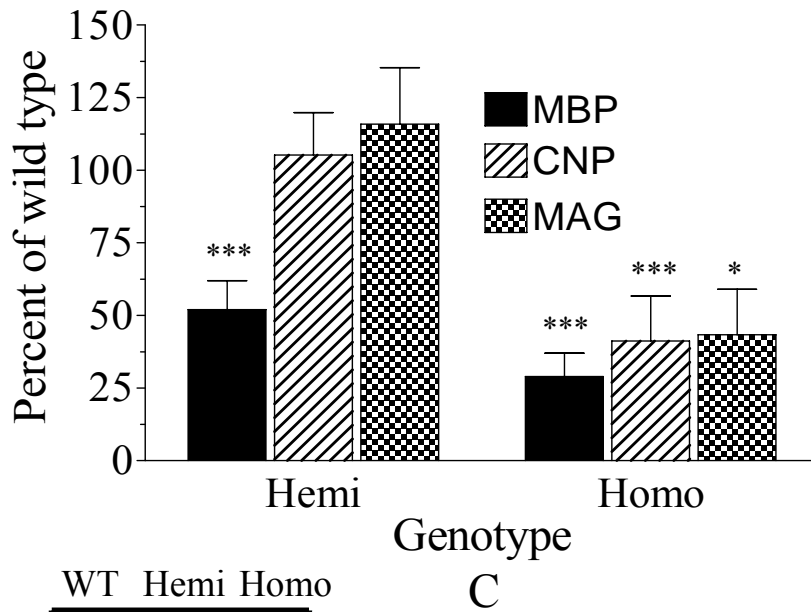


Figure 32 (continued).

C) In myelin enriched fractions from whole brain of P20 mice only MBP ($p < ***0.001$) is reduced in hemizygous animals while all three proteins are lower in homozygous mice ($p < *0.05$, $***0.001$) ($M \pm SEM$). **D)** Coomassie blue staining of $10\mu\text{g}$ myelin separated on a SDS-Page gel showing the positions of PLP and some isoforms of MBP. **E)** Representative western blot of myelin enriched fraction from P20 spinal cord probed for MOBP showing reduction in levels corresponding to genotype, however higher band showing increasing amounts corresponding to genotype (WT wild type, Hemi hemizygous and Homo homozygous).

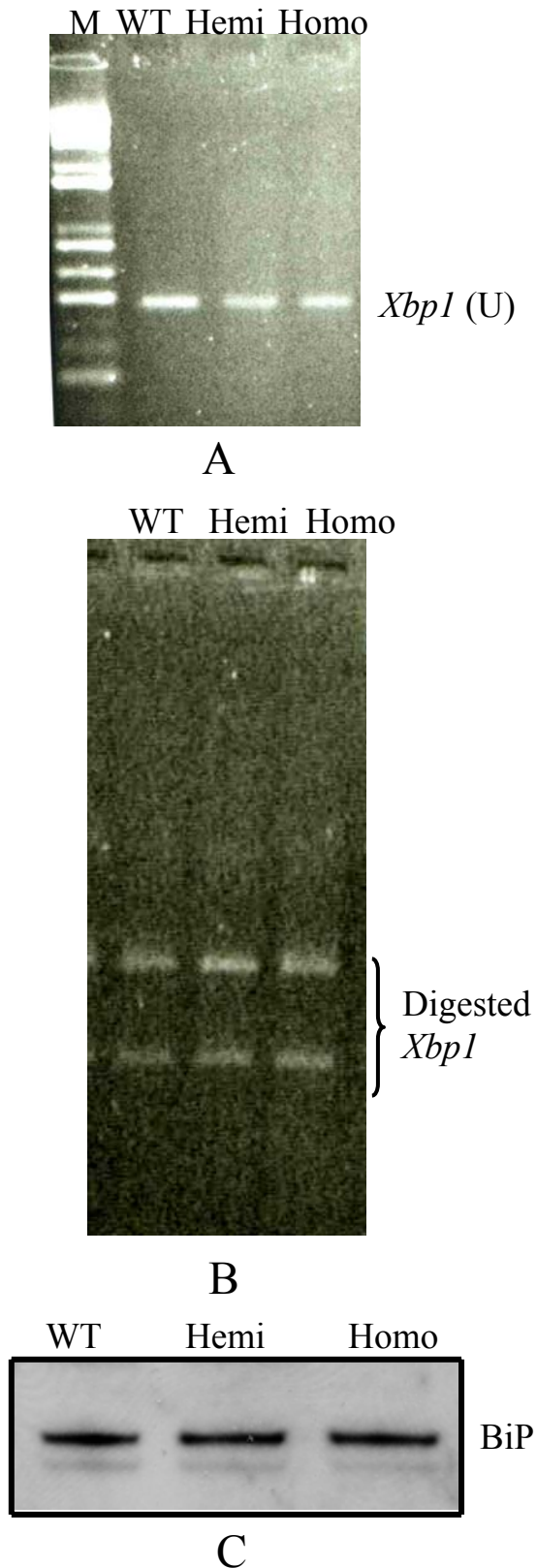


Figure 33. Stress responses in #66 transgenic mice.

A) Agarose gel of *Xbp1* PCR with cDNA from P20 spinal cord of all three genotypes, (WT wild type, Hemi hemizygous, Homo homozygous and M 1kb plus ladder). **B)** Agarose gel image of *PstI* digested *Xbp1* PCR, all PCR product is digested thus was *Xbp1* (U) showing no difference in stress responses in the three genotypes. **C)** Western blot of BiP immunostaining showing no difference between the three genotypes (WT wild type, Hemi hemizygous and Homo homozygous).

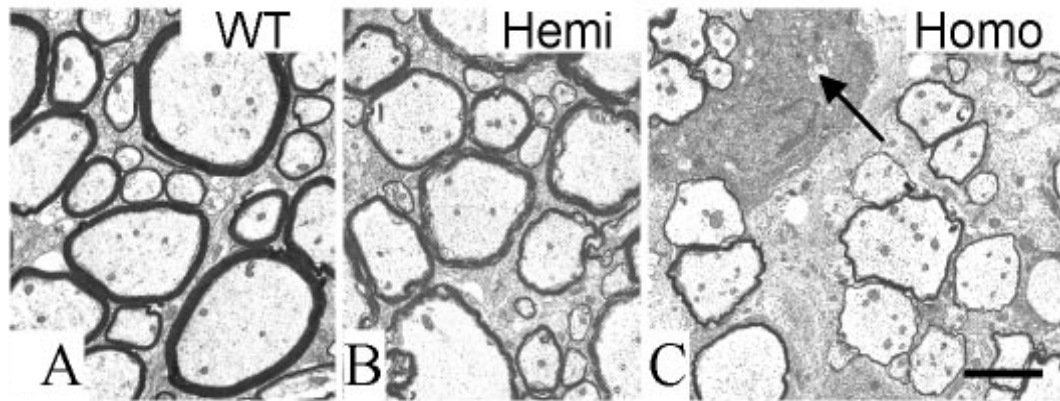


Figure 34. Electron micrographs of white matter in the ventral columns of P20 mice. **A)** Wild type mouse with all axons surrounded by an appropriately thick myelin sheath. **B)** All axons are myelinated in the hemizygous mouse in which the general structure appears normal; morphometric analysis showed that the average sheath was slightly thinner than its wild type counterpart. **C)** The homozygous mouse is dysmyelinated with thin myelin sheaths around the majority of axons. An oligodendrocyte cell body is abnormal and contains numerous autophagic vacuoles (arrow). Bar = 2 μm .

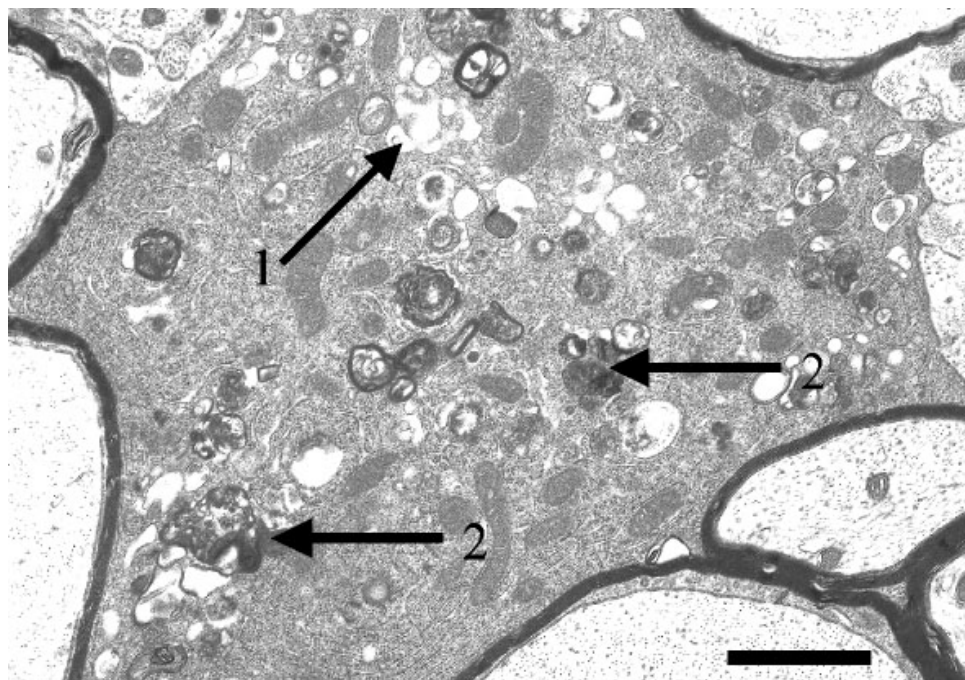


Figure 35. Oligodendrocyte cell body from spinal cord white matter of P20 homozygous transgenic mouse.

There is a well developed RER, which is not obviously disrupted in this cell, vacuolation of the Golgi apparatus (arrow 1) and numerous autophagic vacuoles (arrow 2). Bar = 1 μm .

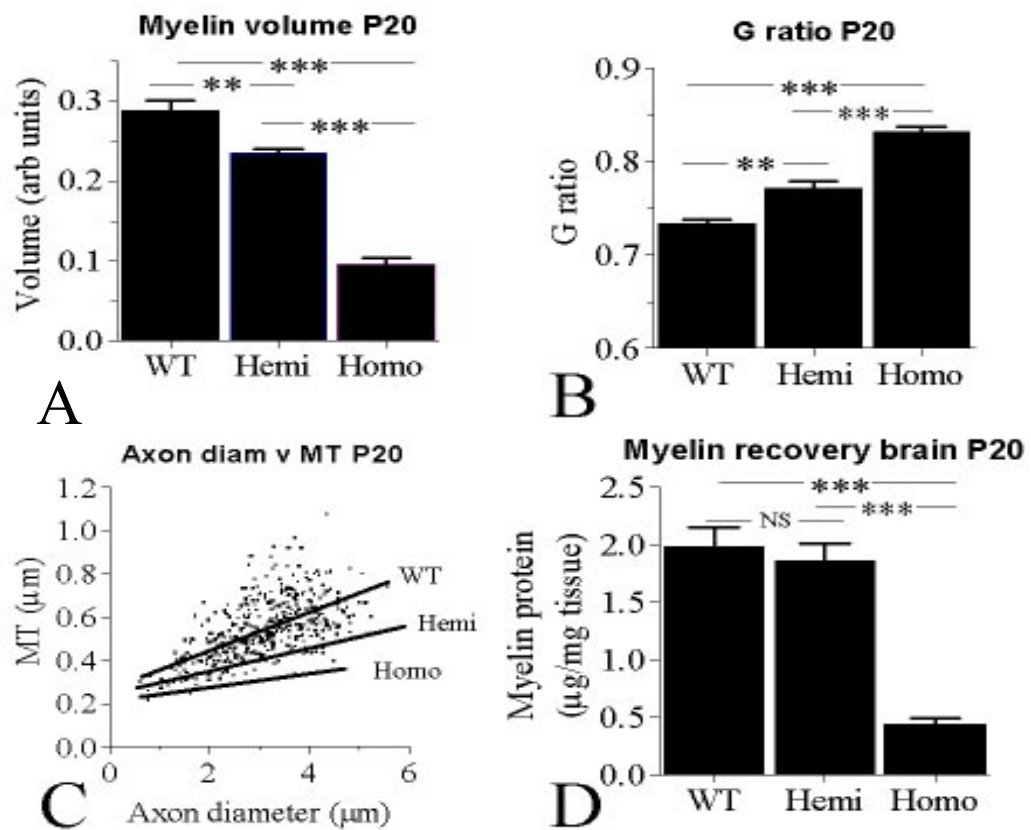


Figure 36. Myelin status of wild type and transgenic mice at P20.

A) Myelin volume in ventral columns of cervical spinal cord was determined from electron micrographs using a point counting method. Values are reduced in both transgenics compared with wild type and also differ with each other. **B)** The g ratio is increased in transgenic mice compared with wild type. The ratio provides an indication of whether the thickness of myelin sheath is appropriate for axon diameter; a higher value indicates a disproportionately thin sheath. **C)** Myelin sheath thickness (MT) should increase with axon diameter as shown by the scatter graph for wild type mice and the corresponding linear regression. The slopes of regression lines for the transgenic mice are reduced compared with wild type and also differ from each other. The individual points for the transgenics are not shown. **D)** Myelin recovery from whole brain is similar in mice hemizygous for the transgene and wild type; both groups differ from homozygous mice. The level of proteins in myelin is expressed as a proportion of the dry weight of whole brain. (The bar charts show $M \pm SEM$, $N = 6$ for A, B, C & 10 for D, $p < ** 0.01$, $***0.001$).

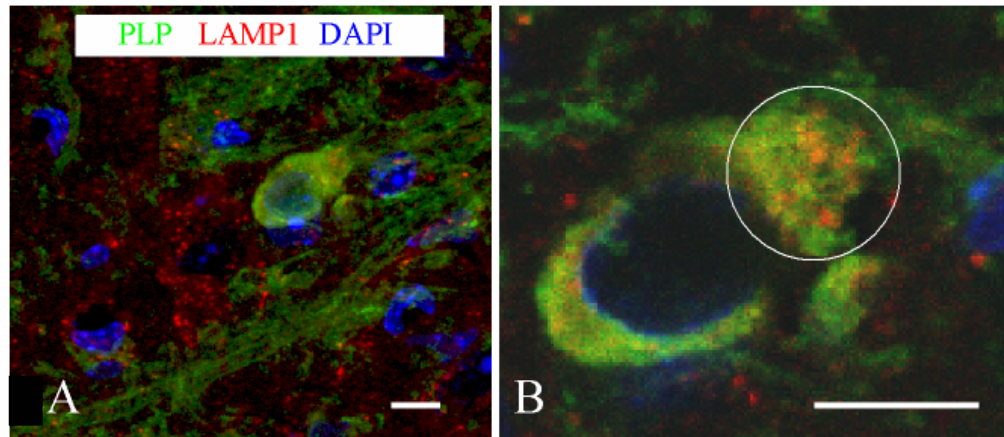


Figure 37. PLP/DM20 immunostaining of P20 homozygous forebrain.

A) Forebrain from P20 homozygous mouse immunostained for PLP/DM20 and Lamp1 and stained for DAPI. **B)** A confocal slice (0.5µm) through the cell body shows several structures co-labelled for PLP/DM20 and Lamp1. Bars = 50µm.

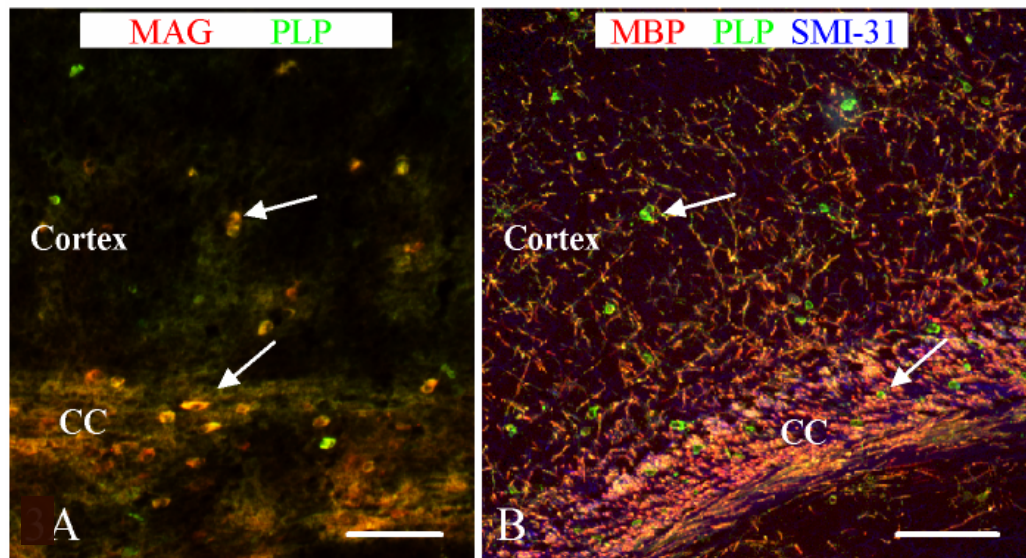


Figure 38. Forebrain from P20 homozygous mice immunostained.

A) Immunostained for MAG and PLP. **B)** MBP, PLP and SMI-31 to show axons. Oligodendrocytes in the cortex and corpus callosum (CC) are intensely stained for PLP and MAG (arrows) but not for MBP. The myelin sheaths are stained for all three myelin proteins. Bars = 100µm.

6 Effects of Increased *Plp1* gene dosage on Maintenance of Myelination (P60)

6.1 Background

Once myelination has occurred, oligodendrocytes in the CNS are involved in maintenance of the myelin. This, as it suggests, does not require as much energy as myelination itself and there is less physiological pressure on the cell. Homozygous #66 mice die prematurely after suffering tremors and developing seizures, as mentioned in the previous chapter. Most are culled as soon as seizures occur or at P20 to avoid any suffering by the animal. Therefore oligodendrocytes in homozygous mice are not involved in the prolonged maintenance of any myelin they may have in their CNS. Hemizygous mice however live for a potentially normal murine life span thus can be used for the study of effects of increased *Plp1* gene dosage on maintenance of myelin.

Myelination in the mouse starts in the spinal cord at birth; therefore the myelination status is more uniform compared to the brain at P20 or P60. Myelination is achieved in most regions in the brain around P45-60 (Baumann and Phin-Dinh, 2001). Anderson *et al.*, (1998) noted that hemizygous #66 mice show signs of late-onset neurodegeneration associated with demyelination. Other phenotypic symptoms include axonal degeneration, astrocytosis and microgliosis. Some animals go on to develop tremors. The age of onset varies greatly between animals with some exhibiting signs of demyelination/neurodegeneration as early as P120 and some remain healthy until they die of old age. However, hemizygous animals at P60 are unlikely to be suffering from any phenotypical abnormalities as this age is prior to any changes previously observed and there is no difference in gross appearance in the mice as the hemizygous animals at P60 are similar in weight to P60 wild type animals (Anderson 1997). These mice may have abnormal pathology but this has not had an effect on the phenotype of these animals.

6.2 Aims

The aims of this study were to describe the effects of increased *Plp1* gene dosage on maintenance of myelin in mature transgenic animals, through comparison to their wild type littermates. The message and protein levels of PLP/DM20 and representative myelin proteins, along with morphometric analysis of CNS myelin composition were chosen as descriptors of the activity.

6.3 Methods

These studies were carried on spinal cord and brain where appropriate from P60 male hemizygous mice and their wild type littermates. P60 mice were chosen in the light of the temporal characteristics of CNS myelination and the late-onset demyelination known to occur in these mice ([see 6.1 Background](#)).

6.3.1 Animal breeding

The breeding of the mice was carried out as described in [2.2 Mouse Breeding](#). The offspring were genotyped as described ([2.3 Isolation and Manipulation of DNA](#)) for the transgene.

6.3.2 Sample Selection

Tissues from wild type mice (n.3) and those hemizygous (n.6) for the #66 transgene were used. Tails were taken for genotyping, spinal cord for tissue culture studies, or RNA and protein extractions.

6.3.3 Transcript Analysis

6.3.3.1 Northern analysis

This experiment was performed on total cellular RNA extracted from spinal cord. The procedure of northern transfer and hybridisation is described in [2.4.6 Northern Blotting](#). The preparation of radiolabelled probes is described also in [2.4.6 Northern Blotting](#).

Staining of the gel with ethidium bromide was used to check for equal loadings of sample and presence of bands in ladder and hybridisation with β -actin (a measure of invariant expression) was used to monitor equivalence of transfer. Hybridisation analysis was

undertaken using labelled cDNA products from PCRs using primers for *Plp1* and *Mbp* (Table 2) (Figure 15). The blot was left for 3-4 weeks to allow the signal to decay then probed for *β-actin*.

6.3.3.2 qRT-PCR analysis

Standard curves were produced using serial dilutions of an appropriate wild type RNA sample as described in [2.4.7 qRT-PCR](#). Once all the parameters for the reactions were set and equivalent for the genes, the test plate, containing *Plp1*, *Mbp* and *β-actin* reactions for the relevant samples selected, was run ([2.4.7 qRT-PCR](#)).

Set up of the experiment was as before and following the analysis protocol laid out in [2.4.7 qRT-PCR](#) the uncorrected concentrations of *Plp1*, *Mbp* and *β-actin* mRNA in 50ng total RNA loaded were calculated. The *Plp1* and *Mbp* concentrations were then normalised to *β-actin* and expressed as a percentage of wild type levels giving the actual concentration of *Plp1* or *Mbp* message in total RNA.

6.3.4 CNS Myelin Analysis

6.3.4.1 Myelin Preparation

Myelin was prepared from spinal cord and brain and protein concentrations were quantified and analysed by western blot as described in [2.5 Protein Analysis](#). Blots were immunostained for PLP/DM20 using C-terminal antibody PLP 226, MAG, MBP and CNP (Table 5). The results of the hemizygous protein analysis were quantified compared with wild type protein amounts. Total homogenates were immunostained for ASPA, a marker for oligodendrocytes and GFAP (Glial fibrillary acidic protein), a protein produced by astrocytes.

6.3.5 Morphometric analysis

To study neural development and maturation, glial cell quantification and myelin morphometry were performed on the ventral columns of spinal cord (C2-3) ([2.6 Myelin Morphological Analysis](#)). Analysis at 60 days was chosen as a stage when neural development was complete and there was no phenotypic abnormalities seen in the animals.

6.4 Results

6.4.1 Identification of Genotype

PCR using the *Plp* and T7 primers identified the presence or absence of the #66 transgene cassette. All animals negative for the PCR product were wild type and all animals positive for the PCR product were considered transgene positive. Dependant on age the transgene positive animals could either be homozygous or hemizygous, as in this chapter the male #66 mice were P60 and all homozygous animals were culled before this age they were all hemizygous. This was confirmed by resin sections as mentioned in previous chapters for genotyping.

6.4.2 Transcript Analysis of P60 wild type and hemizygous #66 male mice

As described previously 20µg total RNA from wild type and hemizygous P60 spinal cord was separated by size through electrophoresis on a denaturing northern gel (Figure 39A). The resulting blot was probed with *Plp/Dm20* and β -*actin* (Figure 39B). The signals of the hemizygous for β -*actin* and *Plp/Dm20* are stronger (Hemi) compared to the signals of the wild type RNA (WT) suggesting a very slight increase in *Plp/Dm20* levels in the hemizygous animals in comparison to the wildtype control. The same blot was then hybridised with *Mbp* identifying a slight reduction in *Mbp* levels in the hemizygous RNA (Hemi) compared to the wild type RNA (Figure 39C).

When analysed and normalised to β -*actin*, the message levels of *Plp/Dm20* and *Mbp* are not statistically different to wild type as demonstrated in Figure 39D. The trend therefore is similar to in P20 hemizygous mice, in fact there is no difference in amounts of *Plp/Dm20* and *Mbp* in the hemizygous animals compared with wild type (previous Chapter).

6.4.3 Protein Analysis of P60 wild type and hemizygous #66 male mice

Proteins from brain and spinal cord were studied in this section. The western blots from the brain tissue are not shown but the data are represented in a graph (Figure 40A). Both PLP and DM20 are increased compared to P60 wild type littermates; however, this increase is not significant. MBP, CNP and MAG are decreased to a varying degree in hemizygous brain myelin compared to levels in wild type brain myelin. Once again this decrease in

levels of myelin proteins is not statistically significant. Two non-myelin proteins, ASPA and GFAP, were also examined. There is also no statistical difference in the amounts of these proteins in comparison to wild type levels.

Figure 41B demonstrates the immunostained blots for the four myelin proteins investigated in this thesis. Visually there is no difference in amounts between the two genotypes (WT wild type and Hemi hemizygous) for any of the proteins (shown in order of size). When plotted as a graph, the average levels for each of these proteins do not differ from the wild type levels. There is less inter-animal variation in protein levels between animals for the spinal cord in comparison to the levels in the brains of the same hemizygous animals (Figure 40A and C).

6.4.4 Morphometric Analysis of P60 Myelin

Electron micrographs of cervical sections of P60 spinal cord are demonstrated in Figure 41A and B. The wild type P60 spinal cord in Figure 41A shows appropriately thick myelin sheaths wrapping all the axons in the spinal cord. The slight distortion of the central large axon's sheath was probably caused by sub-optimal perfusion of the animal. However, the axons are all ensheathed by myelin of the appropriate thickness for the diameter of the axon. A normal looking oligodendrocyte is also in the EM (arrow Figure 41A).

The electron micrograph of the hemizygous spinal cord section is shown in Figure 41B. There is no apparent visual difference in the myelin between the wild type and the #66 hemizygous P60 cords. All axons are ensheathed by tightly packed, highly structured myelin sheaths of appropriate thickness for the axons. There is no difference in myelin volume between P60 wild type and hemizygous spinal cords (Figure 41C). The g ratios in both genotypes are the same (Figure 41D). The variation in the volume of myelin and g ratios as seen by the error bars is very small for the spinal cord.

There is also no difference observed in axon diameter versus myelin thickness (Figure 41E). All these measurements were performed on the spinal cord of P60 wild type and #66 hemizygous animals. Overall, in all aspects of myelin morphology studied, no difference could be observed between the #66 hemizygous animals and their wild type littermates. There is no difference in myelin volume in the brain between the two genotypes (Figure 41F).

6.5 Discussion

In this chapter the effects of *Plp1* gene dosage on the maintenance of myelin at P60 were investigated. Prior to and during peak myelination the hemizygous #66 mice produced similar to wild type levels of *Plp/Dm20* message. This is still the case at P60 when myelination is complete in the spinal cord. There is no increase in *Plp/Dm20* message to the levels implied by *Plp1* copy number at any stage of the myelination process in hemizygous animals. Even with the 7 extra copies of the wild type *Plp1* gene present, in these animals the oligodendrocyte appear to be able to control the expression levels ensuring similar levels to normal are produced. This was also observed when the transgene was on the *Plp1* null background (Chapter 3).

mRNA levels for *Mbp* were also unchanged in the hemizygotes compared with wild type in P60 animals. This was not the case at earlier ages where *Mbp* message levels were reduced even when the *Plp/Dm20* transcript levels were normal. The increased *Plp1* gene dosage even at the low dosage level of hemizygous animals affects *Mbp* message in an adverse manner but the oligodendrocyte is able to correct this imbalance or deficit in transcript by maturation of the myelin at P60.

At the protein level there was again no difference in PLP and DM20 compared to the wild type in either brain or spinal cord. This reflects the observations for message levels for PLP and DM20. When the other myelin proteins were investigated in both brain and spinal cord, levels in hemizygous animals were comparable to wild type levels. There was no difference between the two genotypes in the protein levels of PLP, DM20, MBP, CNP and MAG in myelin from brain or spinal cord. There is however more variation in the protein levels for the hemizygous brain compared to the hemizygous spinal cord. This may be attributed to the status of myelination in the brain in comparison to the spinal cord. The process of myelination is completed in most brain regions by P45-60, therefore it is possibly that the entire brain was not fully myelinated or myelinated to the same extent in the all the animals used in this study.

At peak myelination, MBP and CNP were significantly reduced in hemizygous myelin, MBP protein levels were also reduced in oligodendrocytes *in vitro* and in premyelinating oligodendrocytes at P3. However this difference has resolved during completion of myelination. Neither CNP or MBP are reduced at P60, moreover both proteins are

comparable to wild type levels. As with the message levels for *Mbp*, the hemizygous oligodendrocytes have controls for the decrease of protein and over time compensate for the loss.

Apparently the oligodendrocytes not only have the ability to compensate for the reduction in message or protein but also for the reduction in overall myelin volume. At P20, myelin volume in hemizygous spinal cord was significantly reduced compared to wild type (Chapter 5) yet by P60 the myelin volume in the two genotypes is the same. Concurrently, there is a subtle myelin defect due to a slight reduction in sheath thickness at P20, which also recovers by age P60. There is no variation in the myelin volume, g ratio or axon diameter/myelin thickness relationship in spinal cord at this age either.

Unlike with the variation between genotypes in protein levels in brain compared to spinal cord there are no differences in the overall myelin volume of the brain between the two genotypes. Myelin protein expressed as a proportion of the dry weight of whole brain is shown in Figure 41F. Myelin is prepared from powdered whole brain thus eliminating the variation between regions of the brain. These results concur with the findings by Anderson (1997), who observed no difference in glial cell density or myelin volume between the two genotypes. The cervical cord white matter was also similar between wild type and hemizygous animals.

The recovery of protein levels and myelin volume by P60 in hemizygous animals indicates that there is possibly a recovery mechanism that comes in play during maturation of myelin. The actual mechanism of this possible recovery is not yet known. However this recovery process is likely to be temporary as dependant on age the hemizygous animals suffer from signs of demyelination and neurodegeneration. It is likely as MBP message and protein are the most affected through development and myelination of the CNS that the loss of the oligodendrocytes' ability to sustain normal levels of MBP is a contributing factor to the breakdown of maintenance leading to loss of myelin.

MBP is considered very important in the formation of myelin. Studies on shiverer mice which carry a large deletion of the MBP gene have demonstrated that MBP is essential to the formation of intact myelin (Fitzner *et al.*, 2006). It has been suggested by both Campagnoni and Skoff (2001) and Harauz and colleagues (2004) that it acts as a lipid coupler due to the interaction of the highly positively charged MBP to the negatively

charged cytoplasmic membrane surface. Therefore without MBP there would be no apposition of adjacent membrane surfaces in myelin.

McLaughlin *et al.*, (2006) have also put forward the hypothesis that MBP is the important protein in regards to levels in myelin and loss of myelin. In their study levels of MBP were markedly reduced in *rumpshaker* oligodendrocytes and particularly when the mutation was expressed on the C57BL/6 background (McLaughlin *et al.*, 2006, Al-Saktawi *et al.*, 2003). In ongoing studies (Barrie *et al.*, unpublished) the C57 *rumpshaker* mice were complemented with wild type *Plp1* (#66) transgene, increasing their PLP/DM20 levels to normal. Surprisingly, MBP levels remained low and severe dysmyelination was still present. It is, therefore, possible that the low levels of MBP in *rumpshaker* contribute to the hypomyelination. Unlike protein levels, *Mbp* mRNA levels were only minimally reduced, suggesting the *rumpshaker* mutation operates at a translational or post-translational level to perturb MBP, presumably through the action of misfolded PLP/DM20 through an, as yet, unknown mechanism. This may be true for the #66 mutation where, through excess copies of the wild type gene, the burden on the cell and resulting changes may lead to perturbation of MBP production.

In other transgenic hemizygous animals carrying extra wild type copies of the *Plp1* gene abnormalities show up fairly early on in life. In transgenic heterozygous *4e-Plp* mice generated by Kagawa *et al.*, (1994) containing 2 extra copies of the *Plp1* gene the first sign of myelin degeneration was noted at P71. Heterozygous *4e-Plp* oligodendrocytes contained abnormal vacuoles similar to those observed in #66 homozygous oligodendrocytes. As with the #66 hemizygous mice that show late-onset neurodegeneration, the *4e-Plp* heterozygotes also developed signs consistent with neurodegeneration, such as hind limb tremors and ataxia after several months. The onset of myelin degeneration was 2-3 months after birth in these animals.

In hemizygous *Plp1* transgenic rats profound regional differences in oligodendrocyte physiology were noted (Bauer *et al.*, 2002). Oligodendrocytes and myelin sheaths displayed pathological changes in the CNS gray matter when compared to oligodendrocytes in the white matter. They studied spinal cord sections from 7-week wild type and hemizygous adults and revealed 26% less myelin in the gray matter of hemizygotes. There was no difference seen in the white matter. Vacuolation of myelin in the gray matter was also seen at 7 weeks, as was the presence of abnormal vacuoles in the

cell bodies. Hemizygous transgenic mice eventually progress to clinically overt demyelination, which usually starts 6–7 months or 12–18 months after birth dependant on the line. Interestingly, despite having identical transgene sequences as the transgenic mice, the 18-month-old hemizygous transgenic rats remain healthy and do not develop this profound demyelination.

Later in life the #66 hemizygous animals do go on to develop signs of demyelination with varying age of onset of these signs. What causes this variation is not yet known but one possibility is that the #66 hemizygous animals with the lower end of the MBP levels at a young age develop degeneration sooner than the animals with the higher MBP levels. How this could be investigated is still to be worked out. The possibility that the recovery process between P20 and P60 in the hemizygous animals fails in the run up to the first abnormalities and leads to loss of myelin proteins, volume and overall morphology has to be thoroughly investigated in the future.

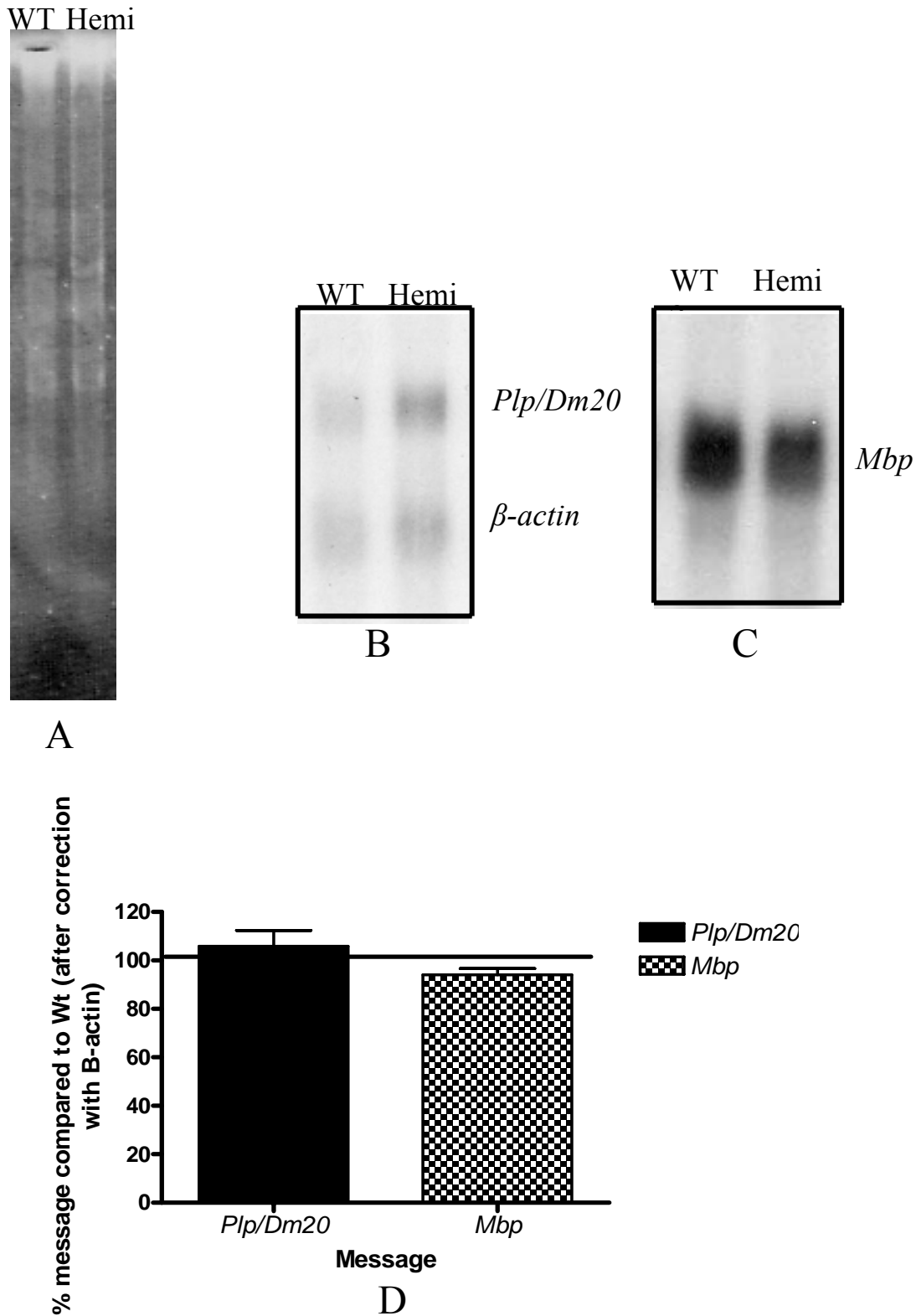


Figure 39. Transcript analysis of P60 wild type and hemizygous message.

A) 20 μ g P60 wild type and hemizygous spinal cord RNA separated on a denaturing gel. **B)** The resulting blot probed for *Plp/Dm20* and β -actin showing similar levels of Plp1 transcript when utilising β -actin levels for the comparison. **C)** The same blot then hybridised with a *Mbp* probe showing lower *Mbp* transcript levels in the Hemi sample. **D)** Transcript analysis graph (northern hybridisation and qRT-PCR) showing mRNA levels of all *Plp/Dm20* and *Mbp* transcripts in P60 hemizygous spinal cord compared to wild type levels (line at 100%).

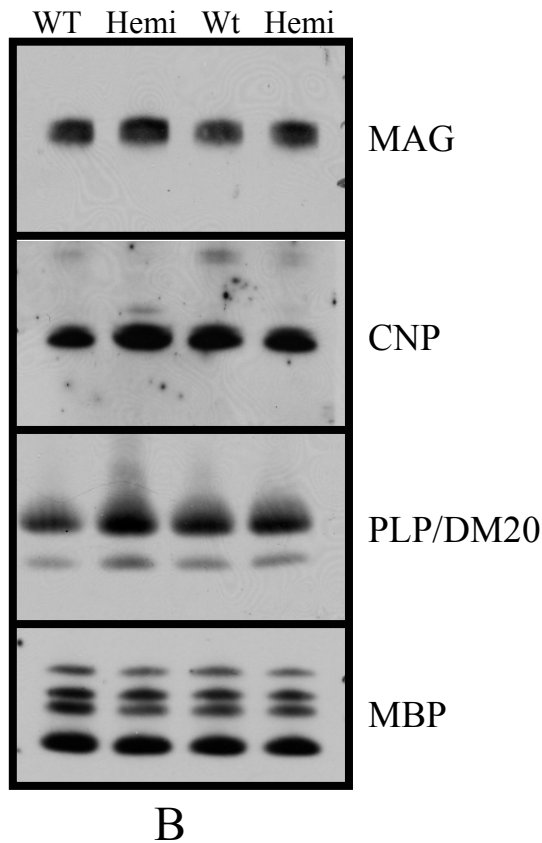
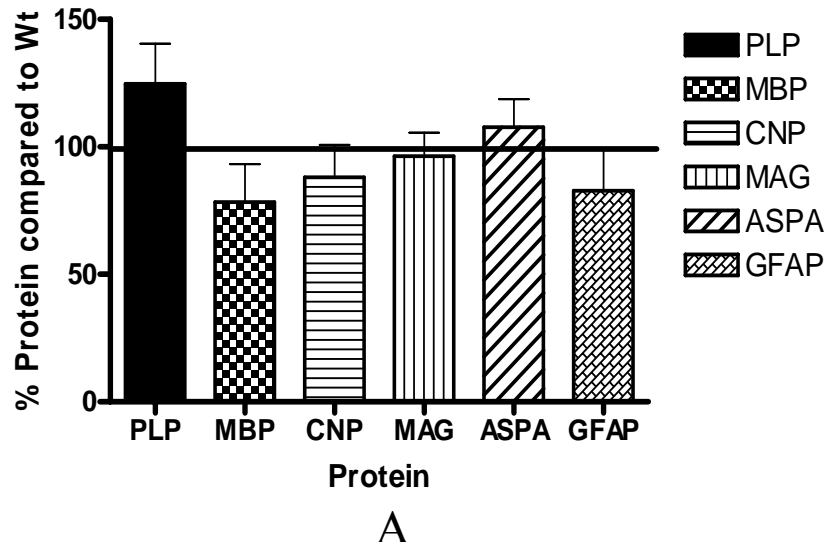


Figure 40. Protein analysis of P60 brain and spinal cord myelin.

A) Graph showing average protein % in P60 hemizygous brain relative to wild type (line at 100%) showing no difference between the two (ASPA and GFAP in total homogenates and others in myelin). **B)** Western blots from P60 spinal cord myelin immunostained for MAG, CNP, PLP/DM20 and MBP highlight the similar levels for the proteins in both wild type and hemizygous CNS (WT wild type and Hemi hemizygous).

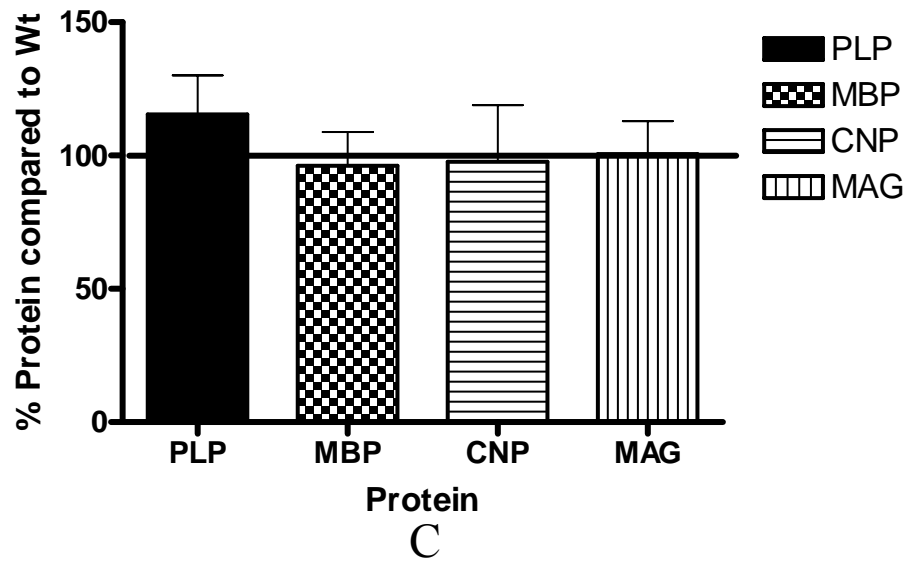


Figure 40 (continued).

C) Graph showing average protein % in P60 hemizygous spinal cord myelin relative to wild type demonstrate the lack of difference for all proteins studied in hemizygous spinal cord compared with wild type (line at 100%).

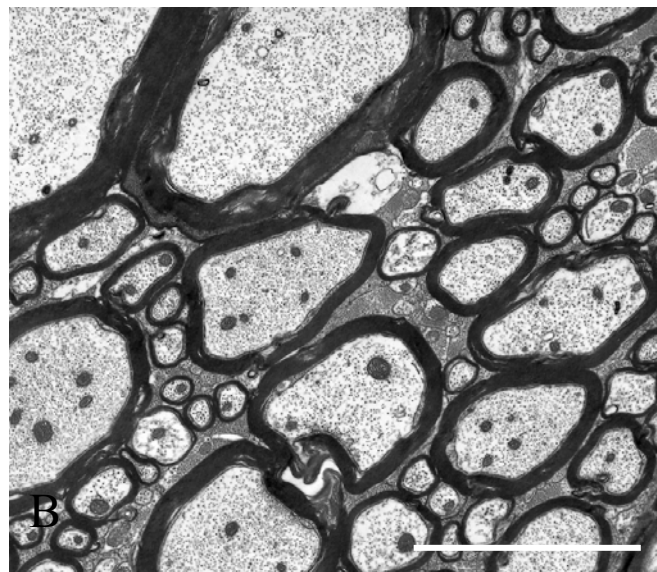
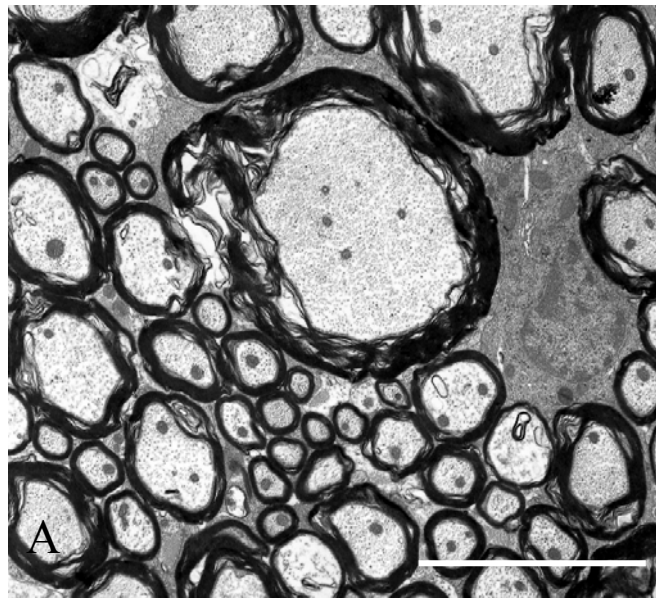
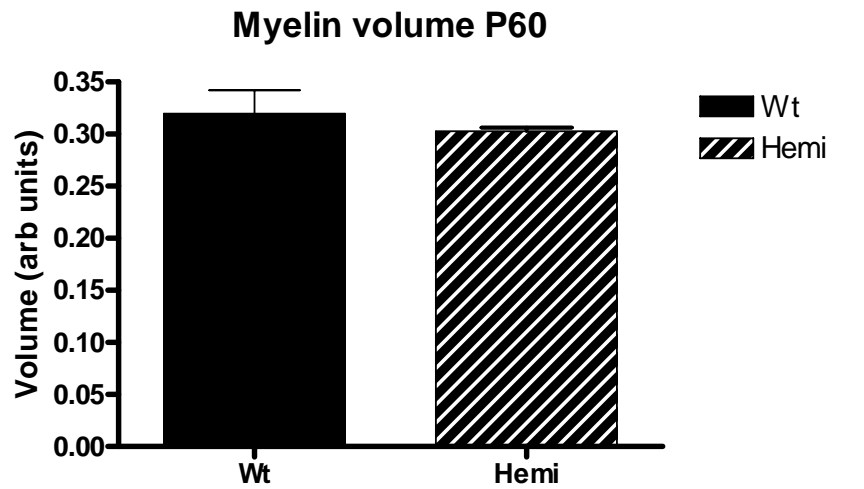
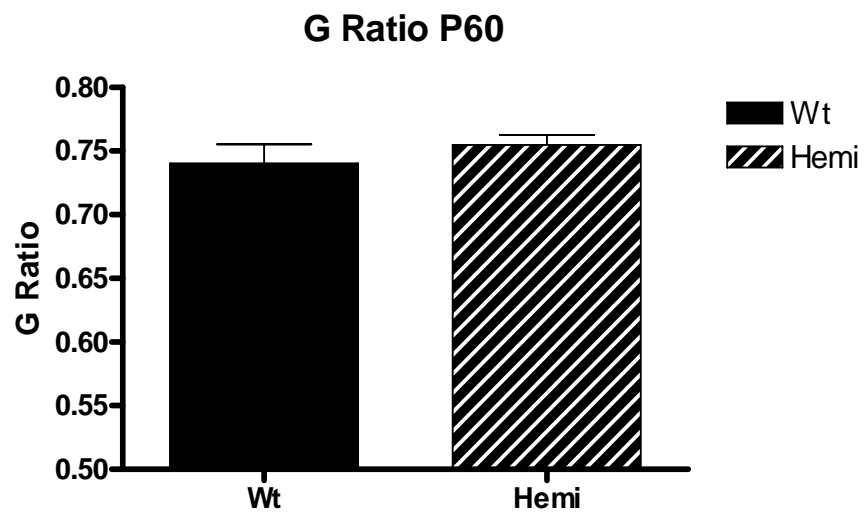


Figure 41. Electron micrographs and graphs of P60 wild type and hemizygous animals' myelin morphology.

A) Electron micrograph of P60 wild type spinal cord section. B) Electron micrograph of P60 hemizygous spinal cord section. No difference in amount of myelin or thickness of sheath can be observed between the two animals. Bar = 5 μ m.



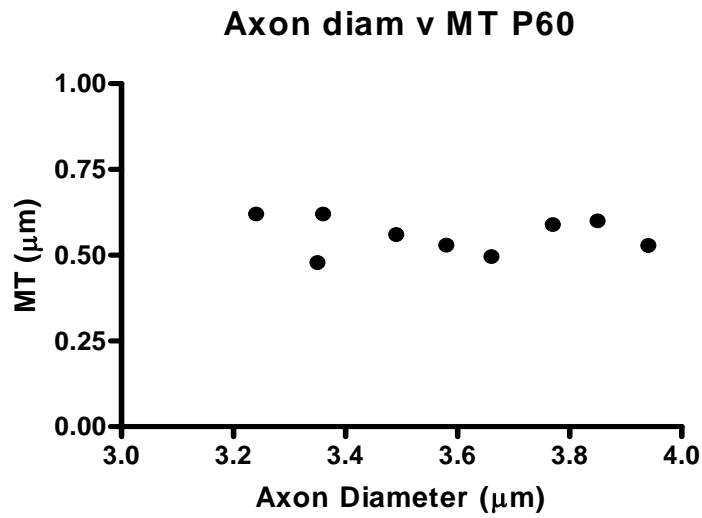
C



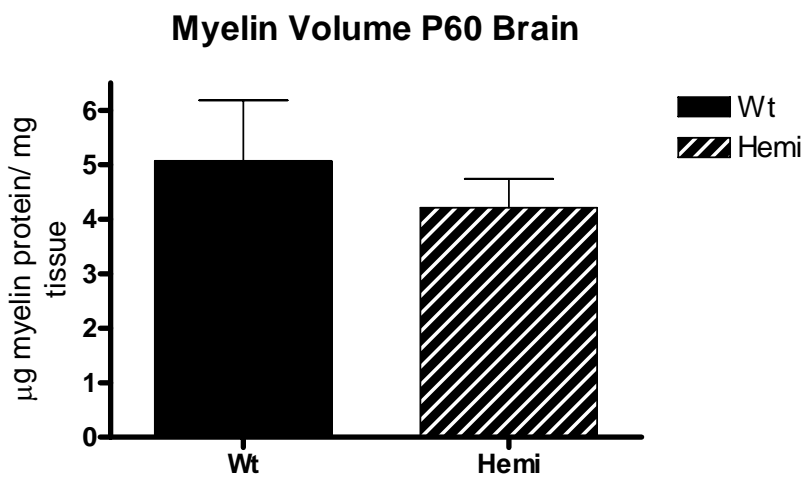
D

Figure 41 (continued).

C) Quantitative data of myelin volume in P60 spinal cord. **D)** Quantitative data of G Ratio between both genotypes. No difference is detected between wild types and hemizygotes using either myelin volume measurements in spinal cord or g ratios.



E



F

Figure 41 (continued).

E) Quantitative data of Axonal Diameter versa Myelin Thickness in P60 spinal cord.

F) Quantitative data of myelin volume in P60 brain of both genotypes. No difference is detected between wild types and hemizygotes using either axon diameter via myelin thickness or myelin volume in brain. (Results $M \pm \text{SEM}$, WT N = 3 Hemi N = 6)

7 Effects of Increased *Plp1* gene dosage on PLP/DM20 Dynamics

7.1 Background

Proteins are constantly synthesised and degraded in cells and the rate is dependant on the protein but can vary under different conditions (Ciechanover 2005) In general proteins can be divided into short-lived rapid turnover proteins and long-lived slow turnover proteins. Their rate of turnover is influenced by their function. Myelination of the CNS requires a mass and concerted production of proteins and lipids and transport of these in the correct proportion to the myelin membrane by the oligodendrocytes. How the oligodendrocyte handles the synthesis, incorporation and degradation of any given protein within the process is an important area of study. In *rumpshaker* animals, synthesis of PLP and DM20 in oligodendrocytes is similar in profile and intensity to that of wild type oligodendrocytes (McLaughlin *et al.*, 2006). The difference between the two genotypes is seen at the degradation level where *rumpshaker* PLP/DM20 is degraded faster than wild type PLP/DM20 (McLaughlin *et al.*, 2006).

The proteasome, which degraded many proteins including wild type proteins, is involved in the degradation of misfolded proteins exiting the ER as part of Endoplasmic Reticulum (ER)-Associated Degradation (ERAD) (Meusser *et al.*, 2005). To elucidate the role of the proteasome in degradation of *rumpshaker* PLP and DM20 in the CNS MG132 an inhibitor of the ubiquitin–proteasome pathway in mammalian cells was utilised. McLaughlin *et al.*, (2006) discovered MG132 blocked the degradation of wild type and *rumpshaker* PLP/DM20 indicating the proteasome is indeed involved the degradation of these proteins in the CNS. Whether this is the case for the PLP and DM20 produced by the #66 transgenic animals is matter for investigation.

Another aspect of the dynamic nature of PLP/DM20 and myelination is the association of proteins in specialised lipid domains that are detergent resistant known as lipid rafts. Simons *et al.*, (2000) discovered that PLP/DM20 was recovered from cultured oligodendrocytes in a low-density CHAPS-insoluble membrane fraction (CIMF) enriched in myelin lipids. PLP was associating with the CIMF after leaving the endoplasmic reticulum but prior to exiting the Golgi apparatus, suggesting that myelin lipid and protein

components assemble in the Golgi complex. Correct association of PLP/DM20 with certain lipids to form myelin rafts may be critical to for the sorting of PLP/DM20 and assembly of myelin (Simons *et al.*, 2000).

7.2 Aims

The main objective of this section was to investigate the effects of increased *Plp1* gene dosage on the dynamics of protein synthesis and degradation. Previously the effects on static transcript and protein levels at various ages were examined. How oligodendrocytes manage the balance of synthesis and degradation normally in the whole myelination process is of vital importance for understanding myelin formation and stability. What happens in the disease state as in PMD with extra copies of the normal gene is therefore an essential part of the understanding of this disease. The possible pathway involved in the degradation of PLP and DM20 was also an area to investigate. Another important aspect of the study was whether oligodendrocytes from #66 transgenic animals could form myelin rafts consisting of PLP and DM20 and essential lipids such as cholesterol.

7.3 Methods

Synthesis rate studies were carried on brain from P20 (early adulthood) male wild type, hemizygous and homozygous littermates for the brain slice experiments. The synthesis, degradation and blocking of proteasome degradation experiments were carried out on primary oligodendrocyte cultures from P5 spinal cord from all three genotypes.

7.3.1 Animal breeding

The breeding of the #66 hemizygous males with #66 hemizygous females was carried out as described in [2.2 Mouse Breeding](#). The offspring were genotyped as described ([2.3 Isolation and Manipulation of DNA](#)) for the transgene and only male animals at P5 or P20 were used for this study.

7.3.2 Sample Selection

Tissues from mice wild type, hemizygous and homozygous for the #66 transgene were used. Tails were taken for genotyping, spinal cord for tissue culture studies and brain for

brain slice experiments. Spinal cords from P5 animals were also used for genotype identification (Chapter 4).

7.3.3 Primary cell cultures

Spinal cord from P5 males pups were used to set up primary cell cultures as described in [2.5.4.1 Primary cell culture](#).

7.3.3.1 Synthesis

Protein synthesis in culture was investigated as described in [2.5.4.4.1 Synthesis](#). All values are expressed relative to the T₀ sample.

7.3.3.2 Degradation

Degradation of newly synthesised proteins was studied in primary oligodendrocyte cultures using the pulse/chase method described in [2.5.4.4.2 Degradation of proteins using Pulse/Chase experiments](#). All values are expressed relative to the T₀ sample.

7.3.3.3 Blocking of Proteasome mediated Degradation

The effects of blocking a degradation pathway using a chemical compound (MG132, an inhibitor of proteasomes and calpains) were investigated ([2.5.4.4.3 Blocking of Degradation](#)). All values are expressed relative to the T₀ sample.

7.3.4 Brain Slice system

Whole brains from P20 male animals were used to study the synthesis rates of PLP and DM20 at peak myelination ([2.5.5 Synthesis at P20](#)). Incorporation of newly synthesised PLP and DM20 in myelin fraction was also investigated. All values are expressed relative to total homogenate/synthesis T₂.

7.3.5 Lipid Rafts

Lipid rafts were isolated from myelin produced from wild type and #66 homozygous CNS tissue as described in [2.5.2.1 Lipid Raft Preparation](#).

7.4 Results

7.4.1 Identification of Genotype

PCR using the *Plp* and T7 primers identified the presence or absence of the #66 transgene cassette. All animals negative for the PCR product were wild type and all animals positive for the PCR product were considered transgene positive. Dependant on age and whether the mice exhibit a phenotype, the transgene positive animals could either be homozygous or hemizygous. Both hemizygous and homozygous animals were available at P5 and P20. The genotype at P20 was confirmed visually prior to tissue collection as the animals have developed tremors by this age. At P5 genotypes were all confirmed by resin sections as shown in Chapter 4.

7.4.2 Newly Synthesised PLP and DM20 in Oligodendrocytes

Due to the nature of genotyping it was only possible to produce only two dishes of cells from each spinal cord. Therefore to study synthesis of protein over time one plate was treated for 45 minutes with [³⁵S]-ProMix (cysteine/methionine) labelled HBSS medium while the other was treated for 90 minutes. Figure 42A shows phosphorimages of newly synthesised (radiolabelled) PLP and DM20 from all three genotypes at the two time points. An increase in the amount of newly synthesised PLP and DM20 can be seen at 90 minutes compared to 45 minutes in all three genotypes. When the blots were then probed with anti-PLP 226 antibody, the total PLP and DM20 present in the lysates was immunostained. The amounts of total PLP and DM20 in the lysates were the same over both time points in each genotype.

The change in newly synthesised PLP and DM20 over time was quantified and illustrated graphically (Figure 42B). There was no significant difference in synthesis of PLP or DM20 over time between wild type and hemizygous mice. However the rate of translation expressed as percentage change per minute of PLP in cultures from homozygous mice was significantly lower, relative to wild type and hemizygous mice, more so compared to wild type. For DM20 the rate was only significantly different between cultures from wild type and homozygous mice. As with all detection techniques there is an optimal range of detection and sensitivity in the system and it is essential to ensure the best exposure for each experiment is found.

7.4.3 Degradation of Newly Synthesised PLP and DM20 over time

Degradation rates were also studied in oligodendrocyte cultures. As before, only two dishes were available from each spinal cord therefore one dish was taken as the start point of 0 hours (T_0) after pulse period and the other taken after the chase period after 24 hours. Figure 43A shows the decrease in levels of newly synthesised PLP and DM20 signals from T_0 to 24 hrs. A visual examination of all genotypes displayed a decrease in following the 24 hr chase. There appears to be a small drop in signal for both labelled PLP and DM20 in the wild type and hemizygous lysates. However, there is a clear decrease in amounts of PLP and DM20 present after 24 hours in the homozygous sample. The magnitude of this decrease is more marked in the homozygotes. Indeed statistical analysis demonstrates that the homozygous decrease (to 40%) is statistically different from the wild type and hemizygous decrease (to 70%) (Figure 42D).

Again, as with the synthesis experiment, when the blot was probed with anti-PLP 226 antibody the levels of PLP and DM20 were the same at both time points. This showed that equal amounts of total PLP and DM20 had been immunoprecipitated from the lysates from both dishes.

7.4.4 Blocking of Proteasome Mediated Degradation

As most proteins in mammalian cells are degraded by the ubiquitin–proteasome pathway and MG132 blocks this pathway (Lee and Goldberg 1998), dishes were treated with 50 μ M MG132 or DMSO (the solvent MG132 was dissolved in) for 24 hours (Figure 43B). This experiment was to establish whether the proteasome pathway contributes to wild type PLP/DM20 degradation in oligodendrocytes. Degradation of PLP and DM20 after 24 hours is reduced in lysates from MG132 treated cells when visually compared to phosphorimages of lysates treated only with DMSO. Once again western blotting highlights the equal loading of total PLP and DM20 when comparing the two dishes of each genotype.

The change in degradation from T_0 to 24 hours under MG132 treatment was then investigated. As before, one dish was taken at T_0 and the other after 24 hours in medium supplemented with MG132 (Figure 43C). The wild type and hemizygous PLP and DM20 signals at 24 hours are similar to the signals at T_0 suggesting MG132 completely blocked the degradation of these proteins in culture. The blocking of degradation in homozygous lysates is not as complete in these cultures as PLP/DM20 levels at 24 hours do not reach T_0 amounts. Western blotting of the membrane with anti-PLP 226 antibody immunostained

the all PLP and DM20 present in the lysates and showed there was no difference in total amounts of protein immunoprecipitated at the two points in each genotypes.

Quantification of the results showed that degradation rates of the wild type and hemizygous PLP/DM20 were very similar (Figure 43D). Newly synthesised or nascent protein levels of PLP/DM20 are down to 80% of T_0 levels for both genotypes whereas, the homozygous levels at 24 hours are reduced to less than 50% of those at T_0 . This is a significant reduction in nascent protein and therefore a significant increase in the proteasome mediated degradation process in the homozygous oligodendrocytes.

The influence of MG132 a proteasome inhibitor, revealed degradation is completely blocked in the wild type and hemizygous oligodendrocytes, stopping almost all PLP/DM20 degradation thus allowing amounts to remain at 100% of T_0 amounts and showing a significant change from the original degradation levels. The homozygous PLP and DM20 levels in MG132 cells also showed a significant increase at 24 hours compared to levels in untreated samples at the same time point and equated to 80% of initial T_0 amounts.

7.4.5 Synthesis in Brain Slices

The synthesis rates of PLP and DM20 were then investigated in P20 brain slices in which the oligodendrocyte/axon unit is intact. Phosphorimages of PLP/DM20 immunoprecipitations from total homogenates and myelin fractions from brain slices are demonstrated in Figure 44A. Between 2 hours to 6 hours an increase in newly synthesised PLP and DM20 is seen in all three genotypes. The total homogenates from wild type and hemizygous mice show a steady increase whereas in the total homogenate from homozygotes 4 hours and 6 hours signals are very similar. The reprobes of each blot with anti-PLP 226 antibody confirmed that the total amounts of PLP and DM20 were equal across the time points.

The percentage increases for PLP synthesis over time (synthesis rate/slope) in wild type and hemizygous total homogenates are very similar over the 6 hours (Figure 44B). The slopes reflect change in signal over time and represent the rate of translation in each genotype. All values are expressed relative to T_2 total homogenate levels. The rates for DM20 are very similar to the PLP synthesis rates. Although the 6 hour signals for PLP and DM20 are stronger in the hemizygous total homogenate phosphorimages there is no difference in the overall synthesis rates (from 100% to approximately 400-500%). On the

other hand the synthesis of PLP and DM20 in the homozygous total homogenates is decreased compared to wild type and hemizygous PLP and DM20 synthesis (100% to approximately 300%) (Figure 44B).

7.4.6 Incorporation of Newly Synthesised PLP and DM20 into Myelin

The PLP and DM20 signals from the myelin fractions are also on the same phosphorimages (Figure 44A). These signals represent the amount of newly synthesised PLP and DM20 incorporating into the myelin over the three time points. At 2 hours, in any of the genotypes, 10-20% of the pool of newly synthesised PLP and DM20 is incorporating into the myelin fraction. At 4 and 6 hours, PLP and DM20 are incorporated into the myelin in all the genotypes to differing extents. Similar amounts of PLP and DM20 are incorporated into myelin in the wild type and hemizygous animals over time. Although PLP and DM20 is synthesised by oligodendrocytes in the homozygous CNS, at 6 hrs only around 80% of the total pool of newly synthesised protein (300%) is incorporated into myelin as can be seen in Figure 44A. More than half of the total pool of wild type and hemizygous newly synthesised PLP and DM20 at 6 hrs is incorporated into myelin.

The resulting western blots show equal amounts of total PLP and DM20 in the myelin fractions between 2, 4 and 6 hours (Figure 44A). Figure 44C shows the rate of incorporation of PLP into myelin over the same 6 hour period as for the synthesis rates. The incorporation of PLP and DM20 in the homozygous #66 myelin is impaired compared wild type and hemizygotes.

7.4.7 PLP and DM20 in Lipid Rafts

Further fractionation of the myelin allows the study of the formation of lipid rafts. As the synthesis rates and incorporation efficiency are compounded in homozygotes, the PLP/DM20 that does associate with myelin may not insert into the correct environment. To test this, a fractionation of myelin using the detergent method by Simons *et al.*, (2000) was carried out. The distribution of PLP and DM20 in different fractions of a sucrose gradient in wild type and homozygous myelin is shown in Figure 45. PLP/DM20 from homozygous myelin is less buoyant than wild type. The majority of PLP and DM20 from wild type myelin are in the 2nd and 3rd fraction with most in the 2nd, while the PLP and DM20 from the homozygote are in present in fractions 2-5 with the majority in fraction 3.

Some PLP and DM20 protein is seen in fraction 5 in the homozygous myelin whereas there is only a very faint signal in the 5th fraction in the wild type myelin.

7.4.8 All Newly Synthesised Proteins in Oligodendrocytes

A proportion of the lysates from oligodendrocyte cultured were examined by phosphorimage (Figure 46). No difference in band amount and strength of signal for the bands present is noted between the two lanes demonstrating no variance in radiolabelled amino acid incorporation between the samples.

7.5 Discussion

The effects of increased *Plp1* gene dosage on dynamics of PLP/DM20 during myelination of the #66 animals were the main focus of this chapter. This included synthesis of the proteins over time in oligodendrocytes prior to contact with axons, rate and pathway of degradation of the proteins in oligodendrocytes, synthesis of PLP/DM20 within a brain slice system and how PLP/DM20 interacts with lipids in myelin. All the controls necessary for each type of experiment were not carried out due to the limits of tissue used. Only two culture dishes were obtainable from each spinal cord at P5 and genotyping necessitated single cultures.

The rate of synthesis of PLP and DM20 in the #66 homozygous CNS was impaired compared to synthesis in wild type and hemizygous oligodendrocytes. The rate of synthesis dropped from a 4% increase of newly synthesised PLP per minute in wild type to a rate of a 2% increase in homozygous oligodendrocytes. No difference was observed between the wild type and hemizygous oligodendrocytes in the synthesis of PLP and DM20. This is not observed in other *Plp1* mutation; in *rumpshaker* for example, oligodendrocytes synthesise PLP at a rate comparable to wild type (McLaughlin *et al.*, 2006). Total steady state levels of PLP and DM20 are reduced in the *rumpshaker* oligodendrocytes unlike in the #66 homozygous oligodendrocytes where there is more PLP/DM20 present (Chapter 4).

Degradation of PLP and DM20 is increased in homozygous oligodendrocytes when compared to their wild type or hemizygous counterparts. Wild type and hemizygous degradation rates for PLP/DM20 are very similar as were total steady state protein amounts at P3 and P20 (Chapters 4 and 5). The differences observed between wild types and

hemizygotes were mainly in other myelin protein such as MBP. Degradation of PLP and DM20 in #66 homozygous is enhanced as is *rumpshaker* and *jimpy-msd* PLP/DM20 (Kramer-Albers *et al.*, 2006, McLaughlin *et al.*, 2006). Only 10% of *jimpy-msd* PLP and DM20 were present after 24 hours, 30% of *rumpshaker* PLP/DM20 and 45% of #66 homozygous PLP and DM20. This difference in degradation is most likely due to the mutation present; *jimpy-msd* (A242V) and *rumpshaker* (I186T) have been identified in humans and are models of severe conatal PMD and mild SPG-2, respectively, whereas in #66 animals, which models classic PMD, PLP and DM20 are wild type.

89-90% of all protein degradation occurs through the ubiquitin-proteasome pathway whereas lysosomal proteolysis accounts for only 10-20% (Lee and Goldberg 1996). MG132 has been reported to be an inhibitor of the ubiquitin-proteasome pathway in mammalian and yeast cells (Lee and Goldberg 1996). Therefore inhibition of proteasome degradation with MG132 should block PLP/DM20 degradation and allow the protein levels/amounts remain near or at initial amounts. When MG132 was used to block degradation in oligodendrocyte cultures, PLP and DM20 amounts in wild type and hemizygotes returned to normal (back to 100% of T₀). In the homozygotes PLP and similarly DM20 amounts went from around 45% to 90% of T₀.

Therefore, in the #66 homozygotes about 50% of nascent PLP/DM20 but not all PLP/DM20 is degraded by a MG132-sensitive mechanism, compared with 30% in wild type and hemizygotes and 70% in the *rumpshaker* mutation (McLaughlin *et al.*, 2006). This suggests that MG132 only partially blocks degradation of these proteins in oligodendrocytes. These findings are supported by Kramer-Albers *et al.*, (2006) who also demonstrated the proteasome was the major site of degradation for both wild type and mutant PLP/DM20 using a different proteasome inhibitor ALLN.

MG132 treatment at the concentrations regularly used for proteasome inhibition has been reported to cause ubiquitination of proteins with cells (Goldbaum and Richter-Landsberg 2004, McLaughlin, M. personal communication). MG132 treatment also induces an increase in heat shock protein levels in cells and in some cases an apoptotic response (Cervello *et al.*, 2004, Goldbaum and Richter-Landsberg 2004). In this study the concentration of MG132 (50µM) used will undoubtedly affect other systems and pathways in the cells. However to ensure oligodendrocyte number were the same between samples, amounts of ASPA, an oligodendrocyte marker, were probed for in the untreated and treated

cell lysates. No difference was observed suggesting no induction of apoptosis in the treated cells and no reduction in oligodendrocyte numbers between the two (data not shown).

When synthesis of PLP and DM20 in P20 #66 animals was investigated using the brain slice experiment, newly synthesised PLP and DM20 accumulated progressively over the 6 hr period. The rate of accumulation of these proteins over the 6 hrs was different for the homozygotes when compared to the wild type and hemizygotes. There was a marked reduction in synthesis of PLP and DM20 in the homozygous CNS. However, *rumpshaker* PLP and DM20 is synthesised at a similar rate to wild type PLP and DM20 in P20 CNS (McLaughlin *et al.*, 2006). This would suggest that the oligodendrocyte “copes” with misfolded PLP and increased dosage of wild type PLP by different mechanisms. Indeed it has been shown that stress molecules such as BiP are elevated in *rumpshaker* but not #66 transgenic animals (Chapter 5).

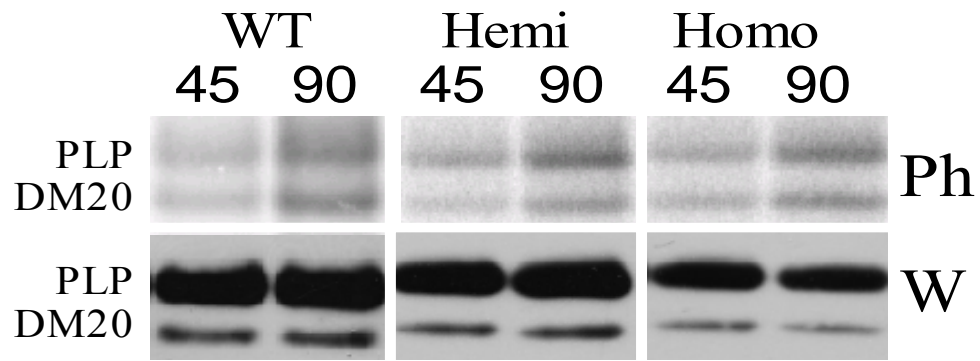
The incorporation of PLP and DM20 into myelin in the brain slice system was also investigated. PLP and DM20 for the wild type and hemizygous brain slices are incorporated into myelin at a similar rate. The incorporation of PLP and DM20 from homozygous brain slices was greatly reduced. There was newly synthesised PLP and DM20 present in myelin of all genotypes at 2 hours but the initial amount of these proteins in myelin from homozygotes was lower compared to wild type and hemizygous. Similar data were seen in *rumpshaker* animals where *rumpshaker* PLP was incorporated at a much lower rate than wild type PLP and the initial amount at 2 hours was also lower (McLaughlin *et al.*, 2006). How extra copies of the *Plp1* gene could effect incorporation of PLP and DM20 into myelin and thus influence the overall stoichiometry of myelin is critical to understand.

One of the initial pieces of evidence to suggest PLP and DM20 is translocated into myelin with lipids comes from the observation that inhibition of glycosphingolipid synthesis in brain slices reduced PLP/DM20 translocation by 50% (Kramer *et al.*, 2001). Saher *et al.*, (2005) discovered that conditional mutations of the squalene synthase (SQS) gene, which is involved in cholesterol production, led to severely perturbed myelin synthesis in oligodendrocytes. This is an indication that oligodendrocytes normally produce cholesterol in brain white matter. However the oligodendrocyte can adapt to the loss of cholesterol by acquiring it from external sources. PLP associates with galactocerebroside and cholesterol in the Golgi apparatus to form lipid rafts which appear to be essential for sorting of PLP

into myelin (Simons *et al.*, 2000). Disruption of the myelin raft pathway may represent a possible pathogenetic mechanism for how *Plp1* mutations can lead to Pelizaeus-Merzbacher disease (Hudson 2004). Myelin assembly could be perturbed by the sequestering of myelin lipids by PLP/DM20 produced due to gene duplication in humans.

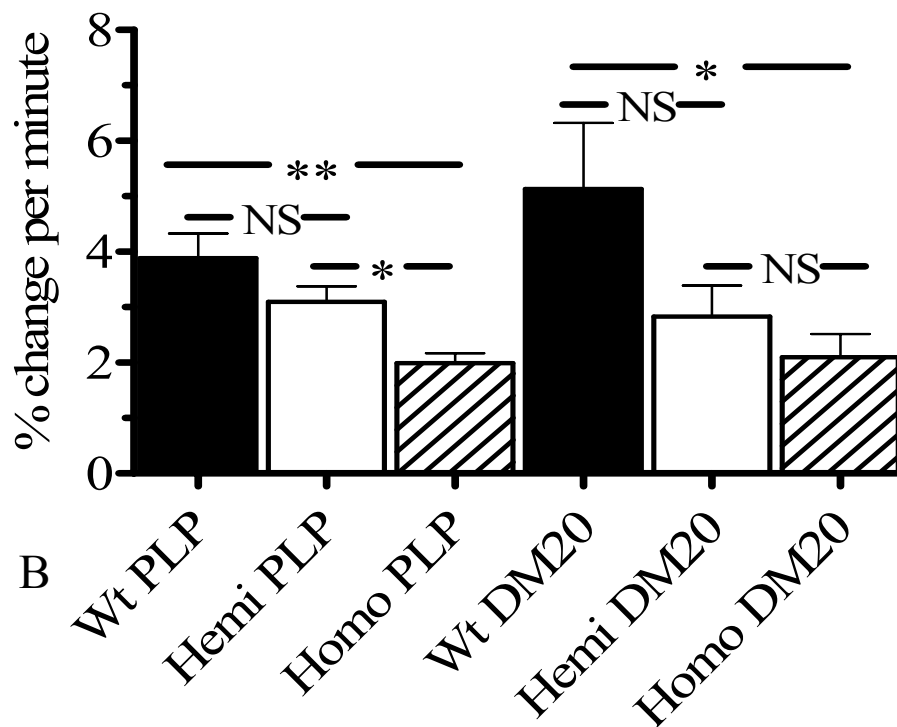
An impairment of the PLP/DM20 and lipid relationship is seen in the #66 homozygous animals. When compared to PLP and DM20 from wild type myelin more of the PLP and DM20 in homozygous myelin is in the lower fractions. As the CIMF float in the sucrose gradient the PLP and DM20 associated with the lipids would be in the higher more buoyant fractions. This is not the case in the homozygous where the PLP and DM20 produced in the CNS is not in the higher fractions, thus, not associated with lipids such as cholesterol and galactosylceramide, a sphingolipid. Overexpressed PLP in oligodendrocytes was found to co-localise with cholesterol in LE/Ls which was unique to overexpressed PLP as it was not observed when MOG was overexpressed in the cells (Simons *et al.*, 2002). This was also observed in sagittal sections of 3 week old brain where labelling with filipin was seen on LAMP-1, PLP-positive structures (Simons *et al.*, 2002).

It appears oligodendrocytes, due to the high rate of myelin synthesis during myelinogenesis, are sensitive to any imbalance in synthesis and turnover of their proteins and lipids. A important aspect of these results is how loss of normal PLP/DM20 interaction with lipids could affect the assembly of the different myelin subdomains and myelin stiochiometry in the #66 mice. How the dysmyelination seen in homozygous animals or human patients is induced by any of the above processes is still an open question. This will be discussed in the following chapter.



A

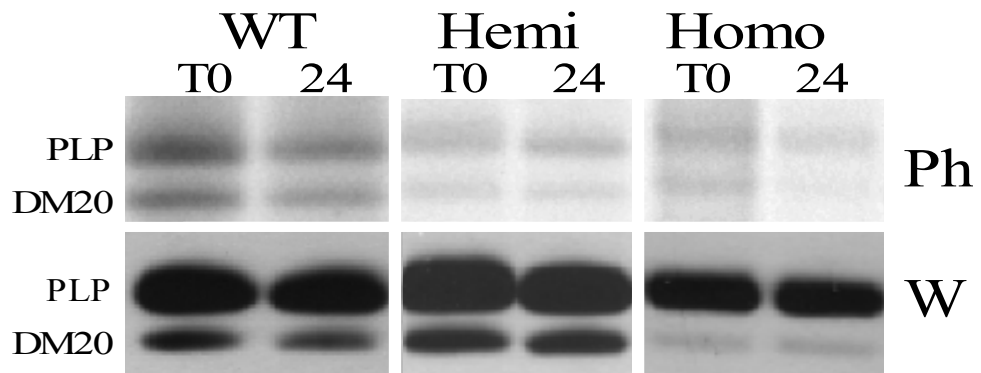
Rate of translation



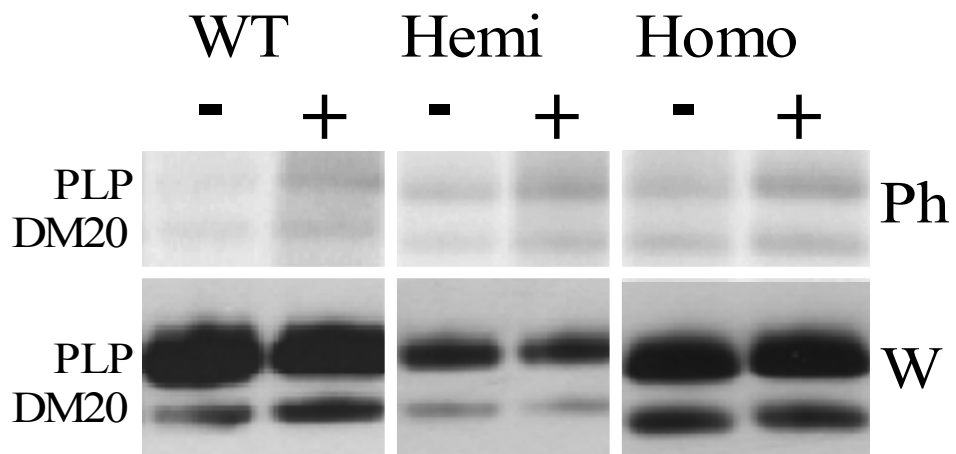
B

Figure 42. Synthesis of PLP and DM20 in wild type, hemizygous and homozygous oligodendrocytes.

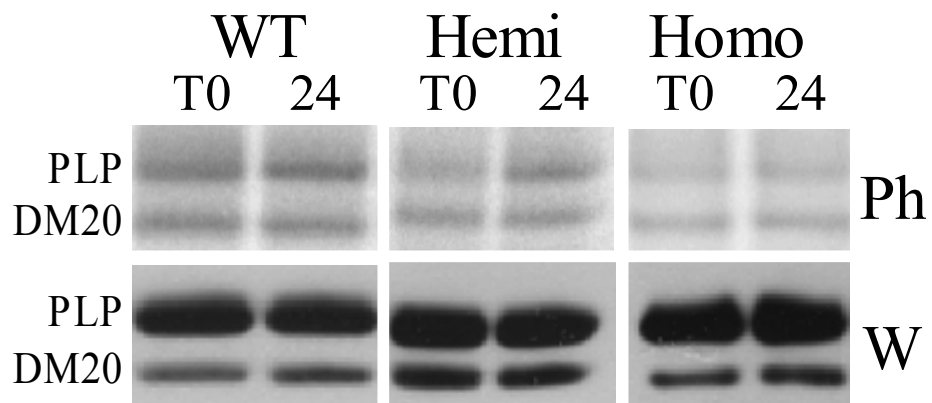
A) Cells were radiolabelled for the time shown above each image prior to lysis and immunoprecipitation. The upper panels are phosphorimages (Ph) and the lower, western blots (W) using an antibody for PLP and DM20 (45, 45 mins 90, 90 mins). B) Quantification of radiolabelled PLP and DM20 over time. The data are expressed relative to the 45 min sample (M ± SEM, NS non significant, N= 4 for wild type and 5 for hemizygous and homozygous, p <*0.05, **0.01).



A



B



C

Figure 43. Degradation of PLP and DM20 in wild type, hemizygous and homozygous oligodendrocytes.

A) Representative experiments from the three genotypes showing the phosphorimages (Ph) and western blots (W). Cells were pulse radiolabelled for 90 mins then chased for the times shown (T0, 0 hours 24, 24 hours). **B)** Representative experiments from the three genotypes showing the phosphorimages (Ph) and western blots (W). Cells were pulse radiolabelled for 90 mins then chased for 24 hours in absence or presence of 50 μ M MG132). **C)** Representative experiments from the three genotypes showing the phosphorimages (Ph) and western blots (W). Cells were pulse radiolabelled for 90 mins then chased for the times shown (T0, 0 hours 24, 24 hours with 50 μ M MG132).

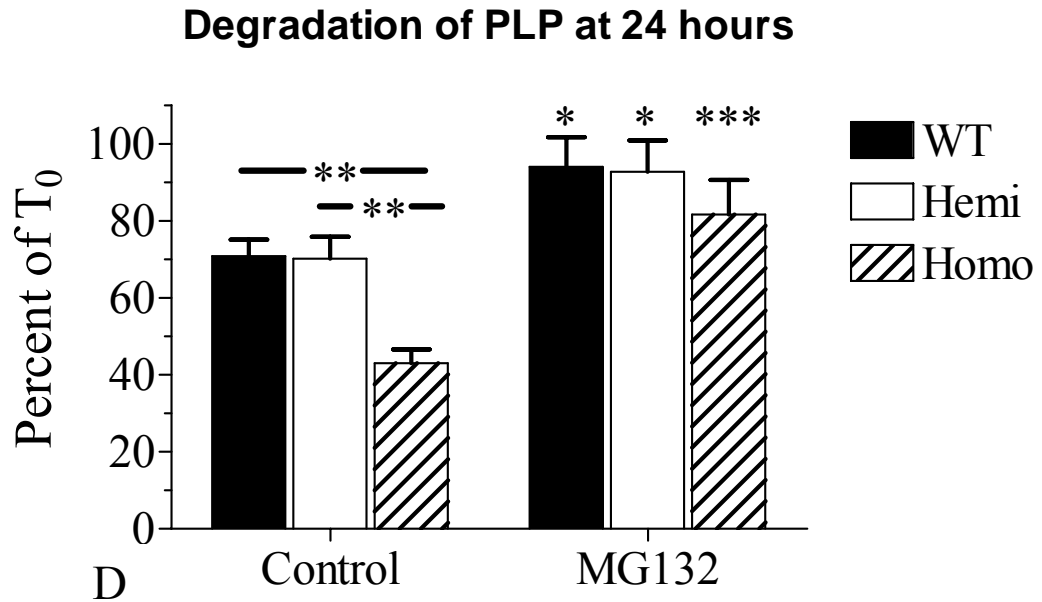


Figure 43 (continued).

D) Quantification of degradation of radiolabelled PLP and DM20 over time (Control, normal degradation over 24 hours; MG132, degradation in presence of MG132 over 24 hours). The data is expressed relative to the T₀ sample in each set (M ± SEM, NS non significant, N= 5 wild type control, 6 wild type MG132, 6 hemizygous control, 5 hemizygous MG132 and 6 homozygous control, 3 homozygous MG132, p <*0.05, **0.01, ***0.001).

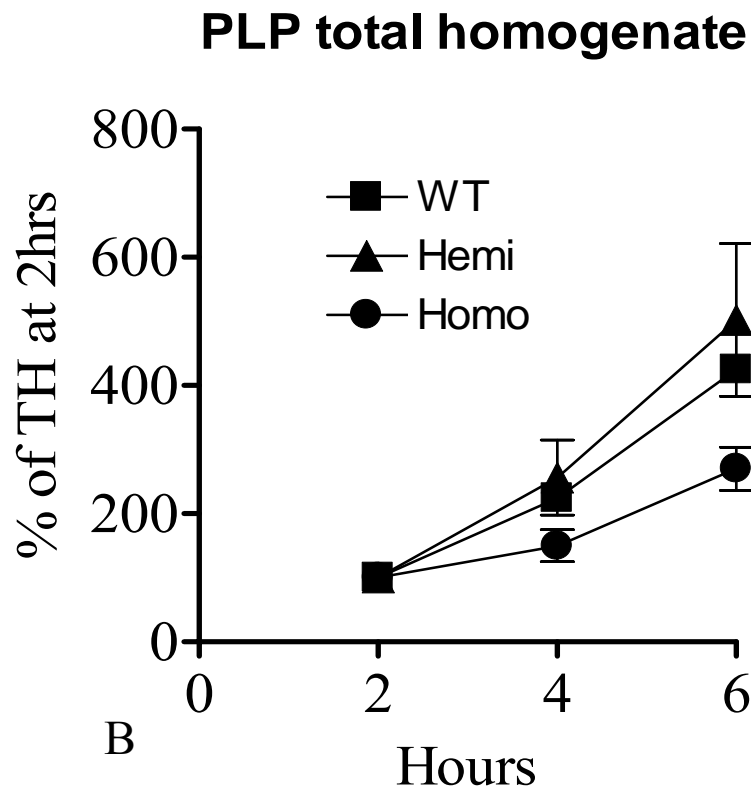
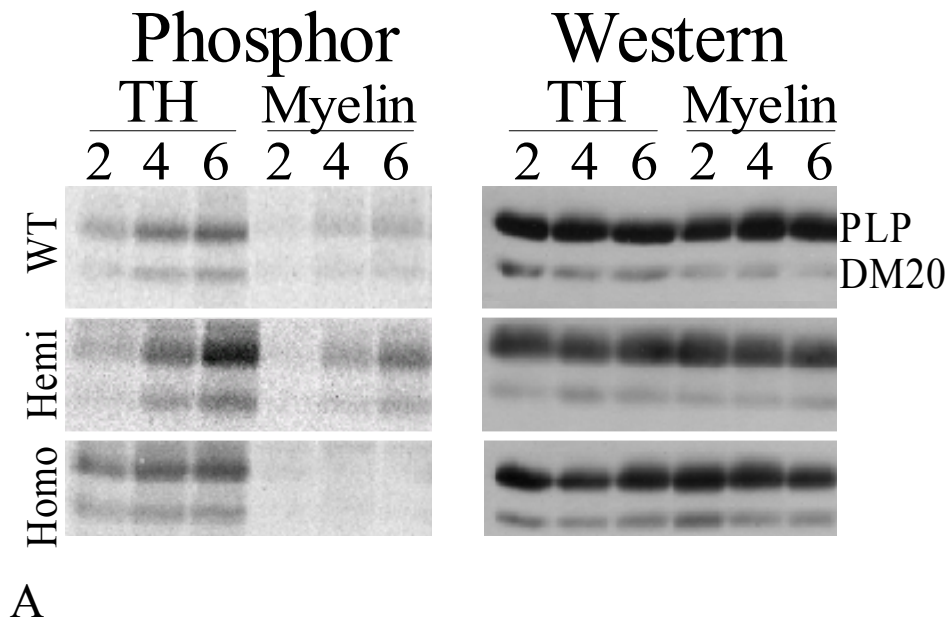


Figure 44. Synthesis and incorporation of newly synthesised PLP and DM20 into myelin in brain slices from P20 wild type, hemizygous and homozygous animals.

A) Phosphorimage of newly synthesised PLP/DM20 in total homogenate and myelin from brain slices of wild type, hemizygous and homozygous mice. **B)** Quantitative data from the above study of translation of PLP over 6 hours in wild type, hemizygous and homozygous mice.

PLP myelin incorporation

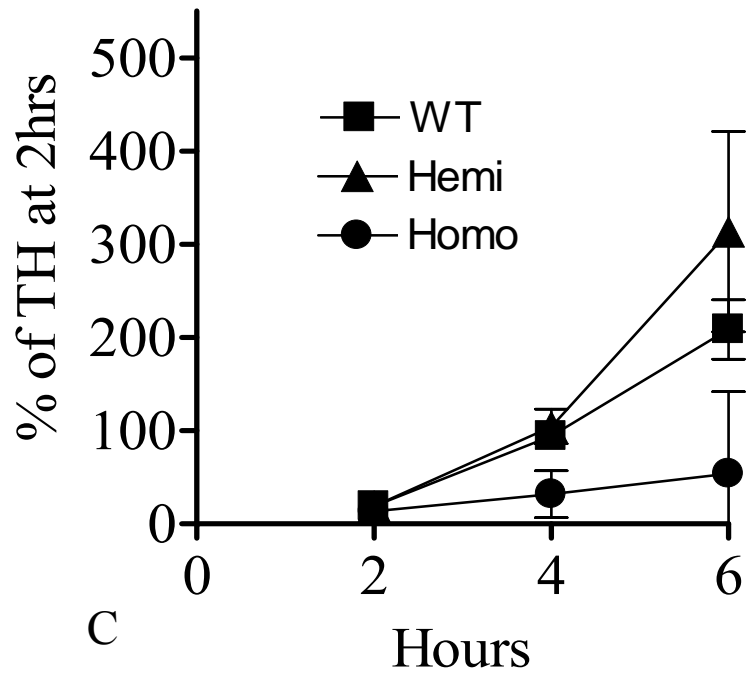


Figure 44 (continued).

C) Incorporation of PLP into myelin in wild type, hemizygous and homozygous mice.

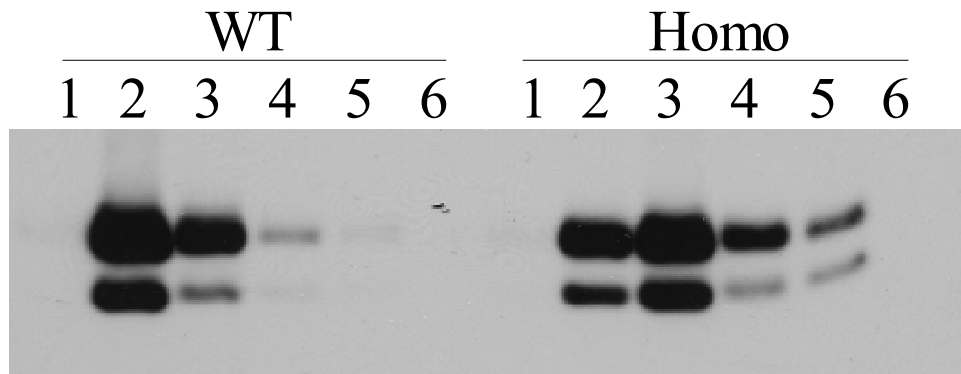


Figure 45. Different association of PLP/DM20 from wild type and homozygous myelin with lipid rafts.

Fractions 1 (light fraction) to 6 (heavy fraction) analysed by western blotting. Whereas, wild type PLP/DM20 is contained more in the lighter fractions, the proteins in homozygous myelin show a more diverse pattern with significant amounts in the dense fractions.



Figure 46. Phosphorimage of lysates from oligodendrocytes after 1 hr of labelling with radiolabelled amino acids.

Shows all newly synthesised labelled protein within the lysates. No difference is shown between the two lanes.

8 Final conclusions and future work

Data presented in this study have provided insights in the effects of increased *Plp1* gene dosage on myelination from message and protein levels all the way to the structure of myelin formed in the transgenic #66 mice. The study aimed to investigate the effects extra copies of a wild type gene would have on the mechanisms associated with myelination that could lead to disease in humans and animals. The two genotypes described in this thesis display very different phenotypes at different ages compared to wild type. The cause of this variation is associated with the number of wild type *Plp1* genes present in their genome. The wild type animals have only the endogenous copy of *Plp1* on the X chromosome whereas the hemizygous animals have one cassette containing 7 extra copies of the gene and homozygous have two cassettes containing in total 14 extra copies of the gene. These animals have been and are currently being used as models of PMD in humans which, in many cases, is caused by *PLP1* gene duplication/triplication. Data presented in this thesis have shown that the underlying effects of this increase in gene dosage differs between the two genotypes compared to wild type and each also between each other and are summarised in Table 9.

For clarity, the hemizygote and homozygote data are discussed separately followed by a comparison between the two genotypes with regards to a mechanistic basis of the findings. In the low gene dosage (hemizygous) mice, at P3, premyelinating oligodendrocytes are able to maintain PLP/DM20 message and protein concentrations at levels similar to wild type expression of the *Plp1* gene. The same observations are made of oligodendrocytes cultured from P5 spinal cord. A single transgene cassette as in hemizygous animals without any endogenous *Plp1* gene, established by expressing the transgene on a *Plp1* null background, has the levels similar to wild type supporting the data for the hemizygous animals.

In cultured oligodendrocytes, the rates of synthesis and degradation of PLP/DM20 over time in hemizygous oligodendrocytes are comparable to wild type rates. These results imply that at early stages of myelination although the cells have to cope with the additional burden imposed by the extra gene dosage, they are able to adapt and maintain a level associated with the normal wild type oligodendrocyte. The potential mechanisms by which the oligodendrocyte could maintain normal *Plp1* message levels either by 1) only transcribing normal levels due to repression of expression of the *Plp1* gene or 2) by

degrading the excess message prior to translation. Whether the downregulation or repression of expression of the *Plp1* gene occurs through the mechanism reported by Mallon and Macklin (2002) utilising the 3' UTR and the possibility this mechanism may play a role in disease in humans requires further investigation. The second hypothesis of degradation of the transcript could be tested using a similar method to that utilised in bacteria. Rifampicin is a chemical used to treat bacterial infections and in *E. coli* it inhibits DNA dependant RNA polymerase and blocks transcription of mRNA (Ludi and Pace 1979). Oligodendrocytes could be treated *in vitro* for different time points, after radiolabelling for a fixed time, with a compound that inhibits the same process in mammalian cells. The levels of *Plp/Dm20* message at each time point would be measured by realtime qRT-PCR.

By P20, when the majority of myelination is occurring in murine CNS, the amount of protein and lipids that oligodendrocytes have to produce to ensheath axons has increased dramatically compared to P3 or P5. In hemizygous mice at P20 although the oligodendrocytes are still maintaining *Plp1* expression at wild type levels, the adaptive response required by the cell to achieve this has a detrimental effect of production of other myelin proteins with a significant reduction in CNP and MBP levels. MAG is not reduced in these animals. There is no difference in the synthesis or degradation rates of PLP/DM20 in these animals when compared to their wild type counterparts. No difference was seen in the raft profile (data not shown) between the two suggesting once again that oligodendrocytes in the hemizygous animals are able to deal with or manage the increase in gene dosage sufficiently to survive and myelinate. By P60 when most of the myelinogenesis has taken place the status of myelin proteins in myelin has changed with all studied myelin proteins including MBP, which showed the greatest reduction at P20, have recovered to wild type levels by P60.

However, these hemizygous animals do go on to develop abnormalities in the CNS leading to phenotypic changes as reported by Anderson *et al.*, (1998). Surprisingly, the point or stage at which this occurs varies from mouse to mouse with some displaying changes by P120 and some only developing abnormalities as late as 18 months. The mechanism behind this variation is not yet understood but MBP may have a role to play. While studying the hemizygous animals, one observation was noted, these mice showed a variation in amount of MBP present in their CNS tissue leading to a higher SEM than any other protein studied. One hypothesis to explain the variation in phenotype is that

phenotypic variation and MBP amount variation are linked. MBP, as mentioned throughout this thesis, is essential to myelin. As mentioned in the introduction of this thesis there are many putative roles for MBP, however, it is known to be important in compaction of myelin. A lower MBP level at P20 may be indicative of an earlier onset of abnormalities while the higher levels of MBP observed may suggest a later onset of myelin changes and abnormalities. This may possibly be related to the turnover of myelin after it has been formed and therefore represent the maintenance phase of myelination and would require further investigation to elucidate.

Homozygous #66 animals behave very differently in terms of protein levels, dynamics axon diameter, g ratios and level of myelination compared to their wild type and hemizygous littermates. From P3 onwards there is marked difference in the fate of PLP/DM20 in these animals. Prior to myelination there is an increase in PLP/DM20 at the protein level, which is inversely related to MBP amounts at both the message and protein level. During peak myelination the homozygous animals still express less MBP either through decreased production or increased degradation or a combination of the two as with PLP/DM20 in this study. This could be tested with the same methods utilised in the PLP/DM20 investigation. At this stage of myelinogenesis the PLP/DM20 levels in total homogenates are also reduced compared to wild type levels but this may be reflective of the low myelin content per unit of tissue. This decrease in PLP/DM20 present in the oligodendrocyte in the effort to control the amount of protein produced affects other myelin proteins such as CNP, MAG and MBP as previously mentioned in this study. This variation in PLP/DM20 present in homozygotes through development of the mature CNS could affect the level of palmitoylation of the protein. Palmitoylation occurs in the Golgi apparatus, is one of the few reversible post-translational modifications and anchors a protein more securely to the plasma membrane than a protein with no post-translational modifications (Basu *et al.*, 2004). The overproduction of PLP/DM20 prior to and at the early stages of myelination could lead to the sequestering of much of the available fatty acid chains thus altering PLP/DM20's hydrophobicity and insertion into myelin membrane. As the increased gene dosage is a universal transformation affecting all oligodendrocytes and in these cells this sequestering of the fatty acid chains could be a global effect in the CNS. A reduction in the incorporation of PLP/DM20 into myelin and steady state levels in myelin at P20 is observed in the homozygous animals.

Another effect of increased gene dosage was reported by Giambonini-Brugnoli *et al.*, (2005). They investigated the effects of increased *PMP22* gene dosage in transgenic mice. *PMP22* is required for the formation of PNS myelin. Increased copy number of the gene was found to cause reduced expression of 58 different genes involved in the cholesterol biosynthesis pathway at P4 compared to wild type animals. This is also observed in the older *PMP22* transgenic mice at P60. It could be hypothesised that the same is occurring in the homozygous #66 mice with proteins involved in lipid biosynthesis affected just as the myelin proteins are. Cholesterol can be obtained by oligodendrocytes from neighbouring cells (Saher *et al.*, 2005). However in homozygous animals all the oligodendrocytes are under the same burden and there can only be a limited supply of cholesterol available for uptake. Therefore the horizontal transfer reported from wild type cells to SQS deficient oligodendrocytes by Saher *et al.*, (2005) is not an option for these homozygous #66 oligodendrocytes. The oligodendrocytes could, however, acquire cholesterol from other cells in the CNS such as astrocytes or neurons but these cells may not be able to provide sufficient amounts of cholesterol for the production of myelin. This could be an avenue for future study in these animals.

The partitioning of PLP/DM20 changes in the homozygotes with more protein present in membranous organelles in the cell body as demonstrated by the increase signal of the protein in the pellet fraction at P20. The membranous organelles were found to be LE/Ls by immunostaining with an anti-Lamp1 antibody. Supporting evidence comes from P0 transgenic mice (Wrabetz *et al.*, 2000) where overexpressed P0 may be targeted to the LE/Ls pathway like PLP/DM20. The accumulation of transgenic wild type PLP/DM20 with lipids such as cholesterol in LE/Ls may be a factor in disease pathology in *PLP1* gene duplications in humans. Simons and Trajkovic (2006) reported PLP/DM20 and cholesterol cycle from the membrane to LE/Ls in the absence of axons. In #66 homozygous oligodendrocytes even in the presence of axons PLP/DM20 and lipids are cycled to the LE/Ls and retained there. The way the oligodendrocyte deals with the increased *Plp1* gene dosage is dependant on whether the cell is generating myelin especially in the presence of axons. These changes in dosage do alter the distribution of PLP/DM20 within the oligodendrocyte and myelin unit. Incorrect partitioning of PLP/DM20 when in lipid rafts must perturb the transport and insertion of PLP/DM20 into myelin and also of other myelin proteins (Simons *et al.*, 2002, Kramer-Albers *et al.*, 2006). This has been demonstrated by colocalisation of PLP/DM20 with MAG in oligodendrocytes in corpus callosum and cortex. PLP/DM20 and MAG share a transport pathway for insertion in myelin (Georgiuo

et al., 2004), whereas MBP is transported as a transcript to myelin and translated at its site of incorporation (Trapp *et al.*, 2004). No colocalisation of MBP with PLP/DM20 was seen in the same oligodendrocytes reiterating the possibility of a selective transport defect in the homozygous #66 oligodendrocytes. Abnormal long lasting immunoreactivity of MBP, MAG and CNP in the cell body of oligodendrocyte-like cells in a patient with PMD have previously noted (Koeppen and Robitaille 2002), suggesting accumulation or abnormal transport of these proteins in the cell body due to the mutation in the *PLP1* gene.

Aberrant insertion of PLP/DM20 into myelin would change the overall protein to lipid ratio and ratios between proteins also. The decrease in available myelin and decreased contact with axons in the homozygous animals could lead to an exacerbation of the accumulation of PLP/DM20 in LE/Ls. Although oligodendrocytes have been hypothesised to be able to sense the imbalance in the protein and lipid ratio and alter expression of genes to suit the change in situation (Saher *et al.*, 2005) this mechanism is likely to be lost in the homozygous animals with high gene dosage.

Steady state levels of this protein are higher in the pellet (membranous fraction) and can be seen to persist through the life of the oligodendrocyte in the cell body from non-myelinating to pre-myelinating and through to the mature peak-myelinating cells. This pool could be classed as long-lived storage pool (Trajkovic *et al.*, 2006) of protein possibly residing in the LE/Ls along with lipids and could have different dynamic properties to the PLP/DM20 transported to myelin or directed for degradation to the proteasome. These pools have been noted in astrocytes for GFAP as there is evidence that there are short and long term pools of GFAP in astrocytes with different decay rates for each (Rolland *et al.*, 1990). The hypothesis required validation and study which could be achieved by radiolabelling oligodendrocytes in culture at an earlier stage such as day 3 and investigating synthesis and degradation at the same end point of day 6 as mentioned in this thesis.

The synthesis rates of PLP and also DM20 at P20 in homozygous animals are similar to the rates of synthesis in oligodendrocytes *in vitro*; however, there is a decrease in the rates of synthesis of PLP and DM20 in both oligodendrocytes *in vitro* and at P20 compared to wild type and hemizygous animals. Overall less PLP/DM20 is produced and less is incorporated into myelin at peak myelination and the degradation rate for PLP/DM20 is also higher. The investigation of the dynamics of PLP/DM20 in conjunction with an assessment of the

distribution of PLP/DM20 would imply that the net reduction of PLP/DM20 observed in myelin is a consequence of the combined alteration in synthesis with accelerated degradation.

The increased degradation rate in homozygous #66 animals along with decreased synthesis and incorporation rates, steady state levels and co-localisation of PLP/DM20 with Lamp-1 in LE/Ls suggests multiple fates for the protein. A proportion of PLP/DM20 is incorporated into myelin correctly as seen by the steady state levels, while some PLP/DM20 along with cholesterol and other lipids is sequestered to the LE/Ls and some of the protein is likely to be synthesised and degraded quickly without even reaching its site of incorporation in compact myelin.

Unlike the *rsh* or *msd* mutations the UPR leading to an apoptotic response does not appear to play a role in the disease/phenotype severity in #66 transgenic mice (Southwood *et al.*, 2002). There is no misfolded protein produced to activate ER stress responses leading to UPR, however, accumulation of PLP/DM20 in the oligodendrocyte cell body could affect other essential cellular processes leading to apoptosis of the cell through different pathway and contribute to the disease phenotype.

In humans increase of *PLP1* gene copy number from 1 to 2 copies causes PMD and an increase from 2 to 3 copies is associated with a more severe disease phenotype. However, an increase from 3 to 5 copies seen in one patient as reported by Wolf *et al.* (2005) showed no significant difference in clinical symptoms from that patient to the other with only 3 copies. This suggests that the threshold for change in gene copy number is; 1) much lower in humans than mice and 2) oligodendrocytes are pushed to their furthest limits at 3 wild type *PLP1* copies in humans. The level of oligodendrocyte cell death may be a contributing factor to the severity of disease and may vary from 2 to 3 copy numbers but not beyond this point. The area of the X-chromosome containing the *PLP1* gene that is duplicated varies in PMD (Inoue *et al.*, 1998, Lee *et al.*, 2006b, Woodward *et al.*, 1998, 2000). The #72 mice and also the *4e-Plp* mice display different degrees of severity (Readhead *et al.*, 1994, Kagawa *et al.*, 1994). This variation in phenotype severity may be caused by the variation in area of duplication or a positional effect due to area of insertion of the duplication. The proposal that PLP overexpression results in arrest of oligodendrocyte and myelin development was put forward by Simons *et al.*, (2002), Kagawa *et al.*, (1994) and Readhead *et al.*, (1994). A similar arrest in Schwann cell

development prior to sorting to axons is seen *P0* transgenic mice with the highest gene copy number (Wrabetz *et al.*, 2000). The increased *Plp1* gene dosage has an impact on oligodendrocyte and myelin development in the #66 transgenic animals as homozygous oligodendrocytes *in vitro* do not produce as much PLP or MBP or membranous sheets as observed in wild type oligodendrocytes. Also PLP and Lamp-1 co-localisation is observed at P20 in the homozygous CNS suggesting the oligodendrocytes are immature even at peak myelination. Whether it causes a complete arrest in development is yet to be determined but a possible experiment could be to culture #66 oligodendrocytes in the presence of axons and astrocytes to produce myelinating cultures (Thomson *et al.*, 2007).

PLP makes up 50% of all CNS myelin proteins while MBP accounts for 30% and this ratio between the two appears also to be essential to myelin formation as alterations in PLP/DM20 levels has a detrimental effect on MBP levels although this is not the case with a complete loss of PLP/DM20. In the case of the *Plp1* null animals, the complete loss of PLP/DM20 may cause the possible activation of another member of the *lipophilin/DM* family present in the genome to replace the protein's function. Also in the absence of MBP a higher proportion of PLP/DM20 is found in heavy fractions in lipid rafts. MBP is critical for myelin formation and influences the amount of myelin formed by an oligodendrocyte (Shine *et al.*, 1992). A series of experiments by Fitzner *et al.*, (2006) demonstrated that MBP is also essential for the reorganisation of the oligodendrocyte plasma membrane and the mediation of raft clustering. There is a likelihood that increasing the levels of MBP to correspond in the correct ratio/proportion to the increase of the *PLP1* gene dosage in these cells may improve myelin formation. This could be achieved by crossing the #66 transgenic animals with *MBP* transgenic animals generated by Readhead *et al.*, (1987) and studying the fate of both PLP/DM20 and MBP and myelin as a whole.

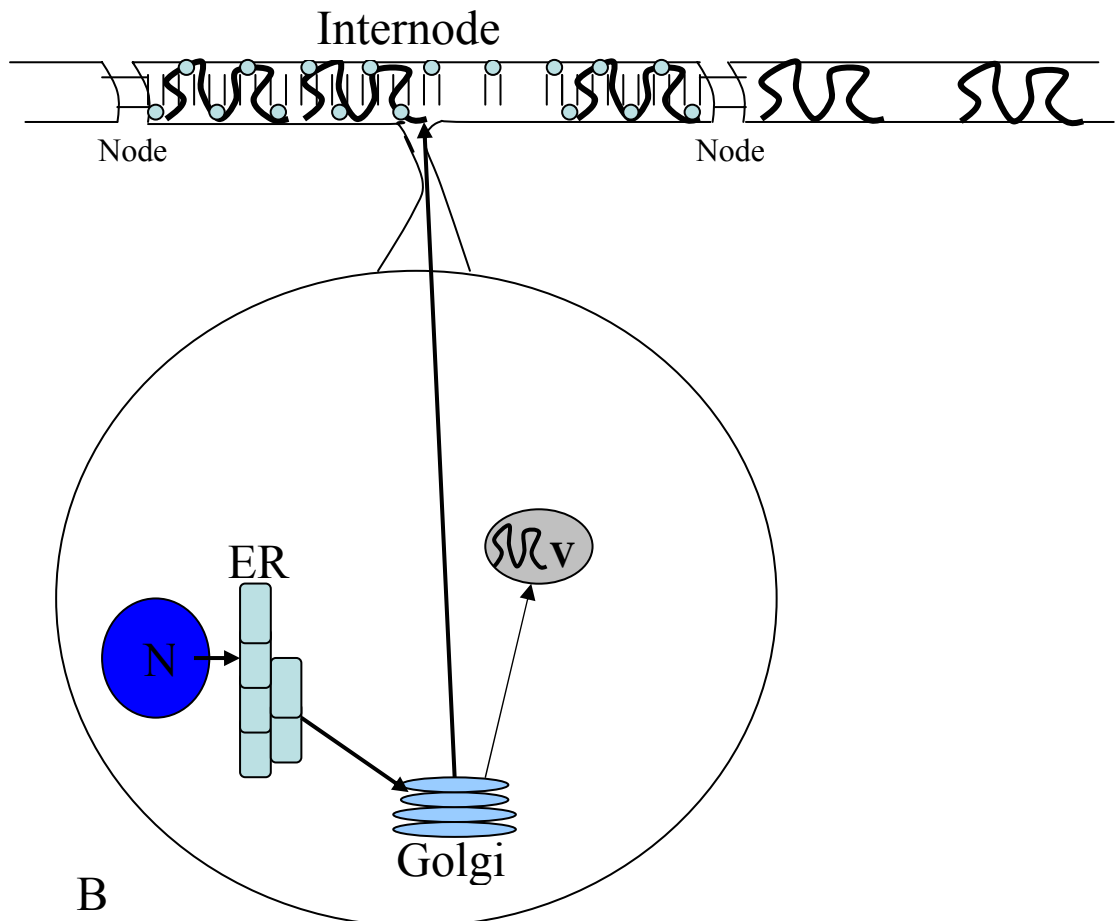
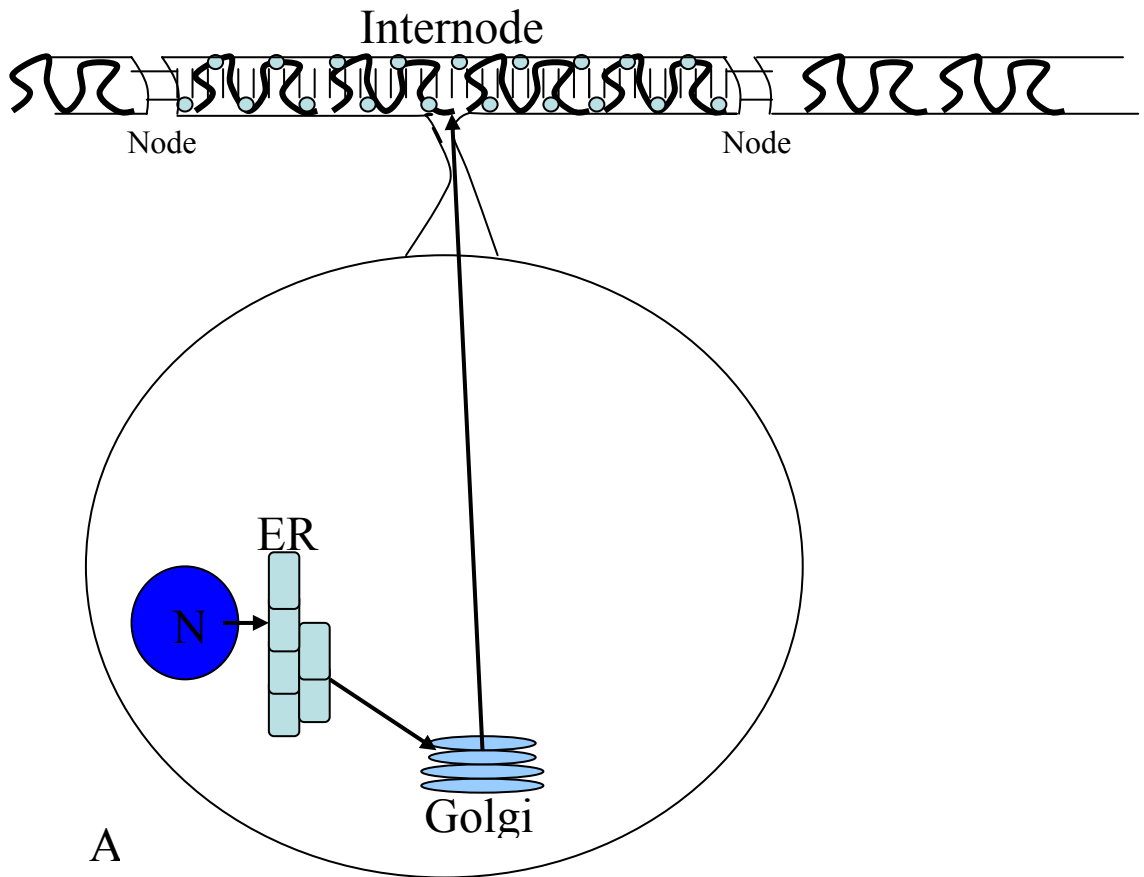
Another avenue of investigation could be similar to the one taken in Rett syndrome (RTT) (Giacometti *et al.*, 2007, Guy *et al.*, 2007). The data from their experiments highlights the potential to rescue an aberrant CNS phenotype. Transgenic mice with a knockout of the X-linked *Mecp2* gene displayed a phenotype caused by a deficiency in neurons. The mice develop RTT-like symptoms from 4-5 weeks which include reduced brain weight, decreased neuron size, hindlimb clasping and impaired locomotor function. However due to the knockout process the investigators retained the ability to turn the gene back on and demonstrated phenotypic reversal in both young and old mice. Although in a different cell type than in #66 mice this displays plasticity to the state of the cells in the CNS and

highlights the possibility a rescue of an aberrant phenotype can occur in the CNS. This is also seen by the recovery of myelin proteins in hemizygous #66 animals by P60 in this study. The causes of the dysmyelination observed in homozygous animals and the later demyelination that occurs in the hemizygous animals are not yet understood but with this study we may be part way in understanding the effects of increased gene dosage on the CNS. Ip *et al.*, (2007) generated #66 heterozygous mice on the C57/Bl6 background then crossbred them with Sialoadhesion (Sn)-deficient mice. Sialoadhesion is a sialic acid binding protein involved in macrophage-lymphocyte interactions and is expressed on 90% of CNS macrophage-like cells in #66 heterozygous PLP mutants. When knocked out in PLP mutants a significant reduction in pathological alterations such as demyelination is observed at 12 months (Ip *et al.*, 2007). In the #66 transgenic mice crossed with Sn deficient mice the improvement in phenotype is indicative of a recovery process by repressing the immune response to the myelin defect. With further investigation into the questions raised from this study we may be able to aid the oligodendrocyte in the as yet unknown recovery process seen and this would be beneficial to PMD patients in the future.

Table 9. Summary of results in this study on #66 transgenic mice.

Stage	Hemizygous (Low gene dosage)	Homozygous (High gene dosage)
Non-myelinating (in culture) Synthesis Degradation MBP OL/Myelin	normal PLP/DM20 normal as WT normal as WT normal MBP normal	increase of PLP/DM20 decrease in rates increase in rates decrease of MBP no membranous sheets lower PLP/DM20 lower MBP
Pre-myelinating MBP OL/Myelin	normal <i>Plp1</i> transcript levels small increase in PLP/DM20 normal <i>Mbp</i> transcript levels normal MBP normal	lower <i>Plp1</i> transcript levels increase of PLP/DM20 lower <i>Mbp</i> transcript levels decrease of MBP autophagic vacuoles distended RER
Peak myelinating TH Myelin Pellet Synthesis Incorporation Rafts Other proteins	normal <i>Plp1</i> transcript levels normal PLP/DM20 normal PLP/DM20 increase of PLP/DM20 normal normal normal (not shown) normal <i>Mbp</i> transcript levels decrease of MBP and CNP	lower <i>Plp1</i> transcript levels small decrease in PLP/DM20 marked decrease in PLP/DM20 increase in PLP/DM20 decreased decreased abnormal raft distribution lower <i>Mbp</i> transcript levels decrease of MBP, CNP and MAG co-localisation of PLP/DM20 with Lamp1 in LE/Ls
Maintaining myelin MBP	normal <i>Plp1</i> transcript normal PLP/DM20 normal <i>Mbp</i> transcript normal MBP	N/A Dead

(OL = oligodendrocytes, N/A = not applicable).



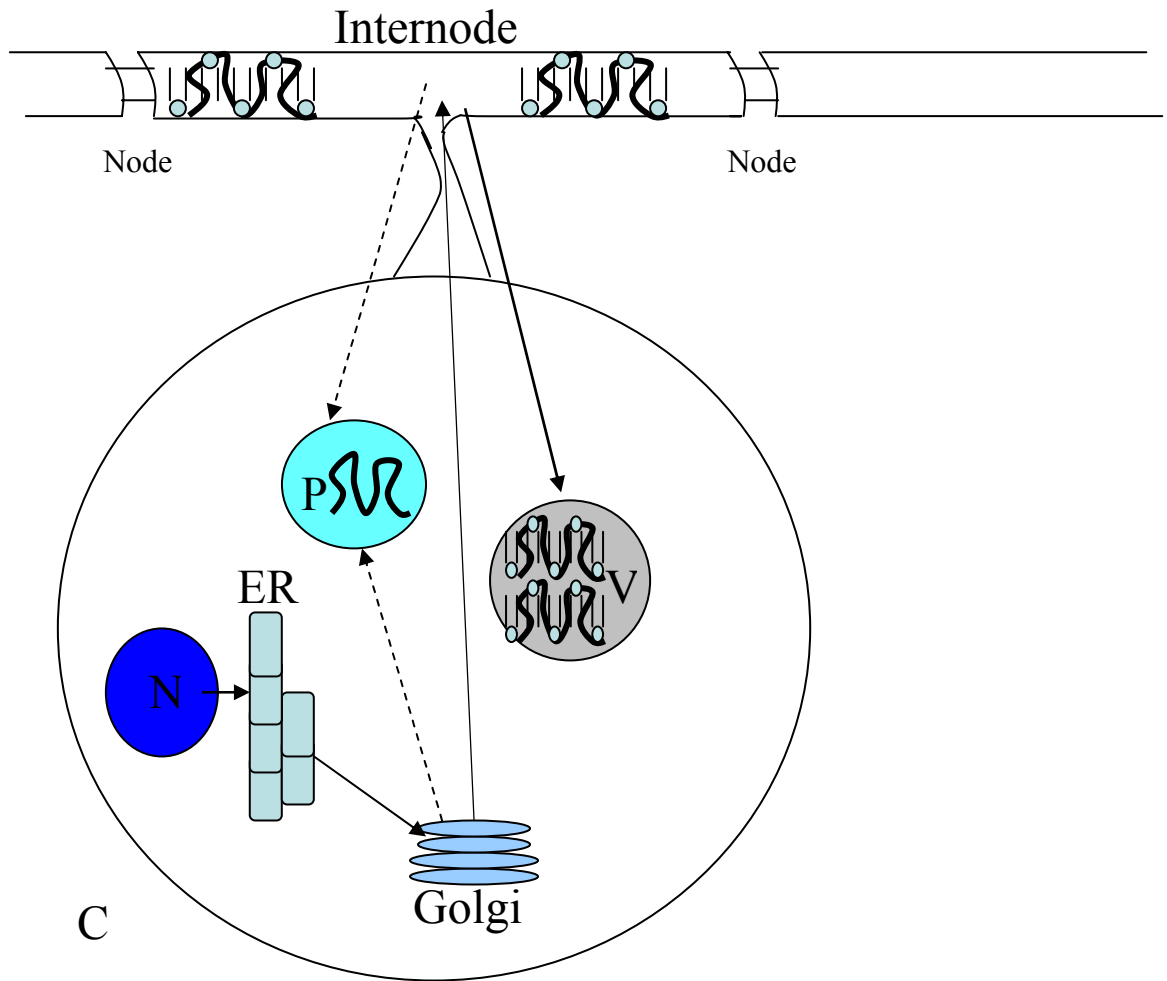


Figure 47. Schematic representation of the fate of PLP/DM20 at P20 in wild type, hemizygous and homozygous #66 oligodendrocytes.

A) Schematic representation of the fate of PLP/DM20 in P20 wild type oligodendrocytes showing the normal processing of the protein via the ER and Golgi apparatus to compact myelin. **B)** Schematic representation of the fate of PLP/DM20 in P20 hemizygous oligodendrocytes showing the processing of the protein via the ER and Golgi apparatus to compact myelin which very similar to wild type. **C)** Schematic representation of the fate of PLP/DM20 in P20 homozygous oligodendrocytes showing the abnormal processing of the protein via the ER and Golgi apparatus to compact myelin and/or vacuoles likely to be LE/Ls in the cell body. (N = nucleus, ER = endoplasmic reticulum, P= proteasome, V = vacuole, thick black line = PLP/DM20,  lipid, solid arrows = established pathways, dashed arrows = possible pathways).

9 Appendix

9.1.1 APES-coated slides

APES-coated slides were generally used for immunohistochemistry because they keep the sections adhered. To clean grease on the slides, they were soaked overnight in 5% Decon 90 (Decon Lab Ltd) then washed in distilled water and oven dried. The dried slides were then soaked in 0.25% APES (Sigma) in methylated spirit in a fume hood for 2 minutes. Finally, the slides were rinsed in DEPC-treated water for 2 minutes and oven dried wrapped in foil. APES-coated slides were stored at room temperature.

9.1.2 DEPC-treated water

0.1% solution of DEPC was made in distilled water and left for at least 12 hours to inactivate contaminating RNases. The water was autoclaved at 151b.in-2 for 20 minutes to destroy the DEPC before use and stored sealed at room temperature until require.

9.1.3 Fixatives

9.1.3.1 Karnovsky's modified fixative (paraformaldehyde/glutaraldehyde 4%/5%)

Preparation of 500 ml of the fixative:

8% Paraformaldehyde: 20 g of paraformaldehyde was added to 250 ml of ddH₂O and heat to 65°C. Few drops of 1M NaOH was added to clear and solution was allowed to cool.

0.08M Cacodylate buffer: 17.1224 sodium cacodylate was dissolved in a 1 litre of dH₂O and adjusted to pH 7.2.

250 ml	8% Paraformaldehyde
100 ml	25% Glutaraldehyde
150 ml	0.08M Cacodylate buffer
250 mg	Calcium chloride

Add appropriate volumes, dissolve calcium chloride, adjust to pH 7.2, filter, and store at 4°C.

9.1.3.2 4% paraformaldehyde

Preparation of 500 ml of the fixative:

20g paraformaldehyde was added to 500ml PBS and heat to 65°C. Few drops of 1M NaOH were added to clear the solution, filtered, cooled, and adjusted to pH 7.2.

9.1.3.3 Periodate-lysine-paraformaldehyde (P-L-P) fixative

Preparation of 1litre of the fixative:

Buffered lysine solution: 13.7g lysine monohydrate dissolved in 375ml ddH₂O. 1.8g sodium hydrogen phosphate dissolved in 100ml ddH₂O. The two solutions were mixed to give 475ml and pH 7.4

10% Paraformaldehyde: 20g paraformaldehyde dissolved in 200 ml ddH₂O and heated to 65°C. Few drops of 1M NaOH were added to clear and allowed to cool.

The two solutions were separately stored at 4°C overnight. Immediately before use the two solutions were mixed and the final volume is made up to 1litre using 0.1M phosphate buffer. 2.14g sodium periodate was also dissolved.

9.1.3.4 Buffered neutral formaldehyde

Preparation of 1 litre of the fixative:

100 ml	40% formaldehyde (Merck)
900 ml	Tap water
4 g	Sodium dihydrogen phosphate
8 g	Di-potassium hydrogen phosphate

9.1.4 Tissue processing protocols

9.1.4.1 Resin processing

CNS tissues were passed through below various solutions and finally blocked in resin:

1-	Isotonic cacodylate buffer	50 min	4°C
2-	1% OsO ₄ in cacodylate buffer	2hr	room temperature
3-	Isotonic cacodylate buffer	30 min	room temperature
4-	50% ethanol	5 min	4°C
5-	50% ethanol	10 min	4°C
6-	70% ethanol	5 min	4°C
7-	70% ethanol	10 min	4°C
8-	80% ethanol	5 min	4°C
9-	80% ethanol	10 min	4°C
10-	90% ethanol	5 min	4°C
11-	90% ethanol	10 min	4°C
12	Ethanol	20 min	4°C

13	Ethanol	20 min	4°C
14-	Propylene oxide	15 min	room temperature
15-	Propylene oxide	15 min	room temperature
16-	1:2 resin: propylene oxide	13 hr	room temperature
17-	1:1 resin: propylene oxide	6 hr	room temperature
18-	2:1 resin: propylene oxide	18 hr	room temperature
19-	Resin	4 hr	30°C

Isotonic cacodylate buffer:

16.05 g	Sodium cacodylate
3.8 g	Sodium chloride
0.055 g	Calcium chloride
0.102 g	Magnesium chloride

Dissolve in 1litre ddH₂O and adjust to pH 7.2

Araldite resin:

1-	30 g	Araldite CY212 (resin)
2-	25.2 g	Dodecanyl succinic anhydride
3-	1.2 ml	2,4,6-tri-dimethylaminomethyl-phenol
4-	0.75 ml	Di-butylphthalate

Add 1 and 2, place in an oven at 65°C for 10-15 min and mix. Add 3 and 4, and stir until mixture well homogenised and store at -20°C.

9.1.5 Staining protocols

9.1.5.1 Dehydration and cleaning of sections

1-	Methylated spirits	2 mins
2-	absolute alcohol	2 mins
3-	absolute alcohol	2 mins
4-	Histoclear	2 mins
5-	Xylene	2 mins

9.1.5.2 Haematoxylin and eosin

1-	Xylene	2 mins
2-	Absolute alcohol	2 mins
3-	Methylated spirits	2 mins
4-	ddH ₂ O	2 mins
5-	Lugols iodine	1 min
6-	ddH ₂ O	1 min
7-	5% sodium thiosulphate	1 min
8-	ddH ₂ O	2 mins
9-	Mayers haematoxylin	10 mins
10	1% acid alcohol	3 dips
11-	ddH ₂ O	2 mins
12-	Scots tap water substitute	1 min
13-	ddH ₂ O	2 mins
14-	Methylated spirits	10 secs
15-	Saturated alcoholic eosin	2 mins

16-	Methylated spirits	10 secs
17-	Absolute alcohol	2 mins
18-	Histoclear	2 mins
19-	Xylene	5 mins

9.1.5.3 Haematoxylin

1-	Running water	2 mins
2-	Mayers haematoxylin	50 secs
3-	Water	wash off excess haematoxylin
4-	Scots tap water substitute	30 secs

9.1.5.4 Staining for electron microscopy

1-	Saturated uranyl acetate in 50% ethanol	15 min
2-	50% ethanol	Rinse
3-	50% ethanol	Rinse
4-	ddH ₂ O	Rinse
5-	ddH ₂ O	Rinse
6-	air dry	
7-	Reynold's lead citrate (Sodium Hydroxide moistened chamber)	10 mins
8-	1M sodium hydroxide	rinse
9-	1M sodium hydroxide	rinse
10-	1M sodium hydroxide	rinse
11	ddH ₂ O	Several rinses

Reynold's lead citrate (1.2mM lead citrate, 1.8mM sodium citrate, pH 12.0)

1-	1.33 g Lead nitrate dissolved in 15 ml ddH ₂ O	1 min vigorous shaking
2-	1.76 g Sodium citrate dissolved in 15 ml ddH ₂ O	1 min vigorous shaking

Add 1 to 2 and equilibrate over 30 minutes with occasional shaking. Clear with 1M NaOH and make up to the final volume of 50 ml with ddH₂O.

9.1.6 Staining solutions

9.1.6.1 Methylene blue/ azure II

1%	Methylene blue
1%	Azure II
1%	Borax

Dilute with ddH₂O and filter before use.

9.1.6.2 Mayers haematoxylin

1 g	Haematoxylin
10 g	Potassium alum
0.2 g	Sodium iodate

Dissolve in 1 litre of ddH₂O, bring to boiling point, allow to cool overnight, and then add:

1 g	Citric acid
50 g	Chloral hydrate

9.1.6.3 Scots tap water substitute

3.5 g	Sodium bicarbonate
20 g	Magnesium sulphate

Dissolve in 1 litre of ddH₂O.

9.1.7 General Buffers**9.1.7.1 Phosphate buffer saline (PBS)**

8 g	Sodium chloride
1.44 g	Disodium hydrogen phosphate
0.24 g	Potassium dihydrogen phosphate
0.2 g	Potassium chloride

Dissolve in 800 ml of ddH₂O. Adjust to pH 7.4 with 1M HCl and make the volume up to 1 litre with ddH₂O.

9.1.7.2 0.1 M phosphate buffer

77.4 ml	1M Disodium hydrogen phosphate
22.6 ml	1M Potassium dihydrogen phosphate

Combine two volumes and adjust to pH 7.4 with 1M HCl.

9.1.7.3 10x Tris buffer saline (10x TBS)

12 g	Tris base pH 7.5
87 g	Sodium chloride

Dissolve in 800 ml ddH₂O. Adjust to pH 7.4 with 1M HCl and make the volume up to 1 litre with ddH₂O.

9.1.7.4 Tris-EDTA buffer (TE buffer)

500 µl	1M Tris pH 8.0
100 µl	0.5M EDTA

Make up volume to 50 ml with ddH₂O.

9.1.7.5 Tris acetate EDTA buffer (TAE buffer)

48.4 g	Tris base
11.4 ml	Glacial acetic acid
20 ml	0.5M EDTA

Volume made up to 1 litre with ddH₂O.

9.1.7.6 20x Sodium chloride/Sodium citrate buffer (SSC buffer)

175 g	Sodium chloride
88 g	Sodium ₃ Citrate.2H ₂ O

Make up to 900mls with ddH₂O. Adjust pH to 7.0 with HCl, then make up to final volume of 1 litre with ddH₂O.

9.1.8 Specific solutions and buffers

9.1.8.1 10x MOPS buffer

200 ml	1M MOPS
20 ml	250mM Sodium acetate
20 ml	0.5M EDTA pH 7.5

Make up 900ml with ddH₂O. Adjust pH to 7.0 with NaOH then make up to final volume of 1 litre with ddH₂O. Filter, wrap bottle in foil and store in dark at RT.

9.1.8.2 6x Orange G loading dye

0.4%	Orange G powder
15%	Ficoll 400 (Glycerol can be used)
500 µl	1M Tris-HCl
5 ml	0.5M EDTA

Make up to 50ml with ddH₂O. Store at RT.

9.1.8.3 6x BPB/XC loading dye

0.04%	Bromophenol Blue powder
0.04%	Xylene Cyanol powder
15%	Ficoll 400 (Glycerol can be used)
500 µl	1M Tris-HCl
5 ml	0.5M EDTA

Make up to 50ml with ddH₂O. Store at RT.

9.1.8.4 RNA loading buffer

250 µl	Formamide (Deionised, COSHH)
83 µl	Fomaldehyde (COSHH)
500 µl	10x MOPS
117 µl	RNase-free H ₂ O

Make up in fume hood.

9.1.8.5 RNA loading dye

50% glycerol in 1x MOPS buffer. Add a few grains of Bromophenol Blue.

9.1.8.6 Cell Lysis Buffer

1 ml	10% Tritin X-100
1 ml	10x TBS
20µl	0.5M EDTA
5 µl	1M DTT
5 µl	10mg/ml Aprotinin
5 µl	10mg/ml Leupeptin
5 µl	10mg/ml Trypsin inhibitor
100 µl	100mM Benzamidine
100 µl	250mM Sodium orthovanadate
100 µl	100mM Sodium pyrophosphate
40 µl	250mM PMSF

Make up to 10ml with ddH₂O. Add PMSF last. Store at 4°C.

9.1.8.7 **Kreb's Buffer**

15.7 ml	2M NaCl
312 µl	2M KCl
300 µl	1M Na ₂ HPO ₄
1.3 ml	250mM MgSO ₄
500 µl	1M CaCl ₂
2.7 ml	1M Glucose
12.5 ml	0.5M NaHCO ₃

Make up 230 mls with ddH₂O. Adjust pH to 7.4 with NaOH, then make up to final volume of 250 mls with ddH₂O. Bubble oxygen through buffer at RT until use.

9.1.8.8 **10x SDS-Page running buffer**

144 g	Glycine
30.3 g	Tris
10 g	SDS

Add the Glycine first, once dissolved add Tris and finally SDS ensuring final volume of 1 litre ddH₂O.

9.1.8.9 **Towbin transfer buffer**

9.1.8.9.1 *Anode 1*

36 g	Tris
74 ml	Methanol

Make up to 1 litre with ddH₂O. Store at 4°C.

9.1.8.9.2 *Anode 2*

3 g	Tris
75 ml	Methanol

Make up to 1 litre with ddH₂O. Store at 4°C.

9.1.8.9.3 *Cathode*

3 g	Glycine
3 g	Tris
74 ml	Methanol

Make up to 1 litre with ddH₂O. Store at 4°C.

9.1.9 **Tissue culture media**

9.1.9.1 **Sato defined medium**

Glucose (1g/l), Glutamine (2mM), Bovine insulin (10µm/ml), Human transferrin (100µm/ml), BSA-pathocyte (0.0286%), Progesterone (0.2µM), Putrescine (0.1µM), Thyroxin (0.45µM), Selenite (0.224µM), Tri-iodo-thyro-nine (0.5µM) in DMEM.

9.1.9.2 Stop solution

Soya bean trypsin inhibitor (0.52mg/ml), Factor V bovine serum albumin (3mg/ml), DNase (0.04mg/ml) made up in HBSS.

References

- Al-Saktawi, K., McLaughlin, M., Klugmann, M., Schneider, A., Barrie, J. A., McCulloch, M. C., Montague, P., Kirkham, D., Nave, K.-A., and Griffiths, I. R. (2003). Genetic background determines phenotypic severity of the *Plp rumpshaker* mutation. *Journal of Neuroscience Research* **72**, 12-24.
- Aldskogius, H. (2005). Repairing CNS myelin - Astrocytes have to do their jobs. *Experimental Neurology* **192**, 7-10.
- Anderson, T. J. Effects of increased dosage of the *Plp* gene: a study in transgenic mice. (1997). University of Glasgow Thesis.
- Anderson, T. J., Montague, P., Nadon, N. L., Nave, K.-A., and Griffiths, I. R. (1997). Modification of Schwann cell phenotype with *Plp* transgenes: evidence that the PLP and DM20 isoproteins are targeted to different cellular domains. *Journal of Neuroscience Research* **50**, 13-22.
- Anderson, T. J., Schneider, A., Barrie, J. A., Klugmann, M., McCulloch, M. C., Kirkham, D., Kyriakides, E., Nave, K.-A., and Griffiths, I. R. (1998). Late-onset neurodegeneration in mice with increased dosage of the proteolipid protein gene. *Journal of Comparative Neurology* **394**, 506-519.
- Anderson, T. J., Klugmann, M., Thomson, C. E., Schneider, A., Readhead, C., Nave, K.-A., and Griffiths, I. R. (1999). Distinct phenotypes associated with increasing dosage of the *Plp* gene: implications for CMT1A due to *Pmp22* gene duplication. *Annals of the New York Academy of Sciences* **883**, 234-246.
- Andrejewski, N., Punnonen, E.-L., Guhde, G., Tanaka, Y., Lullmann-Rauch, R., Hartmann, D., von Figura, K., and Saftig, P. (1999). Normal lysosomal morphology and function in LAMP1-deficient mice. *The Journal of Biological Chemistry* **274**, 12692-12701.
- Aoyagi, Y., Kobayashi, H., Tanaka, K., Ozawa, T., Nitta, H., and Tsuji, S. (1999). A de novo splice donor site mutation causes in-frame deletion of 14 amino acids in the proteolipid protein in Pelizaeus-Merzbacher disease. *Annals of Neurology* **46**, 112-115.
- Arroyo, E. J. and Scherer, S. S. (2000). On the molecular architecture of myelinated fibers. *Histochemical cell biology* **113**, 1-18.
- Awasthi, N. and Wagner, B. J. (2005). Upregulation of heat shock protein expression by proteasome inhibition: An apoptotic mechanism in the lens. *Investigative Ophthalmology and Visual Science* **46**, 2082-2091.
- Barrese, N., Mak, B., Fisher, L., and Moscarello, M. A. (1998). Mechanism of demyelination in DM20 transgenic mice involves increased fatty acylation. *Journal of Neuroscience Research* **53**, 143-152.
- Basu, J. (2004). Protein palmitoylation and dynamic modulation of protein function. *Current Science* **87**, 212-217.
- Bauer, J., Bradl, M., Klein, M., Leisser, M., Deckwerth, T. L., Wekerle, H., and Lassmann, H. (2002). Endoplasmic reticulum stress in PLP-overexpressing transgenic rats: Gray

matter oligodendrocytes are more vulnerable than white matter oligodendrocytes. *Journal of Neuropathology and Experimental Neurology* **61**, 12-22.

Baumann, N. and Pham-Dinh, D. (2001). Biology of oligodendrocyte and myelin in the mammalian central nervous system. *Physiological Reviews* **81**, 871-927.

Bernier, L., Colman, D. R., and D'Eustachio, P. (1988). Chromosomal locations of genes encoding 2',3' cyclic nucleotide 3'-phosphodiesterase and glial fibrillary acidic protein in the mouse. *Journal of Neuroscience Research* **20**, 497-504.

Bifulco, M., Laezza, C., Stingo, S., and Wolff, J. (2002). 2',3'-Cyclic nucleotide 3'-phosphodiesterase: a membrane-bound, microtubule-associated protein and membrane anchor for tubulin. *Proceedings of the National Academy of Sciences USA* **99**, 1807-1812.

Bizzozero, O. A., Malkoski, S. P., Mobarak, C., Bixler, H. A., and Evans, J. E. (2002). Mass-spectrometric analysis of myelin proteolipids reveals new features of this family of palmitoylated membrane proteins. *Journal of Neurochemistry* **81**, 636-645.

Boggs, J. M. (2006). Myelin basic protein: a multifunctional protein. *Cellular and Molecular Life Sciences* **63**, 1945-1961.

Boiko, T. and Winckler, B. (2007). Myelin under construction-teamwork required. *Journal of Cell Biology* **172**, 799-801.

Boison, D., Büssow, H., D'Urso, D., Müller, H.-W., and Stoffel, W. (1995). Adhesive properties of proteolipid protein are responsible for the compaction of CNS myelin sheaths. *Journal of Neuroscience* **15**, 5502-5513.

Bongarzone, E. R., Campagnoni, C. W., Kampf, K., Jacobs, E., Handley, V. W., Schonmann, V., and Campagnoni, A. T. (1999). Identification of a new exon in the myelin proteolipid protein gene encoding novel protein isoforms that are restricted to the somata of oligodendrocytes and neurons. *Journal of Neuroscience* **19**, 8349-8357.

Bö, L., Quarles, R. H., Fujita, N., Bartoszewicz, Z., Sato, S., and Trapp, B. D. (1995). Endocytic depletion of L-MAG from CNS myelin in quaking mice. *Journal of Cell Biology* **131**, 1811-1820.

Bradl, M., Bauer, J., Inomata, T., Zielasek, J., Nave, K. A., Toyka, K., Lassmann, H., and Wekerle, H. (1999). Transgenic Lewis rats overexpressing the proteolipid protein gene: myelin degeneration and its effect on T cell-mediated experimental autoimmune encephalomyelitis. *Acta Neuropathologica* **97**, 595-606.

Bradl, M., Bauer, J., Flügel, A., Wekerle, H., and Lassmann, H. (2005). Complementary contribution of CD4 and CD8 T lymphocytes to T-cell infiltration of the intact and the degenerative spinal cord. *American Journal of Pathology* **166**, 1441-1450.

Brady, S. T., Witt, A. S., Kirkpatrick, L. L., De Waegh, S. M., Readhead, C., Tu, P. H., and Lee, V. M. Y. (1999). Formation of compact myelin is required for maturation of the axonal cytoskeleton. *Journal of Neuroscience* **19**, 7278-7288.

Braun, P. E., Lee, J., and Gravel, M. (2004). 2',3'-Cyclic nucleotide 3'-phosphodiesterase: structure, biology and function. In "Myelin Biology and Disorders" pp. 499-522. Elsevier (USA).

Bray, G. M., Rasminsky, M., and Aguayo, A. J. (1981). Interactions between axons and their sheath cells. *Annual Review of Neuroscience* **4**, 127-162.

Brownell, E., Lee, A. S., Pekar, S. K., Pravtcheva, D., Ruddle, F. H., and Bayney, R. M. (1991). Glial fibrillary acid protein, an astrocytic-specific marker, maps to human chromosome 17. *Genomics* **10**, 1087-1089.

Burnette, W. N. (1981). "Western blotting": electrophoretic transfer of proteins from sodium dodecyl sulfate--polyacrylamide gels to unmodified nitrocellulose and radiographic detection with antibody and radioiodinated protein A. *Annals of Biochemistry* **112**, 195-203.

Bustin, S. A. (2000). Absolute quantification of mRNA using real-time reverse transcription polymerase chain reaction assays. *Journal of Molecular Endocrinology* **25**, 169-193.

Bustin, S. A. (2002). Quantification of mRNA using real-time reverse transcription PCR (RT-PCR): trends and problems. *Journal of Molecular Endocrinology* **29**, 23-29.

Cahill, L. (2006). Why sex matters for neuroscience. *Nature Reviews Neuroscience* **Advance online publication**.

Campagnoni, A. and Skoff, R. P. (2001). The pathobiology of myelin mutants reveal novel biological functions of the MBP and PLP genes. *Brain Pathology* **11**, 74-91.

Campagnoni, A. T. and Campagnoni, C. W. (2004). Myelin basic protein gene. In "Myelin Biology and Disorders" pp. 387-400. Elsevier (USA).

Campagnoni, C. W., Garbay, B., Micevych, P., Pribyl, T., Kampf, K., Handley, V. W., and Campagnoni, A. T. (1992). DM20 mRNA splice product of the myelin proteolipid protein gene is expressed in the murine heart. *Journal of Neuroscience Research* **33**, 148-155.

Carango, P., Funanage, V. L., Quirós, R. E., Debruyne, C. S., and Marks, H. G. (1995). Overexpression of DM20 messenger RNA in two brothers with Pelizaeus-Merzbacher disease. *Annals of Neurology* **38**, 610-617.

Cerghet, M., Bessert, D. A., Nave, K. A., and Skoff, R. P. (2001). Differential expression of apoptotic markers in *jimpy* and in *Plp* overexpressors: evidence for different apoptotic pathways. *Journal of Neurocytology* **30**, 841-855.

Cerghet, M., Skoff, R. P., Bessert, D., Zhang, Z., Mullins, C., and Ghandour, M. S. (2006). Proliferation and Death of Oligodendrocytes and Myelin Proteins Are Differentially Regulated in Male and Female Rodents. *Journal of Neuroscience* **26**, 1439-1447.

Cervello, M., Giannitrapani, L., La Rosa, M., Notarbartolo, M., Labbozzetta, M., Poma, P., Montalto, G., and D'Alessandro, N. (2004). Induction of apoptosis by the proteasome inhibitor MG132 in human HCC cells: Possible correlation with specific caspase-dependant cleavage of B-catenin and inhibition of B-catenin-mediated transactivation. *International Journal of Molecular Medicine* **13**, 741-748.

Chies, R., Nobbio, L., Edomi, P., Schenone, A., Schneider, C., and Brancolini, C. (2003). Alterations in the Arf6-regulated plasma membrane endosomal recycling pathway in cells overexpressing the tetraspan protein Gas3/PMP22. *Journal of Cell Science* **116**, 987-999.

Chomczynski, P. and Sacchi, N. (1987). Single-step method of RNA isolation by acid guanidinium-thiocyanate-phenol-chloroform extraction. *Annals of Biochemistry* **162**, 156-159.

Ciechanover, A. (2005). Proteolysis: from the lysosome to ubiquitin and the proteasome. *Nature Reviews Molecular Cell Biology* **6**, 79-87.

Coetzee, T., Suzuki, K., Nave, K. A., and Popko, B. (1999). Myelination in the absence of galactolipids and proteolipid proteins. *Molecular and Cellular Neuroscience* **14**, 41-51.

Coman, L., Barbin, G., Charles, P., Zalc, B., and Lubetzki, C. (2005). Axonal signals in central nervous system myelination, demyelination and remyelination. *Journal of the Neurological Sciences* **233**, 67-71.

Cook, J. L., Irias-Donaghey, S., and Deininger, P. L. (1992). Regulation of rodent myelin proteolipid protein gene expression. *Neuroscience Letters* **137**, 56-60.

Danielson, P. E., Forss-Petter, S., Brow, M. A., Calavetta, L., Douglass, J., Milner, R. J., and Sutcliffe, J. G. (1988). p1B15: a cDNA clone of the rat mRNA encoding cyclophilin. *DNA* **7**, 261-267.

de Ferra, F., Engh, H., Hudson, L., Kamholz, J., Puckett, C., Molineaux, S., and Lazzarini, R. A. (1985). Alternative splicing accounts for the four forms of myelin basic protein. *Cell* **43**, 721-727.

Deber, C. M. and Reynolds, S. J. (1991). Central nervous system myelin: Structure, function, and pathology. *Clinical Biochemistry* **24**, 113-134.

Dobretsova, A. and Wight, P. A. (1999). Antisilencing: Myelin proteolipid protein gene expression in oligodendrocytes is regulated via derepression. *Journal of Neurochemistry* **72**, 2227-2237.

Dobretsova, A., Kokorina, N. A., and Wight, P. A. (2004). Potentiation of myelin proteolipid protein (Plp) gene expression is mediated through AP-1-like binding sites. *Journal of Neurochemistry* **90**, 1500-1510.

Dubois-Dalcq, M., Behar, T., Hudson, L. D., and Lazzarini, R. A. (1986). Emergence of three myelin proteins in oligodendrocytes cultured without neurons. *Journal of Cell Biology* **102**, 384-392.

Edgar, J. M., McLaughlin, M., Yool, D., Zhang, S. C., Fowler, J., Montague, P., Barrie, J. A., McCulloch, M. C., Duncan, I. D., Garbern, J., Nave, K.-A., and Griffiths, I. R. (2004). Oligodendroglial modulation of fast axonal transport in a mouse model of hereditary spastic paraplegia. *Journal of Cell Biology* **166**, 121-131.

Edgar, J. M., McLaughlin, M., Barrie, J. A., McCulloch, M. C., Garbern, J., and Griffiths, I. R. (2004). Age-related axonal and myelin changes in the *rumpshaker* mutation of the *Plp* gene. *Acta Neuropathologica (Berlin)* **107**, 331-335.

Edgar, J. M. and Garbern, J. (2004). The myelinated axon is dependent on the myelinating cell for support and maintenance: molecules involved. *Journal of Neuroscience Research* **76**, 593-598.

Eskelinen, E.-L. (2006). Roles of LAMP-1 and LAMP-2 in lysosome biogenesis and autophagy. *Molecular Aspects of Medicine* **27**, 495-502.

- Faivre-Sarrailh, C., Gauthier, F., Denisenko-Nehrbass, N., Le Bivic, A., Rougon, G., and Girault, J. A. (2000). The glycosylphosphatidyl inositol-anchored adhesion molecule F3/contactin is required for surface transport of paranodin/contactin-associated protein (caspr). *Journal of Cell Biology* **149**, 491-501.
- Fanarraga, M. L., Sommer, I., and Griffiths, I. R. (1995). O-2A progenitors of the mouse optic nerve exhibit a developmental pattern of antigen expression different from the rat. *Glia* **15**, 95-104.
- Fernandez, P. A., Tang, D. G., Cheng, L. L., Prochiantz, A., Mudge, A. W., and Raff, M. C. (2000). Evidence that axon-derived neuregulin promotes oligodendrocyte survival in the developing rat optic nerve. *Neuron* **28**, 81-90.
- French-Constant, C., Colognato, H., and Franklin, R. J. M. (2004). Neuroscience: The mysteries of myelin unwrapped. *Science* **304**, 688-689.
- Fitzner, D., Schneider, A., Kippert, A., Mobius, W., Willig, K. I., Hell, S. W., Bunt, G., Gaus, K., and Simons, M. (2006). Myelin basic protein-dependant plasma membrane reorganization in the formation of myelin. *EMBO Journal* **25**, 5037-5048.
- Fujita, N., Kemper, A., Dupree, J., Nakayasu, H., Bartsch, U., Schachner, M., Maeda, N., Suzuki, K., and Popko, B. (1998). The cytoplasmic domain of the large myelin-associated glycoprotein isoform is needed for proper CNS but not peripheral nervous system myelination. *Journal of Neuroscience* **18**, 1970-1978.
- Fujiwara, K. (1994). Mouse hepatitis virus. In "Virus infections of rodents and langomorphs" (A. D. M. E. Osterhaus, Ed.), Vol. 1, pp. 249-257. Elsevier Science BV, Amsterdam.
- Garbern, J., Cambi, F., Shy, M., and Kamholz, J. (1999). The molecular pathogenesis of Pelizaeus-Merzbacher disease. *Archives of Neurology* **56**, 1210-1214.
- Garbern, J., Yool, D. A., Moore, G. J., Wilds, I., Faulk, M., Klugmann, M., Nave, K.-A., Siermans, E. A., van der Knaap, M. S., Bird, T. D., Shy, M. E., Kamholz, J., and Griffiths, I. R. (2002). Patients lacking the major CNS myelin protein, proteolipid protein 1, develop length-dependent axonal degeneration in the absence of demyelination and inflammation. *Brain* **125**, 551-561.
- Gardinier, M. V., Macklin, W. B., Diniak, A. J., and Deininger, P. L. (1986). Characterization of myelin proteolipid mRNAs in normal and jimpy mice. *Molecular and Cellular Biology* **6**, 3755-3762.
- Gardinier, V. and Macklin, W. B. (1990). Developmental expression of the myelin proteolipid protein gene. In "Cellular and Molecular Biology of Myelination." (G. Jeserich, Ed.), pp. 517-532. Springer-Verlag, Berlin.
- Georgious, J., Tropak, M. B., and Roder, J. C. (2004). Myelin-associated glycoprotein gene. In "Myelin Biology and Disorders" pp. 421-467. Elsevier (USA).
- Giacometti, E., Luikenhuis, S., Beard, C. and Jaenisch, R. (2007). Partial rescue of MeCP2 deficiency by postnatal activation of MeCP2. *Proceedings of the National Academy of Sciences (USA)* **104**, 1931-1936.

- Giambonini-Brugnoli, G., Buchstaller, J., Sommer, L., Suter, U., and Mantei, N. (2005). Distinct disease mechanisms in peripheral neuropathies due to altered peripheral myelin protein 22 gene dosage or a Pmp22 point mutation. *Neurobiology of Disease* **18**, 656-668.
- Gielen, E., Baron, W., Vandeven, M., Steels, P., Hoekstra, D., and Ameloot, M. (2006). Rafts in oligodendrocytes: Evidence and structure-function relationship. *Glia* **54**, 499-512.
- Giese, K. P., Martini, R., Lemke, G., Soriano, P., and Schachner, M. (1992). Mouse *P₀* gene disruption leads to hypomyelination, abnormal expression of recognition molecules, and degeneration of myelin and axons. *Cell* **71**, 565-576.
- Gillespie, C. S., Bernier, L., Brophy, P. J., and Colman, D. R. (1990). Biosynthesis of the myelin 2',3'-cyclic nucleotide 3'-phosphodiesterases. *Journal of Neurochemistry* **54**, 656-661.
- Goldbaum, O. and Richter-Landsberg, C. (2004). Proteolytic Stress Causes Heat Shock Protein Induction, Tau Ubiquitination, and the Recruitment of Ubiquitin to Tau-Positive Aggregates in Oligodendrocytes in Culture. *Journal of Neuroscience* **24**, 5748-5757.
- Gow, A. (1997). Redefining the lipophilin family of proteolipid proteins. *Journal of Neuroscience Research* **50**, 659-664.
- Gow, A., Southwood, C. M., and Lazzarini, R. A. (1998). Disrupted proteolipid protein trafficking results in oligodendrocyte apoptosis in an animal model of Pelizaeus-Merzbacher disease. *Journal of Cell Biology* **140**, 925-934.
- Gravel, M., Peterson, J., Yong, V. W., Kottis, V., Trapp, B., and Braun, P. E. (1996). Overexpression of 2',3'-cyclic nucleotide 3'-phosphodiesterase in transgenic mice alters oligodendrocyte development and produces aberrant myelination. *Molecular and Cellular Neuroscience* **7**, 453-466.
- Griffiths, I. R., Scott, I., McCulloch, M. C., Barrie, J. A., McPhilemy, K., and Cattanach, B. M. (1990). Rumpshaker mouse: a new X-linked mutation affecting myelination: evidence for a defect in PLP expression. *Journal of Neurocytology* **19**, 273-283.
- Griffiths, I. R., Montague, P., and Dickinson, P. (1995). The proteolipid protein gene. *Neuropathology and Applied Neurobiology* **21**, 85-96.
- Griffiths, I. R., Dickinson, P., and Montague, P. (1995). Expression of the proteolipid protein gene in glial cells of the post-natal peripheral nervous system of rodents. *Neuropathology and Applied Neurobiology* **21**, 97-110.
- Griffiths, I. R., Klugmann, M., Anderson, T. J., Thomson, C. E., Vouyiouklis, D. A., and Nave, K.-A. (1998). Current concepts of PLP and its role in the nervous system. *Microscopy Research and Technique* **41**, 344-358.
- Griffiths, I. R., Klugmann, M., Anderson, T. J., Yool, D., Thomson, C. E., Schwab, M. H., Schneider, A., Zimmermann, F., McCulloch, M. C., Nadon, N. L., and Nave, K.-A. (1998). Axonal swellings and degeneration in mice lacking the major proteolipid of myelin. *Science* **280**, 1610-1613.
- Guy, J., Gan, J., Selfridge, J., Cobb, S and Bird, A. (2007). Reversal of neurological defects in a mouse model of Rett syndrome. *Science* **315**, 1143-1147.

- Hancock, J. F. (2006). Lipid rafts: contentious only from simplistic standpoints. *Nature Review Molecular Cell Biology* **7**, 456-462.
- Hayes, P. C., Wolf, C. R., and Hayes, J. D. (1989). Blotting techniques for the study of DNA, RNA, and proteins. *British Medical Journal* **299**, 965-968.
- Hirano, A. and Dembitzer, H. M. (1967). A structural analysis of the myelin sheath in the central nervous system. *Journal of Cell Biology* **34**, 555-567.
- Hobson, G. M., Davis, A. P., Stowell, N. C., Kolodny, E. H., Sistermans, E. A., De Coo, I. F. M., Funanage, V. L., and Marks, H. G. (2000). Mutations in noncoding regions of the proteolipid protein gene in Pelizaeus-Merzbacher disease. *Neurology* **55**, 1089-1096.
- Hobson, G. M., Huang, Z., Sperle, K., Stabley, D. L., Marks, H. G., and Cambi, F. (2002). A PLP splicing abnormality is associated with an unusual presentation of PMD. *Annals of Neurology* **52**, 477-488.
- Hobson, G. M., Huang, Z., Sperle, K., Stabley, D. L., Marks, H. G., and Cambi, F. (2002). A PLP splicing abnormality is associated with an unusual presentation of PMD. *Annals of Neurology* **52**, 477-488.
- Hobson, G. M., Huang, Z., Sperle, K., Sistermans, E., Rogan, P. K., Garbern, J. Y., Kolodny, E., Naidu, S., and Cambi, F. (2006). Splice-site contribution in alternative splicing of PLP1 and DM20: molecular studies in oligodendrocytes. *Human Mutation* **27**, 69-77.
- Hu, X. and Worton, R. G. (1992). Partial gene duplication as a cause of human disease. *Human Mutation* **1**, 3-12.
- Hubner, C. A., Senning, A., Orth, U., Zerres, K., Urbach, H., Gal, A., and Rudnik-Schoneborn, S. (2005). Mild Pelizaeus-Merzbacher disease caused by a point mutation affecting correct splicing of *PLP1* mRNA. *Neuroscience* **132**, 697-701.
- Hudson, L. D. (1990). Molecular biology of myelin proteins in the central and peripheral nervous systems. *Seminars in the Neurosciences* **2**, 483-496.
- Hudson, L. D. (2003). Pelizaeus-Merzbacher disease and spastic paraplegia type 2: Two faces of myelin loss from mutations in the same gene. *Journal of Child Neurology* **18**, 616-624.
- Hudson, L. D. (2004). Proteolipid protein gene. In "Myelin Biology and Disorders" pp. 401-420. Elsevier (USA).
- Hudson, L. D., Garbern, J. Y., and Kamholz, J. A. (2004). Pelizaeus-Merzbacher disease. In "Myelin Biology and Disorders" pp. 867-885. Elsevier (USA).
- Huxley, C., Passage, E., Robertson, A. M., Youl, B., Huston, S., Manson, A., Sabéran-Djoniedi, D., Figarella-Branger, D., Pellissier, J. F., Thomas, P. K., and Fontés, M. (1998). Correlation between varying levels of PMP22 expression and the degree of demyelination and reduction in nerve conduction velocity in transgenic mice. *Human Molecular Genetics* **7**, 449-458.
- Inoue, K., Osaka, H., Imaizumi, K., Nezu, A., Takanashi, J., Arii, J., Murayama, K., Ono, J., Kikawa, Y., Mito, T., Shaffer, L. G., and Lupski, J. R. (1999). Proteolipid protein gene

duplications causing Pelizaeus-Merzbacher disease: Molecular mechanism and phenotypic manifestations. *Annals of Neurology* **45**, 624-632.

Inoue, K. (2005). *PLP1*-related inherited dysmyelinating disorders: Pelizaeus-Merzbacher disease and spastic paraplegia type 2. *Neurogenetics*. **6**, 1-16.

Ip, C. W., Kroner, A., Bendszus, M., Leder, C., Kobsar, I., Fischer, S., Wiendl, H., Nave, K.-A., and Martini, R. (2006). Immune cells contribute to myelin degeneration and axonopathic changes in mice overexpressing proteolipid protein in oligodendrocytes. *The Journal of Neuroscience* **26**, 8206-8216.

Ip, C.W., Kroner, A., Crocker, P.R., Nave, K.-A. and Martini, R. (2007). Sialoadhesion deficiency ameliorates myelin degeneration and axonopathic changes in the CNS of PLP overexpressing mice. *Neurobiology of Disease* **25**, 105-111.

Ishibashi, T., Dakin, K. A., Stevens, B., Lee, P. R., Kozlov, S. V., Stewart, C. L., and Fields, R. D. (2006). Astrocytes promote myelination in response to electrical impulses. *Neuron* **49**, 823-832.

Ishibashi, T., Dakin, K. A., Stevens, B., Lee, P. R., Kozlov, S. V., Stewart, C. L., and Fields, R. D. (2006). Astrocytes promote myelination in response to electrical impulses. *Neuron* **49**, 823-832.

Jacobs, E. C. (2005). Genetic alterations in the mouse myelin basic proteins result in a range of dysmyelinating disorders. *Journal of the Neurological Sciences* **228**, 195-197.

Jessen, K. R. (2004). Glial cells. *International Journal of Biochemistry and Cell Biology* **36**, 1861-1867.

Johnson, R. S., Roder, J. C., and Riordan, J. R. (1995). Over-expression of the DM-20 myelin proteolipid causes central nervous system demyelination in transgenic mice. *Journal of Neurochemistry* **64**, 967-976.

Jung-Testas, I., Schumacher, M., Robel, P., and Baulieu, E. E. (1994). Actions of steroid hormones and growth factors on glial cells of the central and peripheral nervous system. *Journal of Steroid Biochemistry and Molecular Biology* **48**, 145-154.

Jung, M., Sommer, I., Schachner, M., and Nave, K.-A. (1996). Monoclonal antibody O10 defines a conformationally sensitive cell-surface epitope of proteolipid protein (PLP): evidence that PLP misfolding underlies dysmyelination in mutant mice. *Journal of Neuroscience* **16**, 7920-7929.

Kagawa, T., Ikenaka, K., Inoue, Y., Kuriyama, S., Tsujii, T., Nakao, J., Nakajima, K., Aruga, J., Okano, H., and Mikoshiba, K. (1994). Glial cell degeneration and hypomyelination caused by overexpression of myelin proteolipid protein gene. *Neuron* **13**, 427-442.

Kamholz, J., de Ferra, F., Puckett, C., and Lazzarini, R. (1986). Identification of three forms of human myelin basic protein by cDNA cloning. *Proceedings of the National Academy of Sciences USA* **83**, 4962-4966.

Karim, S. A., Barrie, J. A., McCulloch, M. C., Montague, P., Edgar, J. M., Kirkham, D., Anderson, T. J., Nave, K.-A., Griffiths, I. R., and McLaughlin, M. (2007). PLP overexpression perturbs myelin protein composition and myelination in a mouse model of Pelizaeus-Merzbacher disease. *Glia* **55**, 341-351.

- Kimura, M., Inoko, H., Katsuki, M., Ando, A., Sato, T., Hirose, T., Takashima, H., Inayama, S., Okano, H., Takamatsu, K., and . (1985). Molecular genetic analysis of myelin-deficient mice: shiverer mutant mice show deletion in gene(s) coding for myelin basic protein. *Journal of Neurochemistry* **44**, 692-696.
- Kimura, M., Sato, M., Akatsuka, A., Saito, S., Ando, K., Yokoyama, M., and Katsuki, M. (1998). Overexpression of a minor component of myelin basic protein isoform (17.2 kDa) can restore myelinogenesis in transgenic *shiverer* mice. *Brain Research* **785**, 245-252.
- Kirmani, B. F., Jacobowitz, D. M., Kallaral, A. T., and Namboodiri, M. A. A. (2002). Aspartoacylase is restricted primarily to myelin synthesizing cells in the CNS: therapeutic implications for Canavan disease. *Molecular Brain Research* **107**, 176-182.
- Kirmani, B. F., Jacobowitz, D. M., and Namboodiri, M. A. A. (2003). Developmental increase of aspartoacylase in oligodendrocytes parallels CNS myelination. *Brain Research Developmental Brain Research* **140**, 105-115.
- Kitagawa, K., Sinoway, M. P., Yang, C., Gould, R. M., and Colman, D. R. (1993). A proteolipid protein gene family: Expression in sharks and rays and possible evolution from an ancestral gene encoding a pore-forming polypeptide. *Neuron* **11**, 433-448.
- Klugmann, M., Schwab, M. H., Pühlhofer, A., Schneider, A., Zimmermann, F., Griffiths, I. R., and Nave, K.-A. (1997). Assembly of CNS myelin in the absence of proteolipid protein. *Neuron* **18**, 59-70.
- Klugmann, M., Schwab, M. H., Jung, M., Pühlhofer, A., Schneider, A., Zimmermann, F., Griffiths, I. R., and Nave, K.-A. (1997). Mutations of the X-linked proteolipid protein gene: molecular mechanisms of dysmyelination. In "Cell Biology and Pathology of Myelin: Evolving Biological Concepts and Therapeutic Approaches" (R. M. Devon, J. R. Doucette, B. H. J. Juurlink, D. J. Schreyer, and V. M. K. Verge, Eds.), Plenum Press, New York.
- Kobayashi, H., Hoffman, E. P., and Marks, H. G. (1994). The *rumpshaker* mutation in spastic paraplegia. *Nature Genetics* **7**, 351-352.
- Koeppen, A. H. and Robitaille, Y. (2002). Pelizaeus-Merzbacher disease. *Journal of Neuropathology and Experimental Neurology* **61**, 747-759.
- Koeppen, A. H. (2005). A brief history of Pelizaeus-Merzbacher disease and proteolipid protein. *Journal of the Neurological Sciences* **228**, 198-200.
- Komoly, S., Hudson, L. D., Webster, H. D., and Bondy, C. A. (1992). Insulin-like growth factor I gene expression is induced in astrocytes during experimental demyelination. *Proceedings of the National Academy of Sciences USA* **89**, 1894-1898.
- Kramer-Albers, E.-M., Gehrig-Burger, K., Thiele, C., Trotter, J., and Nave, K.-A. (2006). Perturbed interactions of mutant proteolipid protein/DM20 with cholesterol and lipid rafts in oligodendroglia: implications for dysmyelination in spastic paraplegia. *Journal of Neuroscience* **26**, 11743-11752.
- Krämer, E. M., Schardt, A., and Nave, K. A. (2001). Membrane traffic in myelinating oligodendrocytes. *Microscopy Research and Technique* **52**, 656-671.

Lai, C., Watson, J. B., Bloom, F. E., Sutcliffe, J. G., and Milner, R. J. (1987). Neural protein 1 B236/myelin-associated glycoprotein (MAG) defines a subgroup of the immunoglobulin superfamily. *Immunological Reviews* **100**, 129-151.

Lappe-Siefke, C., Goebbels, S., Gravel, M., Nicksch, E., Lee, J., Braun, P. E., Griffiths, I. R., and Nave, K.-A. (2003). Disruption of the *CNP* gene uncouples oligodendroglial functions in axonal support and myelination. *Nature Genetics* **33**, 366-374.

Le Bras, B., Chatzopoulos, E., Heydon, K., Martinez, S., Ikenaka, K., Prestoz, L., Spassky, N., Zalc, B., and Thomas, J.-L. (2005). Oligodendrocyte development in the embryonic brain: the contribution of the *plp* lineage. *International Journal of Developmental Biology* **49**, 209-220.

Lee, A. G. (2001). Myelin: Delivery by raft. *Current Biology* **11**, R60-R62.

Lee, A. H., Iwakoshi, N. N., and Glimcher, L. H. (2003). XBP-1 regulates a subset of endoplasmic reticulum resident chaperone genes in the unfolded protein response. *Molecular Cell Biology* **23**, 7448-7459.

Lee, D. H. and Goldberg, A. L. (1998). Proteasome inhibitors: valuable new tools for cell biologists. *Trends in Cell Biology* **8**, 397-403.

Lee, J., Gravel, M., Zhang, R., Thibault, P., and Braun, P. E. (2005). Process outgrowth in oligodendrocytes is mediated by CNP, a novel microtubule assembly myelin protein. *Journal of Cell Biology* **170**, 661-673.

Lee, J. A., Madrid, R. E., Sperle, K., Ritterson, C. M., Hobson, G. M., Garbern, J., Lupski, J. R., and Inoue, K. (2006a). Spastic paraplegia type 2 associated with axonal neuropathy and apparent *PLP1* position effect. *Annals of Neurology* **59**, 398-403.

Lee, J. A., Inoue, K., Cheung, S.W., Shaw, C.A., Stankiewicz, P and Lupski, J. R. (2006b). Role of genomic architecture in *PLP1* duplication causing Pelizaeus-Merzbacher disease. *Human Molecular Genetics* **15**, 2250-2265.

Lemke, G. (1986). Molecular biology of the major myelin genes. *Trends in Neurosciences* **9**, 266-270.

Lemke, G. (1988). Unwrapping the genes of myelin. *Neuron* **1**, 535-543.

Lemke, G. (1993). The molecular genetics of myelination: An update. *Glia* **7**, 263-271.

Lerner, P., Campagnoni, A. T., and Sampugna, J. (1972). Proteolipids in the developing brains of normal mice and myelin deficient mutants. *Journal of Neurochemistry* **22**, 163-170.

Leske, D. A., Jianmin, W., Fautsch, M. P., Karger, R. A., Berdahl, J. P., Lanier, W. L., and Holmes, J. M. (2004). The role of VEGF and IGF-1 in a hypercarbic oxygen-induced retinopathy rat model of ROP. *Molecular Vision*.

Li, S. Y., Dobretsova, A., Kokorina, N. A., and Wight, P. A. (2002a). Repression of myelin proteolipid protein gene expression is mediated through both general and cell type-specific negative regulatory elements in nonexpressing cells. *Journal of Neurochemistry* **82**, 159-171.

Li, S. Y., Moore, C. L., Dobretsova, A., and Wight, P. A. (2002b). Myelin proteolipid protein (*Plp*) intron 1 DNA is required to temporally regulate *Plp* gene expression in the brain. *Journal of Neurochemistry* **83**, 193-201.

Li, W.-W., Penderis, J., Zhao, C., Schumacher, M., and Franklin, R. J. M. (2006). Females remyelinate more efficiently than males following demyelination in the aged but not young adult CNS. *Experimental Neurology* **202**, 250-254.

Lie, Y. S. and Petropoulos, C. J. (1998). Advances in quantitative PCR technology: 5' nuclease assays. *Current Opinion in Biotechnology* **9**, 43-48.

Liedtke, W., Edelmann, W., Bieri, P. L., Chiu, F. C., Cowan, N. J., Kucherlapati, R., and Raine, C. S. (1996). GFAP is necessary for the integrity of CNS white matter architecture and long-term maintenance of myelination. *Neuron* **17**, 607-615.

Lipton, H. L., Rozhon, E. J., and Bandyopadhyay, P. (1994). Picornavirus infections. In "Virus infections of rodents and langomorphs" (A. D. M. E. Osterhaus, Ed.), Vol. 1, pp. 373-385. Elsevier Science BV, Amsterdam.

Ludi, G. A. and Pace, N. P. (1979). The use of Ripampicin to evaluate tRNA transcriptional organisation in *Escherichia coli*. *Nucleic Acids Research* **6**, 1269-1286.

Macklin, W. B., Weill, C. L., and Deininger, P. L. (1986). Expression of myelin proteolipid and basic protein mRNAs in cultured cells. *Journal of Neuroscience Research* **16**, 203-217.

Macklin, W. B., Campagnoni, A. T., Deininger, P. L., and Gardinier, M. V. (1987). Structure and expression of the mouse proteolipid protein gene. *Journal of Neuroscience Research* **18**, 383-394.

Madhavarao, C. N., Moffett, J. R., Moore, R. A., Viola, R. E., Namboodiri, M. A. A., and Jacobowitz, D. M. (2004). Immunohistochemical localization of asparoylase in the rat central nervous system. *Journal of Comparative Neurology* **472**, 318-329.

Mallon, B. S. and Macklin, W. B. (2002). Overexpression of the 3'-untranslated region of myelin proteolipid protein mRNA leads to reduced expression of endogenous proteolipid mRNA. *Neurochemical Research* **27**, 1349-1360.

Marciniak, S. J., Yun, C. Y., Oyadomari, S., Novoa, I., Zhang, Y. H., Jungreis, R., Nagata, K., Harding, H. P., and Ron, D. (2004). CHOP induces death by promoting protein synthesis and oxidation in the stressed endoplasmic reticulum. *Genes and Development* **18**, 3066-3077.

Martini, R. and Schachner, M. (1997). Molecular bases of myelin formation as revealed by investigations on mice deficient in glial cell surface molecules. *Glia* **19**, 298-310.

Mastronardi, F. G., Ackerley, C. A., Arsenault, L., Roots, B. I., and Moscarello, M. A. (1993). Demyelination in a transgenic mouse: A model for multiple sclerosis. *Journal of Neuroscience Research* **36**, 315-324.

Maxfield, F. R. and Tabas, I. (2005). Role of cholesterol and lipid organization in disease. *Nature* **438**, 612-621.

- McLaughlin, M., Barrie, J. A., Karim, S. A., Montague, P., Edgar, J. M., Kirkham, D., Thomson, C. E., and Griffiths, I. R. (2006). Processing of PLP in a model of Pelizaeus-Merzbacher disease/SPG2 due to the *rumpshaker* mutation. *Glia* **53**, 715-722.
- McLaughlin, M., Karim, S. A., Montague, P., Barrie, J. A., Kirkham, D., Griffiths, I. R., and Edgar, J. M. (2007). Genetic background influences UPR but not PLP processing in the *rumpshaker* model of PMD/SPG2. *Neurochemical Research* **32**, 167-176.
- McPhilemy, K., Mitchell, L. S., Griffiths, I. R., Morrison, S., Deary, A. W., Sommer, I., and Kennedy, P. G. E. (1990). Effect of optic nerve transection upon myelin protein gene expression by oligodendrocytes: evidence for axonal influences on gene expression. *Journal of Neurocytology* **19**, 494-503.
- Meusser, B., Hirsch, C., Jarosch, E., and Sommer, T. (2005). ERAD: the long road to destruction. *Nature Cell Biology* **7**, 766-772.
- Michailov, G. V., Sereda, M. W., Brinkmann, B. G., Fischer, T. M., Haug, B., Birchmeier, C., Role, L., Lai, C., Schwab, M. H., and Nave, K. A. (2004). Axonal Neuregulin-1 Regulates Myelin Sheath Thickness. *Science* **304**, 700-703.
- Milner, R. J., Lai, C., Nave, K.-A., Lenoir, D., Ogata, J., and Sutcliffe, J. G. (1985). Nucleotide sequence of two mRNAs for rat brain myelin proteolipid protein. *Cell* **42**, 931-939.
- Mimault, C., Giraud, G., Courtois, V., Cailloux, F., Boire, J. Y., Dastugue, B., Boespflug-Tanguy, O., and Clin Eur Network Brain Dysmyelinating (1999). Proteolipoprotein gene analysis in 82 patients with sporadic Pelizaeus-Merzbacher disease: Duplications, the major cause of the disease, originate more frequently in male germ cells, but point mutations do not. *American Journal of Human Genetics* **65**, 360-369.
- Miura, M., Tamura, T., and Mikoshiba, K. (1990). Cell-specific expression of the mouse glial fibrillary acidic protein gene: identification of the *cis*- and *trans*-acting promoter elements for astrocyte-specific expression. *Journal of Neurochemistry* **55**, 1180-1188.
- Montague, P., Dickinson, P. J., McCallion, A. S., Stewart, G. J., Savioz, A., Davies, R. W., Kennedy, P. G. E., and Griffiths, I. R. (1997). Developmental expression of the murine *Mobp* gene. *Journal of Neuroscience Research* **49**, 133-143.
- Montague, P., Barrie, J. A., Thomson, C. E., Kirkham, D., McCallion, A. S., Davies, R. W., Kennedy, P. G. E., and Griffiths, I. R. (1998). Cytoskeletal and nuclear localization of MOBP polypeptides. *European Journal of Neuroscience* **10**, 1321-1328.
- Montague, P., McCallion, A. S., Davies, R. W., and Griffiths, I. R. (2006). MOBP: a family of abundant CNS myelin proteins in search of a function. *Developmental Neuroscience* **28**, 479-487.
- Morell, P. and Norton, W. T. (1980). Myelin. *Scientific American* **242**, 74-89.
- Muncke, N., Wogatzky, B. S., Siermans, E. A., Endris, V., Ross, M., Vetrie, D., Catsman-Berrevoets, C. E., Rappold, G. (2006). Position effect on *PLP1* may cause a subset of Pelizaeus-Merzbacher disease symptoms. *Journal of Medical Genetics* **41**, e121.
- Nadon, N. L., Arnheiter, H., and Hudson, L. D. (1994). A combination of PLP and DM20 transgenes promotes partial myelination in the jimpy mouse. *Journal of Neurochemistry* **63**, 822-833.

- Nadon, N. L., Miller, S., Draeger, K., and Salvaggio, M. (1997). Myelin proteolipid DM20: Evidence for function independent of myelination. *International Journal of Developmental Neuroscience* **15**, 285-293.
- Nandi, D., Tahiliani, P., Kumar, A., and Chandu, D. (2006). The ubiquitin-proteasome system. *Journal of Bioscience* **31**, 137-155.
- Nave, K.-A. and Griffiths, I. R. (2004). Models of Pelizaeus-Merzbacher disease. In "Myelin Biology and Disorders" pp. 1125-1142. Elseviers (USA).
- Nave, K.-A., Lai, C., Bloom, F. E., and Milner, R. J. (1987). Splice site selection in the proteolipid protein (PLP) gene transcript and primary structure of the DM-20 protein of central nervous system myelin. *Proceedings of the National Academy of Sciences USA* **84**, 5665-5669.
- Niemann, S., Sereda, M. W., Suter, U., Griffiths, I. R., and Nave, K. A. (2000). Uncoupling of myelin assembly and Schwann cell differentiation by transgenic overexpression of peripheral myelin protein 22. *Journal of Neuroscience* **20**, 4120-4128.
- Norton, W. T. and Poduslo, S. E. (1973). Myelination in the rat brain: method of myelin isolation. *Journal of Neurochemistry* **21**, 749-757.
- Nussbaum, J. L. and Roussel, G. (1983). Immunocytochemical demonstration of the transport of myelin proteolipids through the Golgi apparatus. *Cell and Tissue Research* **234**, 547-559.
- Perry, V. H. (1994). Functions of microglia. In "Macrophages and the nervous system" (V. H. Perry, Ed.), pp. 44-52. R.G. Landes, Austin.
- Pfeiffer, S. E., Warrington, A. E., and Bansal, R. (1993). The oligodendrocyte and its many cellular processes. *Trends in Cell Biology* **3**, 191-197.
- Poltorak, M., Sadoul, R., Keilhauer, G., Landa, C., Fahrig, T., and Schachner, M. (1987). Myelin-associated glycoprotein, a member of the L2/HNK-1 family of neural cell adhesion molecules, is involved in neuron-oligodendrocyte and oligodendrocyte-oligodendrocyte interaction. *Journal of Cell Biology* **105**, 1893-1899.
- Popko, B., Puckett, C., and Hood, L. (1988). A novel mutation in myelin-deficient mice results in unstable myelin basic protein gene transcripts. *Neuron* **1**, 221-225.
- Pribyl, T. M., Campagnoni, C. W., Kampf, K., Kashima, T., Handley, V. W., McMahon, J., and Campagnoni, A. T. (1996). Expression of the myelin proteolipid protein gene in the human fetal thymus. *Journal of Neuroimmunology* **67**, 125-130.
- Puckett, C., Hudson, L. D., Ono, K., Benecke, J., Dubois-Dalcq, M., and Lazzarini, R. A. (1987). Myelin-specific proteolipid protein is expressed in myelinating Schwann cells but is not incorporated into myelin sheaths. *Journal of Neuroscience Research* **18**, 511-518.
- Rajendran, L. and Simons, K. (2005). Lipid rafts and membrane dynamics. *Journal of Cell Science* **118**, 1099-1102.
- Rasband, M. N. (2006). Neuron-glia interactions at the node of Ranvier. *Results and Problems in Cell Differentiation* **43**, 129-149.

- Readhead, C., Popko, B., Takahashi, N., Shine, H. D., Saavedra, R. A., Sidman, R. L. and Hood, L. (1987). Expression of a myelin basic protein gene in transgenic shiverer mice: correction of the dysmyelinating phenotype. *Cell* **48**, 703-712.
- Readhead, C., Schneider, A., Griffiths, I. R., and Nave, K.-A. (1994). Premature arrest of myelin formation in transgenic mice with increased proteolipid protein gene dosage. *Neuron* **12**, 583-595.
- Regis, S., Grossi, S., Lualdi, S., Biancheri, R., and Filocamo, M. (2005). Diagnosis of Pelizaeus-Merzbacher disease: detection of proteolipid protein gene copy number by real-time PCR. *Neurogenetics* **6**, 73-78.
- Richardson, W. D., Kessaris, N., and Pringle, N. (2006). Oligodendrocyte wars. *Nature Reviews Neuroscience* **7**, 11-18.
- Rios, J. C., Melandez-Vasquez, C. V., Einheber, S., Lustig, M., Grumet, M., Hemperly, J., Peles, E., and Salzer, J. L. (2000). Contactin-associated protein (Caspr) and contactin form a complex that is targeted to the paranodal junctions during myelination. *Journal of Neuroscience* **20**, 8354-8364.
- Roach, A., Takahashi, N., Pravtcheva, D., Ruddle, F., and Hood, L. (1985). Chromosomal mapping of mouse myelin basic protein gene and structure and transcription of the partially deleted gene in shiverer mutant mice. *Cell* **42**, 149-155.
- Rogister, B., Ben Hur, T., and Dubois-Dalcq, M. (1999). From neural stem cells to myelinating oligodendrocytes. *Molecular and Cellular Neuroscience* **14**, 287-300.
- Rosenbluth, J., Nave, K.-A., Mierzwa, A., and Schiff, R. (2006). Subtle myelin defects in Plp-null mice. *Glia* **54**, 172-182.
- Saher, G., Brugger, B., Lappe-Siefke, C., Mobius, W., Tozawa, R., Wehr, M. C., Wieland, F., Ishibashi, S., and Nave, K. A. (2005). High cholesterol level is essential for myelin membrane growth. *Nature Neuroscience* **8**, 468-475.
- Schafer, D. P., and Rasband, M. N. (2006). Glial regulation of the axonal membrane at nodes of Ranvier. *Current Opinions in Neurobiology* **16**, 508-514.
- Scherer, S. S., Vogelbacker, H. H., and Kamholz, J. (1992). Axons modulate the expression of proteolipid protein in the CNS. *Journal of Neuroscience Research* **32**, 138-148.
- Schneider, A., Lander, H., Schulz, G., Wolburg, H., Nave, K. A., Schulz, J. B., and Simons, M. (2005). Palmitoylation is a sorting determinant for transport to the myelin membrane. *Journal of Cell Science* **118**, 2415-2423.
- Schweitzer, J., Becker, T., Schachner, M., Nave, K. A., and Werner, H. (2006). Evolution of myelin proteolipid proteins: gene duplication in teleosts and expression pattern divergence. *Molecular and Cellular Neuroscience* **31**, 161-177.
- Sereda, M., Griffiths, I. R., Pühlhofer, A., Stewart, H., Rossner, M. J., Zimmermann, F., Magyar, J. P., Schneider, A., Hund, E., Meinck, H. M., Suter, U., and Nave, K.-A. (1996). A transgenic rat model of Charcot-Marie-Tooth disease. *Neuron* **16**, 1049-1060.
- Shang, J. (2005). Quantitative measurement of events in the mammalian unfolded protein response. *Methods* **35**, 390-394.

Sherman, D. L. and Brophy, P. J. (2005). Mechanisms of axon ensheathment and myelin growth. *Nature Reviews Neuroscience* **6**, 683-690.

Sherman, D. L., Tait, S., Melrose, S., Johnson, R., Zonta, B., Court, F., Macklin, W. B., Meek, S., Smith, A. J. H., Cottrell, D. F., and Brophy, P. J. (2005). Neurofascins Are Required to Establish Axonal Domains for Saltatory Conduction. *Neuron* **48**, 737-742.

Shine, H. D., Readhead, C., Popko, B., Hood, L., and Sidman, R. L. (1992). Morphometric analysis of normal, mutant and transgenic CNS: correlation of myelin basic protein expression to myelinogenesis. *Journal of Neurochemistry* **58**, 342-349.

Simons, M., Krämer, E. M., Thiele, C., Stoffel, W., and Trotter, J. (2000). Assembly of myelin by association of proteolipid protein with cholesterol- and galactosylceramide-rich membrane domains. *Journal of Cell Biology* **151**, 143-153.

Simons, M., Krämer, E. M., Macchi, P., Rathke-Hartlieb, S., Trotter, J., Nave, K.-A., and Schulz, J. B. (2002). Overexpression of the myelin proteolipid protein leads to accumulation of cholesterol and proteolipid protein in endosomes/lysosomes: implications for Pelizaeus-Merzbacher disease. *Journal of Cell Biology* **157**, 327-336.

Sistermans, E. A., De Wijs, I. J., De Coo, R. F. M., Smit, L. M. E., Menko, F. H., and Van Oost, B. A. (1996). A (G-to-A) mutation in the initiation codon of the proteolipid protein gene causing a relatively mild form of Pelizaeus- Merzbacher disease in a Dutch family. *Human Genetics* **97**, 337-339.

Sistermans, E. A., De Coo, R. F., De Wijs, I. J., and Van Oost, B. A. (1998). Duplication of the proteolipid protein gene is the major cause of Pelizaeus-Merzbacher disease. *Neurology* **50**, 1749-1754.

Sommer, I., Lagenaur, C., and Schachner, M. Stage specific antigens O5 to O11 on oligodendrocyte cell surfaces detected by monoclonal antibodies. Society for Neuroscience Abstracts **8**, 246. 1982.

Southern, E. M. (1975). Detection of specific sequences among DNA fragments separated by gel electrophoresis. *Journal of Molecular Biology* **98**, 517.

Southwood, C. M., Garbern, J., Jiang, W., and Gow, A. (2002). The unfolded protein response modulates disease severity in Pelizaeus- Merzbacher disease. *Neuron* **36**, 585-596.

Spassky, N., Olivier, C., Perez-Villegas, E., Goujet-Zalc, C., Martinez, S., Thomas, J. L., and Zalc, B. (2000). Single or multiple oligodendroglial lineages: A controversy. *Glia* **29**, 143-148.

Stevens, B., Porta, S., Haak, L. L., Gallo, V., and Fields, R. D. (2002). Adenosine: A neuron-glia transmitter promoting myelination in the CNS in response to action potentials. *Neuron* **36**, 855-868.

Streit, W. J., Mrak, R. E., and Griffin, W. S. T. (2004). Microglia and neuroinflammation: a pathological perspective. *Journal of Neuroinflammation* **1**, 14.

Sutcliffe, J. G. (1987). The genes for myelin. *Trends in Genetics* **3**, 73-76.

Takahashi, N., Roach, A., Teplow, D. B., Prusiner, S. B., and Hood, L. (1985). Cloning and characterization of the myelin basic protein gene from mouse: one gene can encode both 14kd and 18.5kd MBPs by alternate use of exons. *Cell* **42**, 139-148.

Taylor, C. M., Marta, C., Bansal, R., and Pfeiffer, S. E. (2004). The transport, assembly, and function of myelin lipids. In "Myelin Biology and Disorders" pp. 57-88. Elsevier (USA).

Thomson, C. E., Vouyiouklis, D. A., Barrie, J. A., Wease, K. N., and Montague, P. (2005). *Plp1* gene regulation in the developing murine optic nerve: correlation with oligodendroglial process alignment along the axons. *Developmental Neuroscience* **27**, 27-36.

Thomson, C. E., Hunter, A. M., Griffiths, I. R., Edgar, J. M., and McCulloch, M. C. (2007). Murine spinal cord explants: A model for evaluating axonal growth and myelination in vitro. *Journal of Neuroscience Research* **84**, 1703-1715.

Trajkovic, K., Dhaunchak, A. S., Goncalves, J. T., Wenzel, D., Schneider, A., Bunt, G., Nave, K. A., and Simons, M. (2006). Neuron to glia signaling triggers myelin membrane exocytosis from endosomal storage sites. *Journal of Cell Biology* **172**, 937-948.

Trapp, B. D., Itoyama, Y., Sternberger, N. H., Quarles, R. H., and Webster, H. d. (1981). Immunocytochemical localization of Po protein in Golgi complex membranes and myelin of developing rat Schwann cells. *Journal of Cell Biology* **90**, 1-6.

Trapp, B. D. and Quarles, R. H. (1984). Immunocytochemical localization of the myelin-associated glycoprotein. Fact or artifact? *Journal of Neuroimmunology* **6**, 231-249.

Trapp, B. D. (1988). Distribution of the myelin-associated glycoprotein and Po protein during myelin compaction in Quaking mouse peripheral nerve. *Journal of Cell Biology* **107**, 675-685.

Trapp, B. D., Andrews, S. B., Wong, A., O'Connell, M., and Griffin, J. W. (1989). Co-localization of the myelin-associated glycoprotein and the microfilament components F-actin and spectrin in Schwann cells of myelinated nerve fibres. *Journal of Neurocytology* **18**, 47-60.

Trapp, B. D., Nishiyama, A., Cheng, D., and Macklin, E. (1997). Differentiation and death of premyelinating oligodendrocytes in developing rodent brain. *Journal of Cell Biology* **137**, 459-468.

Trapp, B. D., Pfeiffer, S. E., Anitei, M., and Kidd, G. J. (2004). Cell biology of myelin assembly. In "Myelin Biology and Disorders" pp. 29-55. Elsevier (USA).

Volterra, A. and Meldolesi, J. (2005). Astrocytes, from brain glue to communication elements: the revolution continues. *Nature Reviews Neuroscience* **6**, 626-640.

von Mikecz, A. (2006). The nuclear ubiquitin-proteasome system. *Journal of Cell Biology* **119**, 1977-1984.

Vouyiouklis, D. A., Barrie, J. A., Griffiths, I. R., and Thomson, C. E. (2000). A proteolipid protein-specific pre-mRNA (*Ppm-1*) contains intron 3 and is upregulated during myelination in the CNS. *Journal of Neurochemistry* **74**, 940-948.

- Vouyiouklis, D. A. (2004). Nervous system myelination: insights from recent experimental findings. *Recent Research Developments in Neurochemistry* **6**, 173-185.
- Wahle, S. and Stoffel, W. (1998). Cotranslational integration of myelin proteolipid protein (PLP) into the membrane of endoplasmic reticulum: Analysis of topology by glycosylation scanning and protease domain protection assay. *Glia* **24**, 226-235.
- Weimbs, T. and Stoffel, W. (1992). Proteolipid protein (PLP) of CNS myelin: Positions of free, disulfide-bonded, and fatty acid thioester-linked cysteine residues and implications for the membrane topology of PLP. *Biochemistry* **31**, 12289-12296.
- Wight, P. A., Dobretsova, A., and Macklin, W. B. (1997). Regulation of murine myelin proteolipid protein gene expression. *Journal of Neuroscience Research* **50**, 917-927.
- Wight, P. A. and Dobretsova, A. (2004). Where, when and how much: regulation of myelin proteolipid protein gene expression. *Cellular Molecular Life Science* **61**, 810-821.
- Wolf, N. I., Sistermans, E. A., Cundall, M., Hobson, G. M., Davis-Williams, A. P., Palmer, R., Stubbs, P., Davies, S., Endziniene, M., Wu, Y., Chong, W. K., Malcolm, S., Surtees, R., Garbern, J. Y., and Woodward, K. J. (2005). Three or more copies of the proteolipid protein gene PLP1 cause severe Pelizaeus-Merzbacher disease. *Brain* **128**, 743-751.
- Woodward, K., Kendall, E., Vetrie, D., and Malcolm, S. (1998). Pelizaeus-Merzbacher disease: Identification of Xq22 proteolipid-protein duplications and characterization of breakpoints by interphase FISH. *American Journal of Human Genetics* **63**, 207-217.
- Woodward, K. and Malcolm, S. (1999). Proteolipid protein gene - Pelizaeus-Merzbacher disease in humans and neurodegeneration in mice. *Trends in Genetics* **15**, 125-128.
- Woodward, K., Kirtland, K., Dlouhy, S., Raskind, W., Bird, T., Malcolm, S., and Abeliovich, D. (2000). X inactivation phenotype in carriers of Pelizaeus-Merzbacher disease: skewed in carriers of a duplication and random in carriers of point mutations. *European Journal of Human Genetics* **8**, 449-454.
- Wrabetz, L., Feltri, M. L., Quattrini, A., Imperiale, D., Previtali, S., D'Antonio, M., Martini, R., Yin, X. H., Trapp, B. D., Zhou, L., Chiu, S. Y., and Messing, A. (2000). P₀ glycoprotein overexpression causes congenital hypomyelination of peripheral nerves. *Journal of Cell Biology* **148**, 1021-1033.
- Yamada, M., Ivanova, A., Yamaguchi, Y., Lees, M. B., and Ikenaka, K. (1999). Proteolipid protein gene product can be secreted and exhibit biological activity during early development. *Journal of Neuroscience* **19**, 2143-2151.
- Yamamoto, Y., Mizuno, R., Nishimura, T., Ogawa, Y., Yoshikawa, H., Fujimura, H., Adachi, E., Kishimoto, T., Yanagihara, T., and Sakoda, S. (1994). Cloning and expression of myelin-associated oligodendrocytic basic protein. A novel basic protein constituting the central nervous system myelin. *Journal of Biological Chemistry* **269**, 31725-31730.
- Yamamoto, Y., Yoshikawa, H., Nagano, S., Kondoh, G., Sadahiro, S., Gotow, T., Yanagihara, T., and Sakoda, S. (1999). Myelin-associated oligodendrocytic basic protein is essential for normal arrangement of the radial component in central nervous system myelin. *European Journal of Neuroscience* **11**, 847-855.

Yamamura, T., Konola, J. T., Wekerle, H., and Lees, M. B. (1991). Monoclonal antibodies against myelin proteolipid protein: Identification and characterization of two major determinants. *Journal of Neurochemistry* **57**, 1671-1680.

Yan, Y., Lagenaur, C., and Narayanan, V. (1993). Molecular cloning of M6: Identification of a PLP/DM20 gene family. *Neuron* **11**, 423-431.

Yin, X., Kidd, G. J., Wrabetz, L., Feltri, M. L., Messing, A., and Trapp, B. D. (2000). Schwann cell myelination requires timely and precise targeting of P₀ protein. *Journal of Cell Biology* **148**, 1009-1020.

Yin, X., Baek, R. C., Kirschner, D. A., Peterson, A., Fujii, Y., Nave, K. A., Macklin, W. B., and Trapp, B. D. (2006). Evolution of a neuroprotective function of central nervous system myelin. *Journal of Cell Biology* **172**, 469-478.

Yin, X. H., Crawford, T. O., Griffin, J. W., Tu, P. H., Lee, V. M., Li, C. M., Roder, J., and Trapp, B. D. (1998). Myelin-associated glycoprotein is a myelin signal that modulates the caliber of myelinated axons. *Journal of Neuroscience* **18**, 1953-1962.

Yool, D. A. Phenotypic analysis of the *Plp*-deficient mouse. (2000). University of Glasgow Thesis.

Yool, D., Montague, P., McLaughlin, M., McCulloch, M. C., Edgar, J. M., Nave, K.-A., Davies, R. W., Griffiths, I. R., and McCallion, A. S. (2002). Phenotypic analysis of mice deficient in the major myelin protein MOBP, and evidence for a novel *Mobp* isoform. *Glia* **39**, 256-267.

Yool, D. A., Edgar, J. M., Montague, P., and Malcolm, S. (2000). The *proteolipid* protein gene and myelin disorders in man and animal models. *Human Molecular Genetics* **9**, 987-992.

Yoshida, H., Oku, M., Suzuki, M., and Mori, K. (2006). pXBP1(U) encoded in XBP1 pre-mRNA negatively regulates unfolded protein response activator pXBP1(S) in mammalian ER stress response. *Journal of Cell Biology* **172**, 565-575.

Yoshida, M. and Colman, D. R. (1996). Parallel evolution and coexpression of the proteolipid proteins and protein zero in vertebrate myelin. *Neuron* **16**, 1115-1126.

Zeller, N. K., Hunkeller, M. J., Campagnoni, A. T., Sprague, J., and Lazzarini, R. A. (1984). Characterization of mouse myelin basic protein messenger RNAs with a myelin basic protein cDNA clone. *Proceedings of the National Academy of Sciences USA* **81**, 18-22.

Zhang, K. Z. and Kaufman, R. J. (2004). Signaling the unfolded protein response from the endoplasmic reticulum. *Journal of Biological Chemistry* **279**, 25935-25938.

Published material from this thesis

Karim, S. A., Barrie, J. A., McCulloch, M. C., Montague, P., Edgar, J. M., Kirkham, D., Anderson, T. J., Nave, K.-A., Griffiths, I. R., and McLaughlin, M. (2007). PLP overexpression perturbs myelin protein composition and myelination in a mouse model of Pelizaeus-Merzbacher disease. *Glia* **55**, 341-351.

PLP Overexpression Perturbs Myelin Protein Composition and Myelination in a Mouse Model of Pelizaeus-Merzbacher Disease

SAADIA A. KARIM,¹ JENNIFER A. BARRIE,¹ MAILIS C. MCCULLOCH,¹ PAUL MONTAGUE,¹ JULIA M. EDGAR,¹ DOUGLAS KIRKHAM,¹ THOMAS J. ANDERSON,¹ KLAUS A. NAVE,² IAN R. GRIFFITHS,^{1*} AND MARK MCLAUGHLIN¹

¹Applied Neurobiology Group, Institute of Comparative Medicine, University of Glasgow, Bearsden, Glasgow G61 1QH, Scotland

²Department of Neurogenetics, Max-Planck-Institute of Experimental Medicine, D-37075 Goettingen, Germany

KEY WORDS

oligodendrocyte; myelin basic protein; autophagic vacuole; dysmyelination

ABSTRACT

Duplication of *PLP1*, an X-linked gene encoding the major myelin membrane protein of the human CNS, is the most frequent cause of Pelizaeus-Merzbacher disease (PMD). Transgenic mice with extra copies of the wild type *Plp1* gene, a valid model of PMD, also develop a dysmyelinating phenotype dependant on gene dosage. In this study we have examined the effect of increasing *Plp1* gene dosage on levels of PLP/DM20 and on other representative myelin proteins. In cultured oligodendrocytes and early myelinating oligodendrocytes in vivo, increased gene dosage leads to elevated levels of PLP/DM20 in the cell body. During myelination, small increases in *Plp1* gene dosage (mice hemizygous for the transgene) elevate the level of PLP/DM20 in oligodendrocyte soma but cause only minimal and transient effects on the protein composition and structure of myelin suggesting that cells can regulate the incorporation of proteins into myelin. However, larger increases in dosage (mice homozygous for the transgene) are not well tolerated, leading to hypomyelination and alteration in the cellular distribution of PLP/DM20. A disproportionate amount of PLP/DM20 is retained in the cell soma, probably in autophagic vacuoles and lysosomes whereas the level in myelin is reduced. Increased *Plp1* gene dosage affects other myelin proteins, particularly MBP, which is transiently reduced in hemizygous mice but consistently and markedly lower in homozygotes in both myelin and naïve or early myelinating oligodendrocytes. Whether the reduced MBP is implicated in the pathogenesis of dysmyelination is yet to be established. © 2006 Wiley-Liss, Inc.

INTRODUCTION

The majority of axons in the CNS have associated myelin sheaths, which optimize conduction and provide support for their structure and function. Myelin is a highly organized, multilamellar structure, rich in lipid and containing numerous specific proteins. Differences in myelin composition occur depending on CNS region (Amaducci et al., 1962; Mehl and Wolfram, 1969) and caliber of fiber (Butt et al., 1998), however, the ratios of myelin proteins are regulated within fairly defined limits. How these ratios are maintained is not known.

The integral membrane proteolipid protein (PLP) and its minor DM20 isoform account for ~50% of total myelin protein with the extrinsic myelin basic proteins (MBP) being ~30%; both are located in compact myelin. Other myelin proteins, such as 2',3'-cyclic nucleotide 3'-phosphodiesterase (CNP) and myelin-associated glycoprotein (MAG) are targeted to uncompacted regions of the myelin sheath.

Mutations or dosage alterations of the X-linked *PLP1* gene cause Pelizaeus-Merzbacher Disease (PMD) and Spastic Paraplegia Type 2 (SPG2) in man (Inoue, 2005) and dysmyelinating disorders in a range of animal species, including mice (Nave and Griffiths, 2004). The *PLP1* gene is highly conserved and the mouse acts as a valid model of these human disorders. The commonest cause of PMD is a duplication of the *PLP1* gene locus causing increased gene dosage; rarely triplications occur (Wolf et al., 2005; Woodward et al., 1998). The size of the duplicated region, its break points, and site of reinsertion are variable, which may account for some of the phenotypic heterogeneity in patients with *PLP1* gene duplication (Woodward et al., 1998). Pathologically, this can vary from virtual absence of myelin formation, through different degrees of dysmyelination to those in whom axonal changes may be a pronounced feature (Harding et al., 1995; Hudson et al., 2004; Koeppen, 2005). The cellular mechanisms that lead to such phenotypes are poorly understood. Although there are no spontaneous models of gene duplication, transgenic mice or rats carrying varying extra copies of wild type *Plp1* genomic transgenes exhibit a similar range of phenotypes (Anderson et al., 1999; Bauer et al., 2002; Bradl et al., 1999; Inoue et al., 1996; Kagawa et al., 1994; Readhead et al., 1994). Typically, mice with high transgene dosage (usually homozygous for the transgene) are dysmyelinated and die prematurely whereas mice with

This article contains supplementary material available via the Internet at <http://www.interscience.wiley.com/jpages/0894-1491/suppmat>

Grant sponsor: Biotechnology and Biological Sciences Research Council (BBSRC).

*Correspondence to: I. R. Griffiths, Applied Neurobiology Group, Division of Cell Sciences, University of Glasgow, Bearsden, Glasgow G61 1QH, Scotland.
E-mail: I.Griffiths@vet.gla.ac.uk

Received 28 August 2006; Accepted 25 October 2006

DOI 10.1002/glia.20465

Published online 27 November 2006 in Wiley InterScience (www.interscience.wiley.com).

low dosage (hemizygous) develop normally but then develop late-onset (15–18 months age) demyelination and axonal degeneration (Anderson et al., 1998).

Although human patients and transgenic animals are often described as “overexpressors” of the *PLP1* gene, elevations of PLP/DM20 protein levels commensurate with alterations in gene dosage have not been reported nor how any such changes might affect other myelin genes.

We are using transgenic mice to address the mechanisms underlying the dysmyelination associated with increased *Plp1* gene dosage. The aims of the present study were to (i) correlate *Plp1* gene dosage with *Plp1* gene expression particularly at the protein level and determine how this affects the distribution of PLP/DM20 within the oligodendrocyte/myelin sheath unit and the amount of myelin formed and (ii) determine if changes in dosage of one myelin gene result in alteration of the proportion of other myelin constituents.

MATERIALS AND METHODS

Mice

Transgenic mice (Line no. 66) were used (Readhead et al., 1994) in all studies. The transgene was derived from a C57BL/6J cosmid library and injected into BDF2 eggs; subsequent generations (>20) were maintained on the C57BL/6NCrIBr (Charles River) background. The transgene comprises seven copies of the wild type murine *Plp1* gene inserted autosomally. Full details of derivation, genotyping and pathology have been published (Anderson et al., 1998, 1999; Readhead et al., 1994).

Plp1 null mice were generated as described (Klugmann et al., 1997). The targeting was performed in Sv129 DNA electroporated into R1 ESCs and injected into C57BL/6J blastocysts. The phenotype of these mice has been described (Griffiths et al., 1998; Klugmann et al., 1997; Yool et al., 2001).

To determine the expression level of transgene encoded PLP/DM20, hemizygous transgenic males were crossed with heterozygous *Plp1* null females to generate *Plp1* wild type and null offspring with or without the transgene. Thus, transgene expression on a null background was compared with wild type PLP/DM20 levels.

For all other studies hemizygous transgenic mice were mated to generate offspring that were wild type and hemizygous or homozygous for the transgene.

Only male mice were used in the current study. Studies were performed at postnatal Day 3 (P3), an age of very early myelination, P20, an age of active myelin formation and at P60 when myelin formation is complete and myelin maintenance is established. Mice for immunostaining were perfused with 4% paraformaldehyde and those for morphometric analysis with a glutaraldehyde/paraformaldehyde mixture; details of processing schedules have been published previously (Al-Saktawi et al., 2003; Griffiths et al., 1981).

Mice were identified as transgenic or wild type using PCR genotyping of genomic DNA, as described (Readhead

et al., 1994). Further differentiation between mice hemizygous or homozygous for the transgene was determined by histological examination of the spinal cord and/or evidence of clinical signs and by the low myelin yield following extraction. Our original publication (Readhead et al., 1994) correlated copy number with pathology and this was verified in subsequent publications (Anderson, 1997; Anderson et al., 1999). Homozygous mice may be distinguished from hemizygotes by the dysmyelination that is evident at all ages in the present study. A small block of cervical spinal cord from mice used for RNA, protein or tissue culture studies was immersion-fixed in paraformaldehyde/glutaraldehyde fixative and processed for resin sections, and where necessary EM. Additionally, by P20 homozygous mice show an obvious clinical tremor.

Cell Culture

Oligodendrocytes were cultured from P5 spinal cords as described (Montague et al., 1998) and used after seven days in vitro. Cells from each spinal cord were divided between two 35 mm poly-D-lysine coated Nunc tissue culture dishes (~250,000 cells/dish); at harvest the cultures comprised 70–80% O4 + cells together with astrocytes, occasional neurons, and other cells (McLaughlin et al., 2006a). To compensate for any differences in oligodendrocyte cell numbers, samples for western analysis were normalized for aspartoacylase (ASPA), a marker of oligodendrocyte cell bodies (Kirmani et al., 2003; Madhavarao et al., 2004). For analysis of protein steady state levels, dishes were rinsed twice in chilled PBS and lysed with Buffer A (10 mM Tris pH 7.4, 150 mM NaCl, 1% triton X-100, and inhibitors of protease and phosphatase activity). The lysates were rotated at 4°C for 30 min and cell debris pelleted by centrifugation at 5,000 rpm for 5 min. Proteins were quantified using the BCA assay system (Perbio Science UK, Tattenhall, UK).

Real Time Quantitative PCR

The ABI prism 7,500 sequence detection system (Applied Biosystems, Foster City, CA) using Taqman technologies (PE Biosystems, Foster City, CA, USA) was employed following the manufacturer’s instructions. Real time PCR was performed using the Platinum Quantitative RT-PCR Thermoscript One-Step System (Invitrogen, Carlsbad, CA). The PCR primer and probe sets were designed using the program Primer-Express™ (Applied Biosystems). Primer and probe sets used were the following: *β-actin* (Accession no. NM_007393) forward 5'-AGAGGGAAATCGTGCGTGACAT-3': reverse 5'-AGGAAGGCTGGAAAACAGCC-3': TaqMan probe 5'-TGGCCACTGCCGCATCCTCTTC-3'. A combined primer probe set that amplified both *Plp* and *Dm20* (*Plp/Dm20*) was also utilized, forward 5'-GTATAGGCAGTCTCTGC-GCTGT-3': reverse 5'-AAGTGGCAGCAATCATGAAGG-3':

TaqMan probe 5'-TGGCAAGGTTTGTGGCTCCAACCTT-3'. Each probe had FAM at the 5' end and Blackhole Quencher at the 3' end (MWG Biotech, Germany).

A standard curve generated for each set using serial dilutions of the RNA prepared from the cultures confirmed the linearity of the method. qRT-PCR was carried out using the following protocol: 30 min at 50°C, 10 min at 95°C followed by 40 cycles of 15 s at 94°C, and 2 min at 64°C for five samples of both genotypes.

Analysis of qRT-PCR was carried out by relative quantification using Ct values of the *Plp/Dm20* probe versus β -actin. Normalized expression of target message probe with respect to β -actin message was determined for all samples using Microsoft excel data spreadsheets to generate [mRNA] per 50 μ g total RNA initially loaded. The relative amounts of transgenic mRNA were expressed as a percentage of wild type.

Northern Blotting

Total RNA was extracted from spinal cord using RNAsol Bee reagent (Tel-Test Friendswood, TX) following the manufacturer's instructions. RNA was extracted from wild type, hemizygous and homozygous mice and reconstituted in DEPC water. RNA quality and integrity were determined using spectrophotometer and gel electrophoresis. Mouse total (20 μ g) RNA was separated on 1% agarose gel containing 2.2 M formaldehyde along with RNA ladders (Invitrogen, Paisley, UK), then stained with ethidium bromide to visualize quality and quantity of RNA. Transfer to Hybond N membrane (Amersham Pharmacia Biotech, Little Chalfont, UK) in 10 \times SSC took place overnight.

Wild type cDNA probes were generated for *Plp/Dm20* and β -actin using the following primers (*Plp/Dm20*, forward 5'-GTATAGGCAGTCTCTGCGCTGT-3': reverse 5'-AAGTGGCAGCAATCATGAAGG-3'; β -actin, 5'-AGAGG-GAAATCGTGCGTGACAT-3': reverse 5'-AGGAAGGCTG-GAAAACAGCC-3'). For generating an *Mbp* probe, a primer set that amplified all *Mbp* isoforms was utilised (forward 5'-AGACCCTCACAGCGATCCAA-3': reverse 5'-CCCCTGTCAACGCTAAAGAAG-3').

The probes were radiolabelled by random priming using α -³²P-dCTP (3,000 Ci/mole) (Amersham Pharmacia Biotech) to specific activity $>5 \times 10^8$ cpm/ μ g. Filters were hybridized for 2 h at 65°C in Rapidhyb buffer (Amersham Pharmacia Biotech). The blots were then washed at high stringency (3 \times 20 min, 0.1 \times SSC, 0.5% SDS) at 60°C and then exposed to film at -70°C.

Antibodies and Immunostaining

PLP/DM20 was detected with either a rabbit polyclonal or rat monoclonal to the common C-terminal (gifts from NP Groome and S Pfeiffer, respectively). MBP was detected with a mouse monoclonal (Clone 12, gift from Prof. NP Groome) or a rabbit polyclonal (Chemicon Europe, Chandlers Ford, UK). CNP was detected with a

mouse monoclonal (Chemicon). Monoclonal and polyclonal antibodies to MAG were obtained from Chemicon (Clone 513) and as gifts from Prof NP Groome and Dr RH Quarles. ASPA was detected with a rabbit polyclonal (gift from Dr J Garbern). The CC-1 antibody (Oncogene Research Products, CN Biosciences, Nottingham, UK) was used to identify oligodendrocytes. β -actin was detected with a mouse monoclonal antibody (Sigma). Anti-Lamp1 (Clone ID4B) was obtained from the Developmental Studies Hybridoma Bank.

Single or double immunofluorescence was performed on cryosections, as described (Al-Saktawi et al., 2003).

Morphometric Analysis

Analyses were performed on resin-embedded tissue from the ventral columns of the second cervical segment (C2) of spinal cord. Myelin volume was calculated from electron micrographs using a point counting method, as described (Al-Saktawi et al., 2003). Axonal area and total fibre area were measured on semi thin sections photographed with a 100 \times oil immersion lens using a digital camera. A computer-generated grid was superimposed on the image and all fibers contacting intercepts were analyzed using Image Pro-Plus 4.1 software (Media Cybernetics, Silver Spring, MD). Axon and total fiber diameters were obtained from the area measurements and used to derive the myelin thickness and *g* ratio (axon diameter/total fiber diameter).

Cell Counts in Spinal White Matter

Oligodendrocytes were immunostained with the CC-1 antibody with DAPI co-staining of nuclei. Cell counts were performed on cryosections of the ventral columns of white matter at approximately C2 segment, as described (Al-Saktawi et al., 2003).

Myelin Extraction and Western Blotting

Myelin enriched fractions were prepared from whole brain and spinal cord and probed for PLP/DM20, MBP, CNP, and MAG; total homogenates were also probed for ASPA as described (Al-Saktawi et al., 2003). The pellets produced by the high-speed centrifugation of the homogenate contained membranous and nuclear fractions and were analyzed for PLP/DM20 content. Lysed oligodendrocyte cultures were blotted for PLP/DM20, MBP, and ASPA. Proteins were visualized by ECL (SuperSignal West Pico, Pierce Biotechnology, Perbio Science UK) and the signal intensity quantified using Scion Image analysis software.

Statistical Analyses

Statistical significance of differences between values was assessed by ANOVA followed by Bonferonni's *post hoc*

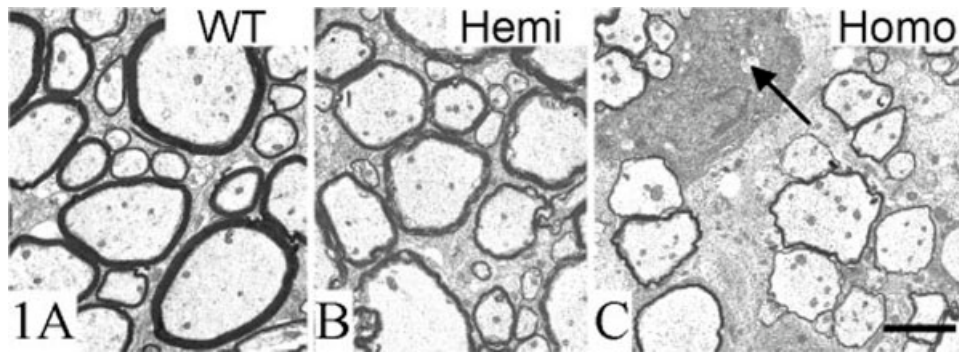


Fig. 1. Electron micrographs of white matter in the ventral columns of P20 mice. **A:** Wild type mouse with all axons surrounded by an appropriately thick myelin sheath. **B:** All axons are myelinated in the hemizygous mouse in which the general structure appears normal; morphometric analysis showed that the average sheath was slightly

thinner than its wild type counterpart. **C:** The homozygous mouse is dysmyelinated with thin myelin sheaths around the majority of axons. An oligodendrocyte cell body is abnormal and contains numerous autophagic vacuoles (arrow). Bar = 2 μ m.

comparison test or by Student's *t* test, as appropriate, with significance $P < 0.05$. Analyses and curve fitting were performed using Graphpad Prism4 software (GraphPad Software, San Diego, CA). In the bar charts, significance of the mutants from wild type is indicated as <0.05 (*), <0.01 (**), and <0.001 (***)

RESULTS

Distinct Phenotypes of *Plp1* Transgenic Mice

Full details of #66 mice have been published (Anderson et al., 1998, 1999; Readhead et al., 1994). Briefly, mice hemizygous for the *Plp1* transgene have no abnormal phenotype until over 1 year, typically 15–18 months, when they lose weight, develop kyphosis, weakness, and ataxia. No obvious pathology is evident in young adults but clinically affected older mice show demyelination and axonal degeneration preferentially affecting smaller diameter fibers. Oligodendrocytes appear normal morphologically. Hemizygous mice in the current study were used prior to the above changes. In contrast, mice homozygous for the transgene exhibit tremor from the second week followed later by seizures, associated with marked dysmyelination, and an increased number of apoptotic oligodendrocytes. Oligodendrocytes show swelling of the Golgi apparatus and numerous autophagic vacuoles. A minority of oligodendrocytes show loss of the normal cisternal pattern of the rough endoplasmic reticulum (RER). Representative images of the morphology at P20 in the three genotypes are shown in Fig. 1 and of the homozygote in supplementary Fig. 1.

Expression of *Plp* Transgene: mRNA and Protein Levels Are Similar to Wild Type

We expressed the autosomal transgene on a *Plp1* null background to assess transgene-derived levels of mRNA

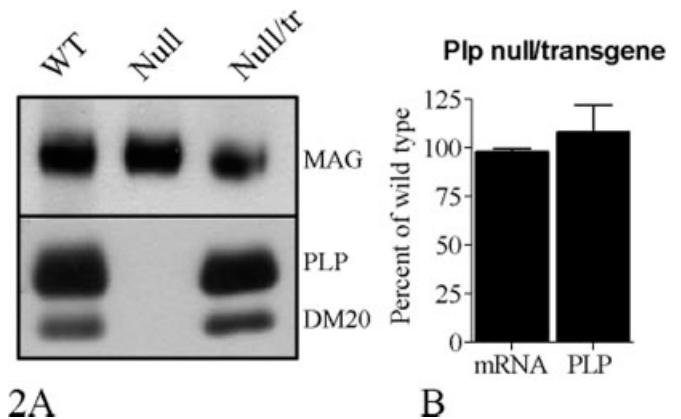


Fig. 2. Expression of the *Plp1* transgene on a *Plp1* null background in spinal cord of P20 mice. **A:** Representative western blot for PLP/DM20 in myelin from wild type (WT), *Plp1* null (Null), and *Plp1* null mice carrying the *Plp1* transgene (Null/tr). The signal is similar in the wild type and null/tr mice. MAG is also shown as a control for loading. **B:** Quantitative data for *Plp/Dm20* mRNA, measured by qRT-PCR and PLP protein, measured by western blotting for *Plp1* null mice carrying the *Plp1* transgene. Results ($M \pm SEM$, $N = 2$) are expressed as a percentage of a wild type mouse from the same litter. There is no difference between groups for either parameter.

and product using qRT-PCR and western blotting, respectively. P20 mice harboring one copy of the transgene cassette on the null background expressed *Plp/Dm20* mRNA and PLP and DM20 proteins in the spinal cord at similar levels to wild type mice generated in the same litter (Figs. 2A,B). Levels of *Mbp* mRNA and myelin MBP in *Plp1* null mice with and without the transgene were also unchanged from wild type (data not shown).

Dosage-Related Expression of the *Plp1* Gene in Oligodendrocytes and Spinal Cord During Myelination

During normal in vivo development the level of *Plp1* gene expression closely parallels myelination. However, expression commences prior to myelin formation and is

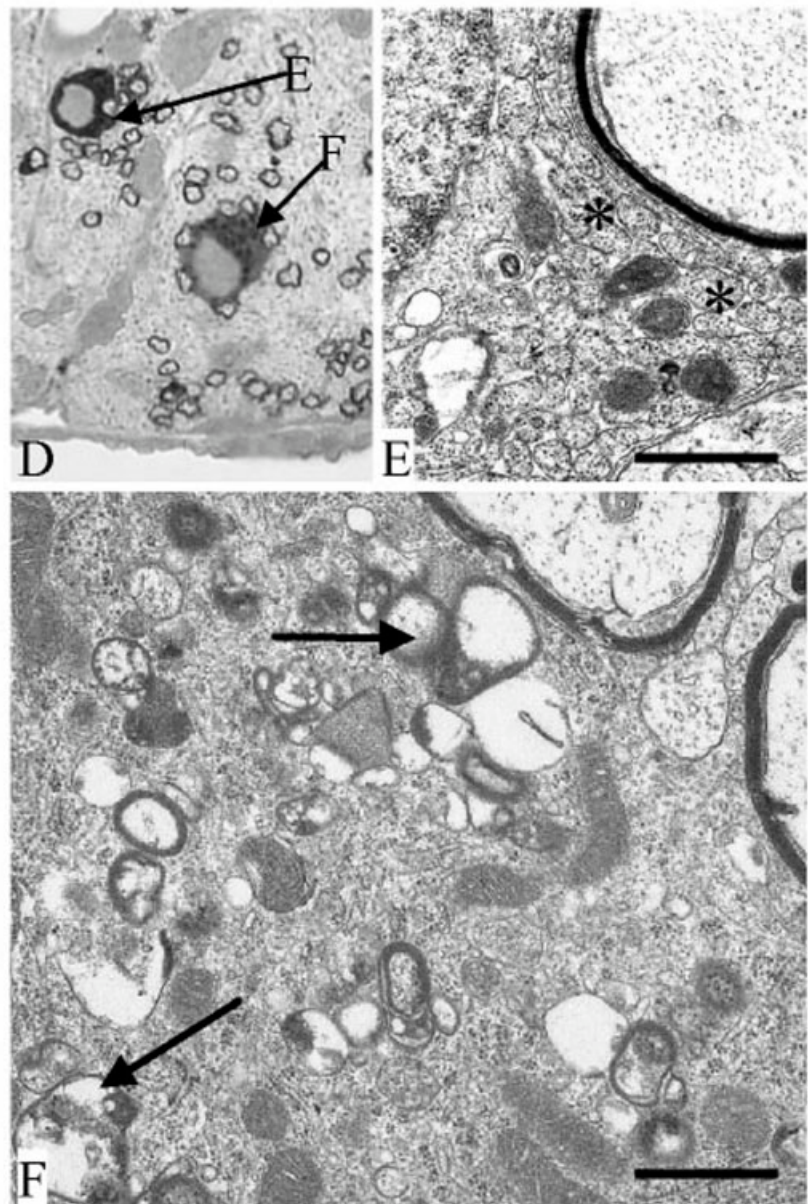
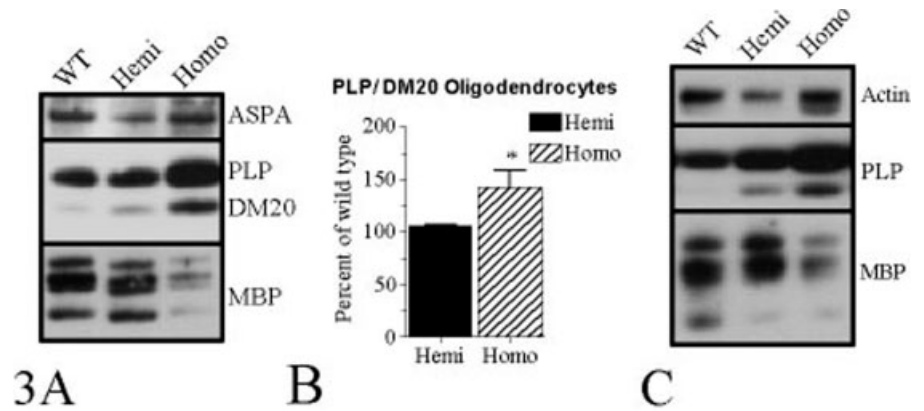


Fig. 3. *Plp1* gene expression in oligodendrocytes and in spinal cord of mice hemizygous and homozygous for the *Plp* transgene. **A**: Representative western blots of cultured oligodendrocytes from wild type (WT), hemizygous (Hemi) and homozygous (Homo) mice probed for PLP/DM20 and for ASPA, an oligodendrocyte-specific cell body protein and for MBP. Whereas the level of PLP/DM20 is elevated in the homozygotes, the amount of the MBP isoforms is decreased in the same cells. **B**: Levels of PLP/DM20 in oligodendrocytes normalized to ASPA and expressed relative to the wild type ($M \pm SEM$, $N = 4$). Values for hemizygotes are similar to wild type whereas the values for homozygotes are elevated ($P < 0.05$). **C**: Representative western blots of total homogenates from P3 spinal cords probed for PLP/DM20 and MBP and normalized with β -actin. The PLP/DM20 levels show a progressive increase with gene dosage whereas the MBP level in the homozygote is considerably lower than the other genotypes. **D**: Accumulation of PLP/DM20 in cell bodies of oligodendrocytes from a P3 mouse homozygous for the transgene. Resin section immunostained for PLP/DM20 showing two oligodendrocytes with strongly immunopositive cell bodies. The thin myelin sheaths are also stained. The ventral pial surface is to the bottom. The arrows (**E**, **F**) indicate the sites of the EM images shown in Figs. **E** and **F**, which were obtained from an immediately adjacent serial thin section. **E**: Part of oligodendrocyte soma showing loss of the normal cristernal arrangement of the RER (*). **F**: Oligodendrocyte soma showing numerous autophagic vacuoles (arrows). Bars = 1 μ m.

influenced by axonal contact and the amount of myelin produced by the cell (McPhilemy et al., 1990; Thomson et al., 2005). To understand how these factors might

interact with increased *Plp1* gene dosage we first studied PLP/DM20 levels in naïve oligodendrocytes with no axonal contact and in the absence of a myelin sheath.

Primary cultures, established from wild type mice and those carrying the transgene in the hemizygous or homozygous state, were probed for PLP/DM20 and aspartoacylase (ASPA), a marker specific for oligodendrocyte cell bodies (Kirmani et al., 2003; Madhavarao et al., 2004) to control for loading and cell numbers between cultures. The normalized levels of total PLP/DM20 protein, relative to wild type, were similar in hemizygous oligodendrocytes but elevated in those from homozygous animals ($P < 0.05$) (Figs. 3A,B).

We next investigated *Plp1* gene expression in spinal cord of P3 and P20 wild type, hemizygous and homozygous transgenic littermates. P3 represents an early stage of myelin formation when oligodendrocytes have established axonal contact but only a small proportion of spinal axons have rudimentary sheaths and the majority of PLP/DM20 is in the cell body whereas P20 is an age of advanced myelination. Levels of PLP/DM20 in total homogenates of P3 spinal cord (Fig. 3C) were elevated relative to wild type in both hemizygotes and homozygotes, more so in the latter. We performed immunostaining and electron microscopy to localize PLP/DM20 in spinal cords of P3 homozygous mice. In 1 μ m immunostained resin sections strongly stained oligodendrocyte cell bodies and myelin sheaths were evident with some cell bodies containing dark immunopositive structures (arrow in Fig. 3D). In immediately adjacent EM sections (Figs. 3E,F) the immunopositive cells had distended RER and autophagic vacuoles/lysosomes, which probably correspond to the dark structures seen in the resin section.

We evaluated *Plp/Dm20* mRNA in the spinal cord of P20 mice by northern blot, using β -actin as an internal standard. At P20 levels in hemizygotes were 122% of wild type ($P > 0.05$) while homozygotes were reduced (60% of wild type) ($P < 0.01$) compared with the two other genotypes (Figs. 4A,B). Very similar changes in mRNA levels were reported in the 4e line of *Plp1* transgenic mice (Kagawa et al., 1994). In the spinal cord of hemizygotes at P20, the levels of PLP and DM20 in myelin-enriched fractions were not different from wild type littermates but were significantly lower in homozygous animals (Figs. 4C,D). Similar results were obtained for myelin fractions from the brain (data not shown). In normal myelinated white matter the vast majority of PLP, the major isoform, is present in the compact sheath while DM20 is located in both myelin and cytoplasm (Trapp et al., 1997). As oligodendrocytes and pre-myelinating spinal cord of homozygous mice contained more PLP/DM20 than wild type (Figs. 3A,C) whereas myelin fractions from P20 mice contained less per unit of extracted myelin protein, we examined the pellet fraction (containing nuclei and membranous organelles) remaining after myelin separation (Fig. 4C). In comparison with wild type (100%), the levels of PLP and DM20 were greater in pellet fractions from hemizygotes ($158\% \pm 9$ and $227\% \pm 28$, respectively, $N = 5$, $P < 0.05$) while for homozygotes PLP was similar ($124\% \pm 10$, NS) and DM20 was elevated ($207\% \pm 38$, $P < 0.05$). A summary of the results is presented in Table 1.

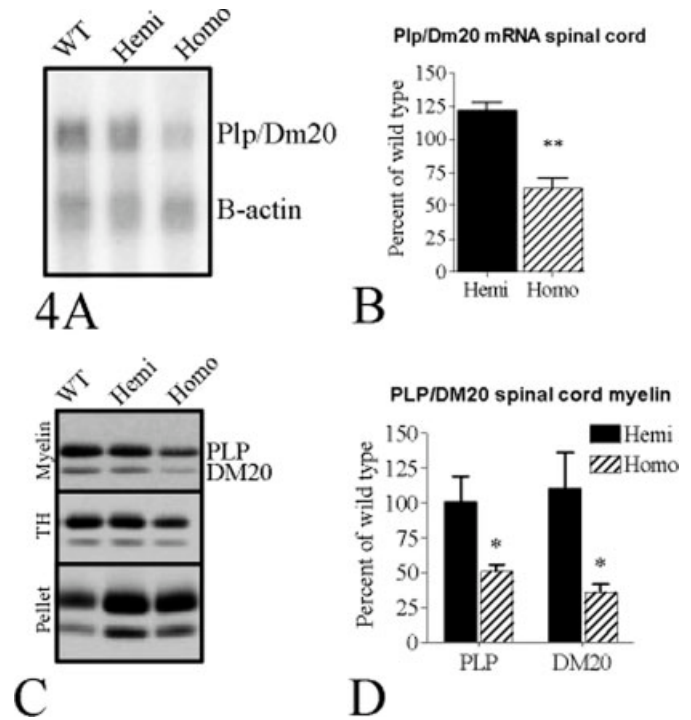


Fig. 4. A: Representative northern blot for *Plp/Dm20* and β -actin mRNA from spinal cord of P20 mice. B: Quantification of *Plp/Dm20* mRNA in P20 spinal cord, ($M \pm SEM$, $N = 5$), expressed relative to wild type. The increase in hemizygotes is not significant whereas the level in homozygotes is reduced ($P < 0.01$). C: Representative western blot for PLP/DM20 of myelin enriched and pellet fractions and the total homogenate (TH) from spinal cord of P20 mice. The levels of PLP/DM20 in the total homogenate and myelin fraction from homozygous mice are reduced compared with wild type whereas in the pellet fraction the converse applies. D: Steady state levels of PLP and DM20 proteins in myelin fractions from P20 mice show no change from wild type in hemizygous animals, but significant reductions in homozygous mice ($M \pm SEM$, $N = 5$, $P < 0.05$).

The data suggest that in oligodendrocytes from homozygous mice a "relative excess" of PLP/DM20 is stored or retained in the cell body with a reduced amount translocated to myelin, in comparison with wild type. Based on the EM, the most probable site for this "stored" PLP/DM20 is the autophagic vacuoles/lysosomes. In immunostained brain sections, significant co-localization of PLP/DM20 and the lysosomal marker, Lamp1, provided further evidence that PLP/DM20 accumulates in these organelles (Supplementary Fig. 2).

Effect of *Plp1* Dosage on Expression of Other Myelin Genes During Myelination

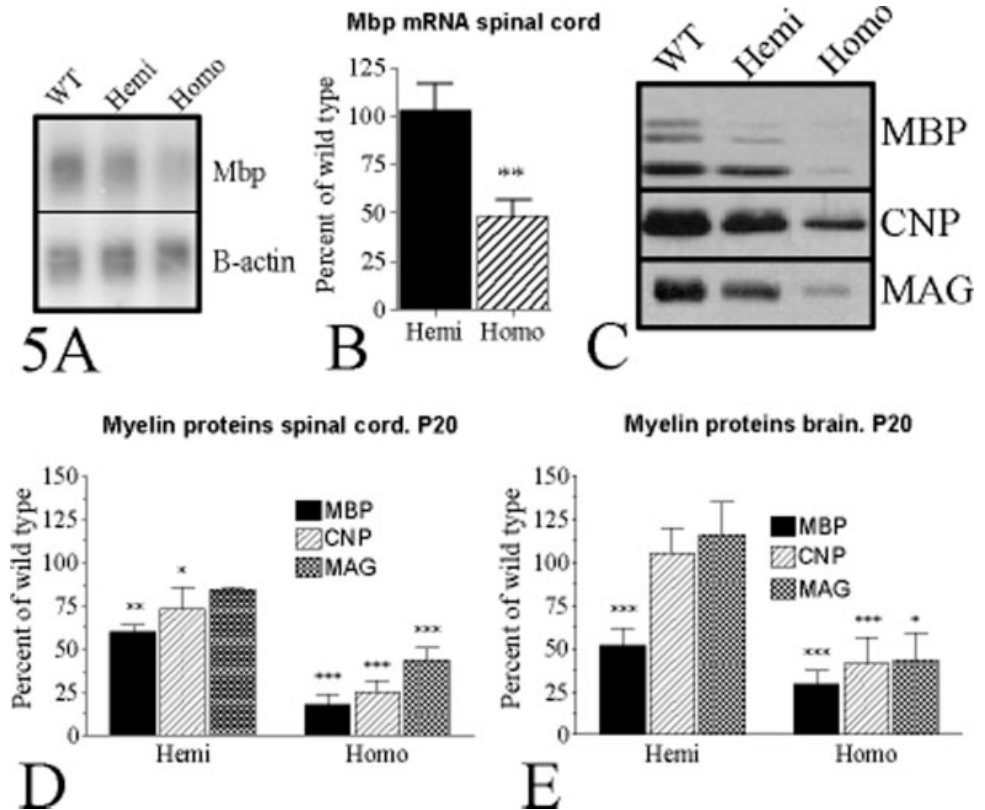
We determined if changes in *Plp1* gene dosage affect the expression of other representative myelin proteins and their incorporation into the myelin sheath. Unexpectedly in homozygous mice, the level of MBP, the second most abundant myelin protein, was decreased even in cultured oligodendrocytes, and prior to myelination in P3 spinal cords (in contrast to the elevated amounts of PLP/DM20 in the same samples) (Figs. 3A,C). This

TABLE 1. Steady State Levels of PLP and MBP Proteins in Cells and Tissues from Mice with Low (Hemizygous) and High (Homozygous) Transgene Dosage, Relative to the Corresponding Wild Type Samples

Stage of myelination	Low dosage		High dosage	
	PLP/DM20	MBP	PLP/DM20	MBP
Nonmyelinating (cultured OLs)	Normal	Normal	Increase	Decrease
Early myelination (P3 spinal cord)	Small increase	Normal	Increase	Decrease
Myelinated (P20 spinal cord)	Normal (T) Increase (P) Normal (M)	Moderate decrease (M)	Small decrease (T) Increase (P) Marked decrease (M)	Marked decrease (M)

OLs, oligodendrocytes. In the P20 spinal cords, samples have been fractionated to examine the distribution of PLP/DM20: T, total homogenate; P, pellet; M, myelin-enriched. For MBP, only myelin-enriched samples were evaluated.

Fig. 5. Increased *Plp* gene dosage affects expression of other myelin protein genes. **A:** Representative northern blot for *Mbp* and β -actin mRNA from spinal cord of P20 mice. **B:** *Mbp* mRNA levels, representative of other myelin genes, are not different from wild type in the spinal cords of P20 hemizygous mice but reduced ($P < 0.01$) in homozygotes. The data ($M \pm SEM$, $N = 5$) are expressed relative to wild type. **C:** Representative western blots of myelin enriched fractions from P20 spinal cord probed for MBP, CNP and MAG. All three proteins are reduced in homozygous mice and MBP and CNP are also lower in hemizygotes, compared with wild type. **D:** Levels of MBP, CNP and MAG in myelin enriched fractions from spinal cord of P20 hemizygous and homozygous mice. In the hemizygotes, MBP ($P < 0.001$) and CNP ($P < 0.05$) are reduced relative to wild type while MAG levels are similar. All proteins are markedly lower ($P < 0.001$) in homozygous mice. **E:** In myelin enriched fractions from whole brain of P20 mice only MBP ($P < 0.001$) is reduced in hemizygotes while all three proteins are lower in homozygous mice.



down regulation extended to later time points where levels of *Mbp* mRNA and MBP protein were reduced in spinal cords of P20 homozygotes. (Figs. 5A–D). In hemizygotes, message levels were normal, but MBP protein was reduced compared with wild type (Figs. 5A–D).

Two proteins, CNP and MAG, found in uncompact myelin membranes were reduced in the homozygous mice while CNP, but not MAG was lower in hemizygous mice (Figs. 5C,D). In myelin fractions derived from whole brain the level of MBP, but not CNP and MAG, was reduced in hemizygous mice while all three proteins were markedly lower in homozygous animals relative to wild type (Fig. 5E). A summary of the MBP data is presented in Table 1.

Thus, overexpression of the *Plp1* gene impacts on other myelin genes, particularly *Mbp*, with downregulation at both mRNA and protein levels.

Myelin Proteins During Myelin Maintenance

P20 represents an age in mice at which myelination in the spinal cord is advanced but incomplete; in the brain the status is more varied with a caudal to rostral gradient of myelin development. To determine the influence of increased *Plp1* gene dosage during myelin maintenance we examined brain and spinal cord of P60 hemizygotes; mice homozygous for the transgene usually died prior to this age. mRNA levels for *Plp/Dm20* and *Mbp* were unchanged in the hemizygotes compared with wild type. There was no difference between the two genotypes in the protein levels of PLP, DM20, MBP, CNP, and MAG in myelin from brain or spinal cord (data not shown) nor in the myelin morphometry (see below), suggesting the differences in CNP and MBP present at P20 had resolved during maturation.

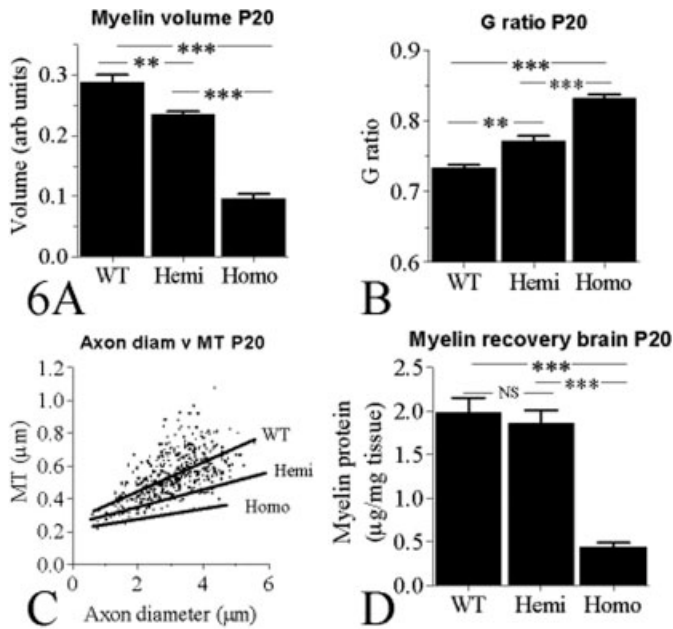


Fig. 6. Myelin status of wild type and transgenic mice at P20. **A:** Myelin volume in ventral columns of cervical spinal cord was determined from electron micrographs using a point counting method. Values are reduced in both transgenics compared with wild type and also differ with each other. **B:** The *g* ratio is increased in transgenic mice compared with wild type. The ratio provides an indication of whether the thickness of myelin sheath is appropriate for axon diameter; a higher value indicates a disproportionately thin sheath. **C:** Myelin sheath thickness (MT) should increase with axon diameter as shown by the scatter graph for wild type mice and the corresponding linear regression. The slopes of regression lines for the transgenic mice are reduced compared with wild type and also differ from each other. The individual points for the transgenics are not shown. **D:** Myelin recovery from whole brain is similar in mice hemizygous for the transgene and wild type; both groups differ from homozygous mice. The level of proteins in myelin is expressed as a proportion of the wet weight of whole brain. (The bar charts show mean \pm SEM, $N = 6$ for A, B, C, and 10 for D).

Effects of *Plp1* Gene Dosage on the Oligodendrocyte/Myelin Unit

As *Plp1* gene dosage influences the formation of myelin we quantified the volume of myelin from electron micrographs of cervical ventral columns at P20 using a point counting method. Hemizygotes contained slightly less myelin (81%) than wild type whereas homozygous mice had considerably less than the other genotypes (Fig. 6A). Morphometric analysis indicated that while axon diameters were similar in the three genotypes, the mean *g* ratio was elevated in hemizygous and more especially homozygous transgenic mice compared with wild type, due to a reduction in myelin thickness (Figs. 6B,C). An increase in *Plp1* gene dosage, therefore, leads to a commensurate reduction in myelin formation in spinal cord, which in the case of hemizygous mice is subtle and due only to slightly thinner myelin sheaths. In the more severely affected homozygous mice the reduction is a combination of markedly thinner sheaths and amyelinated axons. The morphometric changes are reflected by differences in cervical cord area; both hemizygous ($2.54 \pm 0.03 \text{ mm}^2$, $n = 6$) and homozygous (2.14

± 0.02) mice had reduced areas compared with wild type (2.89 ± 0.06 , $P < 0.001$) and the two mutants differed from each other ($P < 0.01$).

We also assessed the myelin recovery from whole brain (expressed as myelin protein per unit weight of brain tissue) obtained during biochemical fractionation. There was no difference in recovery between wild type and hemizygous mice, but markedly less myelin was obtained from the dysmyelinated homozygous mice (Fig. 6D). The failure to detect subtle differences between wild type and hemizygous mice may indicate differences between myelination in brain and spinal cord or reflect the lower sensitivity of this technique compared with the morphometric analyses.

As myelination is incomplete at P20, we evaluated the amount of myelin at P60 in hemizygous and wild type mice. There was no difference in myelin recovery from brain and the myelin volume, *g* ratio or axon diameter/myelin thickness relationship in spinal cord at this age (data not shown).

The calculated number of CC-1 + oligodendrocytes in white matter area per transverse section for P20 wild type, hemizygous and homozygous mice were 337 ± 13 , 358 ± 12 , and 349 ± 52 cells, respectively; these values are not significantly different.

DISCUSSION

Duplication or even triplication of the *PLP1* locus is the most frequent cause of PMD and patients with increased gene dosage and the corresponding transgenic animal models are often referred to as “overexpressors”. Using a transgenic mouse with a “low” or “high” increase in *Plp1* gene dosage we show that the relationship between dosage and steady state PLP/DM20 levels is complex and influenced by whether or not the cell is generating myelin and that changes in dosage alter the proportional distribution of PLP/DM20 within the oligodendrocyte/myelin unit. We further show that changes in *Plp1* gene dosage have profound effects on other myelin proteins, particularly MBP.

The Level and Distribution of PLP/DM20 Are Influenced by Gene Dosage and State of Myelination

Intuitively, one would anticipate increased *Plp1* gene dosage to result in higher levels of PLP/DM20. However, other factors, such as the myelination status, have a major influence. To separate these influences we determined PLP/DM20 levels in cultured oligodendrocytes, which lack myelin sheaths, and showed that levels in cells from homozygous mice were elevated. During very early myelination in P3 spinal cords, PLP/DM20 was also elevated in homozygous mice and to a lesser extent in hemizygous mice. As myelination proceeds the level of gene dosage determines the ability of the oligodendrocyte to deal with the potential protein overload. In

normal myelination the vast majority of PLP/DM20 is concentrated in myelin and myelin gene expression is upregulated to deal with the rapid membrane expansion. With P20 hemizygous mice PLP/DM20 is incorporated into myelin in normal amounts although levels in the cell soma (as indicated by pellet fractions) remain elevated compared with wild type. This suggests the myelinating cell regulates the incorporation of PLP/DM20 into myelin despite changes in levels in the cell body.

With P20 homozygotes the situation is more complex. Total levels of PLP/DM20 (as contained in total homogenates) are slightly lower than wild type, the reduction probably reflecting downregulation of myelin genes associated with dysmyelination and the concomitant reduction in myelin content. What is more striking is the alteration in distribution of PLP/DM20 with the somal pellet fractions containing a disproportionate amount, relative to the low levels in the myelin sheath. This quantitative change is matched by immunocytochemical demonstration of strong PLP/DM20 reactivity in the cell bodies in our mice and in the transgenic rat model (Bauer et al., 2002; Bradl et al., 1999). Immunostaining and EM show that the strongly immunopositive oligodendrocyte cell bodies contain numerous autophagic vacuoles and lysosomes. PLP, when overexpressed, is known to associate with the endosome/lysosome system (Simons et al., 2002). In normal myelination PLP may also associate temporarily with endosomes before axon-derived signals promote its insertion into myelin (Trajkovic et al., 2006). A reduction in the available myelin and decreased axonal contact, as occurs in the homozygotes, would be predicted to exacerbate the accumulation of PLP in lysosomes.

A very similar paradoxical effect has been observed in the nerves of mice "overexpressing" *P0*, the major myelin gene of the PNS. Myelin was maintained with lower levels of *P0* transgene dosage although MBP was reduced, while higher expression led to dysmyelination and decreases in all myelin proteins (Wrabetz et al., 2000). Schwann cells overexpressing *P0* also concentrate the protein in their cell bodies due to the paucity of available myelin (Yin et al., 2000). Similarities also exist with increased dosage of the *PMP22* gene, the commonest cause of Charcot-Marie-Tooth disease Type 1A. Transgenic rodent models of the disorder exhibit dysmyelination proportionate with *Pmp22* dosage (Huxley et al., 1998; Niemann et al., 2000) and Schwann cells contain autophagic vacuoles reminiscent of those seen in oligodendrocytes of the present study (Chies et al., 2003; Niemann et al., 2000). Additionally, increased *Pmp22* dosage causing dysmyelination of the peripheral nerves is associated with reduced levels of myelin proteins (Sereda et al., 1996), as occurred with our other *Plp1* transgenic mice.

We suggest that when using the term "overexpressor" in relation to PLP/DM20 protein a distinction must be drawn between cell soma and myelin. The term may be justified when considering PLP/DM20 levels in the oligodendrocyte cell bodies but does not appear appropriate in relation to myelin where levels are not increased

at either gene dosage. Total tissue levels also show no increase proportionate to gene dosage.

Effect of *Plp1* Gene Dosage on Other Myelin Proteins and Possible Consequences

Although the level of PLP/DM20 in spinal cord myelin from P20 hemizygous mice is normal, MBP is transiently reduced, recovering by the age of P60. Concurrently, there is also a subtle myelin defect due to a slight reduction in sheath thickness, which also recovers by age P60. In P20 homozygous mice, the levels of MBP and other representative proteins are markedly reduced in myelin fractions. While a reduction of MBP, associated with hypomyelination, might be anticipated there must be a more fundamental dysregulation, which is not attributable solely to a lack of myelin, as MBP is substantially reduced in naïve oligodendrocytes and P3 spinal cord, even though PLP/DM20 levels are elevated in the corresponding samples.

Other integral myelin membrane proteins, such as MAG, which share the same biosynthetic pathway as PLP, are also concentrated in oligodendrocyte cell bodies in homozygous mice whereas MBP, which has a different pathway, is not enriched in the soma (Anderson et al., 1999) (Supplementary Fig. 3). A range of membrane proteins of both myelin and non-myelin origin were also concentrated in oligodendrocyte cell bodies in the *Plp1* transgenic rats (Bauer et al., 2002).

The precise cause of the hypomyelination in the homozygotes is still uncertain. Reduced levels of PLP/DM20 do not cause a similar myelin deficit (Klugmann et al., 1997). The reduction in MBP, either singly or in combination with other myelin components, may be significant as MBP is critical for myelin formation and influences the amount of myelin formed (Shine et al., 1992). We are testing whether genetically increasing the level of MBP in *Plp1* transgenic mice improves myelin formation to determine whether the changes in MBP are a causative factor. The autophagic vacuoles also enclose myelin-like membranes in addition to PLP/DM20. A further possible mechanism for dysmyelination may involve accelerated breakdown of any myelin that does form during development so that the sheath never acquires full thickness. An investigation into the turnover dynamics of myelin components is also being undertaken.

Comparison with Other *Plp1* Mutations Causing Dysmyelination

Mutations causing changes in the structure of PLP/DM20, predicted to cause protein misfolding, are a common cause of PMD and also occur spontaneously in animals. The dysmyelination associated with missense mutations and increased gene dosage share similarities with marked hypomyelination and increased cell death. Misfolded PLP/DM20 tends to accumulate in the RER, inducing an unfolded protein response (UPR) and pro-

teasomal degradation (McLaughlin et al., 2006a,b; Southwood and Gow, 2001; Southwood et al., 2002). As PLP/DM20 generated by increased dosage has a normal structure, a UPR is not anticipated and indeed, markers of the UPR, such as caspase 12, *Chop*, and *Atf3* are not induced (Cerghet et al., 2001; Southwood et al., 2002). Additionally, we have not detected elevation in BiP levels nor activation of *X box-1*, which are both induced by misfolded protein (Karim, unpublished data). There is also evidence that apoptosis in the two models occurs via different mechanisms (Cerghet et al., 2001). We are currently investigating the dynamics of PLP/DM20 in *Plp1* transgenic mice. Interestingly, in homozygotes about 55% of nascent PLP/DM20 is degraded by an MG132-sensitive mechanism, probably implicating the proteasome, compared with 30% in wild type and hemizygotes (Karim, unpublished data) and 70% in the *rumpshaker* mutation (McLaughlin et al., 2006a). Our ongoing work suggests there may be at least three fates of newly synthesized PLP/DM20 in the *Plp1* transgenic mice, the labile component, a small amount incorporated into myelin, and a longer-lived pool that persists in the cell soma. How the dysmyelination is induced by any of the above processes is still an open question.

ACKNOWLEDGMENTS

We are grateful to Prof NP Groome and Drs S Pfeiffer, R Quarles, and J Garbern for the gifts of antibodies. The LAMP1 antibody was obtained from the Developmental Studies Hybridoma Bank developed under the auspices of the NICHD and maintained by The University of Iowa, Department of Biological Sciences, Iowa City, IA 52242.

REFERENCES

- Al-Saktawi K, McLaughlin M, Klugmann M, Schneider A, Barrie JA, McCulloch MC, Montague P, Kirkham D, Nave K-A, Griffiths IR. 2003. Genetic background determines phenotypic severity of the *Plp* rumpshaker mutation. *J Neurosci Res* 72:12–24.
- Amaducci L, Pazzagli A, Pessina G. 1962. The relation of proteolipids and phosphatidopeptides to tissue elements in the bovine nervous system. *J Neurochem* 9:309–318.
- Anderson TJ. 1997. Effects of increased dosage of the *Plp* gene: A study in transgenic mice. PhD Thesis, University of Glasgow.
- Anderson TJ, Klugmann M, Thomson CE, Schneider A, Readhead C, Nave K-A, Griffiths IR. 1999. Distinct phenotypes associated with increasing dosage of the *Plp* gene: Implications for CMT1A due to *Pmp22* gene duplication. *Ann NY Acad Sci* 883:234–246.
- Anderson TJ, Schneider A, Barrie JA, Klugmann M, McCulloch MC, Kirkham D, Kyriakides E, Nave K-A, Griffiths IR. 1998. Late-onset neurodegeneration in mice with increased dosage of the proteolipid protein gene. *J Comp Neurol* 394:506–519.
- Bauer J, Bradl M, Klein M, Leisser M, Deckwerth TL, Wekerle H, Lassmann H. 2002. Endoplasmic reticulum stress in PLP-overexpressing transgenic rats: Gray matter oligodendrocytes are more vulnerable than white matter oligodendrocytes. *J Neuropathol Exp Neurol* 61:12–22.
- Bradl M, Bauer J, Inomata T, Zielasek J, Nave KA, Toyka K, Lassmann H, Wekerle H. 1999. Transgenic Lewis rats overexpressing the proteolipid protein gene: Myelin degeneration and its effect on T cell-mediated experimental autoimmune encephalomyelitis. *Acta Neuropathol (Berl)* 97:595–606.
- Butt AM, Ibrahim M, Gregson N, Berry M. 1998. Differential expression of the L- and S-isoforms of myelin associated glycoprotein (MAG) in oligodendrocyte unit phenotypes in the adult rat anterior medullary velum. *J Neurocytol* 27:271–280.
- Cerghet M, Bessert DA, Nave KA, Skoff RP. 2001. Differential expression of apoptotic markers in jimpy and in *Plp* overexpressors: Evidence for different apoptotic pathways. *J Neurocytol* 30:841–855.
- Chies R, Nobbio L, Edomi P, Schenone A, Schneider C, Brancolini C. 2003. Alterations in the Arf6-regulated plasma membrane endosomal recycling pathway in cells overexpressing the tetraspan protein Gas3/PMP22. *J Cell Sci* 116:987–999.
- Griffiths IR, Duncan ID, McCulloch M. 1981. Shaking pup: A disorder of central myelination in the spaniel dog. II. Ultrastructural observations on the white matter of cervical spinal cord. *J Neurocytol* 10:847–858.
- Griffiths IR, Klugmann M, Anderson TJ, Yool D, Thomson CE, Schwab MH, Schneider A, Zimmermann F, McCulloch MC, Nadon NL, Nave K-A. 1998. Axonal swellings and degeneration in mice lacking the major proteolipid of myelin. *Science* 280:1610–1613.
- Harding B, Ellis D, Malcolm S. 1995. A case of Pelizaeus-Merzbacher disease showing increased dosage of the proteolipid protein gene. *Neuropathol Appl Neurobiol* 21:111–115.
- Hudson LD, Garbern JY, Kamholz JA. 2004. Pelizaeus-Merzbacher disease. In: Lazzarini RA, Griffin JW, Lassmann H, Nave K-A, Miller RH, Trapp BD, editors. *Myelin biology and disorders*. Amsterdam: Elsevier. pp 867–885.
- Huxley C, Passage E, Robertson AM, Yool B, Huston S, Manson A, Sab eran-Djionedi D, Figarella-Branger D, Pellissier JF, Thomas PK, Font es M. 1998. Correlation between varying levels of *PMP22* expression and the degree of demyelination and reduction in nerve conduction velocity in transgenic mice. *Hum Mol Genet* 7:449–458.
- Inoue K. 2005. *PLP1*-related inherited dysmyelinating disorders: Pelizaeus-Merzbacher disease and spastic paraplegia type 2. *Neurogenetics* 6:1–16.
- Inoue Y, Kagawa T, Matsumura Y, Ikenaka K, Mikoshiba K. 1996. Cell death of oligodendrocytes or demyelination induced by overexpression of proteolipid protein depending on expressed gene dosage. *Neurosci Res* 25:161–172.
- Kagawa T, Ikenaka K, Inoue Y, Kuriyama S, Tsujii T, Nakao J, Nakajima K, Aruga J, Okano H, Mikoshiba K. 1994. Glial cell degeneration and hypomyelination caused by overexpression of myelin proteolipid protein gene. *Neuron* 13:427–442.
- Kirman BF, Jacobowitz DM, Nambodiri MAA. 2003. Developmental increase of aspartoacylase in oligodendrocytes parallels CNS myelination. *Brain Res Dev Brain Res* 140:105–115.
- Klugmann M, Schwab MH, P uhlhofer A, Schneider A, Zimmermann F, Griffiths IR, Nave K-A. 1997. Assembly of CNS myelin in the absence of proteolipid protein. *Neuron* 18:59–70.
- Koeppen AH. 2005. A brief history of Pelizaeus-Merzbacher disease and proteolipid protein. *J Neurol Sci* 228:198–200.
- Madhavarao CN, Moffett JR, Moore RA, Viola RE, Nambodiri MAA, Jacobowitz DM. 2004. Immunohistochemical localization of aspartoacylase in the rat central nervous system. *J Comp Neurol* 472:318–329.
- McLaughlin M, Barrie JA, Karim SA, Montague P, Edgar JM, Kirkham D, Thomson CE, Griffiths IR. 2006a. Processing of PLP in a model of Pelizaeus-Merzbacher disease/SPG2 due to the *rumpshaker* mutation. *Glia* 53:715–722.
- McLaughlin M, Karim SA, Montague P, Barrie JA, Kirkham D, Griffiths IR, Edgar JM. 2006b. Genetic background influences UPR but not PLP processing in the *rumpshaker* model of PMD/SPG2. *Neurochem Res* (in press).
- McPhilemy K, Mitchell LS, Griffiths IR, Morrison S, Deary AW, Sommer I, Kennedy PGE. 1990. Effect of optic nerve transection upon myelin protein gene expression by oligodendrocytes: Evidence for axonal influences on gene expression. *J Neurocytol* 19:494–503.
- Mehl E, Wolfgram F. 1969. Myelin types with different protein components in the same species. *J Neurochem* 16:1091–1097.
- Montague P, Barrie JA, Thomson CE, Kirkham D, McCallion AS, Davies RW, Kennedy PGE, Griffiths IR. 1998. Cytoskeletal and nuclear localization of MOBP polypeptides. *Eur J Neurosci* 10:1321–1328.
- Nave K-A, Griffiths IR. 2004. Models of Pelizaeus-Merzbacher disease. In: Lazzarini RA, Griffin JW, Lassmann H, Nave K-A, Miller RH, Trapp BD, editors. *Myelin biology and disorders*. Amsterdam: Elsevier. pp 1125–1142.
- Niemann S, Sereda MW, Suter U, Griffiths IR, Nave KA. 2000. Uncoupling of myelin assembly and Schwann cell differentiation by transgenic overexpression of peripheral myelin protein 22. *J Neurosci* 20:4120–4128.
- Readhead C, Schneider A, Griffiths IR, Nave K-A. 1994. Premature arrest of myelin formation in transgenic mice with increased proteolipid protein gene dosage. *Neuron* 12:583–595.

- Sereda M, Griffiths IR, Pühlhofer A, Stewart H, Rossner MJ, Zimmermann F, Magyar JP, Schneider A, Hund E, Meinck HM, Suter U, Nave K-A. 1996. A transgenic rat model of Charcot-Marie-Tooth disease. *Neuron* 16:1049–1060.
- Shine HD, Readhead C, Popko B, Hood L, Sidman RL. 1992. Morphometric analysis of normal, mutant and transgenic CNS: Correlation of myelin basic protein expression to myelinogenesis. *J Neurochem* 58:342–349.
- Simons M, Krämer EM, Macchi P, Rathke-Hartlieb S, Trotter J, Nave K-A, Schulz JB. 2002. Overexpression of the myelin proteolipid protein leads to accumulation of cholesterol and proteolipid protein in endosomes/lysosomes: Implications for Pelizaeus-Merzbacher disease. *J Cell Biol* 157:327–336.
- Southwood C, Gow A. 2001. Molecular pathways of oligodendrocyte apoptosis revealed by mutations in the proteolipid protein gene. *Microsc Res Tech* 52:700–708.
- Southwood CM, Garbern J, Jiang W, Gow A. 2002. The unfolded protein response modulates disease severity in Pelizaeus-Merzbacher disease. *Neuron* 36:585–596.
- Thomson CE, Vouyiouklis DA, Barrie JA, Wease KN, Montague P. 2005. *Plp* Gene regulation in the developing murine optic nerve: Correlation with oligodendroglial process alignment along the axons. *Dev Neurosci* 27:27–36.
- Trajkovic K, Dhaunchak AS, Goncalves JT, Wenzel D, Schneider A, Bunt G, Nave KA, Simons M. 2006. Neuron to glia signaling triggers myelin membrane exocytosis from endosomal storage sites. *J Cell Biol* 172:937–948.
- Trapp BD, Nishiyama A, Cheng D, Macklin E. 1997. Differentiation and death of premyelinating oligodendrocytes in developing rodent brain. *J Cell Biol* 137:459–468.
- Wolf NI, Sistermans EA, Cundall M, Hobson GM, Davis-Williams AP, Palmer R, Stubbs P, Davies S, Endziniene M, Wu Y, Chong WK, Malcolm S, Surtees R, Garbern JY, Woodward KJ. 2005. Three or more copies of the proteolipid protein gene *PLP1* cause severe Pelizaeus-Merzbacher disease. *Brain* 128:743–751.
- Woodward K, Kendall E, Vetrie D, Malcolm S. 1998. Pelizaeus-Merzbacher disease: Identification of Xq22 proteolipid-protein duplications and characterization of breakpoints by interphase FISH. *Am J Hum Genet* 63:207–217.
- Wrabetz L, Feltri ML, Quattrini A, Imperiale D, Previtali S, D'Antonio M, Martini R, Yin XH, Trapp BD, Zhou L, Chiu SY, Messing A. 2000. P₀ Glycoprotein overexpression causes congenital hypomyelination of peripheral nerves. *J Cell Biol* 148:1021–1033.
- Yin X, Kidd GJ, Wrabetz L, Feltri ML, Messing A, Trapp BD. 2000. Schwann cell myelination requires timely and precise targeting of P₀ protein. *J Cell Biol* 148:1009–1020.
- Yool DA, Klugmann M, McLaughlin M, Vouyiouklis DA, Dimou L, Barrie JA, McCulloch MC, Nave K-A, Griffiths IR. 2001. Myelin proteolipid proteins promote the interaction of oligodendrocytes and axons. *J Neurosci Res* 63:151–164.

Genetic Background Influences UPR but not PLP Processing in the *rumpshaker* Model of PMD/SPG2

M. McLaughlin · S. A. Karim · P. Montague ·
J. A. Barrie · D. Kirkham · I. R. Griffiths ·
J. M. Edgar

Accepted: 19 July 2006 / Published online: 31 August 2006
© Springer Science+Business Media, Inc. 2006

Abstract Mutations of the proteolipid protein gene (*PLP1*) cause Pelizaeus-Merzbacher disease (PMD) and Spastic paraplegia type 2 (SPG2). The *rumpshaker* mutation is associated with mild forms of PMD or SPG2 in man and the identical mutation occurs in mice, the phenotype depending on genetic background. The mild phenotype in C3H mice becomes a lethal disease when expressed on the C57BL/6 background. *rumpshaker* PLP is synthesised at a similar rate to wild type but is rapidly degraded by the proteasome. We show that the rates of synthesis, degradation and myelin incorporation of PLP/DM20 are similar in mutants on both backgrounds and therefore differences in PLP processing are unlikely to be the basis of the phenotypic variation. An unfolded protein response (UPR) is activated in *rumpshaker*. Whereas activation of CHOP correlates with phenotypic severity, we find no difference in the response of BiP and X-box protein1 (Xbp1) between the two strains.

Keywords Oligodendrocyte · Myelin · CHOP · Proteolipid protein · Rumpshaker · Misfolded protein · Pelizaeus-Merzbacher disease

Special issue dedicated to Anthony Campagnoni.

Electronic Supplementary Material Supplementary material is available to authorised users in the online version of this article at <http://dx.doi.org/10.1007/s11064-006-9122-y>.

M. McLaughlin · S. A. Karim · P. Montague ·
J. A. Barrie · D. Kirkham · I. R. Griffiths (✉) · J. M. Edgar
Applied Neurobiology Group, Division of Cell Sciences,
Institute of Comparative Medicine,
University of Glasgow, Bearsden, Glasgow G61 1QH,
Scotland
e-mail: I.Griffiths@vet.gla.ac.uk

Introduction

The X-linked proteolipid protein (*PLP1/Plp1*) gene encodes PLP and minor isoforms, such as DM20, which constitute the major proteins of CNS myelin. Mutations of the *PLP1/Plp1* gene cause Pelizaeus-Merzbacher disease (PMD) and Spastic Paraplegia type 2 (SPG2) in man and dysmyelinating disorders in a range of animal species [1, 2]. Missense mutations with single amino acid substitutions are a common cause of PMD/SPG2 and also account for the majority of the spontaneous mutations in animals. Across the whole range of missense mutations there is a wide spectrum of disease severity, which is usually ascribed to the alteration in specific residues and their location within the molecule. We have also shown that in the murine *rumpshaker* mutation (*Plp^{jp-rsh}*) (Ile¹⁸⁶Thr) the phenotype is markedly affected by the background strain, suggesting the influence of modifying gene(s). On the C3H background the phenotype is relatively benign with no seizures and normal longevity whereas expressing the mutation in the C57BL/6 genome results in a severe and lethal disorder [3]. As the genetic mutation and primary sequence of PLP are identical, the *rumpshaker* mutation provides a system in which to compare the pathogenetic mechanisms underlying “mild” and “severe” PMD/SPG2.

Many of the missense mutations in the *PLP1/Plp1* gene are thought to generate misfolded PLP/DM20, which is retained in the rough endoplasmic reticulum (RER) [4] leading to activation of the unfolded protein response (UPR) and oligodendrocyte apoptosis [5–7]. Despite the considerable amount of data on PLP-related disorders the dynamics of PLP processing was relatively under investigated. As a starting point we

determined how the oligodendrocyte handled wild type and *rumpshaker* PLP/DM20 on the C3H background [8]. Surprisingly, the rate of synthesis was similar in wild type and mutant but whereas the half life of normal PLP was ~24 h, the mutant product was degraded twice as fast, largely by a proteasome dependent mechanism. Despite the enhanced degradation a small proportion of *rumpshaker* PLP was incorporated into myelin at a slower rate than normal and was also inserted in the correct topology as shown by immunostaining with the conformation-sensitive O10 antibody [9]. The accelerated degradation of PLP on the C3H background is consistent with a survival response of the oligodendrocyte to accommodate the production of the misfolded mutant protein without activating apoptosis.

We undertook the present study to determine whether differences in the processing of PLP/DM20 or in the magnitude of the UPR might underlie the divergent phenotypes of *rumpshaker* on C3H and C57 backgrounds. Despite the very marked differences in phenotype, we find very little difference in the dynamics of PLP processing. The UPR was more variable with some representative markers, such as BiP and the X box protein 1 (*Xbp1*) showing a similar response in the two mutants while CHOP was activated to a greater extent in the more severe phenotype.

Materials and methods

Animals

The *rumpshaker* (*Plp^{jp-rsh}*) mutation arose originally in C3H mice and was maintained on a hybrid C3H/101 background (referred to hereafter as C3H *rumpshaker*). Female heterozygotes were crossed with wild type C57BL/6NCRIBR males (Charles River) over 10 generations and then intercrossed to generate a stable line (referred to hereafter as C57 *rumpshaker*). Mutant mice were genotyped by PCR amplification of genomic DNA and restriction digest of the novel *AccI* site. Animals for immunostaining were perfused with 4% paraformaldehyde and blocks from cervical cord prepared for cryosections as described [3]. All animal studies were approved by the Ethical Committee of the University of Glasgow and licensed by the UK Home Office.

Antibodies and immunostaining

PLP/DM20 was detected with a rabbit polyclonal antibody recognising the common C-terminal (gift from Prof. NP Groome) or a rat monoclonal (AA3,

gift from Dr. S Pfeiffer). MBP was detected with a mouse monoclonal (clone 12, gift from Prof. NP Groome) or a rabbit polyclonal antibody (Chemicon International Ltd., Harrow, England). CNP was detected with a mouse monoclonal (Chemicon). Monoclonal and polyclonal antibodies to MAG were obtained from Chemicon (clone 513) and as gifts from Prof NP Groome and Dr RH Quarles. A rabbit polyclonal (Santa Cruz Biotechnology Inc. Santa Cruz, CA) and a mouse monoclonal (Affiniti BioReagents, Cambridge Bioscience, Cambridge, UK) against CHOP (GAD153) were used. Rabbit polyclonal anti-BiP (GRP78) was obtained from Stressgen (Bioquote Ltd., York, UK). Anti-caspase-3 was obtained from R&D Systems Europe (Abingdon, UK). Oligodendrocytes were stained with the CC-1 antibody (Oncogene Research Products, CN Biosciences, Nottingham, UK).

Immunostaining of cryosections was performed as described previously [3].

Cell counts in spinal cord

Cryosections of cervical cord ventral funiculi were used to count CHOP+ nuclei, counterstained with DAPI. The methods for cell counting have been described [3].

RT-PCR

RNA was extracted from the spinal cord of mice aged P20 and the reversed transcription reaction performed as described previously [3, 10]. X box protein 1 (*Xbp1*) PCR protocol was performed essentially as described [11] using the primer sequences, forward 5'-AAACA-GAGTAGCTCAGACTGC-3' and reverse 5'-TCCTTCTGGGTAGACCTCTGGGAG-3'. The *Xbp1* PCR products were digested with *Pst1*, which cuts only the unspliced cDNA and the spliced and unspliced products resolved on a 2.5% agarose gel containing ethidium bromide. RNA extracted from cultured oligodendrocytes, which had been exposed to stress inducing conditions were processed in tandem with the cord tissue to serve as controls.

We also assessed levels of *Chop* and *ATF3* using cyclophilin as a control for invariant gene expression. Primers used were; *Chop*, forward 5'-CATACACCA CCACACCTGAAAG-3', reverse 5' CCGTTTCCTA GTTCTTCCTTGC-3' (accession # X67083.1) product size 356 bp; *ATF3*, forward 5'-CAACATCCAGGCC AGGTCT-3', reverse 5'-CTCTGCAATGTTCCTTCT TTT-3' (accession # BC064799.1) product size 532 bp. The primers for cyclophilin and PCR conditions were as described [10]. The products were resolved on a 2%

agarose gel visualised with ethidium bromide staining and the captured images quantified using Scion Image for Windows software (Scion Corporation). The intensity of the signal was corrected for the relative density of cyclophilin.

Primary oligodendrocyte cultures

Oligodendrocytes were isolated and cultured from the spinal cord of male P5 mice as previously described [8, 12]. C3H females homozygous for *rumpshaker* mutation were mated with hemizygous males to generate litters in which all pups were affected. Wild type C3H litters were also produced. As affected C57 mice do not survive to breeding age, C57 *rumpshaker* heterozygotes were mated with wild type males thus generating litters containing wild type and mutant males. Oligodendrocytes from spinal cords of C3H mice were pooled and plated onto two 35 mm poly-L-lysine coated plates per mouse. Oligodendrocytes were prepared from individual C57 mice and divided between two 35 mm plates. The genotype of each pup was confirmed by PCR of genomic DNA extracted from tail tips as previously described [3].

At 7 days in culture, the medium was removed, cells washed twice with Hank's buffered salt (HBS) then incubated for 30 min in HBS. The medium was replaced with 0.5 ml HBS containing [³⁵S]-Pro-Mix (Amersham Pharmacia Biotech, Little Chalfont, UK) at 100 μ Ci/ml. For analysis of protein synthesis, dishes were removed at 45 and 90 min, rinsed twice in chilled PBS and lysed with Buffer A (10 mM Tris pH 7.4, 150 mM NaCl, 1% triton X-100 and inhibitors of protease and phosphatase activity). For pulse chase experiments, cells were labelled for 90 min and chased by replacing the HBS with SATO medium supplemented with 2.5 mM cysteine/2.5 mM methionine. At the appropriate time point, cells were washed twice with chilled PBS then lysed with 75 μ l buffer A. The lysates were rotated at 4°C for 30 min and cell debris pelleted by centrifugation at 5,000 rpm for 5 min [8].

Brain slices and myelin extraction

A brain slice preparation from P20 mice was used to measure incorporation of newly synthesised radiolabelled PLP/DM20 into myelin. Following myelin enrichment on a sucrose gradient and two rounds of osmotic shock, PLP/DM20 was immunoprecipitated and the products resolved by SDS PAGE and transferred to PDVF membranes for exposure to a high sensitivity phosphorimage screen (Amersham) for a period of 1–2 weeks and the image captured on a

Storm phosphorimage system. Western blotting was then performed. Full details have been published [8].

Preparation of tissue for evaluation of UPR

Due to the marked reduction in the myelin content of the *rumpshaker* spinal cord compared with the wild type, a protocol was established which removed the bulk of the myelin and generated an organelle enriched membranous fraction and a cytosolic fraction. Spinal cords were snap frozen in liquid nitrogen and stored at –80°C until required. Tissues were homogenised using a Teflon homogenizer in 2 ml of 0.85 M sucrose, 10 mM Hepes (pH 7.4), 10 mM KCl and 1.5 mM Mg₂SO₄ containing the following protease and phosphatase inhibitors: 1 mM sodium vanadate, 1 mM sodium pyrophosphate, 1 mM benzamidine, 10 μ g/ml leupeptine, 10 μ g/ml aprotinin, 10 μ g/ml trypsin inhibitor, 1 mM EDTA, 1 mM DTT and 1 mM PMSF. 0.5 ml of 0.25 M sucrose with 10 mM Hepes was layered on top and samples centrifuged for 1 h at 100,000 g in a SW50.1 rotor. The myelin containing 0.85/0.25 M sucrose interface was discarded and a sample of the supernatant collected to represent the cytosolic fraction. The membrane rich pellet fraction was sonicated in 0.25 M sucrose, 10 mM Hepes buffer supplemented with the protease and phosphatase inhibitors. About 25 μ g of the appropriate fraction was analyzed by western blotting.

Statistical analysis

Statistical significance of differences between values was assessed by ANOVA followed by Bonferonni's post hoc comparison test with significance $P < 0.05$ using Graphpad Prism software (GraphPad Software Inc.).

Results

Genetic background influences steady state level of myelin proteins in *rumpshaker*

In a previous study we quantified levels of representative proteins in myelin fractions from spinal cords of P20 mice, a time of active myelination [3]. Levels of PLP and DM20 per unit of myelin in C3H mutants were 9 and 15%, respectively, of wild type while in C57 *rumpshaker* values were 6 and 4%, respectively. In the C3H mutant levels of MBP, CNP and MAG were approximately 60, 81 and 71%, respectively relative to wild type whereas in the C57 *rumpshaker* these

proteins were only 30, 26 and 32%, respectively. Levels of Plp mRNA in both mutants were 66–68% of respective wild type while message for the other myelin proteins was very similar to control. Analysis of brain myelin extracts and mRNA levels found changes very similar to those in the spinal cord (data not shown). Thus, the genetic background on which the *rumpshaker* mutation is expressed appears to have a greater influence on the level of myelin proteins other than PLP/DM20, such as MBP.

The rates of PLP synthesis and degradation are not affected by expressing the *rumpshaker* mutation on different genetic backgrounds

Our previous work showed that C3H *rumpshaker* mice synthesised PLP and DM20 at similar rates to wild type although the rate of degradation was markedly enhanced ($T_{1/2}$ *rumpshaker* PLP 11 h, wild type PLP 23 h) [8]. We therefore, compared these parameters in mutants on the C57 background with their corresponding wild type. As cultures have to be prepared from individual C57 mice (see Materials and methods) only 2 time points could be evaluated; a similar protocol was adopted for the C3H genotype. To determine rates of translation, primary oligodendrocyte cultures were radiolabelled with [35 S] Pro-Mix for 45 and 90 min. The rate of accumulation of immunoprecipitated radiolabelled PLP and DM20 was not significantly different between wild type and mutant on either background. However, the total amount of PLP/DM20 (labelled and unlabelled) recovered was considerably lower in the mutants (Fig. 1A, B) compared with wild type.

To study degradation, we pulse labelled the cultures with [35 S] Pro-Mix for 90 min and sampled at 0 h (control) and after 24 h of chase. The decreases in PLP and DM20 over this period were significantly greater in the mutants than their respective wild types (Fig. 2A, B), confirming that *rumpshaker* PLP and DM20 are more labile than the wild type isoforms. The relative decrease of *rumpshaker* product compared with corresponding wild type protein was similar between the two strains at 70 and 78% for PLP and 70 and 73% for DM20 in C3H and C57, respectively.

Genetic background does not influence incorporation of *rumpshaker* PLP into myelin

rumpshaker mice are hypomyelinated compared with wild type and the deficit is accentuated on the C57 background. However, immunostaining and western blotting show both PLP and DM20 to be present in myelin [3] in both genotypes. Additionally, the intra-

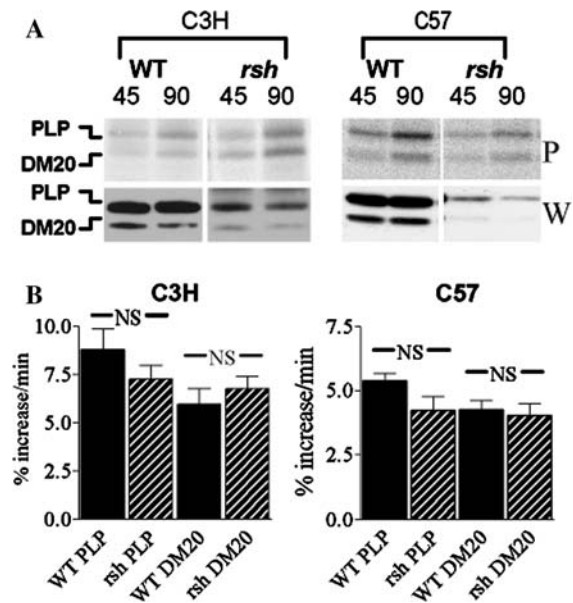


Fig. 1 Synthesis of PLP/DM20 in wild type and mutant oligodendrocytes from C3H and C57 mice. (A) Cells were radiolabelled for 45 or 90 min prior to lysis and immunoprecipitation. The upper panel is a phosphorimage (P) of the radiolabelled precipitates and the lower panel (W) a western blot using an antibody recognising PLP and DM20. The radiolabelled protein increases with time in all mice. The amount of total protein (includes radiolabelled and non-labelled) precipitated from the mutants, particularly C57, is markedly lower than from wild type. (B) Comparison of the synthesis rates for PLP and DM20, expressed as percentage increase in signal per minute, between C3H and C57 mutants relative to their respective wild types ($M \pm SEM$, N for C3H = 5, for C57 = 6). There is no significant difference between mutant and corresponding wild type values

cellular distribution of PLP/DM20 did not appear different between the two mutants with a robust signal co-localised with the RER and a less intense diffuse staining throughout the cytoplasm to the cell membrane (see Fig. 4C of McLaughlin et al., 2006). To compare the correct topographical insertion of PLP/DM20 into membrane, we stained live oligodendrocytes from wild type and mutant mice of both strains with the O10 antibody [9] prior to permeabilisation and immunostaining for PLP/DM20. Virtually 100% of C3H and C57 wild type oligodendrocytes with PLP/DM20+ cell bodies were also surface stained with O10. In contrast, $64 \pm 10\%$ of C3H ($M \pm SEM$, $n = 5$) and $69 \pm 6\%$ of C57 *rumpshaker* oligodendrocytes, respectively, that expressed cytoplasmic PLP/DM20 had surface staining for O10; the values between the mutants are not significantly different. As the intensity of O10 staining in the mutants, particularly for the C57 strain, appeared more variable than for wild type we quantified the rate of PLP/DM20 incorporation into myelin.

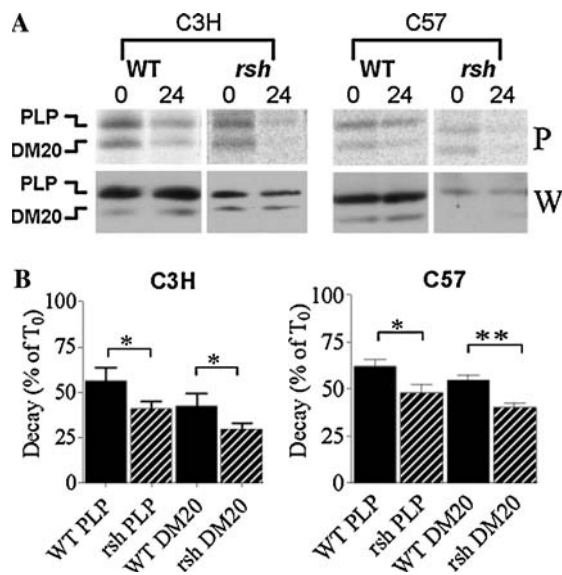


Fig. 2 Degradation of PLP/DM20 in oligodendrocytes from C3H and C57 wild type and *rumpshaker* mice. **(A)** Representative experiment from wild type and mutant mice showing the phosphorimage (P) and corresponding western blot (W) of the immunoprecipitates. Cells were pulse labelled with [³⁵S] Pro-Mix for 90 min and then chased out for 24 h, prior to immunoprecipitation. The accelerated decay of newly synthesised protein in the mutant is evident. **(B)** Decrease in levels of newly synthesised PLP and DM20 in C3H and C57 wild type and *rumpshaker* mice, 24 h after the end of the pulse labelling. The data ($M \pm SEM$, N for C3H = 4, for C57 = 9 or 10) are presented as the percentage of the level after the 90-min pulse (T_0). In both strains of mice the levels of mutant PLP and DM20 are significantly lower than the corresponding wild type value. The ratio (*rumpshaker*:wild type decay) for C3H and C57 PLP is 0.7 and 0.78, respectively and for DM20 is 0.7 and 0.73, respectively

We labelled brain slices with [³⁵S] Pro-Mix for up to 6 h, prepared myelin enriched fractions at 2, 4 and 6 h and compared the labelled, immunoprecipitated products between mutants and their respective wild types. Newly synthesised protein accumulated progressively over the 6-h labelling period in total homogenates from the brain slices. Newly synthesised PLP and DM20 were present in myelin after a 2-h label in wild types and mutants and increased over the subsequent 4 h. Figure 3A, B show the results for C57 mice; the data for C3H mice have been published previously [8]. The rate and amount of newly synthesised PLP accumulating in myelin were significantly lower in mutants of both strains compared with their corresponding wild types. The rate of DM20 incorporation was not significantly different in *rumpshaker* of either strain, relative to wild type although the weak signal of DM20 did influence the accuracy of the quantitation procedure and contribute to the large standard error. The rates of incorporation of PLP and DM20 were not different in C57 *rumpshaker*

compared with the corresponding isoforms in C3H mutants (Fig. 3C).

Some parameters of the UPR are affected by genetic background

Many misfolded proteins induce a cascade of protein activation resulting in the expression of chaperones, such as BiP (GRP78), to assist protein folding and transcription factors such as CHOP and XBP1 [13–15]. By western blotting, BiP protein was elevated in mutants on both genetic backgrounds at $185 \pm 11\%$, ($M \pm SEM$, $n = 4$) for C3H *rumpshaker* and $187 \pm 12\%$ for C57 *rumpshaker*, compared with their respective wild type (100%) (Fig. 4A). The values of the mutants are not significantly different but both are greater than their respective wild type ($P = 0.0002$).

We evaluated levels of *Chop* and *ATF3* mRNA in spinal cords of P20 mice using RT-PCR. Levels of both transcription factors were significantly higher in mutants than corresponding wild type. Additionally, the elevation of *Chop* was greater in the C57 than the C3H *rumpshaker* relative to the respective wild type, whereas the increases in *ATF3* were similar in the two mutants (Fig. 4B, C). The levels of *Chop* and *ATF3* were similar in wild type mice of both genotypes (not shown).

Immunostaining of spinal cord from *rumpshaker* of both backgrounds revealed numerous CHOP+ nuclei, more so in the C57 mutants (Fig. 4D). Double immunostaining showed that the CHOP stained nuclei were associated only with oligodendrocytes (Fig. 4E and supplementary Fig. 1A, B). The proportion of oligodendrocytes with CHOP+ nuclei in C57 *rumpshaker* was approximately double that in C3H mutants when expressed as a percentage of the total DAPI-stained glial nuclei or the CC-1 stained cells (Fig. 4F). The numbers of DAPI nuclei and CC-1+ cells did not differ between the two mutant genotypes. No nuclear CHOP staining was detected in wild type spinal cords. Double immunostaining for CHOP and caspase-3 showed no obvious co-localisation. Additionally, the caspase-3+ oligodendrocytes had pyknotic nuclei whereas the CHOP+ nuclei appeared normal when viewed with the DAPI stain (supplementary Fig. 1C).

We assessed cleavage of the *Xbp1* mRNA from spinal cord of P20 C3H and C57 mice using RT-PCR. No spliced (active) *Xbp1* was detected in wild type tissue with the entire unspliced message being cleaved by *PstI* digestion. An equal amount of spliced transcript was detected in *rumpshaker* mice on both genetic backgrounds but this was small compared with the vigorous response to chemically induced ER stress (Fig. 4F).

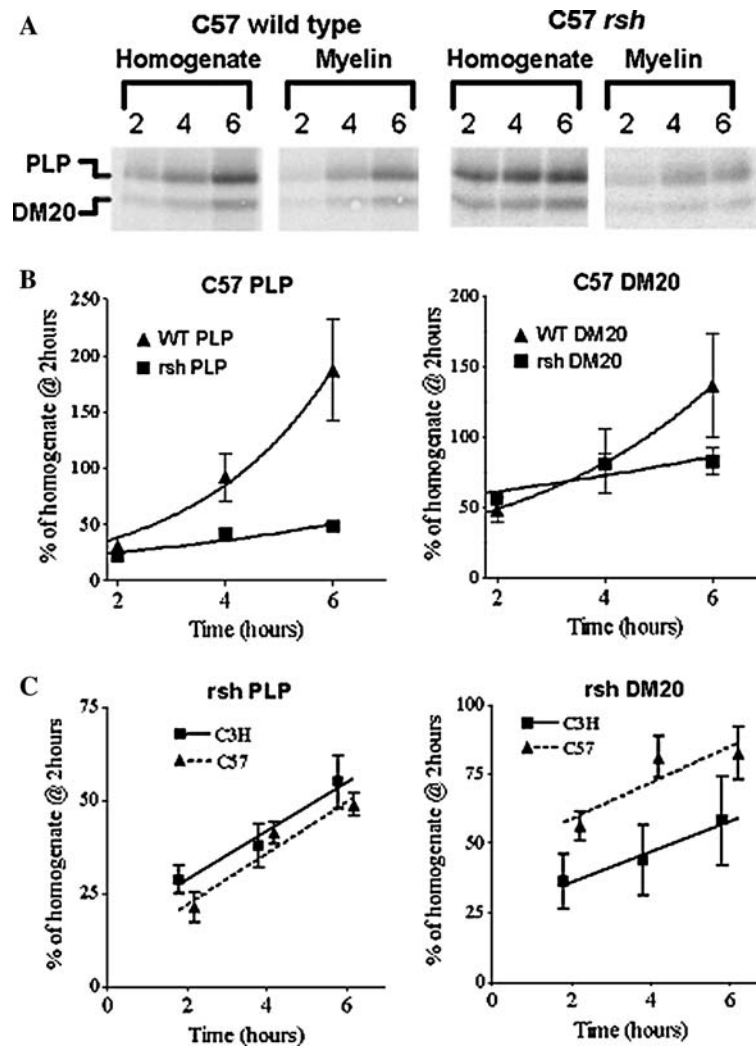


Fig. 3 Incorporation of wild type and mutant PLP/DM20 into myelin. **(A)** Phosphorimage of newly synthesised PLP/DM20 in total homogenate and myelin fractions from brain slices of C57 wild type and *rumpshaker* mice. Slices were radiolabelled for 2, 4 and 6 h and the proteins immunoprecipitated from 400 μ g total homogenate and 20 μ g myelin fractions; this ratio was retained for all studies. The signal intensity increases with time in both fractions from the two genotypes but the myelin signal relative to the homogenate signal is lower in the mutant. **(B)** Quantitative

data from the above study. At each time point the amount of newly synthesised PLP or DM20 incorporated into myelin ($M \pm SEM$, $n = 3$) is expressed as a proportion of the total homogenate signal at 2 h, which was not different between wild type and mutant (not shown). The curves for wild type and mutant are significantly different for PLP but not DM20. **(C)** Comparison of the incorporation rates of radiolabelled PLP and DM20 into myelin between C3H and C57 *rumpshaker*. The slopes are not different between the two mutants for either isoform

The majority of *Xbp1* message in both mutants remained unspliced and therefore susceptible to *PstI* digestion.

We also examined levels of heat shock proteins 70 and 90, which were not elevated in mutants relative to wild type (data not shown).

Discussion

Missense mutations of the *PLP1/Plp1* gene resulting in an amino acid substitution are a common cause of

PMD and SPG2 in man. PMD/SPG2 is markedly heterogeneous, varying from early lethality in severe forms of PMD through to milder clinical signs with longevity associated with SPG2. Similar heterogeneity exists in the animal models where, for example, early death occurs in the *myelin-deficient* rat and the *jimpy* mouse while the *shaking pup* and *paralytic tremor* rabbit have a more protracted disease [17]. The basis for this heterogeneity is unclear but may include differences in the mutated codon and its position in the molecule and the influence of modifying genes. How such factors might affect pathogenetic pathways is also

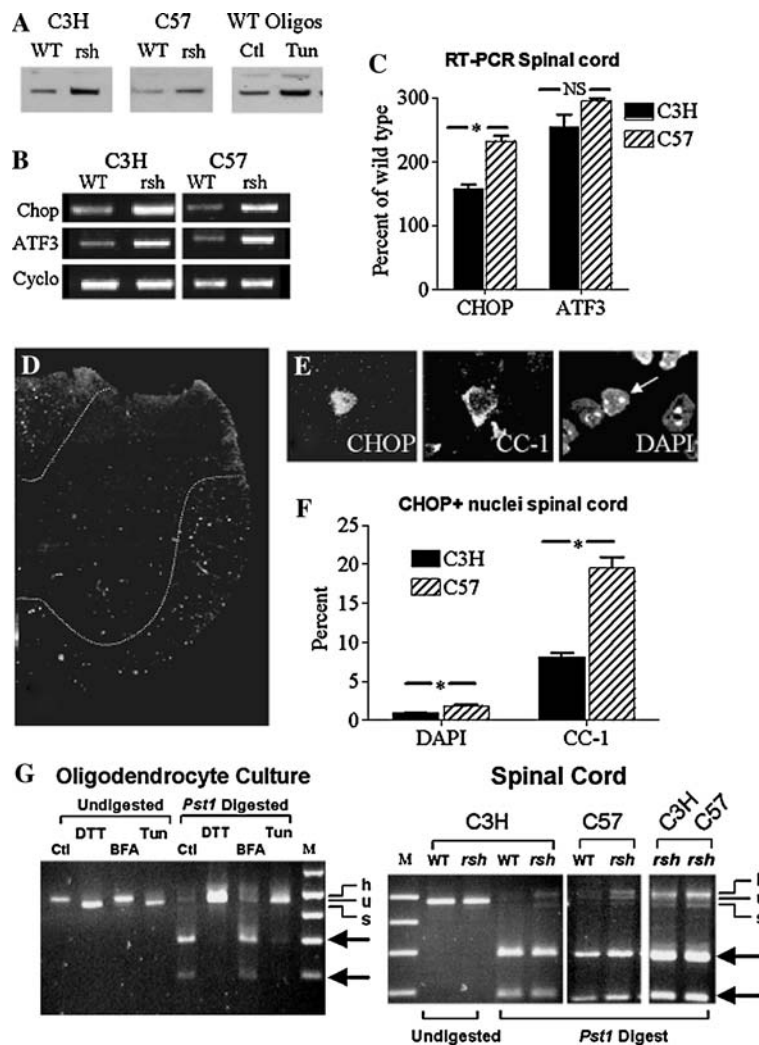


Fig. 4 The UPR is activated in *rumpshaker* but only certain components show differences between the two genetic backgrounds. **(A)** Representative western blots for BiP in spinal cord of wild type (WT) and *rumpshaker* (*rsh*) mice on the C3H and C57 background. As a positive control, wild type oligodendrocytes (WT oligos) have been “stressed” by treating with 2 μg/ml tunicamycin for 18 h (Tun) or left untreated (Ctl). Spinal cords from P20 mice were fractionated to separate membranous, pellet and cytosolic fractions. BiP analysis was performed on 25 μg of pellet or on 10 μg of oligodendrocyte lysis. The induction of BiP in the mutant spinal cord is similar between the two genotypes. The upregulation of BiP after tunicamycin treatment of *rumpshaker* oligodendrocytes was similar to wild type (not shown). **(B)** RT-PCR analysis of P20 spinal cords from C3H and C57 wild type (WT) and *rumpshaker* (*rsh*) mice for *Chop* and *ATF3* mRNA using cyclophilin (*Cyclo*) as an internal control. Both mutants show upregulation of the transcription factors relative to their wild type. **(C)** Quantification of the RT-PCR data for the two mutants ($n = 5$) normalised for cyclophilin and expressed as a percentage of the respective wild type. The upregulation of *Chop* is greater ($P < 0.05$) in the C57 *rumpshaker* whereas *ATF3* shows a similar increase in both mutants. **(D)** Hemisection of spinal cord of C57 *rumpshaker* immunostained for CHOP. Numerous CHOP+ nuclei are evident in the white matter (outlined). Bar = 100 μm. **(E)** Confocal section of spinal cord from C57 *rumpshaker* immunostained for CHOP, CC-1 antibody to label oligodendrocytes and DAPI. The CHOP+ nucleus appears morphologically normal in

the DAPI stain (arrow) (see also Supplementary Fig. 1B, inset). **(F)** The proportion of oligodendrocytes with CHOP+ nuclei in the two mutants is expressed as a percentage of the total DAPI nuclei or the CC-1 stained cells in the ventral column of spinal cord. The proportion in the C57 *rumpshaker* is significantly higher than the C3H mutant. **(G)** Activation of *Xbp1* converts an unspliced to a spliced mRNA that is resistant to digestion by *PstI*. Wild type oligodendrocytes untreated controls (Ctl) or treated with DTT, Brefeldin A (BFA) or tunicamycin (Tun) and then undigested or digested with *PstI*. In the chemically treated, undigested samples the smaller spliced product (s) is evident particularly after DTT treatment whereas very little is evident after BFA treatment. Digestion with *PstI* shows that all the DTT treated product is in the spliced form and resistant to the enzyme whereas the vast majority of the control has yielded the two cleavage products (arrows). In the BFA sample the majority of product has been cleaved, only a small spliced band is present. The tunicamycin treated sample shows a predominant spliced band with small amounts of cleavage products. (M = size markers; s = spliced; u = unspliced; h = a hybrid species, [see 16]. In the spinal cord from C3H wild type and *rumpshaker* the undigested samples show little obvious difference but after *PstI* digestion a small undigested spliced band is evident in *rumpshaker*, however, the majority of the product has been cleaved (arrows). Digestion of samples from C57 wild type and *rumpshaker* mice (middle lanes) produces a pattern very similar to that from the C3H mice. When compared directly (right lanes) the pattern from the two mutants is indistinguishable

uncertain. The *rumpshaker* mutation encodes an isoleucine to threonine substitution (Ile¹⁸⁶Thr) in the putative extracellular “CD” loop of the PLP/DM20 molecule that results in benign or lethal phenotypes dependent on genetic background. As the primary structure of the protein is identical in both situations, the *rumpshaker* mutation provides a system in which to test whether changes in processing of PLP/DM20 or differences in the UPR are associated with the two extreme phenotypes. Surprisingly, we find that there is little difference in PLP processing between the two phenotypes.

Processing of *rumpshaker* PLP is similar in the two phenotypes

The majority of misfolded *rumpshaker* PLP/DM20 is retained in the RER prior to proteasomal degradation, only a minority reaching the cell membrane [8]. No obvious differences were noted between oligodendrocytes from C3H and C57 *rumpshaker* in terms of ultrastructure or cytoplasmic distribution of PLP/DM20 after immunostaining [3 and unpublished observations]. We now find that the rates of PLP/DM20 translation, degradation and myelin incorporation are also very similar in *rumpshaker* on the two genetic backgrounds and different from their respective wild type. Also, the proportion of oligodendrocytes incorporating PLP/DM20 into the plasma membrane is not influenced by background. Although we did not investigate the mechanism of degradation in the C57 mutant it seems safe to assume the proteasome is involved predominantly, as with the C3H *rumpshaker* [8].

The apparently similar processing of PLP/DM20 in two extreme phenotypes caused by the *rumpshaker* mutation does not mean that this pathway is unimportant in other *Plp1* mutants. In the severe phenotypes associated with the *jimpy* and *jimpy^{msd}* mutations PLP/DM20 does not reach the plasma membrane in vitro or in vivo [6, 18], a clear difference from the severe form of *rumpshaker*. Also, *jimpy^{msd}* PLP is complexed with calnexin in the RER [19], whereas we failed to demonstrate a similar interaction with *rumpshaker* PLP [8]. Absence or reduction of wild type PLP/DM20 in myelin does not cause a severe dysmyelinating phenotype in mouse or man [20, 21] and introduction of wild type PLP/DM20 to murine *Plp1* mutants does not reverse the phenotype [22] suggesting that missense mutations may operate by a “gain of function” mechanism. The present study suggests that this putative novel function may not directly involve the PLP/DM20 processing pathway. It is possible that the burden of processing the abundant *rumpshaker*

PLP/DM20 disrupts the dynamics of other myelin components.

Unfolded protein response

Cells have developed mechanisms such as UPR and ERAD to protect themselves against protein misfolding. The presence of unfolded protein within the ER may activate a cascade of protein interactions and dissociations initiated primarily by the chaperone BiP whose association with three stress sensors PERK, IRE1 and ATF6 maintains these proteins in an inactive state. Upon stress induction, BiP dissociates, translocates to the ER lumen to assist in protein folding, and the sensor proteins adopt an active status. The activated proteins induce a series of interacting pathways constituting the UPR [23]. PERK activation inhibits eif2 α leading to reduced translation of the misfolded protein [24] although, conversely, other pathways involving GADD34 promote protein synthesis [11]. We find no evidence for reduced PLP/DM20 synthesis, even in the phenotypically severe C57 *rumpshaker*. Other aspects of the UPR, such as the induction of BiP, ATF3 and to a lesser extent the generation of spliced *Xbp1* mRNA, are clearly activated in *rumpshaker*. However, there is no difference in the magnitude of the responses between the two phenotypes and overall, the response is modest compared with the chemically induced changes in oligodendrocytes. The only clear distinction in the parameters examined between the two phenotypes is the CHOP response, where there is at least twice the number of CHOP+ nuclei in a section of C57 *rumpshaker* spinal cord and a corresponding upregulation of *Chop* mRNA. In many cell types CHOP acts as a pro-apoptotic factor, which is activated upstream of effector caspases, such as caspase-3. A pro-apoptotic action of CHOP would correlate with the increased number of apoptotic cells in the C57 mutant [3]. However, a previous report suggested that in *rumpshaker*, CHOP may act as a protective factor, as mutant mice carrying a null *Chop* allele fared worse than the unmodified *rumpshaker* [7]. This apparent discrepancy will need further study.

Pathogenesis of the dysmyelinating phenotype

The present study does not fully resolve the basis of phenotypic severity in *rumpshaker* or other *PLP1/Plp1* missense mutations. It seems unlikely that differences in PLP/DM20 processing, such as the rate of degradation or rate of incorporation into myelin, fully account for such a diversity of phenotypes. As demonstrated in this

and other studies, the UPR is clearly activated and some pathways, most notably CHOP, do correlate with phenotypic severity. We propose that the level of glial cell apoptosis may be related to the magnitude of the CHOP induction although, as the overall rates of translation and degradation appear similar in C3H and C57 mutants, it is not obvious why CHOP induction is greater in the latter. We found no cells simultaneously expressing CHOP and caspase-3 and whereas the nuclei in caspase+ cells were pyknotic, the majority of CHOP+ nuclei appeared normal.

The temporal nature of CHOP induction and the appearance of apoptotic markers vary depending on the cell type and nature of the stress inducer. In general, caspase-3 cleavage is considered to be an end stage event in apoptosis, downstream of CHOP expression [25, 26] and the above findings may reflect this temporal difference. Alternatively, the lack of colocalisation of these markers may reflect two distinct cellular populations where the response to ER stress is either terminal (caspase-3) or survivable (CHOP) in cells [7, 27]. This requires clarification and perhaps examination of markers implicated in events upstream of caspase-3 would identify a divergence in the stress/apoptotic response of both populations.

Acknowledgments We are grateful to Prof. NP Groome and Drs S Pfeiffer and RH Quarles for the gift of antibodies and to Dr H. Harding for advice on the UPR. Grant Information. This work was supported by The Wellcome Trust and Birth Defects Foundation.

References

- Hudson LD (2003) Pelizaeus-Merzbacher disease and spastic paraplegia type 2: two faces of myelin loss from mutations in the same gene. *J Child Neurol* 18:616–624
- Nave K-A, Griffiths IR (2004) Models of Pelizaeus-Merzbacher disease. In: Lazzarini RA, Griffin JW, Lassmann H, Nave K-A, Miller RH, Trapp BD (eds) *Myelin biology and disorders*. Elsevier, Amsterdam, pp 1125–1142
- Al-Saktawi K, McLaughlin M, Klugmann M, Schneider A, Barrie JA, McCulloch MC, Montague P, Kirkham D, Nave K-A, Griffiths IR (2003) Genetic background determines phenotypic severity of the *Plp rumpshaker* mutation. *J Neurosci Res* 72:12–24
- Gow A, Lazzarini RA (1996) A cellular mechanism governing the severity of Pelizaeus-Merzbacher disease. *Nat Genet* 13:422–428
- Gow A, Southwood CM, Lazzarini RA (1998) Disrupted proteolipid protein trafficking results in oligodendrocyte apoptosis in an animal model of Pelizaeus-Merzbacher disease. *J Cell Biol* 140:925–934
- Southwood C, Gow A (2001) Molecular pathways of oligodendrocyte apoptosis revealed by mutations in the proteolipid protein gene. *Microsc Res Tech* 52:700–708
- Southwood CM, Garbern J, Jiang W, Gow A (2002) The unfolded protein response modulates disease severity in Pelizaeus-Merzbacher disease. *Neuron* 36:585–596
- McLaughlin M, Barrie JA, Karim SA, Montague P, Edgar JM, Kirkham D, Thomson CE, Griffiths IR (2006) Processing of PLP in a model of Pelizaeus-Merzbacher disease/SPG2 due to the *rumpshaker* mutation. *Glia* 53:715–722
- Jung M, Sommer I, Schachner M, Nave K-A (1996) Monoclonal antibody O10 defines a conformationally sensitive cell-surface epitope of proteolipid protein (PLP): evidence that PLP misfolding underlies dysmyelination in mutant mice. *J Neurosci* 16:7920–7929
- Montague P, Dickinson PJ, McCallion AS, Stewart GJ, Savioz A, Davies RW, Kennedy PGE, Griffiths IR (1997) Developmental expression of the murine *Mobp* gene. *J Neurosci Res* 49:133–143
- Marciniak SJ, Yun CY, Oyadomari S, Novoa I, Zhang YH, Jungreis R, Nagata K, Harding HP, Ron D (2004) CHOP induces death by promoting protein synthesis and oxidation in the stressed endoplasmic reticulum. *Genes Dev* 18:3066–3077
- Montague P, Barrie JA, Thomson CE, Kirkham D, McCallion AS, Davies RW, Kennedy PGE, Griffiths IR (1998) Cytoskeletal and nuclear localization of MOBP polypeptides. *Europ J Neurosci* 10:1321–1328
- Rutkowski DT, Kaufman RJ (2004) A trip to the ER: coping with stress. *Trends Cell Biol* 14:20–28
- Zhang KZ, Kaufman RJ (2004) Signaling the unfolded protein response from the endoplasmic reticulum. *J Biol Chem* 279:25935–25938
- Harding HP, Calton M, Urano F, Novoa I, Ron D (2002) Transcriptional and translational control in the mammalian unfolded protein response. *Annu Rev Cell Dev Biol* 18:575–599
- Shang J (2005) Quantitative measurement of events in the mammalian unfolded protein response. *Methods* 35:390–394
- Duncan ID (1995) Inherited disorders of myelination of the central nervous system. In: Kettenmann H, Ransom BR (eds) *Neuroglia*, Oxford University Press, Oxford, pp 843–858
- Gow A, Friedrich VL Jr, Lazzarini RA (1994) Many naturally occurring mutations of myelin proteolipid protein impair its intracellular transport. *J Neurosci Res* 37:574–583
- Swanton E, High S, Woodman P (2003) Role of calnexin in the glycan-independent quality control of proteolipid protein. *EMBO J* 22:2948–2958
- Garbern J, Yool DA, Moore GJ, Wilds I, Faulk M, Klugmann M, Nave K-A, Siermans EA, van der Knaap MS, Bird TD, Shy ME, Kamholz J, Griffiths IR (2002) Patients lacking the major CNS myelin protein, proteolipid protein 1, develop length-dependent axonal degeneration in the absence of demyelination and inflammation. *Brain* 125:551–561
- Klugmann M, Schwab MH, Pühlhofer A, Schneider A, Zimmermann F, Griffiths IR, Nave K-A (1997) Assembly of CNS myelin in the absence of proteolipid protein. *Neuron* 18:59–70
- Schneider A, Griffiths IR, Readhead C, Nave K-A (1995) Dominant-negative action of the *jimpy* mutation in mice complemented with an autosomal transgene for myelin proteolipid protein. *Proc Natl Acad Sci USA* 92:4447–4451
- Ma YJ, Hendershot LM (2001) The unfolding tale of the unfolded protein response. *Cell* 107:827–830
- Harding HP, Zhang YH, Ron D (1999) Protein translation and folding are coupled by an endoplasmic-reticulum-resident kinase. *Nature* 397:271–274

25. Vlug AS, Teuling E, Haasdijk ED, French P, Hoogenraad CC, Jaarsma D (2005) ATF3 expression precedes death of spinal motoneurons in amyotrophic lateral sclerosis-SOD1 transgenic mice and correlates with c-Jun phosphorylation, CHOP expression, somato-dendritic ubiquitination and Golgi fragmentation. *Eur J Neurosci* 22:1881–1894
26. Liu N, Kuang X, Kim HT, Stoica G, Qiang W, Scofield VL, Wong PK (2004) Possible involvement of both endoplasmic reticulum- and mitochondria-dependent pathways in Mo-MuLV-ts1-induced apoptosis in astrocytes. *J Neurovirol* 10:189–198
27. Lin W, Harding HP, Ron D, Popko B (2005) Endoplasmic reticulum stress modulates the response of myelinating oligodendrocytes to the immune cytokine interferon-gamma. *J Cell Biol* 169:603–612

Processing of PLP in a Model of Pelizaeus-Merzbacher Disease/SPG2 due to the *rumpshaker* Mutation

MARK McLAUGHLIN, JENNIFER A. BARRIE, SAADIA KARIM, PAUL MONTAGUE, JULIA M. EDGAR, DOUGLAS KIRKHAM, CHRISTINE E. THOMSON, AND IAN R GRIFFITHS*

Applied Neurobiology Group, Institute of Comparative Medicine, University of Glasgow, Bearsden Glasgow G61 1QH, Scotland

KEY WORDS

oligodendrocyte; myelin; misfolded protein; dysmyelination; spastic paraplegia type 2

ABSTRACT

The *rumpshaker* mutation of the X-linked myelin proteolipid protein (*PLP1*) gene causes spastic paraplegia type 2 or a mild form of Pelizaeus-Merzbacher disease in man. The identical mutation occurs spontaneously in mice. Both human and murine diseases are associated with dysmyelination. Using the mouse model, we show that the low steady state levels of PLP result from accelerated proteasomal degradation rather than decreased synthesis. The $T_{1/2}$ for degradation of *rumpshaker* PLP is 11 h compared with 23 h for wild type. A minority of newly synthesized PLP is incorporated into myelin in the correct orientation but at a reduced rate compared with wild type. However, inhibition of proteasomal degradation does not increase the level of PLP incorporated into myelin. As *Plp* null mice do not have a similar myelin deficiency, it is unlikely that the reduced PLP levels are the main cause of the dysmyelination. *Rumpshaker* oligodendrocytes also have a reduced level of other myelin proteins, such as MBP, although the mechanisms are not yet defined but are likely to operate at a translational or post-translational level. © 2006 Wiley-Liss, Inc.

INTRODUCTION

Proteolipid protein (PLP) and the smaller DM20 isoform constitute the major proteins of CNS myelin. The functions of PLP/DM20 have been partly clarified through the study of PLP-deficient mice and humans. Despite its abundance, the protein is not essential for myelin formation but is required for the formation of a normal intra-period line (IPL) and maintenance of axonal integrity (Garbern et al., 2002; Griffiths et al., 1998; Klugmann et al., 1997). Both PLP and DM20 seem necessary for completely normal function, although each is capable, individually, of insertion into myelin (McLaughlin et al., 2002).

Mutations of the X-linked myelin *PLP1/Plp1* gene cause Pelizaeus-Merzbacher disease (PMD) and spastic paraplegia type 2 (SPG2) in man and dysmyelinating disorders in a range of animal species (Hudson, 2003; Inoue, 2005). In man, gene duplication is the most frequent cause of PMD, with a range of missense mutations accounting for the majority of the remaining cases. Typically, missense mutations are associated with dysmyelination characterized by hypomyelination, increased apoptosis of oligodendro-

cytes, and gliosis (Al-Saktawi et al., 2003; Skoff, 1995), although the severity of each parameter varies between different mutations. The lack of a similar phenotype in PLP-deficient mice and humans (Garbern et al., 2002; Klugmann et al., 1997) suggests that missense mutations cause disease through a “gain of function” effect.

The *rumpshaker* mutation of the *PLP1/Plp1* gene (*Plp*^{*jp-rsh*}) causes disease in both man and mouse and provides an excellent model of mild forms of PMD and of SPG2. The distinction between mild PMD and SPG2 is blurred depending on the clinical presentation, which may change over time and also on individual clinicians; both syndromes have been ascribed to the *rumpshaker* mutation, with spastic paraparesis as a major sign (Johnston and McKusick, 1962; Kobayashi et al., 1994; Naidu et al., 1997). The mutation, an amino acid substitution (Ile¹⁸⁶Thr), was described first in mice of the C3H.HeH strain, in which it causes a relatively benign phenotype with normal longevity and fertility and is characterized by mild to moderate dysmyelination with oligodendrocyte numbers being maintained (Al-Saktawi et al., 2003; Griffiths et al., 1990). Many larger axons are either naked or surrounded by thin sheaths, whereas the smaller axons obtain sheaths of appropriate thickness by 12 to 18 months (Edgar et al., 2004). An outstanding question is why the surviving oligodendrocytes fail to assemble normal amounts of myelin, particularly around larger axons.

Misfolding of proteins is a common mechanism by which mutations cause disease (Sanders and Myers, 2004), and cells have evolved the unfolded protein response (UPR) and endoplasmic reticulum-associated degradation (ERAD) to deal with this event (Ellgaard and Helenius, 2003; Jarosch et al., 2003; Rutkowski and Kaufman, 2004). Evidence for a UPR is present in *rumpshaker* mice (Southwood and Gow, 2001; Southwood et al., 2002), suggesting that PLP/DM20 is misfolded. As oligodendrocytes generate massive amounts of membrane during myelination and PLP accounts for ~50% of protein in myelin, the *rumpshaker* mutation provides an ideal model to dissect how the cell deals with a misfolded, non-

Grant sponsor: The Wellcome Trust; Grant sponsor: Birth Defects Foundation.

*Correspondence to: I.R. Griffiths, Applied Neurobiology Group, Division of Cell Sciences, University of Glasgow, Bearsden, Glasgow G61 1QH, Scotland.
E-mail: I.Griffiths@vet.gla.ac.uk

Received 26 October 2005; Accepted 10 January 2006

DOI 10.1002/glia.20325

Published online 27 February 2006 in Wiley InterScience (www.interscience.wiley.com).

glycosylated, polytopic membrane protein. Very little is known about the dynamics of PLP/DM20 encoded by missense mutations or how this may influence the processing of other myelin components. Evidence, largely from transfected heterologous cells, has implicated impaired protein trafficking in that the products are retained within the rough endoplasmic reticulum (RER) (Gow and Lazzarini, 1996). Variations in trafficking between different *PLP1/Plp1* mutations have been demonstrated in such systems and, in general, suggest that the impairment correlates with phenotypic severity of the natural disease (Thomson et al., 1997). The purpose of this study was to establish how the oligodendrocyte handles misfolded *rumpshaker* PLP.

We find that *rumpshaker* oligodendrocytes synthesize PLP/DM20 as efficiently as their wild type counterparts but, once formed, much of the protein is rapidly degraded, most probably by the proteasome, with a minority inserting correctly into the myelin membrane.

MATERIALS AND METHODS

Animals

The *rumpshaker* (*Plp^{jp-rsh}*) mutation arose originally in C3H.HeH mice and was maintained on a hybrid C3H/101 background. Mutant mice were genotyped by PCR amplification of genomic DNA and restriction digest of the novel *AccI* site (Schneider et al., 1992). All animal studies were approved by the Ethical Committee of the University of Glasgow and licensed by the UK Home Office.

Quantitative Real Time PCR (qRT-PCR)

Total RNA was extracted from oligodendrocyte cultures using RNazol Bee reagent (Tel-Test Inc, Friendswood, TX) following the manufacturer's instructions. RNA was extracted from wild type and *rumpshaker* cultures and reconstituted in DEPC water. RNA quality and integrity were determined using spectrophotometry and gel electrophoresis. The ABI prism 7500 sequence detection system (Applied Biosystems, Foster City, CA) using Taqman technologies (PE Biosystems, Foster City, CA, USA) was employed following the manufacturer's instructions. Real time PCR was performed using the Platinum Quantitative RT-PCR ThermoScript One-Step System (Invitrogen, Carlsbad, CA). Full details of the primers, probes, and method are in Supplementary Information. The relative amount of *rumpshaker Plp* and *Plp/Dm20* mRNA was expressed as a percentage of wild type.

Antibodies and Immunostaining

Antibodies

PLP/DM20 was detected with a rabbit polyclonal antibody recognizing the common C-terminal (gift from Prof. N.P. Groome) or a rat monoclonal (AA3, gift from Dr. S. Pfeif-

fer). MBP was detected with a mouse monoclonal (clone 12, gift from Prof. N.P. Groome). CNP was detected with a mouse monoclonal (Chemicon Europe, Chandlers Ford, UK). Monoclonal and polyclonal antibodies to MAG were obtained from Chemicon (clone 513) and as gifts from Prof. N.P. Groome and Dr. R.H. Quarles. Aspartoacylase (ASPA) was detected with a rabbit polyclonal (gift from Dr. J. Garbern). Anti ubiquitin monoclonal was obtained from Santa Cruz (sc 8017, Autogen Bioclear UK Ltd, Calne, UK) and a rabbit polyclonal against p27^{kip1} from Upstate (Lake Placid, NY). A rabbit polyclonal against GRP78 was obtained from Stressgen (Bioquote Ltd., York, UK) and a mouse monoclonal GM130 antibody for Golgi membranes from Chemicon.

Immunostaining

Immunostaining of cells or tissue sections by indirect immunofluorescence was performed as described previously (Al-Saktawi et al., 2003; Edgar et al., 2002; Thomson et al., 1999). Fluorescent images were obtained using an Olympus IX70 microscope and a Photonic Sciences Colour CoolView camera. Contrast and brightness were adjusted using Adobe Photoshop 6.

Primary Oligodendrocyte Cultures

Oligodendrocytes were isolated and cultured from the spinal cords of P5 mice as previously described (Montague et al., 1998). Females homozygous for the *rumpshaker* mutation were mated with hemizygous males to generate litters in which all pups were affected. Cells from spinal cords were pooled and plated onto two 30mm poly-L-lysine coated plates per mouse. The resultant cultures contained a mixed population—70–80% O4+ cells together with astrocytes, occasional neurons, and other cells.

At 7 days in culture, the medium was removed, cells washed twice with Hank's buffered salt (HBS), then incubated for 30 min in HBS. The medium was replaced with 0.5 ml HBS containing [³⁵S]-Pro-Mix (Amersham) at 100 μ Ci/ml. For analysis of protein synthesis, dishes were removed at the indicated times, rinsed twice in chilled PBS, and lysed with Buffer A (10mM Tris pH 7.4, 150 mM NaCl, 1% triton X-100, and inhibitors of protease and phosphatase activity). For pulse chase experiments, cells were labeled for 1.5 h and chased by replacing the HBS with SATO medium supplemented with 2.5mM cysteine/2.5mM methionine. At the appropriate time point, cells were washed twice with chilled PBS, then lysed with 75 μ l buffer A. The lysates were rotated at 4°C for 30 min and cell debris pelleted by centrifugation at 5,000 rpm for 5 min. Proteins were quantified using the BCA assay system (Perbio Science UK Ltd, Tattenhall, UK).

Brain Slices, Myelin Extraction, and Fractionation Procedures

A brain slice system was used to investigate the incorporation of newly synthesized, radiolabeled PLP/DM20

into myelin. Full details of the methods are presented in Supplementary Information.

Western Blotting and Immunoprecipitation

Western blotting and immunoprecipitation analysis were conducted as described in detail elsewhere (McLaughlin et al., 2002; Yool et al., 2001), except that in the present study the immunoprecipitation reactions were conducted with buffer A, which contains 1% triton X-100 as the major solubilization detergent. Following SDS PAGE separation, the proteins were transferred to PVDF and the membrane exposed to a low energy, high sensitivity phosphorimage screen (Amersham) for a period of 1–2 weeks and the image captured on a Storm phosphorimage system. Quantitation was performed using ImageQuant densitometry software. The PVDF membranes were then processed for western blotting.

Statistical Analysis

Statistical significance of differences between values was assessed by ANOVA followed by Bonferonni's post hoc comparison test or by Student's *t*-test, as appropriate, with significance $P < 0.05$. Analyses and curve fitting were performed using Graphpad Prism4 software (GraphPad Software Inc., San Diego, CA). In the bar charts, significance is indicated as <0.05 (*), <0.01 (**), and <0.001 (***)

RESULTS

Myelin Protein Levels Are Disproportionately Low Compared with mRNA

In a previous study we quantified levels of representative proteins in myelin fractions from spinal cords of post-natal day 20 (P20) mice, a time of active myelination (Al-Saktawi et al., 2003). Levels of PLP and DM20 per unit of myelin in mutants were 9 and 15%, respectively, of wild type while levels of myelin basic protein (MBP), 2',3'-cyclic nucleotide 3'phosphodiesterase (CNP), and myelin-associated glycoprotein (MAG) were approximately 60, 81, and 71%. Levels of *Plp* mRNA in mutants were 66% of wild type, while message for the other myelin proteins was similar to control. Analysis of brain myelin extracts and mRNA levels found changes comparable with those in the spinal cord (data not shown).

In the CNS, myelin acts as the main repository of these proteins. To determine if the mutation had a comparable effect in the oligodendrocytes per se, we examined similar parameters in cultured primary oligodendrocytes, which do not elaborate a compact myelin sheath. *Rumpshaker* *Plp/Dm20* mRNA (combined probe) and the *Plp* specific isoform levels by qRT-PCR were $89 \pm 0.04\%$ and $83 \pm 0.08\%$ ($M \pm SEM$, $N = 5$), respectively, of wild type (data not shown), whereas the PLP and DM20 protein levels were 2 and 4%. MBP, MAG, and CNP were 16%, 54%, and

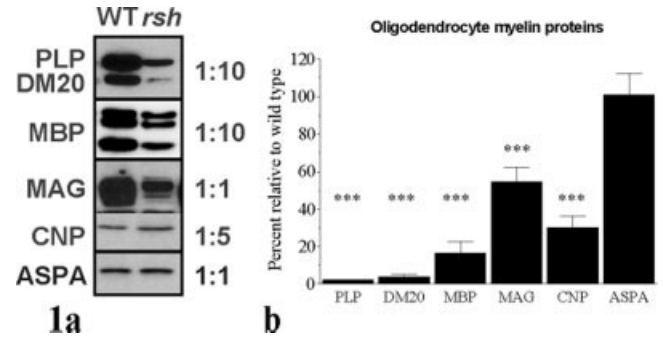


Fig. 1. Steady state levels of myelin proteins in cultured oligodendrocytes. **a**: Representative western blots from wild type (WT) and *rumpshaker* (*rsh*) oligodendrocytes. In order to visualize the signal in *rumpshaker*, some lanes were loaded with 5 (1:5) or 10 (1:10) times the amount of wild type protein. **b**: Quantitation of protein levels relative to wild type (100%) ($M \pm SEM$, $n = 4$). Equality in the number of oligodendrocytes and of loading between samples is verified by the level of aspartoacylase (ASPA), an oligodendrocyte-specific protein, which is identical in wild type and mutant.

30% (Fig. 1); all MBP isoforms were reduced to a similar extent. Levels of ASPA, a specific oligodendrocyte cell body marker (Kirmani et al., 2002) used as a control between samples, were unchanged from wild type.

Rumpshaker Oligodendrocytes Synthesize PLP at Normal Rate

In view of the discrepancy between message and product, we determined if translation was proceeding efficiently. Primary oligodendrocyte cultures from wild type and mutant mice were radiolabeled with Pro-Mix for between 10 and 90 min. The overall profile and signal intensity of radiolabeled proteins present in the cell lysates was similar for wild type and *rumpshaker* (data not shown). Analysis of immunoprecipitated products showed a similar accumulation of PLP and DM20 over time in both groups (Figs. 2a,b). Despite the similar levels of radiolabeled PLP and DM20, the total amount of both proteins recovered from the immunoprecipitation was consistently lower in the *rumpshaker* than wild type. These data demonstrate that *rumpshaker* oligodendrocytes synthesize PLP and DM20 with the same efficiency as wild type oligodendrocytes and indicate that other factors are responsible for the reduced steady state level of these proteins.

The Degradation of *rumpshaker* PLP Is Enhanced

The combination of normal rates of synthesis and low protein levels suggested that the mutant protein was being degraded rapidly. To confirm this, we pulsed cultured oligodendrocytes with [35 S] Pro-Mix for 1.5 h and then chased the labeled proteins for periods of up to 64 h. The level of labeled PLP declined exponentially with a $T_{1/2}$ of 23 h in wild type cells compared with 11 h in *rump-*

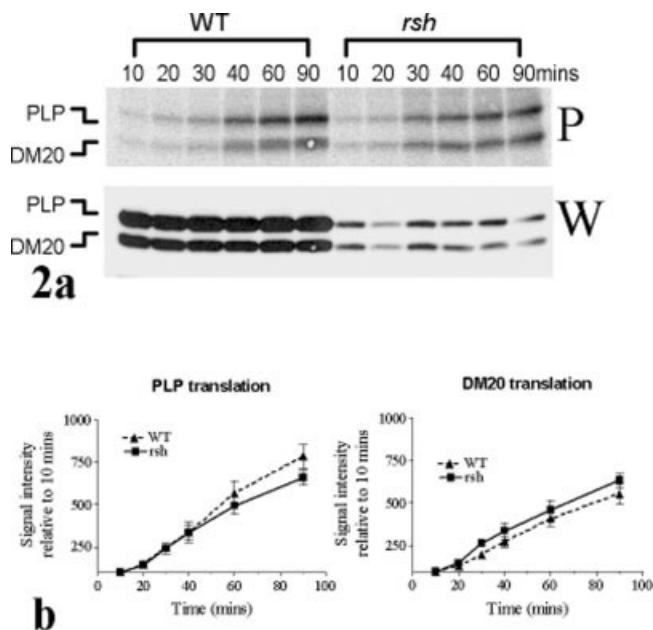


Fig. 2. Synthesis of PLP/DM20 in wild type and mutant oligodendrocytes. **a:** Cells were radiolabeled for the times shown above each lane prior to lysis and immunoprecipitation. The upper panel is a phosphorimage (P) of the radiolabeled precipitates, and the lower panel a western blot (W) using an antibody recognizing PLP/DM20. The radiolabeled protein increases with time in both genotypes. The amount of total protein (includes radiolabeled and non-labeled) precipitated from the mutants is lower than from wild type. **b:** Quantification of radiolabeled PLP and DM20 at times from 10 to 90 min. The data are expressed relative to the 10-min sample. ($M \pm SEM$, $n = 6$). There is no significant difference between mutant and wild type.

shaker (Figs. 3a,b); for DM20 the equivalent times were 11.7 h and 8.4 h, respectively. The decay curves of wild type and mutant were significantly different ($P < 0.05$).

The Proteasome Is Probably Involved in the Degradation of Wild Type and *rumpshaker* PLP

A common degradation pathway involves degradation by the proteasome system, a process known as ER-associated degradation (ERAD) (Jarosch et al., 2003). We investigated the influence of increasing doses of MG132, a proteasome inhibitor (Lee and Goldberg, 1996), on protein degradation. We first confirmed the effectiveness of MG132 in decreasing degradation of p27^{kip1} in oligodendrocytes (Fig. 4a), a process known to involve the proteasome (Pasquini et al., 2000). Using the same approach, we found that degradation of both wild type and *rumpshaker* PLP/DM20 was markedly ameliorated in a dose-dependant manner by MG132 (Figs. 4a, b). Whereas approximately 30% of wild type PLP was degraded by the proteasome and recovered after treatment with 50 μ M MG132, two thirds of *rumpshaker* PLP was lost and restored to 90% of normal by inhibiting the proteasome (Fig. 4b). Although MG132 treatment resulted in a marked increase in the ubiquitination profile of the cell lysates and an increase in the level of PLP/DM20 (data not shown), we were unable to demonstrate an interaction

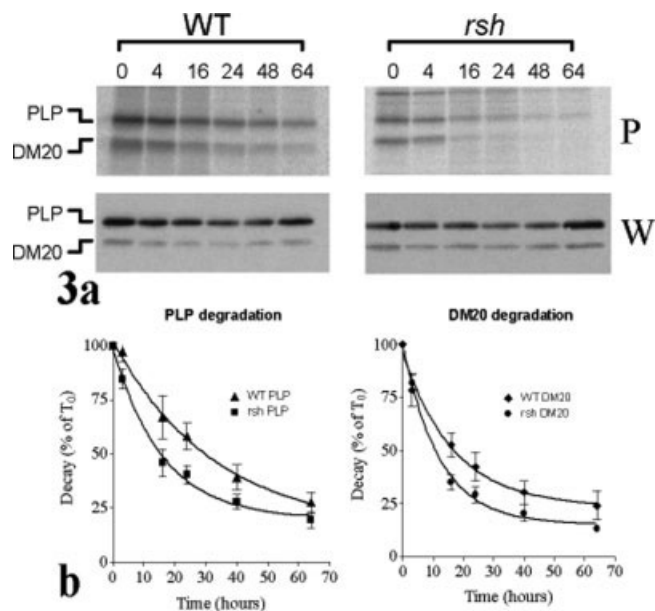


Fig. 3. Degradation of PLP/DM20 in oligodendrocytes from wild type and *rumpshaker* mice. **a:** Representative experiment from wild type and mutant mice showing the phosphorimage (P) and corresponding western blot (W) of the immunoprecipitates. Cells were pulse labeled with [³⁵S] Pro-Mix for 90 min and chased for the times shown, prior to immunoprecipitation. The accelerated decay of newly synthesized protein in the mutant is evident. The total amount of PLP/DM20 recovered over the 64-h period of chase remains constant for each genotype. For the western blots, a higher antibody concentration has been used in *rumpshaker* than wild type (due to the lower levels of PLP/DM20); therefore, the western blots of mutant and wild type are not directly comparable. **b:** Decay profiles for PLP and DM20 from wild type and mutant mice. The points represent $M \pm SEM$, $n = 4$; the curves show the exponential decay. The $T_{1/2}$ for mutant PLP is 11 h compared with 23 h for wild type PLP; the two DM20 profiles have $T_{1/2}$ of 8 and 11 h, respectively.

of PLP and ubiquitin by co-immunoprecipitation. Co-immunostaining of *rumpshaker* oligodendrocytes for PLP/DM20 and the ER marker GRP78 showed strong PLP/DM20 staining in the ER but also extending through the cytoplasm to the cell membrane, indicating that at least some of the mutant protein was escaping ERAD (Fig. 4c).

We immunostained wild type and *rumpshaker* oligodendrocytes for PLP/DM20, ubiquitin, and HSP70 following treatment with the proteasomal inhibitor but were unable to demonstrate any evidence of aggresomes (data not shown).

The *rumpshaker* Mutation Impairs the Insertion of PLP into Myelin

Despite the accelerated degradation, *rumpshaker* PLP/DM20 (Al-Saktawi et al., 2003) and PLP (Fig. 5a) integrate into myelin. We examined the insertion of the molecule into the plasma membrane by immunostaining live cells with the O10 antibody (Jung et al., 1996) and then detecting cytoplasmic PLP/DM20 after permeabilization. The O10 antibody detects a conformation-sensitive epitope on the extracellular "CD" loop of PLP/DM20, thus indicating the molecule is inserted correctly into the

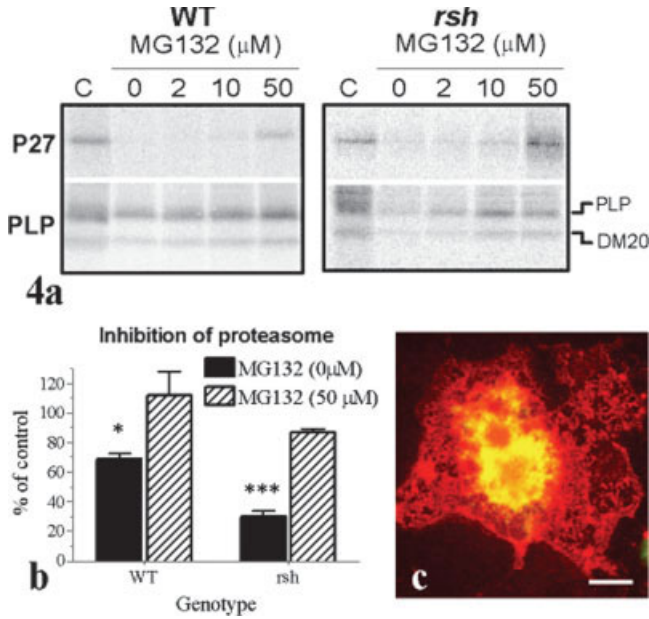


Fig. 4. Wild type and mutant PLP/DM20 are degraded via the proteasome. **a:** Wild type (WT) or *rumpshaker* (*rsh*) cells were pulsed with [³⁵S] Pro-Mix for 90 min to obtain a control (C) labeling and chased for 24 and 16 h, respectively, without (0) or with (2, 10, 50 μM) MG132. Lysates were immunoprecipitated with p27^{kip1} (P27) or PLP/DM20 (PLP) antibodies. The p27^{kip1}, a known substrate for proteasomal degradation, acts as a control system, showing a dose-dependent rescue by MG132. The decline in levels of PLP and DM20 is ameliorated by proteasome inhibition, more so in the wild type cells. **b:** Inhibition of the proteasome by 50 μM MG132 (a concentration with maximum effect in the dose-response studies) reverses the decline in levels of PLP. Cells were labeled, as above, and the intensity of the PLP band in wild type and *rumpshaker* quantified at 24 or 16 h, respectively, without (0 μM) or with (50 μM) MG132 treatment. The data (M ± SEM, n = 4) are expressed relative to the control level after the 90-min pulse. The level of wild type PLP is completely restored, while *rumpshaker* PLP is 86% of control. **c:** *rumpshaker* oligodendrocyte immunostained for PLP/DM20 (red) and for the ER marker, GRP78 (green). A proportion of PLP/DM20 has exited the ER and extends through the cytoplasm to the plasma membrane. Bar = 10 μm.

plasma membrane (Jung et al., 1996). After 7 days in culture, virtually 100% of wild type oligodendrocytes that expressed PLP/DM20 were also surface stained with O10, whereas significantly fewer, 64 ± 10% (M ± SEM, n = 5), of *rumpshaker* cells stained in a similar manner (Fig. 5b). The O10 staining intensity of the mutant cells showed variability, whereas most wild type cells were intensely stained.

We used brain slices to compare the kinetics of radiolabeled PLP and DM20 incorporation into myelin between the genotypes. Newly synthesized protein accumulated progressively over the 6-h labeling period in total homogenates from the brain slices. The rate of accumulation in total homogenate was not different between wild type and mutant (data not shown), again suggesting that the rate of synthesis was similar in the two genotypes. Newly synthesized PLP and DM20 were present in myelin after a 2-h label in both wild type and mutant and increased over the subsequent 4 h (Figs. 5c, d). The amount and rate of incorporation of PLP into myelin was significantly less in *rumpshaker* so that at 6 h the relative intensity of *rumpshaker* PLP was similar to the wild type signal

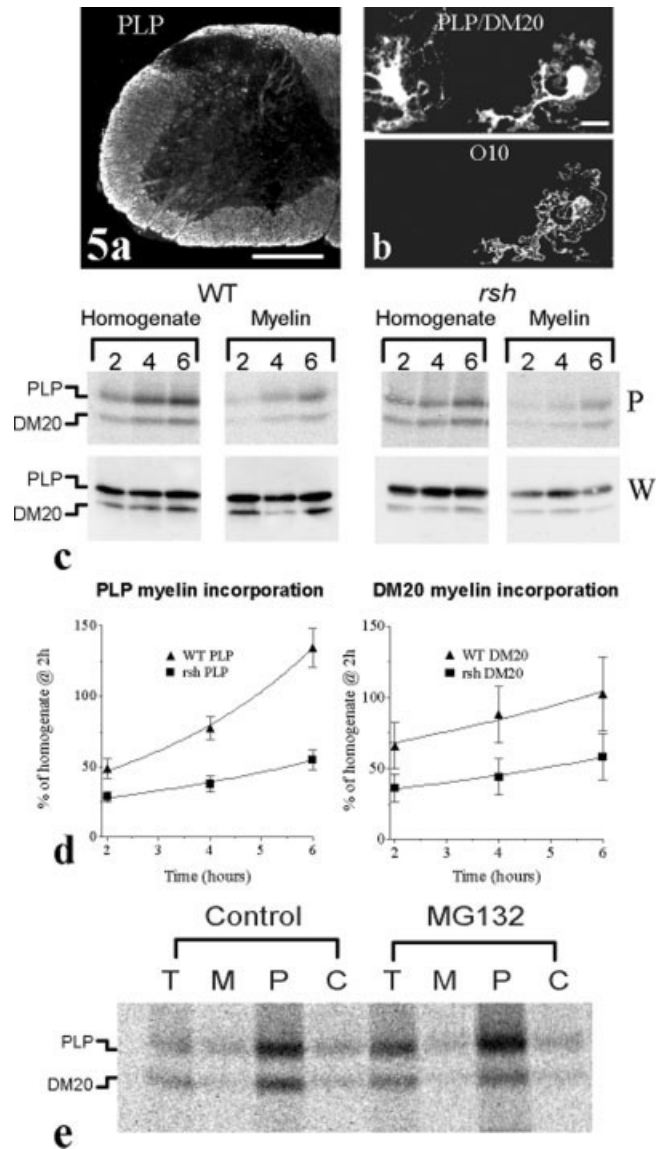


Fig. 5. Incorporation of wild type and mutant PLP/DM20 into myelin membrane. **a:** Immunostaining of *rumpshaker* spinal cord with an antibody specific to PLP demonstrates this isoform is incorporated into myelin. Bar = 400 μm. **b:** Oligodendrocytes from *rumpshaker* spinal cord were cultured for 7 days and surface stained with the O10 antibody before being permeabilized and immunostained for PLP/DM20. Two cells are shown, only one of which has correctly inserted PLP/DM20 into its plasma membrane. Bar = 20 μm. **c:** Incorporation of newly synthesized PLP/DM20 into myelin in brain slices from P20 wild type and *rumpshaker* mice. Slices were radiolabeled for 2, 4, and 6 h and the proteins immunoprecipitated from 400 μg total homogenate and 20 μg myelin fractions; this ratio was retained for all studies. The panels show the phosphorimage (P) of newly synthesized, radiolabeled PLP and DM20 and the corresponding western blots (W) of total (labeled and unlabeled) PLP and DM20. **d:** Incorporation of PLP and DM20 into myelin in wild type and *rumpshaker* mice. At each time point, the signal intensity of newly synthesized PLP and DM20 in myelin is expressed relative to the signal of the total homogenate at 2 h. The rate of incorporation of newly synthesized wild type PLP into myelin is significantly greater than in the mutant ($P = 0.04$), whereas DM20 is not different between the two genotypes ($P = 0.5$). **e:** Inhibition of the proteasome does not increase incorporation of PLP/DM20 into myelin in *rumpshaker*. Brain slices labeled with [³⁵S] Pro-Mix for 2 h were treated with MG132 or the DMSO vehicle (control) for an additional 4 h before fractionation and immunoprecipitation. Whereas the signal increased in the total homogenate (T) and pellet (P) fractions with treatment, no corresponding increase occurred in the myelin (M) or supernatant/cytosolic (C) fractions.

observed after 2 h, indicating a significant delay in incorporation. The rate at which *rumpshaker* DM20 incorporated into myelin was similar to wild type, although the amounts were considerably lower. Western blot analysis of the immunoprecipitated products (Fig. 5c) showed that the ratio of PLP recovered from the homogenate compared with the myelin fraction was similar for wild type and *rumpshaker*. The difference in myelin incorporation rates is not simply a reflection of the amount of PLP recovered from the myelin fraction in *rumpshaker*.

As inhibition of ERAD resulted in a significant elevation of the level of PLP in cultured *rumpshaker* cells, we asked whether there would be a similar increase in myelin incorporation. However, treatment of brain slices with 50 μ M MG132 failed to increase PLP/DM20 incorporation into the myelin fraction, although signal in both the total homogenate and pellet fractions was elevated (Fig. 5e).

DISCUSSION

Missense mutations of the *PLP1/Plp1* gene resulting in an amino acid substitution are a cause of PMD in man and account for the majority of spontaneous disorders in animals. Dysmyelination is a major feature of the pathology and probably accounts for many of the clinical signs, yet its basis is not clear. Indeed, how the abnormal PLP/DM20 is handled by the oligodendrocyte is only partly resolved and is the focus of the present study. The *rumpshaker* mutation encodes an isoleucine to threonine substitution in the putative extracellular CD loop of the PLP/DM20 molecule that results in mild or lethal phenotypes dependent on genetic background, suggesting the influence of other modifying genes (Al-Saktawi et al., 2003). Using a model of the mild form of PMD/SPG2, we show that the reduced steady state level of PLP/DM20 is caused principally by enhanced degradation, most probably via the proteasome, rather than a reduced rate of translation. The majority of *rumpshaker* PLP/DM20 that escapes ERAD is targeted to the developing myelin sheath, where it inserts correctly into the membrane, albeit more slowly than in wild type.

Translational Efficiency of PLP Is Not Affected by the *rumpshaker* Mutation

The level of *Plp/Dm20* mRNA is only minimally reduced compared with PLP/DM20 protein, suggesting that a translational or post-translational defect is responsible for the low protein level. Misfolded proteins in the RER can inhibit translation by activating PERK, leading to phosphorylation of the eIF2 α factor (Harding et al., 1999), although this is often a transient effect and is not necessarily operative. For example, in the Akita diabetic mouse, misfolded proinsulin accumulates in the RER yet translation proceeds normally (Izumi et al., 2003). Similarly, translational efficiency of PLP/DM20 in *rumpshaker* oligodendrocytes is comparable with wild type, indicating that the low protein levels are due to post-translational mechanisms.

The Fate of the *rumpshaker* PLP/DM20

The exit of most misfolded membrane proteins from the RER tends to be perturbed (Ellgaard and Helenius, 2003). Transfection and in vivo studies have shown that products encoded by many missense mutations of the *PLP1/Plp1* gene accumulate in the RER rather than reach the plasma membrane (Gow and Lazzarini, 1996). The majority of information has been gathered from microscopic images, which create the impression of a static protein mass in the RER cisternae and provide little kinetic information. We show that *rumpshaker* PLP is a dynamic protein, the majority of which is degraded by an MG132-sensitive pathway at twice the rate of the wild type product, causing the low steady state levels. The rate of DM20 breakdown is also accelerated by the mutation. Only a minority of PLP/DM20 reaches its correct destination in the myelin sheath.

The majority of proteins destined for proteasomal degradation are polyubiquitinated, although there are examples of non-ubiquitinated proteins being degraded by this pathway (Asher et al., 2002; Jarosch et al., 2003; Shringarpure et al., 2003). Despite numerous attempts, we were unable to demonstrate polyubiquitination of PLP/DM20. We cannot exclude the possibility that the putative pool of ubiquitin-conjugated PLP is rapidly deubiquitinated by the activity of isopeptidases (Kim et al., 2003). There are also examples of wild type or misfolded RER proteins being degraded by non-proteasomal pathways (Donoso et al., 2005; Schmitz and Herzog, 2004). Sensitivity to MG132 is a well-accepted indicator of proteasomal involvement; and despite the failure to demonstrate polyubiquitination, it seems most probable that the proteasome is the main degradative pathway for *rumpshaker* PLP/DM20.

Rumpshaker PLP Is Incorporated into Myelin Less Efficiently than Wild Type

The amount and rate of incorporation of newly synthesized PLP into myelin, relative to the total pool of labeled PLP, were reduced in *rumpshaker* consistent with a delay in the processing pathway at an earlier stage. Evidence for the insertion of PLP and/or DM20 into the myelin membrane was obtained by surface staining with the O10 antibody, which recognizes an epitope on the extracellular CD loop (Jung et al., 1996), a region that also contains the *rumpshaker* mutation. While the amino acid substitution compromises the function of PLP/DM20, it does not appear sufficient to prevent the membrane insertion of the fraction that escapes ERAD.

The presence of misfolded PLP influences the structure of myelin. In common with other *Plp1* mutants (Duncan et al., 1987), *rumpshaker* mice have thin myelin sheaths with abnormal, condensed, intraperiod lines (IPL), compared with the closely apposed double IPL of normal myelin (Griffiths et al., 1990). In contrast, *Plp1* null mice have widened or absent IPL (Yool et al., 2002). Although PMD is classed as a dysmyelinating rather than a demyelinating

ing disorder, it is possible that individual components, such as misfolded PLP, have an enhanced rate of turnover in myelin, thus making the myelin unstable and unable to achieve the appropriate thickness.

Increasing the amount of *rumpshaker* PLP/DM20 potentially available to myelin by inhibiting proteasomal degradation does not lead to an enhanced incorporation, suggesting the system is handling the maximum amount of mutated product or that other mechanisms of degradation also operate (Schmitz and Herzog, 2004). One candidate is the endosomes/lysosome system, which is involved in clearing excess wild type PLP generated by increased *Plp1* gene dosage (Simons et al., 2002). It is possible that this pathway also degrades a minority of the *rumpshaker* PLP/DM20.

Relevance to the Dysmyelinating Phenotype

Most forms of PMD and its spontaneous animal models are characterized by the inability of surviving oligodendrocytes to assemble and maintain normal amounts of myelin. Although the level of PLP/DM20 is markedly reduced in *rumpshaker* myelin, this is unlikely to be the cause of the hypomyelination, as a similar phenotype does not occur in *Plp* null mice or humans (Garbern et al., 2002; Klugmann et al., 1997). Also, introducing wild type PLP/DM20 into mutant myelin through transgenic complementation does not rescue the phenotype (Schneider et al., 1995). One potential mechanism is the effect of the *rumpshaker* mutation on other myelin components, particularly MBP, which is critical for myelin formation (Shine et al., 1992). Levels of MBP are markedly reduced in *rumpshaker* oligodendrocytes (present study), and particularly when the mutation is expressed on the C57BL/6 background (Al-Saktawi et al., 2003). In ongoing studies (Barrie et al., unpublished) we have complemented the C57 *rumpshaker* mice with a wild type *Plp* transgene, increasing their PLP/DM20 levels to normal. However, MBP levels remain low and severe dysmyelination is still present. It is, therefore, possible that the low levels of MBP in *rumpshaker* contribute to the hypomyelination. *Mbp* mRNA levels are only minimally reduced, suggesting the *rumpshaker* mutation operates at a translational or post-translational level to perturb MBP, presumably through the action of misfolded PLP/DM20 through an, as yet, unknown mechanism.

ACKNOWLEDGMENTS

This work was supported by The Wellcome Trust and Birth Defects Foundation. We are grateful to Prof. N.P. Groome and Drs. J. Garbern, S. Pfeiffer, and R.H. Quarles for the gift of antibodies.

REFERENCES

Al-Saktawi K, McLaughlin M, Klugmann M, Schneider A, Barrie JA, McCulloch MC, Montague P, Kirkham D, Nave K-A, Griffiths IR. 2003. Genetic background determines phenotypic severity of the *Plp rumpshaker* mutation. *J Neurosci Res* 72:12–24.

Asher G, Lotem J, Sachs L, Kahana C, Shaul Y. 2002. Mdm-2 and ubiquitin-independent p53 proteasomal degradation regulated by NQO1. *Proc Natl Acad Sci USA* 99:13125–13130.

Donoso G, Herzog V, Schmitz A. 2005. Misfolded BiP is degraded by a proteasome-independent endoplasmic-reticulum-associated degradation pathway. *Biochem J* 387:897–903.

Duncan ID, Hammang JP, Trapp BD. 1987. Abnormal compact myelin in the myelin-deficient rat: absence of proteolipid protein correlates with a defect in the intraperiod line. *Proc Natl Acad Sci USA* 84:6287–6291.

Edgar JM, Anderson TJ, Dickinson PJ, Barrie JA, McCulloch MC, Nave K-A, Griffiths IR. 2002. Survival of, and competition between, oligodendrocytes expressing different alleles of the *Plp* gene. *J Cell Biol* 158:719–729.

Edgar JM, McLaughlin M, Barrie JA, McCulloch MC, Garbern J, Griffiths IR. 2004. Age-related axonal and myelin changes in the *rumpshaker* mutation of the *Plp* gene. *Acta Neuropath (Berl)* 107:331–335.

Ellgaard L, Helenius A. 2003. Quality control in the endoplasmic reticulum. *Nat Rev Mol Cell Biol* 4:181–191.

Garbern J, Yool DA, Moore GJ, Wilds I, Faulk M, Klugmann M, Nave K-A, Siermans EA, van der Knaap MS, Bird TD, et al. 2002. Patients lacking the major CNS myelin protein, proteolipid protein 1, develop length-dependent axonal degeneration in the absence of demyelination and inflammation. *Brain* 125:551–561.

Gow A, Lazzarini RA. 1996. A cellular mechanism governing the severity of Pelizaeus-Merzbacher disease. *Nat Genet* 13:422–428.

Griffiths IR, Klugmann M, Anderson TJ, Yool D, Thomson CE, Schwab MH, Schneider A, Zimmermann F, McCulloch MC, Nodon NL, et al. 1998. Axonal swellings and degeneration in mice lacking the major proteolipid of myelin. *Science* 280:1610–1613.

Griffiths IR, Scott I, McCulloch MC, Barrie JA, McPhilemy K, Cattanauch BM. 1990. Rumpshaker mouse: a new X-linked mutation affecting myelination: evidence for a defect in PLP expression. *J Neurocytol* 19:273–283.

Harding HP, Zhang YH, Ron D. 1999. Protein translation and folding are coupled by an endoplasmic-reticulum-resident kinase. *Nature* 397:271–274.

Hudson LD. 2003. Pelizaeus-Merzbacher disease and spastic paraplegia type 2: two faces of myelin loss from mutations in the same gene. *J Child Neurol* 18:616–624.

Inoue K. 2005. PLP1-related inherited dysmyelinating disorders: Pelizaeus-Merzbacher disease and spastic paraplegia type 2. *Neurogenetics* 6:1–16.

Izumi T, Yokota-Hashimoto H, Zhao S, Wang J, Halban PA, Takeuchi T. 2003. Dominant negative pathogenesis by mutant proinsulin in the Akita diabetic mouse. *Diabetes* 52:409–416.

Jarosch E, Lenk U, Sommer T. 2003. Endoplasmic reticulum-associated protein degradation. *Int Rev Cytol* 223:39–81.

Johnston AW, McKusick VA. 1962. A sex-linked recessive form of spastic paraplegia. *Am J Hum Genet* 14:83–94.

Jung M, Sommer I, Schachner M, Nave K-A. 1996. Monoclonal antibody O10 defines a conformationally sensitive cell-surface epitope of proteolipid protein (PLP): evidence that PLP misfolding underlies dysmyelination in mutant mice. *J Neurosci* 16:7920–7929.

Kim JH, Park KC, Chung SS, Bang O, Chung CH. 2003. Deubiquitinating enzymes as cellular regulators. *J Biochem (Tokyo)* 134:9–18.

Kirmani BF, Jacobowitz DM, Kallarakal AT, Nambodiri MAA. 2002. Aspartoacylase is restricted primarily to myelin synthesizing cells in the CNS: therapeutic implications for Canavan disease. *Mol Brain Res* 107:176–182.

Klugmann M, Schwab MH, Pühlhofer A, Schneider A, Zimmermann F, Griffiths IR, Nave K-A. 1997. Assembly of CNS myelin in the absence of proteolipid protein. *Neuron* 18:59–70.

Kobayashi H, Hoffman EP, Marks HG. 1994. The *rumpshaker* mutation in spastic paraplegia. *Nat Genet* 7:351–352.

Lee DH, Goldberg AL. 1996. Selective inhibitors of the proteasome-dependent and vacuolar pathways of protein degradation in *Saccharomyces cerevisiae*. *J Biol Chem* 271:27280–27284.

McLaughlin M, Hunter DJB, Thomson CE, Yool D, Kirkham D, Freer AA, Griffiths IR. 2002. Evidence for possible interactions between PLP, DM20 within the myelin sheath. *Glia* 39:31–36.

Montague P, Barrie JA, Thomson CE, Kirkham D, McCallion AS, Davies RW, Kennedy PGE, Griffiths IR. 1998. Cytoskeletal and nuclear localization of MOBP polypeptides. *Europ J Neurosci* 10:1321–1328.

Naidu S, Dlouhy SR, Geraghty MT, Hodes ME. 1997. A male child with the *rumpshaker* mutation, X-linked spastic paraplegia Pelizaeus-Merzbacher disease and lysinuria. *J Inherited Metab Dis* 20:811–816.

Pasquini LA, Moreno MB, Adamo AM, Pasquini JM, Soto EF. 2000. Lactacystin, a specific inhibitor of the proteasome, induces apoptosis and activates caspase-3 in cultured cerebellar granule cells. *J Neurosci Res* 59:601–611.

- Rutkowski DT, Kaufman RJ. 2004. A trip to the ER: coping with stress. *Trends Cell Biol* 14:20–28.
- Sanders CR, Myers JK. 2004. Disease-related misassembly of membrane proteins. *Annu Rev Biophys Biomol Struct* 33:25–51.
- Schmitz A, Herzog V. 2004. Endoplasmic reticulum-associated degradation: exceptions to the rule. *Eur J Cell Biol* 83:501–509.
- Schneider A, Griffiths IR, Readhead C, Nave K-A. 1995. Dominant-negative action of the *jimpy* mutation in mice complemented with an autosomal transgene for myelin proteolipid protein. *Proc Natl Acad Sci USA* 92:4447–4451.
- Schneider A, Montague P, Griffiths IR, Fanarraga ML, Kennedy PGE, Brophy PJ, Nave K-A. 1992. Uncoupling of hypomyelination and glial cell death by a mutation in the proteolipid protein gene. *Nature* 358:758–761.
- Shine HD, Readhead C, Popko B, Hood L, Sidman RL. 1992. Morphometric analysis of normal, mutant and transgenic CNS: correlation of myelin basic protein expression to myelinogenesis. *J Neurochem* 58:342–349.
- Shringarpure R, Grune T, Mehlhase J, Davies KJ. 2003. Ubiquitin conjugation is not required for the degradation of oxidized proteins by proteasome. *J Biol Chem* 278:311–318.
- Simons M, Krämer EM, Macchi P, Rathke-Hartlieb S, Trotter J, Nave K-A, Schulz JB. 2002. Overexpression of the myelin proteolipid protein leads to accumulation of cholesterol and proteolipid protein in endosomes/lysosomes: implications for Pelizaeus-Merzbacher disease. *J Cell Biol* 157:327–336.
- Skoff RP. 1995. Programmed cell death in the dysmyelinating mutants. *Brain Pathol* 5:283–288.
- Southwood C, Gow A. 2001. Molecular pathways of oligodendrocyte apoptosis revealed by mutations in the proteolipid protein gene. *Microsc Res Tech* 52:700–708.
- Southwood CM, Garbern J, Jiang W, Gow A. 2002. The unfolded protein response modulates disease severity in Pelizaeus-Merzbacher disease. *Neuron* 36:585–596.
- Thomson CE, Anderson TJ, McCulloch MC, Dickinson PJ, Vouyiouklis DA, Griffiths IR. 1999. The early phenotype associated with the *jimpy* mutation of the proteolipid protein gene. *J Neurocytol* 28:207–221.
- Thomson CE, Montague P, Jung M, Nave K-A, Griffiths IR, Nave KA. 1997. Phenotypic severity of murine *Plp* mutants reflects in vivo and in vitro variations in transport of PLP isoproteins. *Glia* 20:322–332.
- Yool D, Klugmann M, Barrie JA, McCulloch MC, Nave K-A, Griffiths IR. 2002. Observations on the structure of myelin lacking the major proteolipid protein. *Neuropath Appl Neurobiol* 28:75–78.
- Yool DA, Klugmann M, McLaughlin M, Vouyiouklis DA, Dimou L, Barrie JA, McCulloch MC, Nave K-A, Griffiths IR. 2001. Myelin proteolipid proteins promote the interaction of oligodendrocytes and axons. *J Neurosci Res* 63:151–164.

A physical map of the genomic region on mouse chromosome 3 containing the *hindshaker* (*hsh*) mutation

Saadia A. Karim,^a Keith J. Johnson,^{b,1} Ian R. Griffiths,^a and Demetrius A. Vouyiouklis^{a,*}

^aApplied Neurobiology Group, Institute of Comparative Medicine, Veterinary School, United Kingdom

^bIBLS Molecular Genetics, Anderson College, University of Glasgow, Glasgow G12 8QQ, Scotland, United Kingdom

Received 12 May 2003; accepted 13 August 2003

Abstract

Hindshaker (*hsh*), a spontaneous, autosomal recessive mouse mutation, displays a developmentally dependent tremor of the hindquarters due to hypomyelination in the CNS. This myelin deficit is followed by progressive, but incomplete, recovery by postnatal day 42. Herein we describe the construction of a genomic contig spanning the interval between the markers *D3Mit187* (42.4 cM) and *D3Mit232* (45.2 cM) on mouse chromosome 3, which we have previously shown to contain the *hsh* mutation. A physical map, covering approximately 3.5 Mb, was constructed from a series of overlapping yeast and bacterial artificial chromosomes. A 1.2- to 1.4-Mb segment central to the contig was compared extensively with the syntenic regions in human (chromosome 1q21–q23) and rat (chromosome 2). We present new data on 10 genes erroneously assigned to this area and on another 6 genes previously assigned elsewhere. For absent genes, our work suggests that they are telomeric to the region encompassed in our map. Accordingly, our findings both map the area surrounding the *hsh* mutation and present important corrections to the current maps in an area rich in genes related to the nervous system.

© 2003 Elsevier Inc. All rights reserved.

Keywords: *Hindshaker*; Gene; Contig; Genomic map

The recent completion of the human and mouse genome sequences has contributed to the mapping of genes linked to diseases with similar phenotypes in humans and mice [1–4]. One phenotype in mouse is *hindshaker* (*hsh*), a spontaneous autosomal recessive mutation characterized by a tremor of the hindquarters due to hypomyelination of the CNS. Unlike many other CNS myelin disorders in which the brain is predominantly affected, in *hsh* the spinal cord is the main site of dysmyelination. Progressive, but incomplete, improvement in myelination follows after approximately postnatal day 20 (when the *hsh* phenotype is most evident) [5,6]. Although myelin deficiency has serious clinical consequences in humans, the underlying molecular mechanisms involved in myelin assembly are not fully understood. Therefore, positional cloning and analysis of mouse muta-

tions, such as *hsh*, can give insights into either novel or uncharacterized genes involved in myelination. Additionally, such mouse mutants may serve as models of human myelin diseases [7,8].

The *hsh* mutation was previously mapped to a region near the centromere of mouse chromosome 3 [9]. In the present paper we report the completion of a YAC/BAC contig spanning the interval 42.4–45.2 cM on this chromosome. Our map of the area includes several published genes such as brevicin (*Bcan*), brain link protein 1 (*Bral1*), chaperonin subunit 3 (*Cct3*), death-associated protein 3 (*Dap3*), glucocerebrosidase precursor (*Gba*), and recombination activating gene 1 gene activation (*Rga*). However, other genes placed in this region on the mouse genomic map (<http://www.ncbi.nlm.nih.gov/mapview/maps.cgi?ORG=mouse&CHR=3>) are absent from our map. We report that the bone γ -carboxyglutamate protein gene 1 (*Bglap1*) (which has the same sequence as *Bglap-rs1*), semaphorin 4 (*Sema4*), lamin A (*Lmna*), and possibly other genes contained within an area of approximately 250 kb are absent between 42.4 and 45.2 cM. These genes may, nevertheless, belong on mouse chromosome 3 but nearer the telomere, as suggested by the Identify Unknown Nucleic Sequence (NIX)

* Corresponding author. Fax: +44-141-330-5659.

E-mail address: dv2u@udcf.gla.ac.uk (D.A. Vouyiouklis).

¹ Present address: Pfizer Corp., 2800 Plymouth Road, Ann Arbor, MI, USA.

² Present address: Yoshitomi Research Institute for Neuroscience in Glasgow (YRING), West Medical Building Room 307, University of Glasgow, Glasgow, G12 8QQ, UK.

analysis program (<http://www.hgmp.mrc.ac.uk/Registered/Webapp/nix/>). By contrast, the genes selenium binding protein 1 (*Selenbp1*), *Selenbp2*, proteasome (prosome, macropain) subunit β type 4 (*Psmb4*), and regulatory factor X5 (*Rfx5*) and the mouse homologues to human IQ motif-containing GTPase activating protein 3 (*IQGAP3*) and human cingulin (*CGN*), which have been mapped closer to the telomere of chromosome 3 on other maps, are present in our contig. Therefore, our new physical map both introduces new genes in specific positions on mouse chromosome 3 that may be related to the *hsh* phenotype and corrects misassignments in the current databases.

Results

A contig spanning a region of the mouse chromosome 3 genetic map, corresponding to 2.8 cM between the markers

D3Mit187 (centromeric end of the *hsh* interval) and *D3Mit232* (telomeric end), was assembled from 5 YAC and 11 BAC clones. Our experimental evidence (unpublished) placed the *hsh* gene in the center of this interval; hence we mapped the region with this central area as the main focus. Three methods were used to screen for clones: marker/gene PCR, BAC end-sequence (BES) screening, and YAC library screening. A contig map representing the positions of selected clones is shown in Fig. 1. Not all the clones identified by each method are shown if they contributed no new or extra information to the results. Based on clone sizes and overlaps, approximately 3.5 Mb of chromosomal DNA is covered by these clones.

Bioinformatics analysis and contig construction

We obtained mapping information on YAC clones containing the *D3Mit187* and *D3Mit232* markers from the

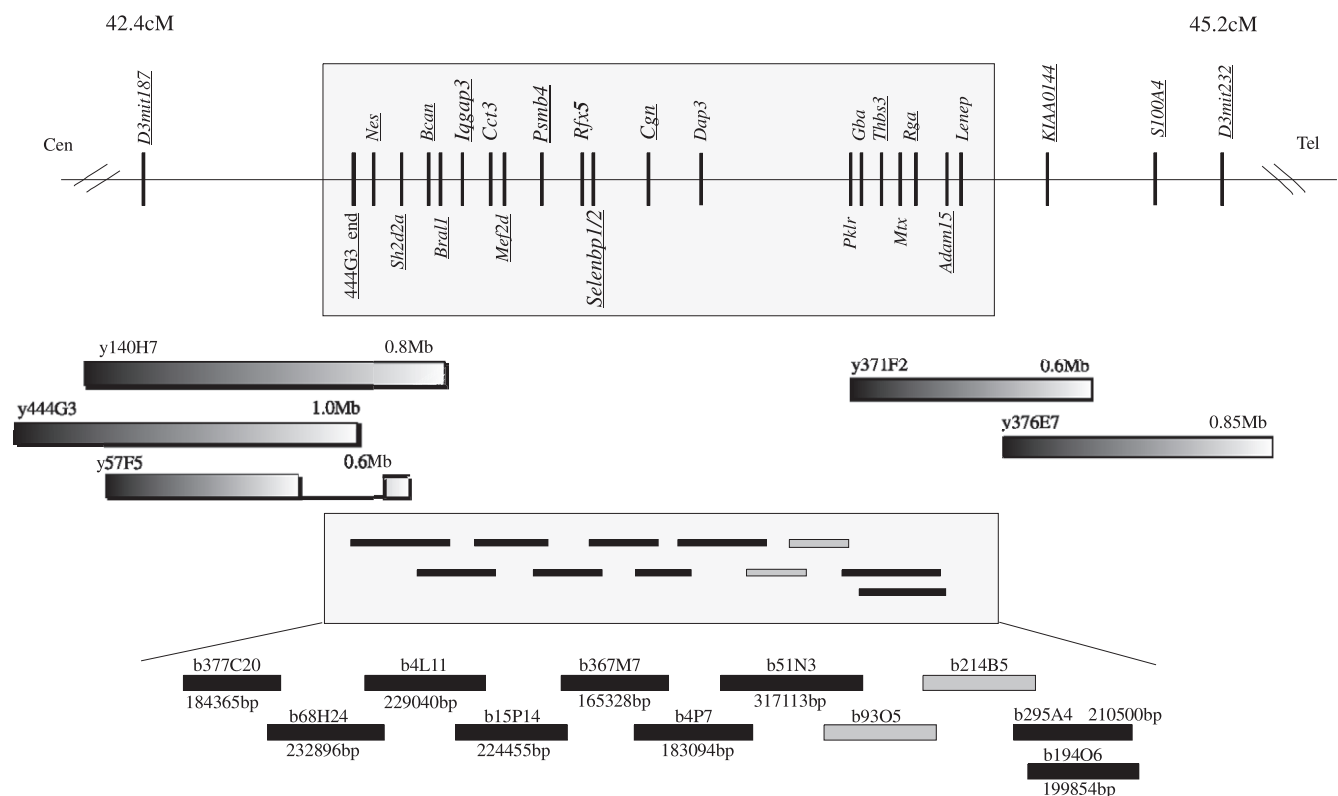


Fig. 1. Contig of area 42.4–45.2 cM in mouse chromosome 3. The region is encompassed by 5 YAC and 11 BAC clones. The YAC clones are in sliding gray scale and the BAC clones in black or light gray, the former denoting known sizes. Boxed area corresponds to the BAC tile. Underlined genes/markers were placed on the map by both PCR and Southern blotting, the rest by NIX analysis. Genes in larger font and bold were ascribed by others to an area nearer the telomere of mouse chromosome 3; however, we have mapped them to this region. YAC clone 57F5, which contains the intact *Sh2d2a* gene in its telomeric end, appears to have an internal deletion, since the terminus sequence of YAC clone 444G3 and the nestin gene are missing. Cen, centromere; *Nes*, nestin; *Sh2*, sh2 domain 2A protein; *Bcan*, brevicain; *Brnl1*, brain link protein 1; *Iqgap3*, IQ motif containing GTPase activating protein 3; *Cct3*, chaperonin subunit 3; *Mef2d*, myocyte enhancer factor 2D; *Psmb4*, proteasome (prosome, macropain) subunit, β type 4; *Rfx5*, regulatory factor X 5; *Selenbp1*, selenium binding protein 1; *Selenbp2*, selenium binding protein 2; *Cgn*, cingulin; *Dap3*, death-associated protein 3; *Pklr*, pyruvate kinase; *Gba*, glucocerebrosidase precursor; *Thbs3*, thrombospondin 3; *Mtx1*, metaxin 1; *Rga*, recombination activating gene 1; *Adam15*, metalloprotease-disintegrin MDC15; *Lenep*, lens epithelial protein; *KIAA0144*, potential phospholipid transporting ATPase; *S100A4*, s100calcium-binding protein A4; and Tel, telomere.

Whitehead/MIT database (<http://www.genome.wi.mit.edu/cgi-bin/mouse/index>) and also screened by PCR for genes and markers. Clones 444G3 and 376E7 contained *D3Mit187* and *D3Mit232*, respectively.

Two other YAC clones, 57F5 and 140H7, were also positive for *D3Mit187*. Clone 57F5 appeared to have an internal deletion and was missing the entire SH2 domain protein 2A (*Sh2d2a*) gene; however, clone 140H7 was positive for *Sh2d2a*. Using the 444G3 end sequence as probe, BAC 377C20 was cloned from the BAC RP23 library. NIX analysis of the sequence of 377C20 (available at <http://www.ncbi.nlm.nih.gov>) revealed the presence of several genes (*Nes*; *Sh2d2a*; *Bcan*; and *Brall*). These were also present in YAC 140H7, as confirmed by PCR and Southern blotting.

Analysis of YAC clone 376E7 showed it contained the gene *S100A4* and the mouse sequence orthologous for *KIAA0144*, a putative gene homologous to organic cation transporter (*OCT1*) transcription factor [10]. YAC clone 371F2 was obtained by screening with a *KIAA0144* probe. This clone also contained the intact a disintegrin and metalloproteinase domain 15 (*Adam15*) and recombination activating gene 1 (*Rga*) genes proximally, which helped us extend the contig farther in the upstream direction. We were unable to detect YAC clones containing the genes published in the gap between *Brall* and *Rga*. To map this area more precisely, we decided to complete the contig with clones isolated from the mouse BAC RP23 and RP24 libraries.

BAC clone analysis and build of an internal BAC tile

Computational analysis of BAC clone sequences, whether full or BESs, utilized electronic PCR (<http://www.ncbi.nlm.nih.gov/ePCR>) and pair-wise and standard nucleotide–nucleotide BLAST. These analyses provided sufficient numbers of unique overlaps to build a BAC tile within the final contig. Initially, data and sequence analysis of known clones on chromosome 3 were carried out to identify possible overlaps. From these we identified the BAC clones RP23-68H24, RP23-4L11, RP23-15P14, RP23-367M7, RP23-4P7, RP23-51N3, RP24-194O6, and RP23-295A4. However, there was no overlap between BAC clones RP23-51N3 and RP24-194O6. For this gap, the cytoview of chromosome 3 at Ensembl (http://www.ensembl.org/Mus_musculus/cytoview) (version 16.30.1, May 2003) was used. BAC clones RP23-93O5 and RP23-214B5 had not been fully sequenced; however, our analysis showed that their BESs were unique. Analysis revealed a single overlap between these clones and also single (opposite end) overlaps with clones RP23-51N3 and RP24-194O6, respectively (Fig. 1).

Comparative analysis with supercontig NW_000191 suggested that the physical gap between *Brall* and *Rga* was approximately 1.3 Mb. In agreement, estimating the sizes of the two unsequenced clones and taking overlaps

into account, the BAC contig tile length was calculated to be 1.2–1.4 Mb.

Discussion

Mapping anomalies

In the process of constructing the contig, we came across several irregularities. As the public maps were updated, genes such as *Ctsk*, *Ctss*, and *Mcl1* were removed from the region. However, other genes such as *Bglap1* (which has the same sequence as *Bglap-rs1*, as verified by BLAST analysis) are still present on the public maps (August 2003). We found that *Bglap1* is contained within both the 0.35-Mb YAC clone 331A8 and the BAC clone RP24-298F19; however, *Bglap1* is absent from the *D3Mit187–D3Mit232* region. In addition, both PCR and Southern blot analysis confirmed that YAC clone 331A8 does not contain several of the genes shown in public mouse maps near *Bglap1* (such as *Sema4a* and *Lmna*). However, the 331A8 clone does contain the polyamine-modulated factor-1 (*Pmf-1*)-like gene. We found that the BAC clone RP24-298F19 also contains *Pmf-1*, *Sema4a*, and *Lmna* (Table 1), and it is therefore possible that clone 331A8 is chimeric. In human, *PMF-1* is located on chromosome 1q12 next to tropomodulin 4 (*TMOD4*), the mouse orthologue of which is present in chromosome 3 between 49 and 52 cM.

Genes present in the contig but shown elsewhere in public databases

We have also mapped genes present in clones within the contig, which, in public databases, are shown nearer the telomere (Fig. 1, Table 1). Using NIX analysis of sequenced BAC clones (NCBI) containing *Iqgap3*, *Psemb4*, *Rfx5*, *Selenpb1*, *Selenpb2*, and a gene homologous to human *CGN*, followed by colony PCR and Southern blotting experiments, these genes have been assigned to BAC clones in the center of our contig (Table 1, Fig. 1).

The genomic interval 42.4–45.2 cM and flanking areas on mouse chromosome 3 are rich in genes that are actively transcribed in the nervous system. Such genes are *Bcan*, neurotrophic tyrosine kinase receptor type 1 (*Ntrk1*) at the same map location as hepatoma-derived growth factor (*Hdgf*), *Brall*, and potassium channel calcium-activated intermediate/small conductance subfamily n member 3 (*Kenn3*) at 90.85 Mb. This is also true for the human and rat syntenic regions in chromosomes 1q21–q23 and 2, respectively (<http://www.ensembl.org> human version 16.33.1, July 2003, and <http://www.rgd.mcw.edu> rat version 5.0_HS, August 2003). Our previous results mapped the *hsh* gene to this interval [9] and due to the relatively poor genomic maps available at that time, we undertook to construct a contig across this region to help identify the

Table 1

Differences between the map presented in this paper and the ones presented at <http://www.ncbi.nlm.nih.gov/mapview/maps.cgi?ORG=mouse&CHR=3>, <http://www.jax.org/resources/documents/cmdata/rhmap/3data.html>, and http://www.ensembl.org/Mus_musculus/mapview?chr=3

Genes markers	Accession No./Refseq	YAC/BAC clone	NCBI map	JAX map	ENSEMBL map	Our map	Human/rat syntenic region
<i>Genes removed from area of interest</i>							
<i>Bglap1</i> (sequence identical to that of <i>Bglap1-rs1</i>)	NM_007541 NM_013480	y331A8 bRP24 298F19	+	+	+	–	1q21/?
<i>Sema4a</i>	NM_013658	bRP23 93E19	+	+	+	–	1q21/2
<i>Lmna</i>	NM_019390	bRP24 298F19	+	+	+	–	1q21.2–q21.3/2
<i>Rab25</i>	NM_018899	bRP23 76F18	+	+	+	–	1q21.3/2
<i>Mapbpip</i>	NM_031248	bRP23 18J1	+	+	+	–	1q21.3/?
<i>Ubin</i>	NM_033526	bRP23 76F18	+	+	+	–	1q21/?
<i>Lbcl1</i>	NM_008487	bRP23 199B2	+	+	+	–	1q/2
<i>Rit1</i>	NM_009069	bRP23 199B2	+	+	+	–	1q21.3/?
<i>Syt11</i>	NM_018804	bRP23 199B2	+	+	+	–	1q21–q23/UN
<i>Fdps</i>	NM_134469	bRP23 318I15	+	+	+	–	1q21.3/4
<i>Genes added to area of interest</i>							
<i>Iqgap3</i>	NM_178229	bRP23 68H24	–	–	–	+	1q22/?
<i>Psemb4</i>	XM_203986	bRP23 4L11 bRP23 15P14	–	+	–	+	1q21.2/UN
<i>Rfx5</i>	NM_017395	bRP23 15P14	–	+	–	+	1q21/?
<i>Selenbp1</i>	NM_009150	bRP23 15p14 bRP23 367m7	–	–	–	+	1q21–q22/2
<i>Selenbp2</i>	NM_019414	bRP23 15p14 bRP23 367M7	–	–	–	+	1q21–q22/2
<i>Cgn</i>	XM_194107 (human seq)	bRP23 4P7 bRP23 367M7	–	+	–	+	1q21.3/?

hsh gene. We calculate that the region 42.4–45.2 cM consists of approximately 3.5 Mb, with the internal BAC tile accounting for 1.2–1.4 Mb. Since the *hsh* phenotype locus was mapped approximately in the center, greater emphasis was placed on mapping this region and therefore additional genes were studied. Currently, we are evaluating the expression of potential candidate genes within the CNS of wild-type and *hsh* mice. Over the course of constructing the contig, several genes such as *Ctss*, *Ctsk*, and *Mcl1* were moved out of the area (42.4–45.2 cM in public databases) and are now placed around 48 cM [1,4]. In addition, we revealed several other differences by comparison with the most recent releases of data (August 2003). Several genes are absent from our contig, and our experimental results confirmed that *Bglap1*, *Sema4a*, *Lmna*, *Rab25*, *Mapbpip*, *Ubin*, *Lbcl1*, *Rit1*, *Syt11*, and *Fdps* are missing from the clones representing this region (42.4–45.2 cM). However, our analysis showed that these genes are present in other BAC clones (Table 1), suggesting that these genes exist toward the telomere on mouse chromosome 3 at 49–52 cM, adjacent to the genes *Oaz3*, *Rorc*, *Tcf1*, and *Tmod4*.

We also discovered that six other genes are present within the contig, four of which (*Psemb4*, *Rfx5*, *Selenbp1*, and *Selenbp2*) were previously mapped at 50 cM on mouse chromosome 3 (Fig. 1, Table 1) (July 2003). The fifth gene, *Iqgap3*, was recently mapped to human chromosome 1q22 (April 2003); however, in the mouse there are only two mapped *Iqgap* genes, *Iqgap1* on chromosome 15 and *Iqgap2*

on chromosome 7. Genscan analysis (<http://genes.mit.edu/GENSCAN.html>) of mouse BAC RP23-68H24, which contains the entire gene, shows that *Iqgap3* is present in this clone (bases 170905 to 130160); however, it differs from the published human mRNA by 108 bases. The sixth gene, *Cgn*, also maps on human chromosome 1. These six genes are now mapped between 42.4 and 45.2 cM on mouse chromosome 3.

All the genes reported in this paper are in cytogenetic bands F1–F2 on mouse chromosome 3 in all publicly held data (www.ncbi.nlm.nih.gov, August 2003; www.ensembl.org, August 2003; and www.jax.org, August 2003). We have highlighted the differences between our map and that at NCBI, Ensembl, and the Radiation Hybrid (RH) map at The Jackson Laboratory (Table 1). There are, however, differences in gene location between each source of information, with some more frequently updated than others. As yet, this region in mouse chromosome 3 has not been completely mapped in any of the above maps. The Ensembl database has an incomplete BAC contig, which contains unsequenced BACs and at least one gap between 89 and 89.9 Mb. The information at Mouse Genome Informatics at www.jax.org appears to correlate better (than other public maps) with our findings (Table 1). The complete mouse, human, and eventually rat genomic sequence will allow researchers to speed up positioning of genes and allow further refinement in genomic maps, facilitating functional studies and analysis of positional effects and modifications.

Materials and methods

To prepare the physical map from 42.4 to 45.2 cM on chromosome 3, we analyzed the Jackson Mouse RH map (June 2003) between markers *D3Mit187* and *D3Mit232* (<http://www.jax.org/resources/documents/cmdata/rhmap/3data.html>) [11,12]. This region in the RH map contained many ESTs expressed in the brain, suggesting that this area might warrant further research. The polymorphic markers identified were then checked in the Whitehead database to match YAC clones (<http://www-genome.wi.mit.edu/cgi-bin/mouse/index>). All the clones that corresponded to a specific marker were obtained through HGMP (<http://www.hgmp.mrc.ac.uk/geneservice/reagents/products/index.shtml>). For the markers and genes that did not belong to known YAC clones, screening by PCR with appropriate primers was performed on the WI/MIT C57BL/6J female mouse genomic YAC library [13,14]. PCR and Southern blotting analysis confirmed the presence of either the gene or the marker in the clone.

Database analysis

The mouse chromosome 3 cytogenetic map spanning bases 88.6–90.3Mb (http://www.ensembl.org/Mus_musculus/cytoview) and the Jackson RH map permitted us to bridge the gap between YAC clones placed at either end of our region of interest. This also allowed us to indicate the potential positions of genes within the area containing *hsh* that were used to search the High Throughput Genomic Sequence database (restricted to mouse) and the NCBI Non-Redundant protein database using BLAST (<http://www.ncbi.nlm.nih.gov/blast>). The results showed all the significant overlaps in the sequences. From this, sequences of genes that gave only two/three highly significant and specific overlaps were used to design PCR primers. BAC clones were selected from Ensembl (http://www.ensembl.org/Mus_musculus/cytoview) (mouse version 16.30.1, May 2003). Their BES (http://www.tigr.org/tdb/humgen/bac_end_search/bac_end_search.html) was analyzed using BLAST and the resulting clones using NIX. The results confirmed our gene placements and revealed additional genes that might belong to the region of interest. The latter genes were examined in a similar fashion to generate the contig. Once the overlaps within the area were confirmed using bioinformatics, the appropriate clones were obtained from BACPAC Resources at <http://www.chori.org/bacpac/> [15].

NIX analysis

NIX is a free access tool to perform several analysis programs on large (20–100 kb) DNA sequences simultaneously. It aids identification of regions such as promoters, exons, CpG islands, and poly(A) tails. The output page allows viewing of all the results and can be used to highlight

areas of interest. If a consensus is found between analysis packages, then it may warrant experimental research to confirm. NIX analysis is carried out on all regions of interest by entering the genomic sequence at the HGMP Web site (www.menu.hgmp.mrc.ac.uk/menu-bin/Nix/Nix.pl). If a sequence is larger than 100 kb then the sequence is entered as overlapping segments.

YAC and BAC clone culturing

YAC clones were either streaked on AHC plates (0.17% w/v yeast nitrogen base without amino acids, 0.5% w/v ammonium sulfate, 1% w/v casein hydrosylate acid, 0.50 mg/ml adenine hemisulfate, 2% w/v Bactoagar, and, added after autoclaving, 2% w/v glucose) (Becton–Dickinson, UK) or grown in AHC broth [13,14]. BAC clones were grown either in LB medium containing 20 µg/ml chloramphenicol or on agar plates. Freshly plated YAC and BAC clones from the original stocks were routinely tested for genes and markers by single-colony PCR [16].

PCR and Southern blotting

A general colony PCR amplification protocol was a single cycle of 94°C for 3 min, 62°C for 1 min, 72°C for 3 min 30 s (preamplification step); 34 step cycles of 93°C for 30 s, 63°C for 45 s, and 72°C for 25 s (amplification steps); and 93°C for 30 s, 63°C for 1 min, and 72°C for 3 min (chain termination step). The annealing temperature and extension time varied depending on the primer pairs. The products were separated in 2% agarose gels and viewed by ethidium bromide (0.5 µg/ml) staining. In all cases only the predicted clones yielded PCR products of the appropriate sizes, and the results were confirmed by sequencing and/or Southern blot analysis.

Pulsed-field gel electrophoresis

PFGE was used to calculate the size of the YAC clones. The clones were grown in AHC broth and intact cells were embedded in agarose [17]. The cell wall was removed by lyticase (Sigma–Aldrich, UK) (0.13 mg/ml) in SCEM (20 mM β-mercaptoethanol, 1 M sorbitol, 100 mM sodium citrate, 10 mM EDTA), rendering the DNA accessible. Electrophoresis was performed on a Chef III Pulsed Field Gel System (Bio-Rad, UK) (24-h run time, switch time 60–120 s). After electrophoresis, the gels were stained with ethidium bromide and photographed. Transfer to nylon membrane for Southern blotting was in 10 × SSC. The filters were baked at 80°C for 2 h, followed by probing with well-characterized gene-specific probes labeled with [α -³²P] dCTP. The membranes were washed to a final stringency of 0.1 × SSC at 65°C and then exposed to X-ray film. This permitted sizing of the YAC inserts, confirmation of the PCR results, and analysis of appropriate digestion products.

Acknowledgments

This work was supported by the Wellcome Trust (Grants 059262/Z/99/AR/KM/JAT and 064736/GM/MK/RL to D.A.V.). We thank our colleagues at IBLS Molecular Genetics and the Applied Neurobiology Group at the Veterinary School in Glasgow, particularly Dr. G. Brock, Dr. M. Bailey, and Dr. J. Anderson for their helpful advice, as well as Mr. T. Rachmamurthy and Mr. G. Richardson for help during the project. We also wish to thank our colleagues at the Sir Henry Wellcome Functional Genomics Facility, IBLS, University of Glasgow for an excellent sequencing service. Homology data for this paper were retrieved from the Mouse Genome Database, Mouse Genome Informatics, The Jackson Laboratory, Bar Harbor, Maine, USA (URL: <http://www.informatics.jax.org/>) (August 2003), and the Rat Genome Database, Rat Genome Database Web Site, Medical College of Wisconsin, Milwaukee, Wisconsin, USA (URL: www.rgd.mcw.edu/) (August 2003). Additional homology data for the paper were retrieved from Mouse Genome Resources, National Center for Biotechnology Information, U.S. National Library of Medicine, 8600 Rockville, Bethesda, Maryland 20894, USA (URL: <http://www.ncbi.nlm.nih.gov/genome/guide/mouse/>) (August 2003), and the Ensembl Genome Browser, European Bioinformatics Institute, and the Sanger Centre, Wellcome Trust Genome Campus, Cambridge, United Kingdom (URL: www.ensembl.org) (August 2003).

References

- [1] R.H. Waterston, K. Lindblad-Toh, E. Birney, J. Rogers, J.F. Abril, et al., Initial sequencing and comparative analysis of the mouse genome, *Nature* 420 (2002) 520–562.
- [2] E. Pennisi, Genomics: sequence tells mouse, human genome secrets, *Science* 298 (2002) 1863–1865.
- [3] S. Mayor, Mouse genome shows many disease genes shared with humans, *BMJ* 325 (2002) 1319.
- [4] S.G. Gregory, et al., A physical map of the mouse genome, *Nature* 418 (2002) 743–750.
- [5] C.V. Beechey, A new spontaneous neurological mutant, *Mouse Genome* 91 (1993) 114–115.
- [6] H. King, *hindshaker*, a novel myelin mutant showing hypomyelination preferentially affecting the spinal cord, *J. Neurocytol.* 26 (1997) 557–566.
- [7] K.A. Nave, Neurological mouse mutants and the genes of myelin, *J. Neurosci. Res.* 15 (1994) 38607–38612.
- [8] I.R. Griffiths, Myelin mutants: model systems for the study of normal and abnormal myelination, *Bioessays* 18 (1996) 789–797.
- [9] D.A. Vouyiouklis, T.J. Anderson, H.E. King, D. Kirkham, S.A. Karim, et al., Mapping of the dysmyelinating murine *hindshaker* mutation to a 1.2-cM interval on chromosome 3, *Genomics* 80 (2002) 126–128.
- [10] K.I. Mills, V. Walsh, A.F. Gilkes, L.J. Woodgate, G. Brown, et al., Identification of transcription factors expressed during ATRA-induced neutrophil differentiation of HL60 cells, *Br. J. Haematol.* 103 (1998) 87–92.
- [11] L.B. Rowe, M.E. Barter, J.T. Eppig, Cross-referencing radiation hybrid data to the recombination map: lessons from mouse chromosome 18, *Genomics* 69 (2000) 27–36.
- [12] L.B. Rowe, M.E. Barter, J.A. Kelmenson, J.T. Eppig, The comprehensive Mouse Radiation Hybrid map densely cross-referenced to the Recombination map: a tool to support the sequence assemblies, *Genome Res.* 13 (2003) 122–133.
- [13] F. Spencer, Targeted recombination-based cloning and manipulation of large DNA segments in yeast, *Methods: Companion Methods Enzymol.* 5 (1993) 161–175.
- [14] M.L. Haldi, C. Strickland, P. Lim, V. VanBerkel, X. Chen, et al., A comprehensive large-insert yeast artificial chromosome library for physical mapping of the mouse genome, *Mamm. Genome* 7 (1996) 767–769.
- [15] K. Osoegawa, M. Tateno, P.Y. Woon, E. Frengen, A.G. Mammoser, et al., Bacterial artificial chromosome libraries for mouse sequencing and functional analysis, *Genome Res.* 10 (2000) 116–128.
- [16] E. Frengen, D. Weichenhan, B. Zhao, K. Osoegawa, M. van Geel, et al., A modular, positive selection bacterial artificial chromosome vector with multiple cloning sites, *Genomics* 58 (1999) 250–253.
- [17] D.C. Schwartz, C.R. Cantor, Separation of yeast chromosome-sized DNAs by pulsed field gradient gel electrophoresis, *Cell* 37 (1984) 67–75.